LITHUANIAN ENERGY INSTITUTE

INNA PITAK

SOLID RECOVERED FUEL: EXTRACTION FROM MUNICIPAL SOLID WASTE AND USE IN INDUSTRY

Doctoral Dissertation
Technological Sciences, Environmental Engineering (T 004)

2023, Kaunas

This doctoral dissertation was prepared at Lithuanian Energy Institute, Laboratory of Materials Research and Testing during the period of 2019–2023. The studies were supported by Research Council of Lithuania.
The doctoral right has been granted to Kaunas University of Technology together with Vytautas Magnus University and Lithuanian Energy Institute.

Scientific Supervisor:

Prof. Dr Gintaras DENAFAS (Lithuanian Energy Institute, Technological Sciences, Environmental Engineering, T 004).

Edited by: English language editor Enrika Švenytė (UAB "BELLA VERBA"), Lithuanian language editor Irma Urbonavičienė (Nr. 670485).

Dissertation Defence Board of Environmental Engineering Scientific Field:

Prof. Dr Jolanta DVARIONIENĖ (Kaunas University of Technology, Technological Sciences, Environmental Engineering, T 004) − **chairperson**;
Assoc. Prof. Dr Anatolijus EISINAS (Kaunas University of Technology, Technological Sciences, Chemical Engineering, T 005);
Prof. Dr Mika HORTTANAINEN (Lappeenranta-Lahti University of Technology, Finland, Technological Sciences, Environmental Engineering, T 004);
Dr Jūratė KRIAUČIŪNIENĖ (Lithuanian Energy Institute, Technological Sciences, Environmental Engineering, T 004);
Prof. Dr Dalia ŠTREIMIKIENĖ (Lithuanian Energy Institute, Social sciences, Economics, S 004).

The public defense of the dissertation will be held at 10 a.m. on 15 December, 2023 at the public meeting of Dissertation Defense Board of Environmental Engineering Science Field in the Conference room at Lithuanian Energy Institute.

Address: Breslaujos 3-202, Kaunas, LT-44403, Lithuania
Phone: (+370) 374 01 809; e-mail : studijos@lei.lt

The doctoral dissertation was sent out on 15 November, 2023.
The doctoral dissertation is available on the internet http://ktu.edu and at the libraries of Kaunas University of Technology (Gedimino 50, Kaunas, LT-44239, Lithuania), Lithuanian Energy Institute (Breslaujos 3, Kaunas, LT-44403, Lithuania) and Vytautas Magnus University (K. Donelaičio 52, Kaunas, LT-44244, Lithuania).

LIETUVOS ENERGETIKOS INSTITUTAS

INNA PITAK

KIETASIS ATGAUTASIS KURAS: GAVYBA IŠ KIETŲJŲ KOMUNALINIŲ ATLIEKŲ IR PANAUDOJIMAS PRAMONĖJE

Daktaro disertacija
Technologijos mokslai, aplinkos inžinerija (T 004)

2023, Kaunas

Disertacija rengta 2019–2023 metais Lietuvos energetikos instituto Medžiagų tyrimų ir bandymų laboratorijoje. Mokslinius tyrimus rėmė Lietuvos mokslo taryba.
Doktorantūros teisė Kauno technologijos universitetui suteikta kartu su Vytauto Didžiojo universitetu ir Lietuvos energetikos institutu.

Mokslinis vadovas:
prof. dr. Gintaras DENAFAS (Lietuvos energetikos institutas, technologijos mokslai, aplinkos inžinerija, T004).

Redagavo: anglų kalbos redaktorė Enrika Švenytė (UAB „BELLA VERBA“), lietuvių kalbos redaktorė Irma Urbonavičienė (IVP Nr. 670485).

Aplinkos inžinerijos mokslo krypties disertacijos gynimo taryba:
prof. dr. Jolanta DVARIONIENĖ (Kauno technologijos universitetas, technologijos mokslai, aplinkos inžinerija, T 004) – **pirmininkė**;
doc. dr. Anatolijus EISINAS (Kauno technologijos universitetas, technologijos mokslai, chemijos inžinerija, T 005);
prof. dr. Mika HORTTANAINEN (Lapenrantos-Lahti technologijos universitetas, Suomija, technologijos mokslai, aplinkos inžinerija, T 004);
dr. Jūratė KRIAUČIŪNIENĖ (Lietuvos energetikos institutas, technologijos mokslai, aplinkos inžinerija, T 004);
prof. dr. Dalia ŠTREIMIKIENĖ (Lietuvos energetikos institutas, socialiniai mokslai, ekonomika, S 004).

Disertacija bus ginama viešame Aplinkos inžinerijos mokslo krypties disertacijos gynimo tarybos posėdyje 2023 m. gruodžio 15 d. 10.00 val. Lietuvos energetikos instituto Posėdžių salėje.

Adresas: Breslaujos g. 3, LT-44403 Kaunas, Lietuva
Tel. (+370) 374 01 809; el. paštas: studijos@lei.lt

Disertacija išsiųsta 2023 m. lapkričio 15 d.
Su disertacija galima susipažinti interneto svetainėje http://ktu.edu, Kauno technologijos universiteto (Gedimino g. 50, Kaunas, LT-44239, Lietuva), Lietuvos energetikos instituto (Breslaujos g. 3, Kaunas, LT-44403, Lietuva) ir Vytauto Didžiojo universiteto (K. Donelaičio g. 52, Kaunas, LT-44244, Lietuva) bibliotekose.

CONTENTS

LIST OF TABLES

LIST OF FIGURES

LIST OF ABBREVIATIONS

AC	Ash content
Afm	Calcium monosulfo-, hemicarboaluminate or calcium monocarboaluminate phases
Aft	Ettringite
BA	Bottom Ash
BET	Brunauer-Emmett-Teller Analysis
BJH	Barrett-Joyner-Halenda method
CC	Decarbonises calcium carbonates
CH	Portlandite
CSH	Calcium Silicate Hydrate
C&DW	Construction and Demolition Waste
CPP	Cogeneration Power Plant
ERFO	European Recovered Fuel Organisation
DFT	Density Functional Theory
DTA	Differential Thermal Analysis
EDS	Energy-Dispersive X-ray Spectroscopy
EU	European Union
FTIR	Fourier-Transform Infrared spectroscopy
Hy	Calcium phosphate hydrates
IUPAC	International Union of Pure and Applied Chemistry
LMRs	Landfill Mined Residues
MBT	Mechanical Biological Treatment
MC	Moisture Content
MSW	Municipal Solid Waste
NCV	Net Calorific Value
RDF	Refuse-Derived Fuel
SEM-EDS	Scanning Electron Microscopy-Energy Dispersive Spectroscopy
SRF	Solid-Recovered Fuel
TGA	Thermo-Gravimetric Analysis
VM	Volatile Matter
wb	Bound water
XRD	X-ray powder Diffraction

1. INTRODUCTION

1.1. Motivation and relevance of the problem

The amount of waste generated worldwide has increased over the past decade and continues to widen. According to the World Bank[1], by 2050, the amount of waste generated (in the world) will increase by 70.4% to 3.4 billion tons. The total amount of waste generated in the European Union (EU) increased by 19.8% between 2005 and 2020, with 505 kg of municipal solid waste (MSW) generated per capita in 2020. This trend suggests that it is necessary to take serious and concrete actions to reduce the generation and recycling of waste.

Waste management and disposal are some of the most pressing global problems today. Appropriate management of MSW is a critical priority for achieving the EU's sustainable development goal of reducing negative environmental and human health impacts[2]. The main improvements in this area have been achieved by commissioning mechanical biological treatment (MBT) and cogeneration power plants (CPP). However, a significant amount of waste is still sent to landfills, indicating that the problem of waste disposal remains unresolved[3,4]. In some countries, more than 50% of household waste has been recycled, composted and anaerobically digested[5].

In 2020, countries like Norway, the Czech Republic, Slovakia, and Iceland were among the top per capita household waste producers, showing significant growth over a 15-year period. This means that these countries generated a considerable amount of household waste per person, and this amount has increased significantly over the past 15 years. As presented in **Figure 1.1**, Lithuania is among the countries that, since 2005, have seen an increase in MSW generation.

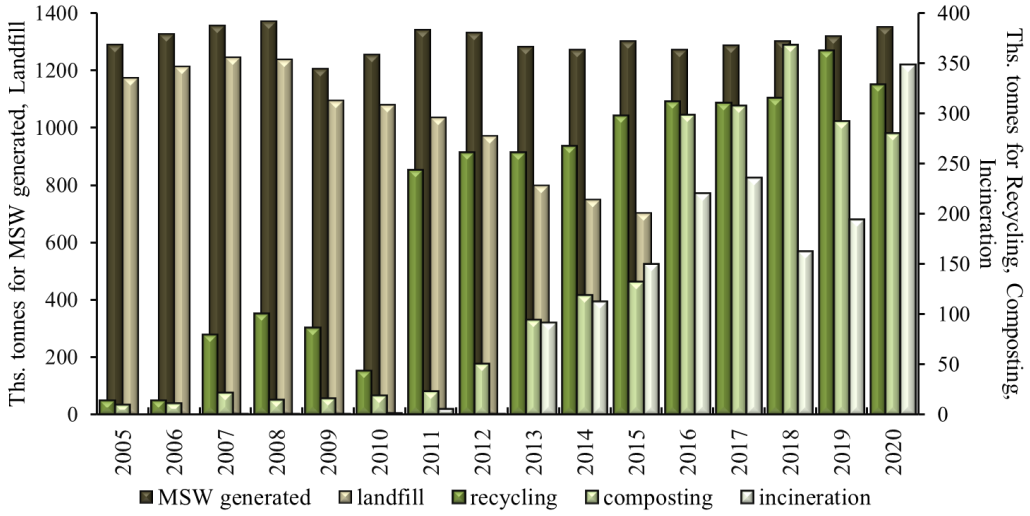

*Eurostat. 2021. Municipal Waste Statistics

Fig. 1.1. Municipal solid waste of Lithuania: generated and recovering.

EU strategic objectives include reducing waste generation and achieving a circular economy[6]. The circular economy is a regenerative system in which the

number of resources used and the waste, emissions and energy losses generated are minimised by slowing down, closing and narrowing the energy and material use cycles. This can be achieved through sustainable design, maintenance, reuse, total refurbishment, and recycling. The critical components of the EU environmental policy are environmentally sound waste management and recycled materials.

In this context, the waste management sector should become a responsible unit, including creating new business models, focusing on the prevention of household waste, targeted monitoring, waste generation forecasting, the introduction of digitisation technologies and the extraction of resources from landfills. In particular, recycling and reuse will be vital to achieving the goals of sustainable environmental protection.

Developed and developing countries are trying to achieve a minimum amount of waste sent to landfills. This desire, in turn, leads to increased incinerated, recycled and compostable household waste. Recovery of energy from waste in CPP is a more sustainable way of managing waste than burying it in landfills. Using sorted and burnable waste as fuel for power generation and district heating, CPP works in synergy with the circular economy and promotes responsible waste management. The aggregate of waste generated in Lithuania is $1.34 \cdot 10^6$ tons per year, of which about $203 \cdot 10^3$ tons, which is ≈15.15%, are currently incinerated at Lithuanian CPPs[7–9]. Currently, on the territory of Lithuania located and working three CPPs in Vilnius, Kaunas and Klaipeda cities (**Fig. 1.2**).

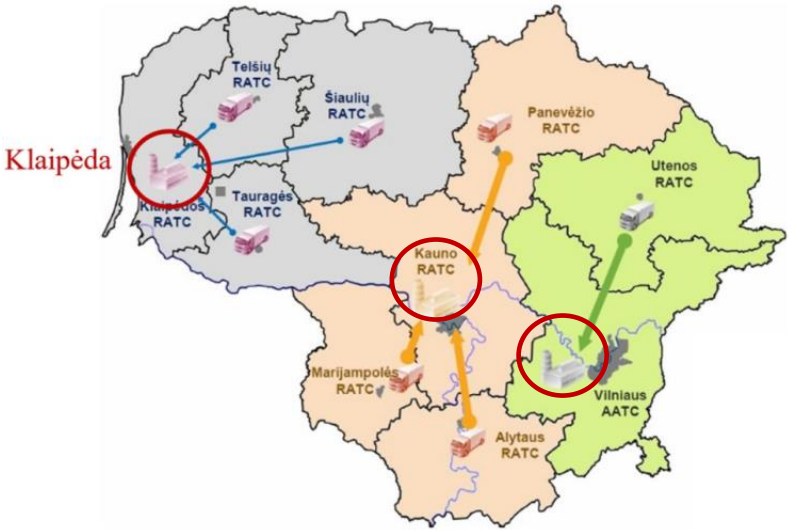

Fig. 1.2. The explication of the location of the cogeneration power plants in Lithuania and supply waste for producing heat and energy.

Waste incineration generates heat and power; the by-product, bottom ash (BA), comprises about 11%. After the extraction of metals, BA is taken to the landfill and used for dumping the landfill. However, there is a real opportunity to use the formed ash residue in the construction industry. Studies of the physical and mechanical characteristics of BA have shown its potential suitability for civil engineering, especially for road construction and the production of clay bricks and tiles[10–12].

Along with the authors[13] statement that the best way to get rid of waste and move closer to a circular economy is to reuse and produce heat and energy, it is also necessary to take into account the fact that waste can be used as a replacement fuel for energy-intensive industries, such as cement industry. The authors[14–16] also believe that waste and materials can be sustainable energy sources. Such a strategy will save companies a lot of money, ensure controlled waste disposal and reduce the consumption of non-renewable natural energy resources.

Waste-derived fuels are becoming a viable and popular alternative to fossil fuels. This fuel type falls into two main categories: Refuse-Derived Fuel (RDF) and Solid-Recovered Fuel (SRF). RDF is a term that refers to waste that has not undergone proper processing. RDF is not standardised, its functions are not defined, and the quality of the finished product cannot be guaranteed. SRF is a fuel obtained by sorting, drying and shredding of solid waste. SRF usually consists of combustible components derived from municipal solid waste. It is typically produced from MSW, industrial and commercial waste, or construction and demolition waste (C&DW). The typical SRF production scheme is shown in **Fig. 1.3**, according to the European Recovered Fuel Organisation (ERFO)[17].

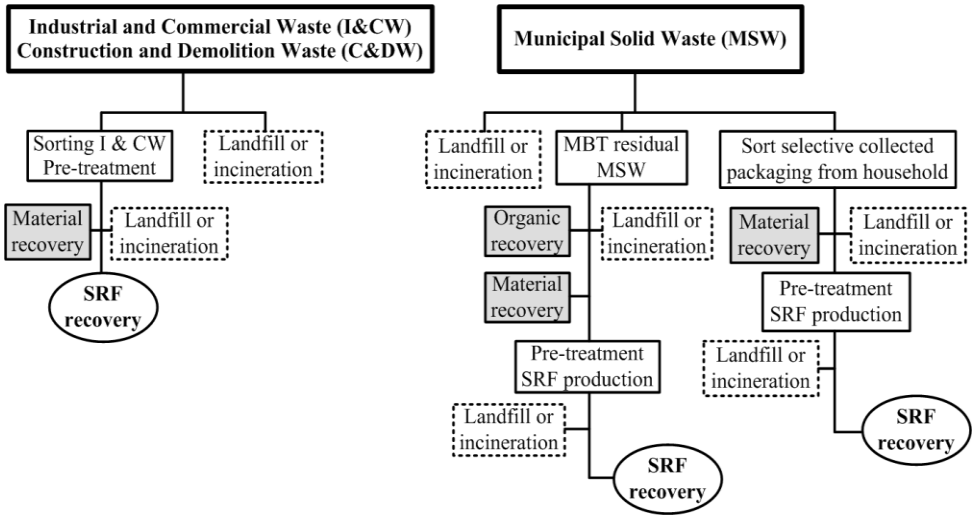

Fig. 1.3. Process of the production SRF.

However, it should be noted that recently the issue of producing alternative energy sources using not natural energy resource streams became topical, but this is waste from landfills, which were once taken out for disposal. Landfill mining is the term most commonly used to describe the extraction of resources from landfills[18–19]. Landfill mining should be understood as an integrated resource extraction and conservation activity in which deposited resource wastes (metals, plastics, fuels and building materials) are recovered, and problems with leachate utilisation and other environmental issues associated with landfills are addressed[18,20]. Once the waste is extracted from the landfill, more space is freed through recycling, avoiding the need for new landfills. The primary way behind mining in landfills is that the deposited material will be more useful elsewhere. By extracting resources from landfills, waste,

once landfilled, is given a new chance to climb up the waste hierarchy towards energy recovery, recycling or reuse. So, the waste extracted from the landfill can be recycled to produce alternative fuels. The production of SRF is not a competing recycling process but an integral part of it. SRF is known in Lithuania but is not used as an alternative fuel, although it is an important element in the waste management system. Only SRF can be used as a replacement fuel (instead of coal or natural gas) during the clinker firing process. Using produced fuel from waste in the clinker firing process will reduce the consumption of non-renewable natural energy resources and greenhouse gas emissions.

Thus, waste disposal through the production of high-quality alternative fuel and its use in the cement kiln in the clinker firing process has economic and environmental benefits and is crucial in achieving the goals of the circular economy. The production of SRF will also entail less dependence on non-renewable natural energy resources, a reduced carbon footprint, and a constant supply of "quality" fuel at a relatively stable price.

According to the presented data regarding the generation and management of waste, it was found that there is a real problem in the field of waste management both in the world and in Lithuania. The global community is striving to achieve the goals of the circular economy, and Lithuania is no exception. In this dissertation, potential steps were proposed for creating an alternative type of fuel, and a mechanism was proposed for the disposal of ash residues generated during the waste incineration process. The studies carried out in work, and the proposed mechanisms will bring Lithuania closer to achieving the goals of the circular economy.

1.2. The aim, objectives and scientific novelty

Aim of dissertation

The aim of the dissertation is to investigate the possibility of utilising waste by producing solid recovered fuel for energy-intensive industries and using by-products as replacement components in ceramic bricks production and cement-based materials.

Objectives

1. to determine the main characteristics of RDF, SRF, and ash obtained after the incineration of SRF and develop the concept of an SRF production line;
2. to establish the possibility of excavating waste from the landfill and producing alternative fuel;
3. to prove the environmental feasibility of utilising bottom ash as the replacement component in clay brick production;
4. to prove the possibility of using ash after gasifying biomass-sludge waste as a partial substitute in cement-based materials.

Thesis statements:

1. Refuse-derived fuel (RDF), as a product of the mechanical processing of mixed municipal waste generated in the Kaunas region, is a suitable raw material for solid recovered fuel (SRF), the use of which in the cement industry increases its sustainability.

2. Municipal solid waste landfills are sources of quality materials suitable for the production of qualitative SRF.
3. The use of SRF bottom ash as a partial substitute for clay in the brick production process would influence the reduction of waste amount and would not deteriorate the quality of the obtained product.
4. Residual ash generated during SRF gasifying can partly replace cement-based materials and reduce the use of natural sources.

Scientific novelty

1. Developed the concept of the line for RDF conversion to SRF and selected the optimal conditions for alternative fuel production for the Kaunas region;
2. Developed a two-stage mechanism of LMR extraction and further SRF production.
3. Proposed more sustainable technology for producing clay bricks by replacing a part of clay with SRF bottom ash having low calcium content.
4. Based on the similarity of the mineral composition of SRF and sewage sludge, the optimal parameters for using SRF gasification residue ash as a hybrid filler in cement-base materials have been developed and confirmed.

Practical value

This study provides essential practical information on the possibilities of recycling the burnable fraction of municipal solid waste through producing alternative fuels (SRF) for the cement industry, which has largely not been considered and used in processing municipal waste at MBT and landfills in Lithuania. A methodology has been developed to dispose of by-products formed during heat and energy production.

The research results can be used to reduce the consumption of natural resources, greenhouse gas emissions and waste accumulation in landfills by reusing and recycling the non-utilisable fraction of MSW and their by-products.

The content and scope of the dissertation

This doctoral dissertation consists of the following chapters: introduction, results and discussion, conclusions and recommendations, references, curriculum vitae, list of publications, copies of scientific papers and acknowledgements appendixes. The doctoral dissertation consists of 160 pages, the main part of the work consists of 86 pages, 2 tables, 39 figures and 1 appendix. The dissertation consists of material previously published in the articles, reproduced with the publishers' permission.

1.3. Papers and co-authors' contributions to papers

1. **Inna Pitak**; Darius Rinkevičius; Regina Kalpokaitė-Dičkuvienė; Arūnas Baltušnikas; Gintaras Denafas. The strategy for conservation of non-renewable natural resources through producing and application solid recovery fuel in the cement industry: a case study for Lithuania // Environmental science and pollution research. Heidelberg: Springer. ISSN 0944-1344. eISSN 1614-7499. 2022, vol. 29, p. 69618–69634. https://doi.org/10.1007/s11356-022-20793-y

[Science Citation Index Expanded (Web of Science); Scopus; MEDLINE] [IF: 5,190; AIF: 6,309; IF/AIF: 0,822; Q2 (2021, InCites JCR SCIE)] [CiteScore: 6,60; SNIP: 1,154; SJR: 0,831; Q1 (2021, Scopus Sources)] [Field: T 004] [Input: 0,5].

2. **Inna Pitak;** Gintaras Denafas; Arūnas Baltušnikas; Marius Praspaliauskas; Stasė Irena Lukošiūtė. Proposal for implementation of extraction mechanism of raw materials during landfill mining and its application in alternative fuel production // Sustainability. Basel: MDPI. ISSN 2071-1050. 2023, vol. 15(5), 4538, p. 1–22. https://doi.org/10.3390/su15054538 [Science Citation Index Expanded (Web of Science); Scopus; DOAJ] [IF: 3,889; AIF: 6,732; IF/AIF: 0,577; Q2 (2021, InCites JCR SCIE)] [Field: T 004, T 008] [Input: 0,5].
3. **Inna Pitak**; Arūnas Baltušnikas; Regina Kalpokaitė-Dičkuvienė; Rita Kriūkienė; Gintaras Denafas. Experimental study effect of bottom ash and temperature of firing on the properties, microstructure and pore size distribution of clay bricks: a Lithuania point of view // Case Studies in Construction Materials. Elsevier BV. ISSN 2214-5095. 2022, vol. 17, p. e01230. https://doi.org/10.1016/j.cscm.2022.e01230 [Science Citation Index Expanded (Web of Science); Scopus] [IF: 4.934; AIF: 4.885; IF/AIF: 1.010; Q1 (2021, InCites JCR SCIE)] [CiteScore: 5.2; SNIP: 1,932; SJR: 1.01; Q1 (2021, InCites JCR SCIE)] [Field: T 004, T 008] [Input: 0,7].
4. Regina Kalpokaitė-Dičkuvienė; **Inna Pitak**; Arūnas Baltušnikas; Stasė Irena Lukošiutė; Gintaras Denafas; Jūratė Česnienė. Cement substitution by sludge-biomass gasification waste: the synergy with silica fume // Construction and Building Materials. Oxford: Elsevier BV. ISSN 0950-0618. 2022, vol. 326, 126902, p. 1–14. https://doi.org/10.1016/j.conbuildmat.2022.126902. [Science Citation Index Expanded (Web of Science); Scopus] [IF: 7,693; AIF: 5,545; IF/AIF: 1,387; Q1 (2021, InCites JCR SCIE)] [Cite Score: 10.6; SNIP: 2.362; SJR: 1.777; Q1 (2021, InCites JCR SCIE)] [Field: T 004, T 008] [Input: 0,2].

Personal input of the author

P1: A concept of SRF production line production from RDF was developed by extracting prohibited materials, shredding and drying, and the energy potential for using SRF in the cement industry as an alternative fuel was evaluated[21]: contribution from each co-author is reported at the end of the publication. The first and corresponding author Inna Pitak contributed to conceptualisation, methodology, software for numerical analysis and data processing, data acquisition and experimental investigations, visualisation, writing of original draft, review and editing. Darius Rinkevičius contributed to data curation and worked with software to analyse data. Arūnas Baltušnikas and Regina Kalpokaitė-Dičkuvienė contributed to conceptualisation, methodology, validation of results, supervision, writing review and editing. Gintaras Denafas contributed to conceptualisation, data curation, validation of the results, formal analysis, writing review and editing.

P2: There was the development of an extraction mechanism for raw materials during the landfill mining process and using its application in alternative fuel

production[24]. The first and corresponding author Inna Pitak contributed to conceptualisation, data curation, formal analysis, methodology, resources, software, writing original draft, review and editing. The second author Gintaras Denafas contributed to the conceptualisation, data curation, formal analysis, review and supervision. Arūnas Baltušnikas contributed to the investigation, formal analysis, methodology and validation. The author Marius Praspaliauskas contributed to methodology, formal analysis and software. Stasė Irena Lukošiūtė contributed to conceptualisation, resources and supervision.

P3: Proved the feasibility of using the bottom ash obtained after incineration of not a recyclable fraction of municipal solid waste in clay bricks production[33]. The first and corresponding author Inna Pitak contributed to conceptualisation, data curation, formal analysis, investigation, methodology, software, visualisation, and writing the original draft. Arūnas Baltušnikas and Regina Kalpokaitė-Dičkuvienė contributed to the investigation, methodology, software, writing review and editing. Rita Kriūkienė contributed to the formal analysis of data. Gintaras Denafas contributed to supervision, validation, writing review and editing.

P4: Proved the possible application of residue derived from industrial sewage sludge-biomass gasification plants, with silica fume as a partial binder substitute in cement-based materials[46]: first co-author Regina Kalpokaitė-Dičkuvienė contributed to the conceptualisation, methodology, data curation and experimental investigation, formal analysis, visualisation of figures, writing review and editing. Inna Pitak contributed by the writing-original draft of the work, visualisation of data, formal analysis, review and editing. Arūnas Baltušnikas contributed to the Investigation of materials by TGA and XRD analysis, methodology, formal analysis and validation obtained results. Stasė Irena Lukošiūtė contributed to funding acquisition, conceptualisation, finding resources, and project supervision. Gintaras Denafas and Jūratė Česnienė contributed with formal analysis and editing.

Inter-relation of the articles

The first article addresses the first task of the dissertation, which is to determine the main characteristics of RDF, SRF, and ash obtained after the incineration of SRF. It delves into developing a robust SRF production line, encompassing crucial stages such as prohibited material extraction, shredding, and drying. The central objective is to produce high-quality SRF from RDF and evaluate its suitability as an alternative fuel for the cement industry in Lithuania.

Article 2 directly addresses the second task by proposing an innovative mechanism for extracting raw materials during landfill mining and its application in alternative fuel production. This study explores the extraction of valuable materials from LMRs and their transformation into alternative fuel, thereby contributing to sustainable waste management practices and meeting the energy needs of intensive industries. Furthermore, this article investigates the composition and characteristics of LMRs at various depths of the landfill, establishing the optimal depth for LMR extraction and calculating the energy potential of the studied landfill sections.

The third article aligns with the third task of the dissertation, which aims to prove the environmental feasibility of utilising bottom ash as a replacement

component in clay brick production. Through experimental studies, this research examines the effects of bottom ash and firing temperature on clay bricks' properties, microstructure, and pore size distribution. With a specific focus on Lithuania, this article contributes valuable insights into sustainable construction practices by demonstrating the potential of bottom ash as a viable replacement component.

Article 4 serves the fourth task of the dissertation, aiming to prove the possibility of using ash generated from the gasification of biomass-sludge waste as a partial substitute in cement-based materials. The study explores the synergy between gasification waste and silica fume, a common additive in cement production. This research demonstrates the technical and environmental feasibility of incorporating gasification waste into cement-based materials, offering an innovative solution for waste valorisation.

Together, these four articles form a cohesive body of work that advances the aim of the dissertation. Each article contributes unique insights and findings, collectively promoting sustainable resource management, waste-to-energy solutions, and by-product utilisation within the Lithuanian context.

1.4 Brief review of scientific literature

Possibilities of recycling MSW and saving natural resources

Increasing MSW generation is considered a serious environmental problem in many countries, including Lithuania, and it is regarded as an unavoidable by-product of economic activity. In[13], the authors argue that the amount of waste available for energy production is larger than unsorted residual waste and that the best disposal type is material recycling and energy production. It can be assumed that waste and biomass materials can be used as sustainable renewable energy sources. This step will save companies money, reduce greenhouse gas emissions, and reduce the consumption of non-renewable natural resources.

As shown[21], in recent years, interest in the combustion of high caloric fractions for energy production has arisen in many countries. The reasons considered by the authors explain the increased interest in waste incineration for energy production: depletion of natural resources, increase in the amount of waste produced, lack of space for waste disposal, reduction of greenhouse gas emissions and reduced dependence on imported energy sources. However, there is no emphasis on the difficulties a business may face in using waste as an alternative fuel. Such challenges are discussed [22]: energy consumption, high product quality standards, and environmental concerns (reduction of greenhouse gas emissions). The combustion of fossil fuels is the main cause of anthropogenic CO_2 emissions. According to[23], the cement industry has been a leader in the consumption of natural resources and the emission of gaseous substances into the atmosphere. A significant amount of energy consumption and greenhouse gas emissions have been reported[24].

CO_2 emissions depend on clinker production technology, fuels and cement production. Depletion of natural resources and increasing fuel prices pushing cement plants to use alternative fuels in clinker kiln production is the major problem discussed in this paper. The production and use of SRF in the cement industry as an alternative fuel can reduce greenhouse gas emissions compared to emissions from fossil fuels, as

described in[25]. According to[26], co-combusting SRF with fossil fuels can provide economic and environmental benefits by reducing fossil fuel consumption and CO_2 emissions. According to[27], every 5–10% reduction in carbon dioxide intensity in cement production by 2050 could reduce emissions by about $0.4 \cdot 10^9$ tonnes of CO_2 and contribute to slowing climate change and global warming. In[28], the experience of European countries was analysed, which shows that using waste fuels for the cement industry can save companies a lot of money, ensure controlled waste disposal, and reduce the consumption of non-renewable natural resources. However, there are still unresolved issues related to the production of SRF.

Landfill reclamation and recovery of energy-intensive raw materials

Landfills can pose several environmental problems, primarily due to the improper disposal and management of waste. Some of the key environmental issues associated with landfills include[29–31]:

– air pollution: landfills emit various gases, including methane, a potent greenhouse gas that contributes to climate change. Landfills can also release volatile organic compounds (VOCs) and other air pollutants, contributing to poor air quality and health problems;

– water contamination: improperly managed landfills can contaminate groundwater and surface water sources;

– soil degradation: landfills can lead to soil degradation and loss of productive land.

Landfills contain various waste materials, including organic waste, plastics, paper, and other combustible items. The burnable fraction typically consists of materials that have a high calorific value and can be effectively incinerated to produce heat or electricity. Landfill mining, despite its complexities and challenges, can offer several potential advantages[32, 33]:

– resource recovery: landfills contain various materials that can still have value and be recovered for reuse or recycling. Landfill mining allows for extracting valuable resources such as metals, plastics, and organic materials that can be redirected into the production cycle. This reduces the demand for virgin resources and promotes a more circular economy;

– land reclamation: landfills occupy significant land areas that can be repurposed once the waste is excavated. Landfill mining allows reclaiming and rehabilitating these lands for other beneficial uses such as green spaces, parks, or renewable energy installations. It can contribute to the restoration of landscapes and enhance environmental quality;

– environmental remediation: old landfills may have been poorly managed or lack proper environmental safeguards. By excavating and treating the waste, landfill mining can help remediate and mitigate environmental hazards associated with historical landfill sites. It allows for proper containment and treatment of toxic or hazardous substances, preventing their migration into surrounding soil and water;

– energy recovery: some landfills can be a source of landfill gas, mainly composed of methane.

It is important to note that the feasibility and advantages of landfill mining vary

depending on factors such as the composition of the landfill, local regulations, available technologies, and economic considerations. Each landfill site needs to be assessed individually to determine whether landfill mining is viable and beneficial.

Generation, accumulation and utilisation of bottom ash

Bottom ash is the residue obtained after the incineration of a burnable fraction of MSW at CPP. Every year, a huge amount of BA is generated and accumulated in the environment. The potential disadvantages and challenges associated with BA accumulation[34]:

– environmental concerns: bottom ash may contain trace amounts of heavy metals and other potentially harmful substances that could leach into the environment if not properly managed. Adequate safeguards and monitoring are necessary to prevent groundwater contamination and mitigate potential environmental risks;

– waste management: bottom ash accumulation requires dedicated space and appropriate infrastructure. As bottom ash is continually generated in CPP, accumulating large volumes of ash can strain landfill capacities and necessitate proper waste management practices to prevent potential issues related to storage and disposal;

– quality control: bottom ash composition can vary depending on the fuel source and combustion process, which may affect its suitability as a replacement component.

Bottom ash, the residue left after RDF combustion at CPP, can be used as a replacement component in clay brick production. Some advantages of using bottom ash in clay brick production[35,36]:

– waste utilisation: by using bottom ash, a byproduct of power generation, as a replacement material, it reduces the amount of waste sent to landfills and promotes its beneficial reuse. This contributes to sustainable waste management practices;

– resource conservation: clay, a primary raw material for brick production, can be conserved by partially substituting it with bottom ash. This helps preserve natural clay resources and reduces the environmental impact of clay extraction;

– improved brick properties: bottom ash contains reactive components, such as unburned carbon and amorphous silica, which can contribute to the strength and durability of bricks;

– reduced environmental impact: incorporating bottom ash into clay brick production can reduce carbon emissions. By replacing a portion of the clay content, the carbon footprint associated with brick manufacturing can be minimised.

It's important to note that using bottom ash as a replacement component in clay bricks production requires careful testing and optimisation to ensure the desired quality and performance of the final product.

Pross, cons and possibilities of utilisation of ash residue in cement-based materials

The ash residue obtained after the incineration of pellet wood with sewage sludge in a gasifier is a by-product of the combustion process. This ash residue is commonly referred to as gasification ash or gasification slag. It consists of the inorganic materials that remain after the organic matter in the pellet wood and sewage

sludge has been converted into gas through gasification[37,38]. There are several factors to consider regarding the ash residue obtained from the gasification of pellet wood with sewage sludge:

– composition: the exact composition of the ash residue can vary depending on the characteristics of the pellet wood, sewage sludge, and the gasification process. It typically contains minerals, unburned carbon, metals, and other inorganic compounds;

– contaminant levels: the ash residue may contain trace amounts of heavy metals and other pollutants that were present in the pellet wood or sewage sludge. The levels of contaminants can vary depending on the source and quality of the feedstock. Proper characterisation and testing of the ash residue are necessary to assess potential environmental and health risks;

– waste management: the ash residue must be properly managed and disposed of to prevent environmental contamination. Specific regulations and guidelines may exist regarding gasification ash handling, storage, and disposal. Compliance with these regulations is crucial to minimise the environmental impact of the ash residue;

– potential utilisation: gasification ash can potentially be utilised in various applications, such as construction materials, cement production, or soil amendment. However, the suitability of the ash residue for these applications would depend on its composition, including contaminant levels and physical properties. Extensive testing and characterisation would be required to determine the feasibility and suitability of utilising the ash residue;

– environmental impacts: the ash residue could pose environmental risks if not managed properly. Contaminants may leach into soil and water, potentially impacting ecosystems and water quality. Careful handling and disposal practices, such as appropriate containment and monitoring, are necessary to minimise potential environmental impacts.

Proper management, testing, and adherence to regulations are essential when dealing with the ash residue obtained from the gasification of pellet wood with sewage sludge. Evaluating its composition, potential utilisation options and environmental considerations can help ensure the safe and sustainable handling of the ash residue.

2. RESEARCH METHODOLOGY

The concept of an SRF production line was developed by extracting prohibited materials from RDF, shredding, drying, and evaluating the economic and environmental feasibility of using SRF in the cement industry (**Paper 1**). During four seasons (2020–2021) composition of RDF was obtained after the extraction of biological fractions from the stream of MSW. The RDF was taken out through three sieves with square holes 80, 40 and 20 mm in diameter. The fractions were subdivided into subfractions on each sieve, weighed, and the granulometric and morphological composition was determined. Additional sorting of waste fraction 40 mm>d>20 mm was practically impossible since it was difficult to separate the materials visually. At the same time, visual sorting was impossible for small fractions d<20 mm. Morphological separation was performed manually. After morphological analysis, each fraction was weighed, placed in containers and transported to the laboratory for further study. Prohibited materials (Cl- and Hg- containing) were previously extracted. The SRF fraction was shredded in an SM 300 mill. After SRF preparation, the main characteristics (moisture content and ash content, high calorific value, Cl- and Hg- content) were determined by EU standards. The elemental composition (%, in ash) was determined using scanning electron microscopy (SEM). The structure and phase composition of crystalline materials (ash of SRF and SS) were determined using X-ray diffraction (XRD), for which SRF and sewage sludge samples were prepared by burning in a muffle furnace at 950°C for an hour.

The flow rate of the SRF production line was calculated using the formulas:

$$FR_{SRF} = FRP_{RDF} - X - Y - Z - FR_W \quad (1.1)$$

$$X = \left(FRP_{RDF} \cdot a\right)/100\% \quad (1.2)$$

$$Y = [(FRP_{RDF} - X) \cdot b]/100\% \quad (1.3)$$

$$Z = [(FRP_{RDF} - Y) \cdot c)/100\% \quad (1.4)$$

$$FR_{MC} = [(FRP_{RDF} - Z) \cdot MC_L]/100\%, \quad (1.5)$$

if FR_{SRF} is the flow rate of the SRF in the production process (t/h); FRP_{RDF} is the flow rate of the combustible fraction obtained at the MBT plant (6.6 t/h); X, Y, and Z are the flow rates of materials extracted from the RDF at each stage of the process (inert, ferrous, nonferrous metal) (t/h); a, b, and c are the number of extraction materials at each stage of separation (inert, ferrous, nonferrous metal) (%); MC_L is the amount of moisture lost (%); FR_W is the flow rate after moisture loss (t/h).

The economic and environmental feasibilities of using the SRF in the cement industry were calculated using methods (Appendix 1).

The mechanism for extracting LMRs was developed, and the characteristics and possibilities of SRF production from landfill waste and use in the cement industry were studied (**Paper 2**). The Kaunas regional non-hazardous waste landfill (Lapes) was the object of the study. The landfill consists of three sections. The drillings were carried out at the landfill with a 15 cm drill on the landfill sections; waste samples were taken every two meters at a depth of 1 to 20 m. In Section I, drilling was carried out up to 10 m; in Section II, up to 14 m; and in Section III, up to 20 m. The drilling depth was determined on-site at the time of the study. The composition of unprocessed

LMRs was determined through manual sorting after drilling every 2 m. The studies were conducted according to the Standard Test Method for Determining the Composition of Unprocessed Municipal Solid Waste (ASTM D5231-92 (2016). Excavated materials were sieved to fine (<20 mm) and course (> 20 mm) fractions. The fine fraction was backfilled. The coarse fraction was sorted. Afterwards, the coarse fraction was processed for material recovery whenever possible (e.g., plastic, wood, rubber and others) and used as materials to produce SRF. After drilling, the samples of LMRs were shredded and mixed and, after these manipulations, tested. The samples were heterogeneous, and their composition could fluctuate. The material was obtained and subsequently subjected to research to prove the feasibility of extracting LMRs from the landfill and using them in alternative fuel production.

The possibility of reusing the bottom ash to produce clay bricks was studied (**Paper 3**). The BA was obtained by incinerating RDF at the Kaunas CPP. After four months of BA ageing in the atmosphere, the material samples for investigation were taken. The clay Technik-3 used to form the samples was mined in the largest Andreevsky deposit in Ukraine, located near Druzhkovka, Donetsk region, Ukraine. Both materials were dried at 105±5°C, crushed, sieved through a 0.63 mm sieve and tested before forming samples. The samples were prepared from clay and BA, previously dried to constant humidity. The components were mixed under dry conditions; water was added to the mixture (8%). The clay bricks samples were prepared with the replacement of clay with BA from 10 to 40%. The samples were formed, pressed (120 kg/cm^2), dried and fired at 900 and 1000°C. The fired products were cooled down to the ambient temperature in the kiln. After sample formation, drying and firing, it was analysed to confirm or deny the feasibility of using the BA as a replacement material during clay brick production.

The potential application of solid ash residue obtained after the gasification of SS with wood, in binary compositions with silica fume, to utilise solid wastes was investigated (**Paper 4**). The studies were carried out using industrial materials such as commercial Portland cement, micro silica and sand. AR was obtained after gasifying pelleted wood and sewage sludge. The resulting ash was milled in a laboratory ball mill to establish the homogeneity of the material. To prepare each batch of samples, all binder components (cement, micro silica and ash residue) were dry-blended until homogeneous before adding the required amount of water. Fresh mortar mass was poured into moulds and left for 24 hours. Then the samples from the mould were kept at a temperature of (21±2)ºC and a relative humidity of 95% for a time. Mortar cubes and prisms were prepared to determine the mechanical strength at a binder to the sand ratio of 2.5 and water to binder ratio (w/b). 0.4. Various combinations of silica fume with gasification residues have been used to replace cement at replacement levels of 10% and 12% by weight of cement. The dry content of superplasticizer Gaia (pH=5, ρ=1.15 g/mL, Spain) was constant at 0.8 g for all mortar formulations. Eight cubic and three prismatic samples of each composition were used to determine the compressive and flexural strength, respectively. After the samples were formed, it was subjected to the tests.

3. RESULTS AND DISCUSSION

3.1. Determination of the main characteristics of RDF, SRF and ash obtained after incinerating SRF and development of the SRF production line concept (Paper 1)

In this pilot study, an attempt was made to develop an SRF production line from RDF based on the Kaunas MBT, and the energy potential, economic and environmental of using SRF in the clinker firing process was also assessed[39].

Throughout four seasons, during 2020 and 2021, studies were carried out to study the morphological composition of the RDF formed after the extraction of the biological fraction, metals, and inert materials from the general flow of municipal waste. **Fig. 3.1** shows the averaged results (based on the results of four seasons) of granulometric studies of the combustible fraction of materials.

Fig. 3.1. Average granulometric composition of the RDF fraction.

It was found that the combustible fraction of RDF, in the majority, is represented by the size of materials with a size of more than 80 mm; there is no fine fraction. This is a good indicator since the presence of a fine fraction worsens the calorific value of potential waste fuel. The results of the morphological analysis established that the RDF dominant materials are plastics, paper, textiles, and other combustible materials (**Fig. 3.2**).

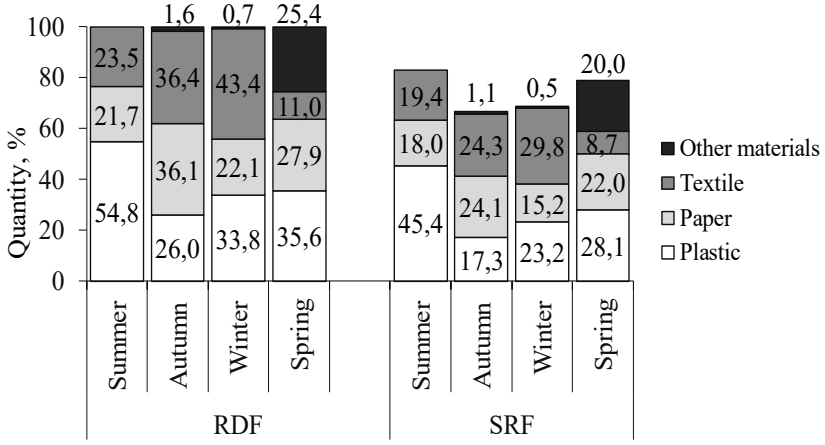

Fig. 3.2. Morphological characteristics of RDF and SRF.

The morphological characteristics of the RDF combustible fraction change depending on the season. **Fig. 3.2** shows the characteristics of the produced SRF from RDF. SRF is proposed to be produced on the technological line presented in the work. The morphological characteristics of the SRF differed from the RDFs, as were extracted prohibited materials (chlorine-containing plastics, mercury-containing materials) and the loss of materials through extraction, screening, grinding and drying. **Fig. 3.2** also shows the characteristics of sewage sludge, which is currently used as a replacement fuel in the clinker firing process. In the work, sewage sludge was compared with the characteristics of the produced SRF.

As seen in **Fig. 3.3**, according to the results of the studies conducted to determine the main characteristics of the RDF and the produced SRF, it was found that they directly depend on the morphological composition and the season of municipal waste generation. A clear dependence of the characteristics of the RDF on the season can be traced based on the data on humidity determination. The highest moisture content of the combustible waste fraction was observed in the autumn and winter periods. Moisture content (MC), ash content (AC) and net calorific value (NCV) depend on the waste's morphological composition and the season of its formation.

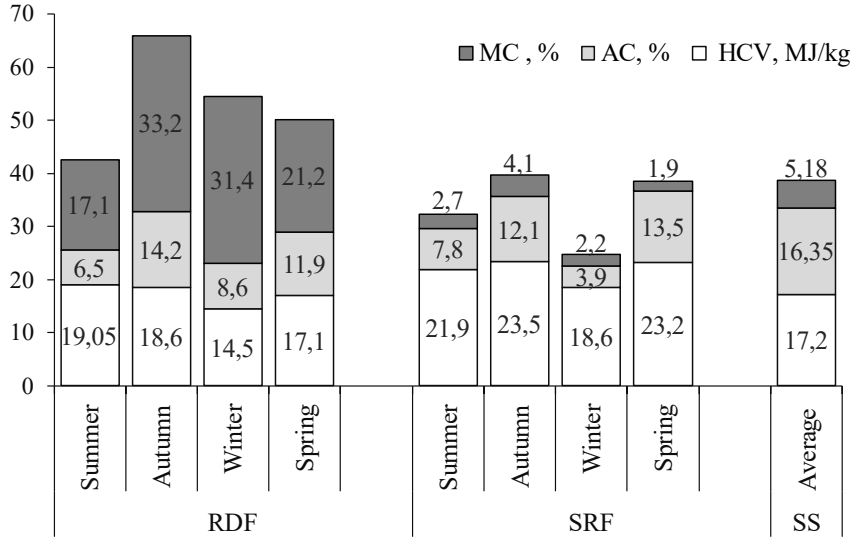

Fig. 3.3. RDF, SRF and sewage sludge seasonal testing results.

As for the characteristics of the produced SRF, in **Fig. 3.3**, it can be seen that the moisture content of the produced SRF is within the allowable limits set for fuel from waste (1.9–4.1%). The calorific value of SRF is relatively high and can compete with solid fuel. Sewage sludge from wastewater treatment plants, prepared for use as a replacement fuel, has a relatively high calorific value (17.2 MJ/kg), MC is 5.18% and high ash content compared to SRF (16.35%).

Chlorine and mercury content is also an essential factor that must be constantly monitored for environmental and technical reasons. The chlorine content for the RDF samples ranged from 1.18 to 1.04% (**Fig. 3.4**).

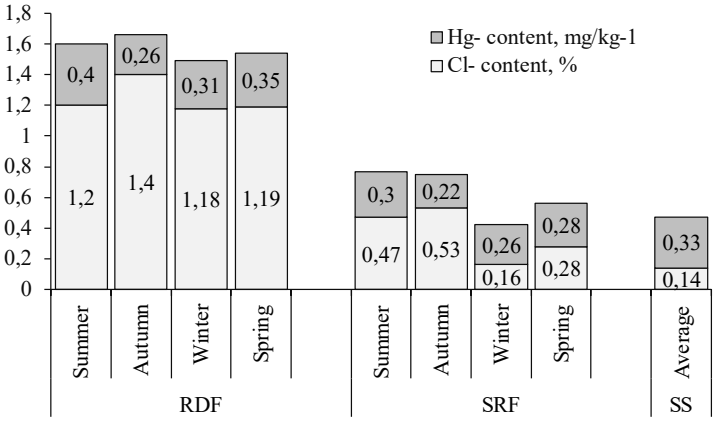

Fig. 3.4. Chlorine and mercury content in RDF, SRF and sewage sludge.

The relatively high chlorine content in the combustible fraction of RDF is associated with chlorine-containing materials. However, in the prepared SRF, the chlorine content is much lower and amounts to 0.16–0.53%. The relatively low chlorine content in the produced SRF is due to the absence of prohibited chlorine-containing plastics in the fuel.

The mercury content in any fuel is a limiting factor that must be constantly monitored. Fuel from waste is no exception. The mercury content in RDF samples varied depending on the season and, consequently, on the morphological composition of the waste generated in a given season, ranging from 0.26 to 0.4 mg/kg^{-1}. The mercury content in the produced SRF had lower values than RDF and ranged from 0.22 to 0.3 mg/kg^{-1} (**Fig. 3.4**). According to the results of the studies carried out to determine the main characteristics of alternative fuel for the cement industry, the following was established:

– RDF obtained at the Kaunas MBT has thermal and energy properties and can be used for combustion at a cogeneration power plant. The combustible RDF fraction can only be used to produce heat and energy and cannot serve as an alternative fuel for energy-intensive industries due to the high moisture content, Cl and Hg in it;

– produced SRF by extraction of prohibited materials, shredding, sieving, and drying had better results than RDF. Produced SRF had a class rating according to EN 15359 and could be used as a replacement fuel in the cement industry.

Today, the Lithuanian cement plant uses sewage sludge as a replacement fuel during the clinker firing process.

Sewage sludge has been subject to the same studies as RDF and SRF. The main characteristics of sewage sludge had the following results: calorific value is 17.2 MJ/kg, chlorine and mercury content is 0.14% and 0.33 mg/kg^{-1}, respectively. It has been established that the sewage sludge and the SRF produced, according to the main characteristics required for fuels from waste, comply with the EU standard and can be used in clinker firing as an alternative fuel.

Kaunas MBT plant has sufficient equipment to extract the biological fraction from the general flow of municipal solid waste. The following equipment removes the biological fraction, inert materials and metals: a drum sieve, magnetic separators for

metal recovery, NIR separators and manual extraction at the final stage. However, these pieces of equipment are not enough to make the final product (RDF) suitable as an alternative fuel for the clinker firing process. The work was proposed to supplement the existing MBT line with additional operations and equipment. The developed SRF production line will contain six additional pieces of equipment (**Fig. 3.5**).

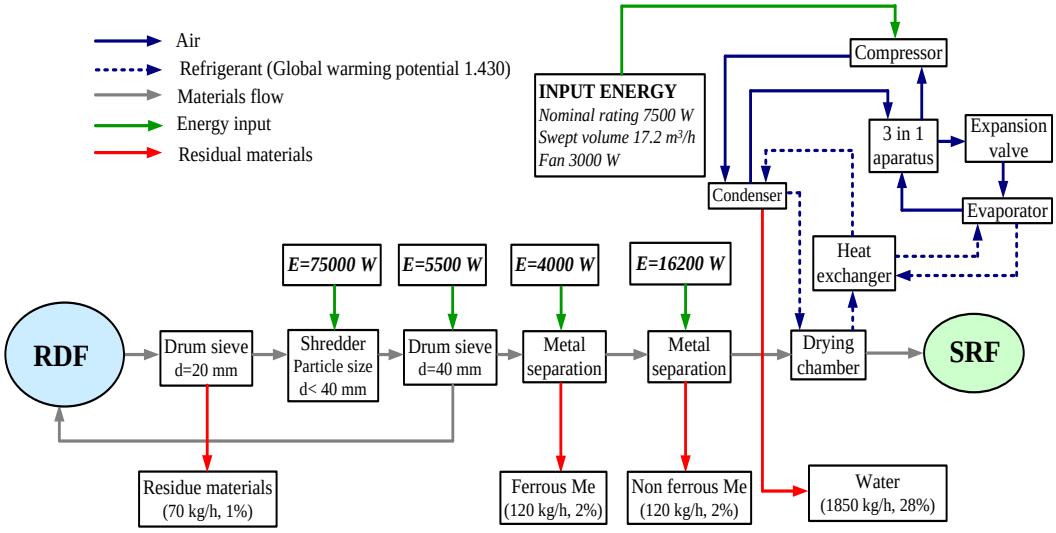

Fig. 3.5. SRF production line.

The first stage of SRF production begins with the first drum sieve, where the biological and fine fraction, inert materials are extracted. After that, the potential combustible fraction is subjected to shredding with a d<40 mm; the larger materials that are not shredded are again sent to the second drum sieve for homogenisation and improvement of the combustible properties of the material. The second drum sieve provides the required size of the SRF, as larger particles are sent to the starting position of the production line. To minimise the presence of metals in SRF, the shredded materials pass through separators to recover metals.

Subsequently, the extracted metals can be sent for sale or recycling. In the final stage of the production line, pre-drying of the finished material is provided, if required, in a drum chamber. The proposed drum chamber has low operating costs, is easy to operate and can handle large volumes of products. The SRF produced from RDF, using all the necessary technological operations with the stages of separation, extraction, grinding and drying, is shown in **Fig. 3.6**. The produced alternative fuel for use in the cement industry has a relatively homogeneous structure, shredded, dried, i.e., prepared for use. To achieve SRF production according to EU standards, it was necessary to develop an additional line for the production of SRF. Turning all the incinerated waste generated at the Kaunas MBT into fuel additives for the cement industry is impossible.

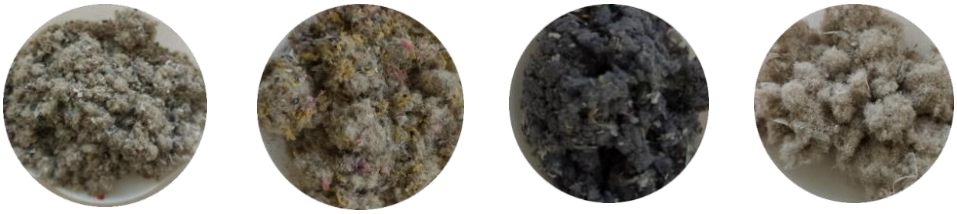

Fig. 3.6. SRF produced from RDF (seasonal variants).

Otherwise, it will disrupt the operation of the Kaunas cogeneration power plant. To avoid this, it is necessary to calculate the amount of RDF for Kaunas CPP and SRF for the cement plant. To not disrupt the technological process of Kaunas CPP, the cement plant waste should be approximately 50% of the waste incinerated (6.6 t/h).

The consumption of the production line was calculated to be 4.47 t/h.

The advantage of kilns is that when materials are burned, including waste, no additional waste remains due to high temperatures (1300–1400°C). The ash generated during the high-temperature roasting process, together with limestone, clay, sand and iron ore, turns into clinker without affecting the quality of the product.

It was proposed to use the produced SRF in the operating technological line to produce clinker at the Lithuanian cement plant. The main characteristics of SRF and sewage sludge (calorific value, humidity, ash-, chlorine- and mercury content) allow them to be used as a replacement fuel in the clinker firing process. The value of these parameters may vary depending on the season, but these changes will be within acceptable limits and will not affect the quality of the finished product. A general view of the ash residue obtained in the incinerating SRF and sewage sludge is shown in **Fig. 3.7.**

Analysis of elemental oxides (%, in ash) obtained by SEM-EDS and presented in **Table 3.1** confirms that the oxide composition of the SRF and sewage sludge is consistent with the oxide composition of the finished clinker.

Fig. 3.7. Image of the ash of sewage sludge **(a)** and SRF **(b).**

The dominant elements reportedly are Si and Ca, the two main elements in clinker production. Al, Fe, Mg and other important elements in the cement industry have also been observed. However, it should be noted that the percentage of oxides in SRF, sewage sludge, and clinker varied. It can be concluded that SRF can be used as a fuel for clinker firing in the same way as sewage sludge but in a particular proportion. This is because there are some oxides (e.g., Na, P, Al, Fe), and their amount must be strictly controlled.

Table 3.1. Elemental oxide analysis ($\%_{in\ ash}$) based on SEM-EDS measurements.

Oxides / Products	CaO	Fe_2O_3	SiO_2	P_2O_5	Al_2O_3	SO_3	MgO	Na_2O	TiO_2	K_2O	Cr_2O_3	CuO	MnO	ZnO
Sewage sludge	32.8	19.3	12.6	20.2	3.8	4.3	2.2	0.9	0.8	1.2	0.1	0.2	1.7	
SRF	30.5	8.8	35.5	1.3	8.7	2.6	3.7	5.5	1.6	0.7	0.1	0.4		0.6
Clinker	65.5	3.0	23.0	0.2	6.0	0.2	2.8	0.3	0.2	0.3				

The chromium, copper and manganese content did not exceed 3%; at high temperatures of 1200–1450°C and above, these elements do not pose a danger to clinker. Although Zn has been added to the list of environmentally harmful elements, its relatively low content (less than one per cent) can be interpreted as an inert element based on waste acceptance criteria[40].

It has been experimentally established that the ash obtained after the combustion of SRF and sewage sludge has a crystalline structure and consists of sodium-, calcium-potassium-, iron- and silicon-containing phases (**Fig. 3.8**).

XRD analysis of sewage sludge and SRF in **Fig. 3.8** showed that in materials presented next minerals: quartz (SiO_2), iron oxide (Fe_2O_3), monalbite ($NaAlSi_3O_8$), whitlockite ($Ca_{18.53}Fe_4Mg_{1.6}(PO_4)_{14}$), calcite ($Ca(CO_3)$), microcline ($KAlSi_3O_8$), cristobalite ($SiO_2$), akermanite ($(Ca_{1.53}Na_{.51})(Mg_{.39}Al_{.41}Fe_{.16})(Si_2O_7)$), albite ($Na(AlSi_3O_8)$), perovskite ($CaTiO_3$), brushite ($CaPO_3(OH)_2H_2O$), and monetite ($CaHPO_4$).

The presence of the crystalline phase in both materials, which can be seen in **Fig. 3.9**, has a positive effect on the production of building materials.

The elemental composition obtained by SEM-EDS and the X-ray pattern of sewage sludge and SRF after incineration at 950 °C confirmed the presence of crystalline phases in the obtained materials, which ensures the possibility of using SRF as an alternative fuel in the clinker firing process.

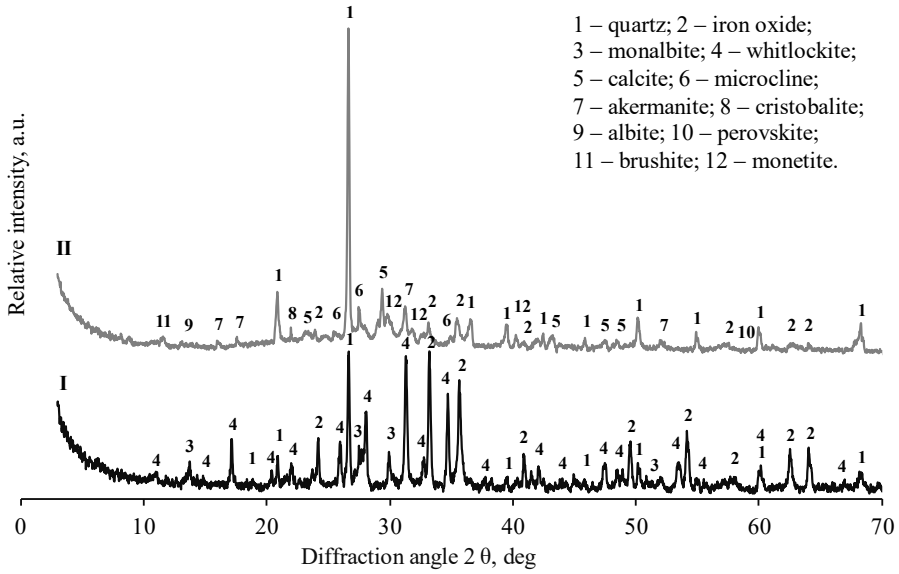

Fig. 3.8. The X-ray diffraction pattern of sewage sludge **(I)** and SRF ash **(II)**

Elemental analysis by SEM-EDS confirmed that the oxide composition of SRF and sewage sludge consists of clinker-forming oxides but with different percentages of oxides.

According to the cement plant, introducing up to 25% of non-hazardous waste as a replacement fuel in the clinker firing process does not impair the quality of the finished product and does not lead to the formation of other flue gas emissions into the atmosphere. According to Directive 2000/763, about 3.52 MJ is required to produce one kilogram of clinker. Some research in this area has shown the potential environmental and economic benefits associated with the production of SRF and its use as an alternative fuel in clinker firing. On the one hand, the production and use of SRF as an alternative fuel positively affect the environment by reducing non-renewable energy natural resources.

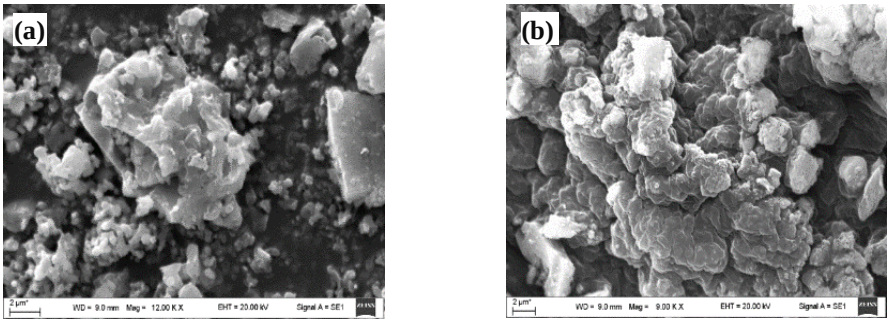

Fig. 3.9. SEM image of the ash of sewage sludge **(a)** and SRF **(b)**.

On the other hand, replacing traditional fossil fuels with SRF results in energy recovery and reduced air emissions. An assessment was made of the possible use of the produced SRF as a replacement additive to the main fuel during clinker firing. This calculation included an analysis of the share of CO_2 in greenhouse gas emissions and the determination of the energy required to burn clinker by replacing coal with SRF.

To assess the economic benefits of using SRF, four options were proposed for adding SRF as a replacement fuel. Options for this calculation were based on publications[41] and actual data. For the economic evaluation of adding SRF to the main fuel (coal), various options were selected in the proportions of 10, 15, 20 and 25%. The economic feasibility of using SRF as a replacement fuel for clinker firing was calculated. Thus, when using 10% of the produced SRF (which is 16,634 t/year) as replacement fuel instead of coal during the clinker firing process, it will save 37,948 t/year of coal and 5,198,978 USD/year from the cost of coal imports and 1,870,873 USD/year from greenhouse gas emissions, and the net savings will be 6,520,911 USD/year. According to the World Bank data using the SRF as a replacement fuel during the clinker firing process in the amount of 10% can help Lithuania to achieve the CO_2 emissions as in Estonia (10175.4 kt). However, using the SRF of 25% instead of coal can help Lithuania move closer to achieving the CO_2 emissions as in Latvia (7569.2 kt). Calculations show that replacing coal with SRF at 10% to 25% will reduce fossil resource consumption and greenhouse gas emissions and bring Lithuania closer to a circular economy.

3.2. Establishing the possibility of excavating waste from the landfill and producing SRF (Paper 2)

The paper studies assessed the feasibility of extracting and recovering energy-intensive raw materials from landfills by developing a waste extraction mechanism and creating an SRF production line for using it as a replacement fuel in the cement industry[42].

The object of the study was the Kaunas regional non-hazardous waste landfill (**Fig. 3.10**). The landfill has been operating since 1973. The area occupied is 37.4 hectares. The landfill disposes of mixed household waste from Kaunas and other Lithuanian municipalities.

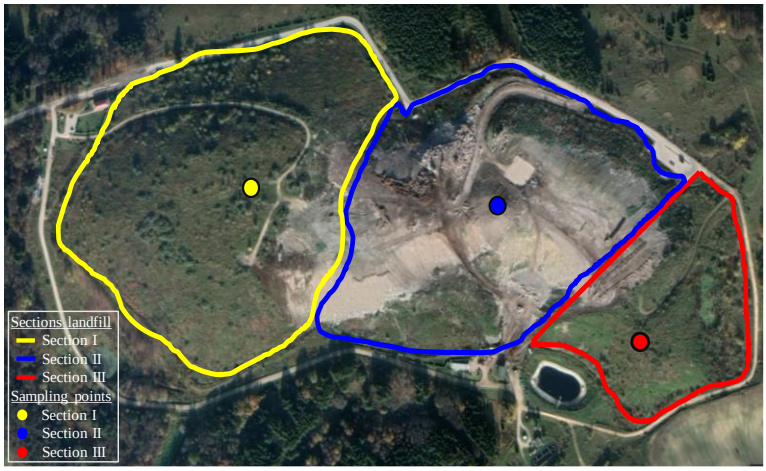

Fig. 3.10. Kaunas regional Lapės landfill sections and sampling points.

According to the data obtained during the research (the result of drilling), the granulometric characteristic of the landfill mined residues (LMRs) was obtained (**Fig. 3.11**).

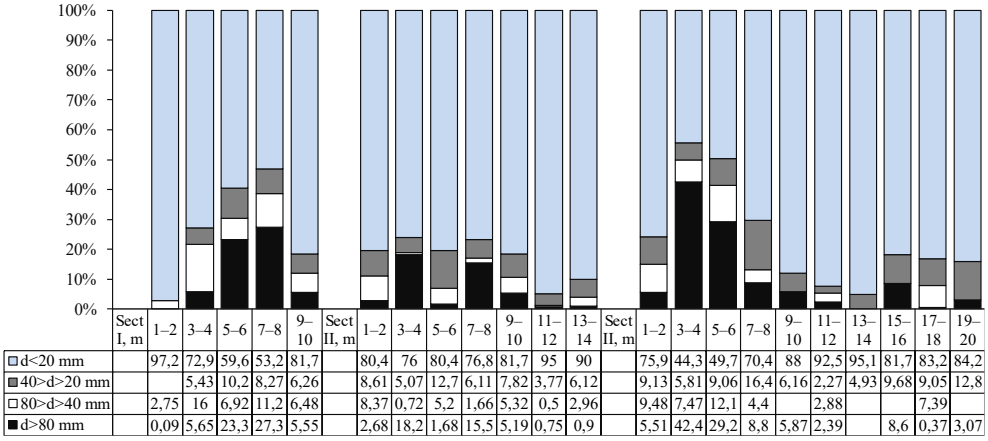

Sect I, m	1–2	3–4	5–6	7–8	9–10	Sect II, m	1–2	3–4	5–6	7–8	9–10	11–12	13–14	Sect II, m	1–2	3–4	5–6	7–8	9–10	11–12	13–14	15–16	17–18	19–20
d<20 mm	97,2	72,9	59,6	53,2	81,7		80,4	76	80,4	76,8	81,7	95	90		75,9	44,3	49,7	70,4	88	92,5	95,1	81,7	83,2	84,2
40>d>20 mm		5,43	10,2	8,27	6,26		8,61	5,07	12,7	6,11	7,82	3,77	6,12		9,13	5,81	9,06	16,4	6,16	2,27	4,93	9,68	9,05	12,8
80>d>40 mm	2,75	16	6,92	11,2	6,48		8,37	0,72	5,2	1,66	5,32	0,5	2,96		9,48	7,47	12,1	4,4		2,88			7,39	
d>80 mm	0,09	5,65	23,3	27,3	5,55		2,68	18,2	1,68	15,5	5,19	0,75	0,9		5,51	42,4	29,2	8,8	5,87	2,39		8,6	0,37	3,07

Fig. 3.11. Granulometric analysis of samples in the sections of Kaunas regional Lapės landfill.

It was established that in all sections of the landfill (I–III), a fine fraction (d<20 mm) predominates, regardless of the depth of the waste. In the upper layers of the landfill, it reaches 97% and increases with the depth of the waste, especially after 10 m. It has also been found that a more significant waste fraction is present (d>20 mm), which is a potential burnable fraction that can be considered as a potential alternative fuel. In landfill areas, the coarse fraction percentage reaches up to 60%.

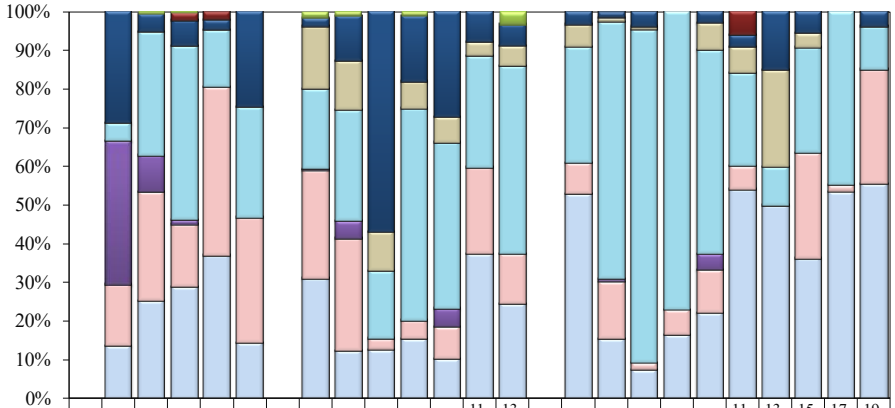

	I	1-2	3-4	5-6	7-8	9-10	II	1-2	3-4	5-6	7-8	9-10	11-12	13-14	III	1-2	3-4	5-6	7-8	9-10	11-12	13-14	15-16	17-18	19-20
Multilayer composites			0,6	0,3				1,6	1,1		1,1			3,3											
Other				1,8	2,0																6,0				
Wood		28,6	4,5	6,6	2,6	24,6		2,1	11,4	56,8	16,8	26,9	7,7	5,3		3,3	1,3	3,7		2,8	3,0	15,0	5,5	0,0	3,7
Paper								16,1	12,8	10,2	7,0	6,7	3,5	5,3		5,7	1,1	0,9		6,9	6,6	25,0	3,6	0,0	0,0
Textile		4,7	32,0	44,9	14,9	28,4		20,9	28,7	17,4	54,7	43,0	28,9	48,6		30,1	66,6	86,0	76,9	52,8	24,1	10,0	27,3	44,6	11,1
Rubber		37,2	9,6	1,3				0,3	4,5			4,7					0,7			4,2					
Hard plastic		15,8	28,0	16,1	43,5	32,6		28,0	29,0	2,9	4,9	8,3	22,5	13,1		8,1	14,8	1,9	6,6	11,1	6,0		27,3	1,8	29,6
Soft plastic		13,7	25,4	28,9	37,1	14,4		31,1	12,5	12,7	15,4	10,4	37,3	24,5		52,8	15,5	7,5	16,5	22,2	54,2	50,0	36,4	53,6	55,6

Fig. 3.12. Composition of the burnable fraction in the sections of Kaunas regional Lapės landfill.

Fig. 3.12 shows the amount of the total burnable fraction. The research results correlate with the data[29, 30] obtained in the study of landfills in European countries. The primary materials that make up the burnable fraction are soft and hard plastics, rubber, textiles, paper, wood, multilayer composites and other burnable materials. The burnable fraction was mainly represented by textiles and contained the least multilayer composites. The content of textiles varied by section and was in the range of 4.7 to 76%. It should be noted that in Section III, no multilayer packing was found at any of the considered depth intervals. The results made it possible to view the burnable fraction of the landfill as a potential "energy object". The composition of LMRs directly depends on the socio-economic situation in a particular region. LMRs from Lape's landfill had characteristics typical for most countries with a high moisture content and the presence of a fine fraction, changing with increasing depth.

MC, AC values and the content of combustible components (carbon and hydrogen) are MSW's main fuel characteristics. The limits of fluctuations of the considered parameters are significant and differ depending on the depth of the waste at the landfill and its composition. The MC of the waste excavated during drilling varied from 18 to 84%, the volatile matter (VM) value from 34.2 to 86%, and the AC, in turn, from 3.8 to 45.5% (**Fig. 3.13**).

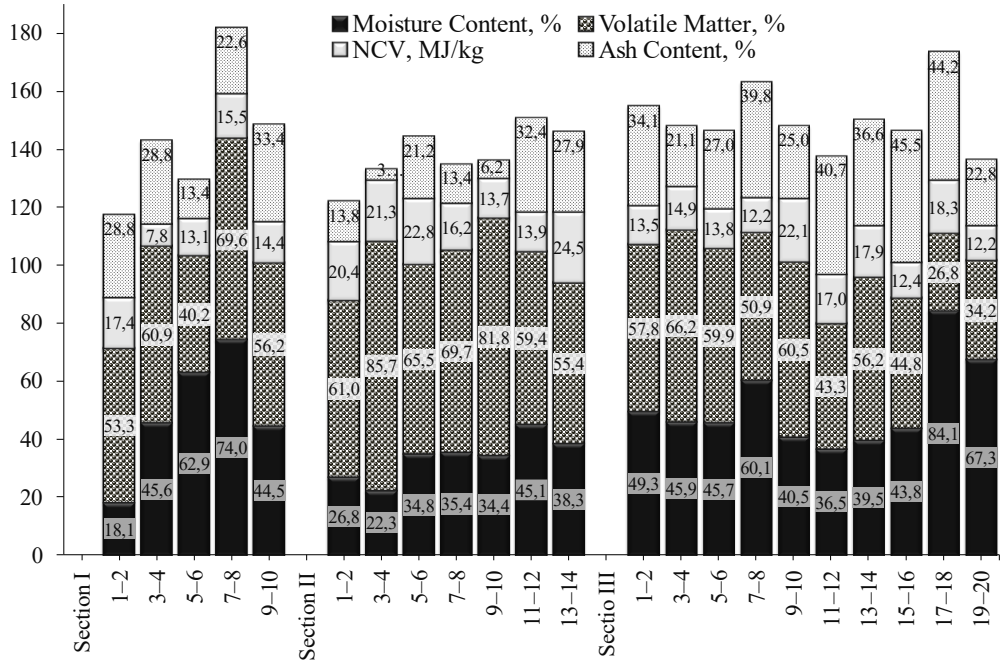

Fig. 3.13. Characteristics of burnable fractions in the sections of Kaunas regional Lapės landfill.

Compared to solid fuel such as coal, which has a VM value of up to 44%, pre-treated fuel from waste has a higher VM value, almost twice as high and is up to 87%. The value of volatile substances strongly depends on the nature of the material, combustion conditions, temperature and heating rate. It increases with an increase in the amount of hydrogen and decreases with an increase in the moisture content of the fuel. The biomass content in the studied samples was established, especially in Section II. These results confirm that Section II is in operation, and in the relatively recent past (before the commissioning of the MBT plant), waste was taken to the landfill without carrying out technological operations (extraction of biological fraction from MSW). In general, the burnable fraction extracted from the landfill has all the necessary properties that allow it to be considered as a fuel: chemical activity ensures the possibility of combustion in atmospheric oxygen; continuous reproduction enables us to consider their reserves sufficient for industrial use; the energy value is comparable to the energy value of low-calorie fuel used in the power industry[31–33,43]. The HCV of the burnable fraction of waste in the studied areas of the landfill does not depend on depth but directly depends on municipal waste, which was once taken to the landfill for deposition.

Chlorine is an element that must be strictly controlled, as high concentrations cause high-temperature corrosion and low efficiency in waste-to-energy incinerators. It is necessary to control the amount of chlorine-containing waste in the composition to prevent operational problems with equipment. The chlorine content in the samples under consideration did not depend on the depth of the waste but strictly relied on the chlorine-containing materials once taken to a landfill for disposal. The maximum

chlorine content was established in Section I at a depth of 7–8 m and amounted to 4.3%. The mercury content in the studied samples had the same trend as chlorine and depended on mercury-containing wastes taken to the landfill. The mercury content was within the allowable parameters for fuel from waste; the maximum value of mercury content was established in Section III in the upper layer and amounted to 0.304 mg/kg^{-1}.

X-ray powder diffraction analysis of the ash obtained after incineration of the LMRs after two stages of separation confirmed the presence of clinker-forming minerals in all sections and depths considered (**Fig. 3.14**).

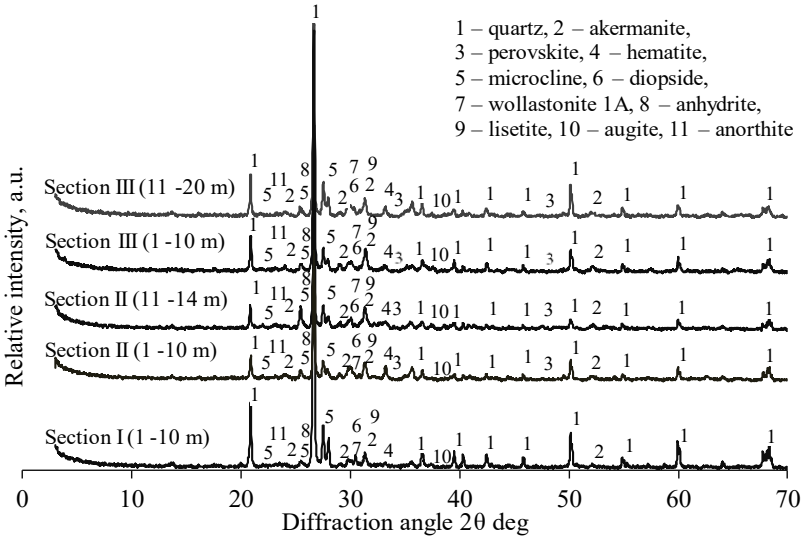

Fig. 3.14. XRD analysis for ashes of burnable fractions from Kaunas regional Lapės landfill

During XRD analysis were found quartz (SiO_2), akermanite ($Ca_2Mg(SiO_2O_7)$), perovskite ($CaTiO_3$), hematite (Fe_2O_3), microcline ($KAlSi_3O_8$), diopside ($CaMg(Si_2O_6)$), wollastonite 1A ($CaSiO_3$), anhydrite ($CaSO_4$), lisetite ($CaNa_2Al_4Si_4O_{16}$), augite ($Ca_xMg_yFe_z)(Mg_{y1}Fe_{z1})\cdot SiO_6$), anorthite ($Ca(Al_2Si_2O_8)$.

Results of XRD analysis by Rietveld refinement are presented in **Fig. 3.15** and contain the following information. It has been established that quartz is the main mineral in the samples. The content of quartz varied depending on the section and depth of the landfill and ranged from 36.32 to 72.23%.

Wollastonite is a mineral composed of calcium, silicon and oxygen. In the studied samples, the amount of wollastonite was in the range of 0.54 to 5.85% and did not depend on the depth but on the composition of the waste. Akkermanite – just like wollastonite, is called a technogenic mineral. As with previous minerals, the content of akermanite did not depend on depth but strictly relied on the composition of the waste and was in the range of 5.35 to 11.28%. The presence of hematite, a relatively strong mineral, in the samples did not tend to increase or decrease depending on the depth but relied only on the composition (0.6–13.39%).

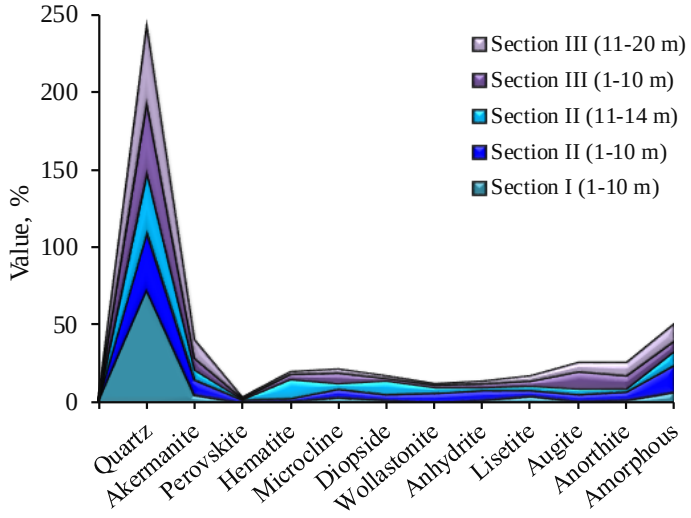

Fig. 3.15. Results of XRD analysis by Rietveld refinement for burnable fractions from Kaunas regional Lapės landfill

The microcline content in the samples ranged from 2.74 to 6.60%. The diopside content in the analysed samples varied from 1.53 to 9.44%, depending on the section of the landfill. The presence of perovskite, anhydrite, lisetite, augite and anorthite in the ash is typical for this type of ash and is not dependent on the depth of the waste at the landfill but relies only on the composition of the source material.

The quantitative composition of these minerals is from 0.54 to 1.87%; from 1.43 to 6.68%; from 3.19 to 4.85%; from 1.20 to 10.84%, and from 1.73 to 8.84%, respectively. The presence of the amorphous phase ranged from 6.75 to 17.26% for the considered sections of the landfill.

The elemental-oxide composition of the ash obtained based on SEM-EDS analysis made it possible to determine the chemical elements and calculate the composition of the oxides. It has been established that the ash consists of an inorganic part, and the oxide composition of the ash corresponds to the oxide composition of the clinker but in different amounts[44].

It has been established that oxides of Ca, Fe, Si, Al and Mg predominate in the oxide composition of the ash; their quantity was more than one $\%_{wt}$. The content of oxides Na-, S-, K-, Ti- and Mg in the ash was less than one $\%_{wt}$. Thus, according to[45], the ash does not contain forbidden oxides. This confirmation has allowed us to consider landfill waste as a subject for the production of alternative fuels and, ultimately, will comply with the EU standard.

Based on the data obtained during the research, a conceptual line for the production of SRF was developed, shown in **Figure 3.16**. The productivity of the SRF production line was calculated, which amounted to 4.9 t/h.

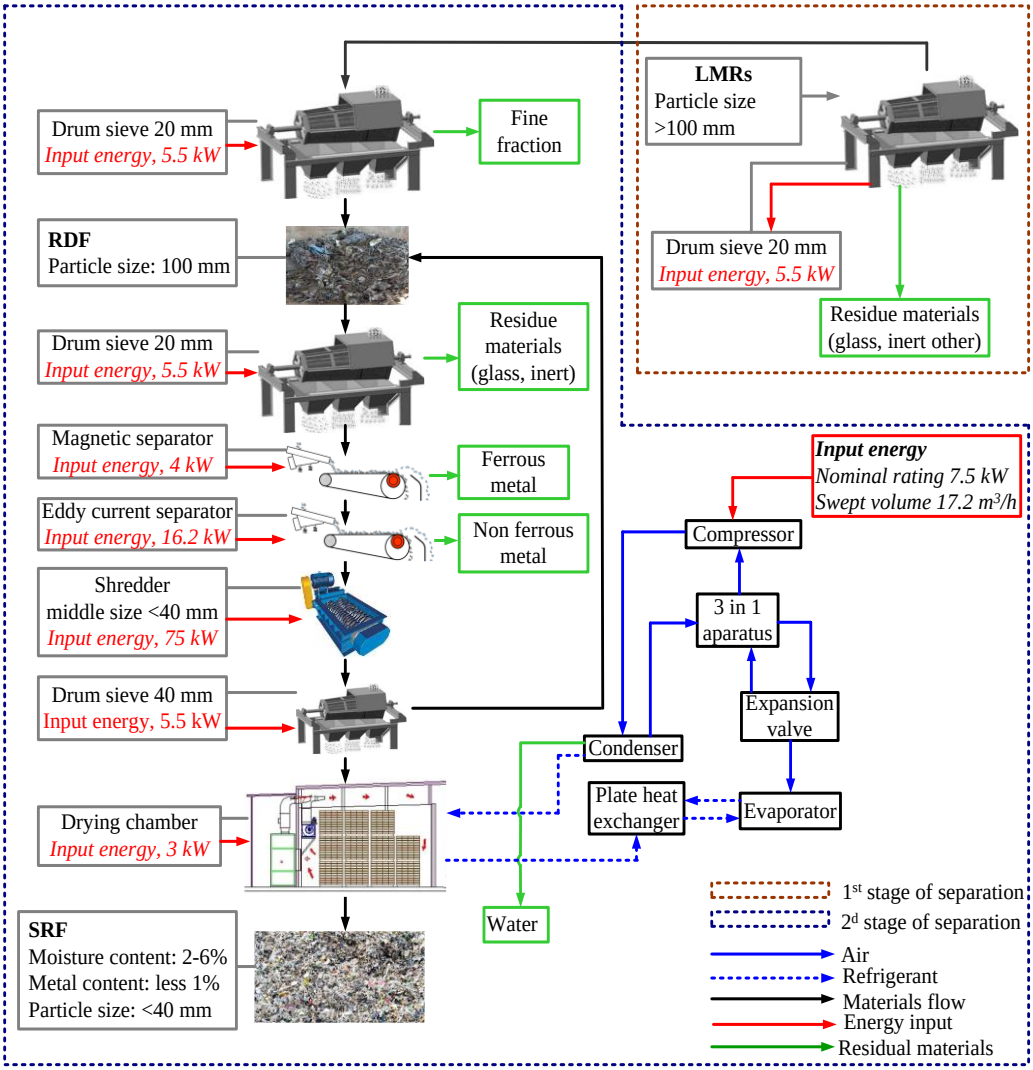

Fig. 3.16. SRF production line from LMRs.

The developed mechanism for LMRs extraction and SRF production consisted of two stages. In the first stage, inert, huge materials and fine fractions are extracted using a drum sieve (on the territory of the landfill). The amount of fine fraction extracted from the LMRs was 43%. At the second, final stage, the re-extraction of the fine fraction and the production of SRF are proposed to be carried out on the territory of the Kaunas MBT. At the second stage of SRF production, another 50% of the fine fraction is removed by secondary sieving. At the end of the second stage, the fine content is 1.3%. The second stage includes six additional pieces of equipment, each of which plays an important role.

After removing the fine fraction and the huge inert material, the remaining fraction is directed to the extraction of ferrous and non-ferrous metals. It is proposed to extract ferrous metals with a magnetic separator and non-ferrous metals with an

eddy current separator. After the extraction of metals, the material is subjected to shredding (up to 40 mm) until a homogeneous material is obtained.

After shredding, the material is sent to a repeated drum sieve to homogenise and remove large particles. Material more than 40 mm is sent for shredding to the desired size. At the end of the grinding stage, the moisture content of the material decreased by 86.7% and amounted to 2.5%.

Installing a drying chamber at the end of the production line is recommended. The tumble dryer is the optimal unit, as it has low capital costs, is easy to operate and allows you to produce large volumes of products.

At the end of the production line, an alternative fuel was obtained with the characteristics shown in **Figure 3.17.** The fines fraction, MC, AC, VM and NCV, was 1.3%$_{wt}$, 2.5%$_{wt}$, 44.3%$_{wt}$, 8%$_{wt}$ and 16 MJ/kg, respectively. The data obtained indicate that the extraction of the fine fraction by double sieving significantly improves the characteristics of the finished SRF.

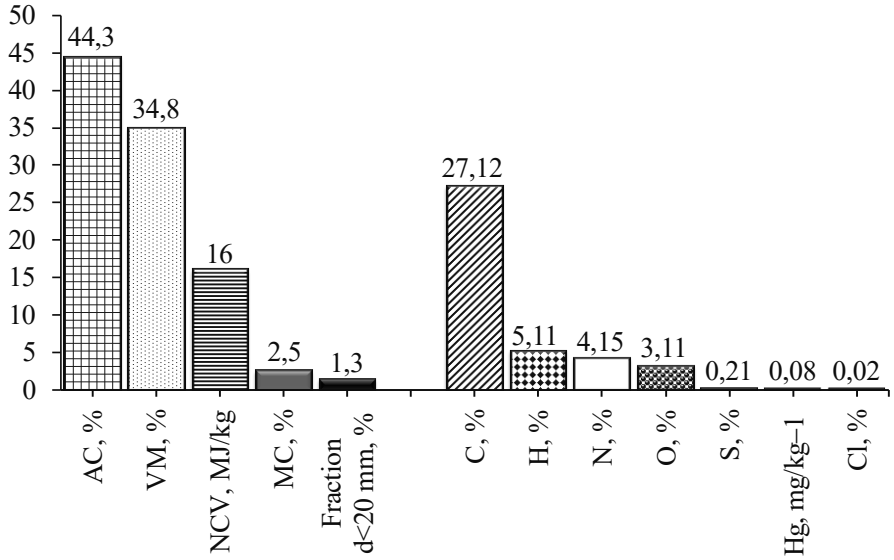

Fig. 3.17. Characteristics of SRF produced from LMRs

Fuel is a hydrocarbon, which includes carbon, hydrogen and some amount of sulphur, nitrogen, oxygen and minerals in the range, with the content of C from 20 to 70 %$_{wt}$, H from 3 to 8%$_{wt}$ and N from 1 up to 5 %$_{wt}$. As can be seen in **Figure 3.17**, the SRF produced is a good combination of C, H and N ratios for combustion. As for sulphur, the sulphur content in the analysed materials was in the usual for any fuel in the range from 0.2 to 1%$_{wt}$. As for the halogen elements, the concentration of chlorine was measured, which was 0.02%$_{wt}$, the mercury content was within acceptable limits for fuel from waste and met the acceptable standards for use in cement kilns.

In the course of research, it was found that the ash obtained after burning SRF has a crystalline structure and contains crystalline Ca-, Na-, K-, Fe- and Si-containing phases. The crystalline phase in the materials is favourable for the production of clinker (**Fig. 3.18**).

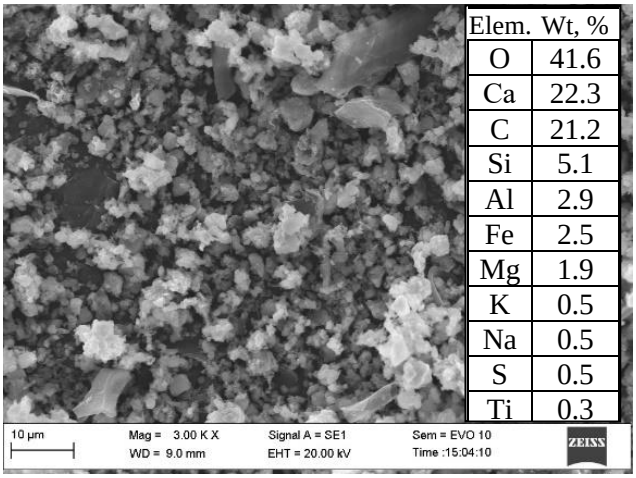

Fig. 3.18. SEM image and EDS analysis of SRF incineration ash.

The structure of materials and granulometric characteristics are related to the features of their crystal structure. Morphology provides information about the conditions for forming minerals and is used in their determination. In our case, the ash particles had different colours, changing with depth from light grey to dark grey, and had a lamellar-crystalline form. The particle size of the ash was in the range of 1 to 20 µm and was not uniformly distributed.

Quantitative-elemental analysis of RDF (obtained by extracting a fraction d<20 mm and large-sized inert materials from LMRs) and SRF obtained by re-extraction of a fine fraction, inert and forbidden materials showed that RDF and SRF consist of 14 elements: aluminium, calcium, cadmium, chromium, copper, iron, potassium, magnesium, manganese, sodium, phosphorous, silicon, titanium, zinc, but it should be noted that their number was different (**Table 3.2**). It has been established that the predominant elements are silicon, calcium, iron, potassium, sodium and magnesium. The presence of certain chemical elements is determined by the composition of the waste taken to the landfill.

Table 3.2. Quantity element analysis of SRF and RDF

	Value, g/kg													
	Al	**Ca**	**Cd**	**Cr**	**Cu**	**Fe**	**K**	**Mg**	**Mn**	**Na**	**P**	**Si**	**Ti**	**Zn**
RDF	7.67	162.03	0.0005	0.352	0.435	22.32	12.87	3.94	0.24	5.98	1.87	406.86	1.77	0.52
SRF	3.95	86.56	0.0005	0.122	0.183	17.43	9.45	3.52	0.21	5.47	1.07	208.65	1.09	0.39

It is established that silicon is the predominant element in the RDF and SRF. The amount of silicon in RDF was 406.86 g/kg, and in SRF, 208.65 g/kg. As a result of the double sieving of LMRs at the drum sieve, the amount of silicon in the SRF decreased to 48.7%. The quantitative content of calcium in RDF was 162.03 g/kg, and in SRF, it was 86.56 g/kg. The iron content in SRF decreased by almost 22% compared with the RDF content and consisted of 17.43 g/kg. The amount of potassium in SRF was 9.45 g/kg, and sodium was 5.47 g/kg. Sufficiently high concentrations of magnesium in SRF indicate the presence of inert materials and garden waste. The

magnesium content in SRF decreased by 10.7% and amounted to 3.52 g/kg. As for the remaining elements in the obtained SRF, their amount was reduced because of the double sieving. The amount of aluminium decreased by 48.5%, chromium by 65.3%, copper by 57.9%, manganese by 10.9%, phosphorus by 42.5%, titanium by 38.1%, and zinc by 25.4%. The amount of cadmium in SRF before and after separation remained unchanged.

After a detailed study of the composition of waste from the Kaunas landfill, the energy potential of the investigated landfill sections was calculated. During the conducted studies, it is recommended to extract waste from a landfill with a depth of up to 10 m inclusive. Extraction of waste from great depths is not reasonable and does not have positive prospects. Calculations of the energy potential of the considered landfill parts amounted to 196,700 GJ.

3.3. Proof of feasibility using bottom ash as a replacement component in producing clay bricks (Paper 3)

The possibility of reusing the bottom ash from SRF incineration to produce clay bricks was studied[46]. To generate energy, many countries use waste incineration. For incineration in a CPP, sending waste that cannot be recycled or reused is recommended. In this case, the incineration process is integral to the waste management strategy. By burning waste, we obtain energy, save non-renewable natural resources and reduce waste sent to landfills. However, any technological process has advantages and disadvantages. One of these disadvantages is the significant amount of bottom ash generated during the waste incineration process.

Waste incineration at a thermal power plant occurs in a boiler at a temperature of 920–990°C[47]. This type of heat treatment of materials has advantages for domestic and industrial waste.

An excellent solution to the problem associated with the accumulation of BA is to use it as a replacement component in the production of ceramic products. It is reported in scientific works[34–36,48] that the ash residue obtained after waste incineration can produce silicate bricks, ceramic tiles and glass.

The characteristics of BA were studied, and composite mixtures of clay with different percentages of BA (10–40%) were prepared to investigate the possibility of reusing BA in the production of bricks. The physical and mechanical properties of clay bricks have been studied; a quantitative phase analysis of clay bricks fired at 900 and 1000°C was performed, and the characteristics of the porous structure of the materials, in particular the average pore size and pore size distribution, were determined. The composition and structure of samples of clay, ash and clay bodies fired at temperatures of 900 and 1000°C were determined by Fourier-transform infrared (FTIR) spectroscopy to study the interaction of clay minerals with inorganic or organic compounds.

The bottom ash was obtained by burning the CPP's burnable waste fraction. Clay for making samples was obtained from the Andreevsky deposit in Ukraine. SEM-EDS analysis data established that clay consists of SiO_2 content are 66.65%, Al_2O_3+TiO_2 content is 27.64%, CaO content is 0.2%, and Fe_2O_3 content is 1.51% (**Fig. 3.19**).

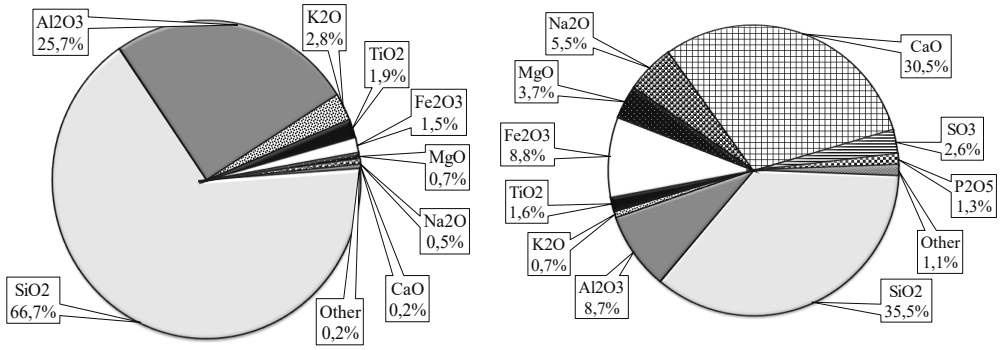

Fig. 3.19. Chemical composition of the clay **(a)** and BA **(b)**.

The results of the oxide composition of bottom ash showed that SiO_2 content in the BA is 35.53%, Al_2O_3+TiO_2 content is 10.3%, and Fe_2O_3 content is 8.83%.

The analysis microstructure of clay and BA is presented in **Fig. 3.20**. Clay particles had a size of 1.5–10 μm and were distributed almost evenly. Clay particles are predominantly lamellar, but there are also elongated plates, stripes and tubular and fibrous particles. The BA particles were dark grey and had a lamellar and crystal shape. The bottom ash particle size was from 1 μm to 10 μm.

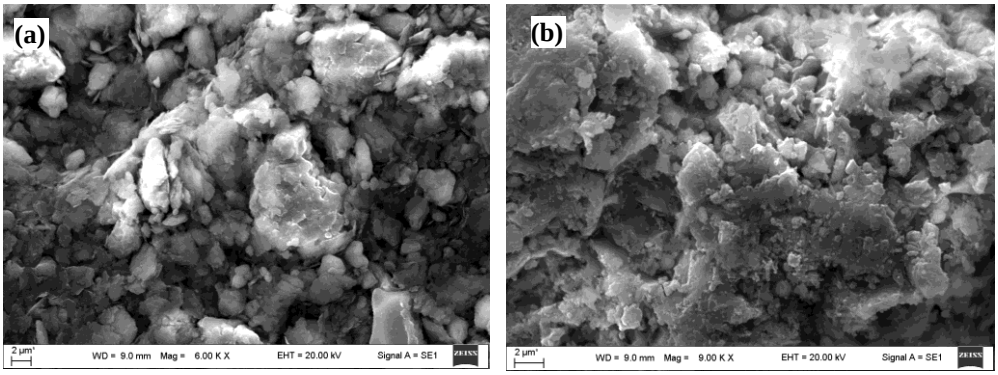

Fig. 3.20. Microstructure of clay **(a)** and bottom ash**(b)**.

Municipal solid waste incineration converts organic materials into CO_2 and H_2O and obtains inorganic residues from ferrous and non-ferrous metals, silicates, and other components. Fourier-transform infrared spectroscopy results and XRD analysis of BA and clay (**Fig. 3.21**) indicate the presence of inorganic elements in the studied materials.

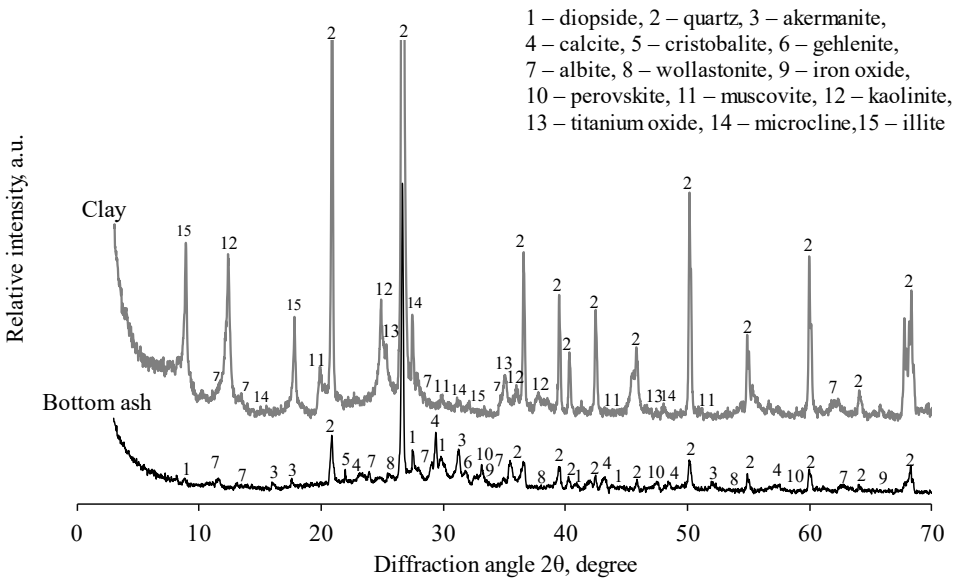

Fig. 3.21. XRD analysis of bottom ash and clay

The prevailing minerals in the clay and BA detected by XRD analysis are quartz, muscovite, titanium oxide, kaolinite, illite, microcline, and others and correspond to the data[49]. **Fig. 3.22** presents the results of a quantitative elemental analysis of the ash residue and clay.

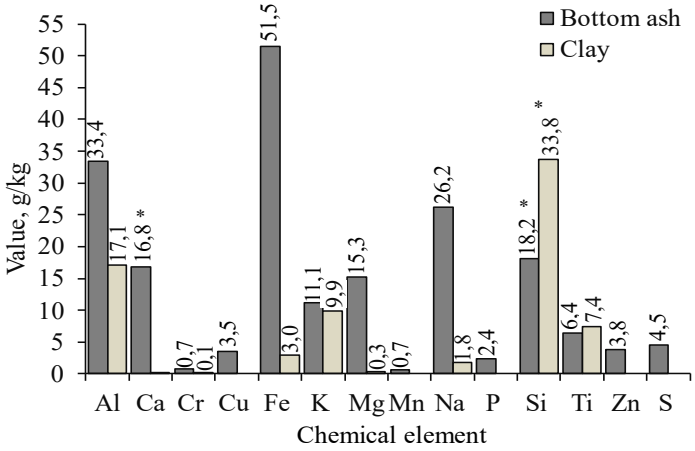

Fig. 3.22. Quantitative element analysis of bottom ash and clay (*the value is multiplied by 10).

Based on the available results, it can be said that the chemical elements contained in clay and BA do not pose a severe threat to the environment since they do not contain heavy metals. Thus, bottom ash is classified as non-hazardous waste and can be used as an additive in brick production.

Fig. 3.23 presents differential thermal analysis (DTA) and thermo-gravimetric

analysis (TGA) curves for clay and bottom ash. The clay DTA curve has three distinct peaks endothermic peaks. The first peak is at 95°C, the second at 505°C and the third at 569°C. The TGA curve with the first peak shows a 1.45% weight loss at 120°C and a 1.38% weight loss from 120 to 405°C. The second and third TGA peak curves show a weight loss of 3.12% in the temperature range of 410 and 592°C. The total mass loss in the studied temperature range was 7.84%. The endothermic peak and weight loss in the temperature range of 100–200°C are due to the heating of the products and the removal of interlayer and partially adsorbed water. In the temperature range of 200–300°C, the removal of bound water and the burning of a part of organic substances are completed. Distinct endothermic peaks and weight loss in the temperature range of 505 and 569°C are due to the dehydration of clay minerals and the release of chemically bound water entering their crystal lattice[50].

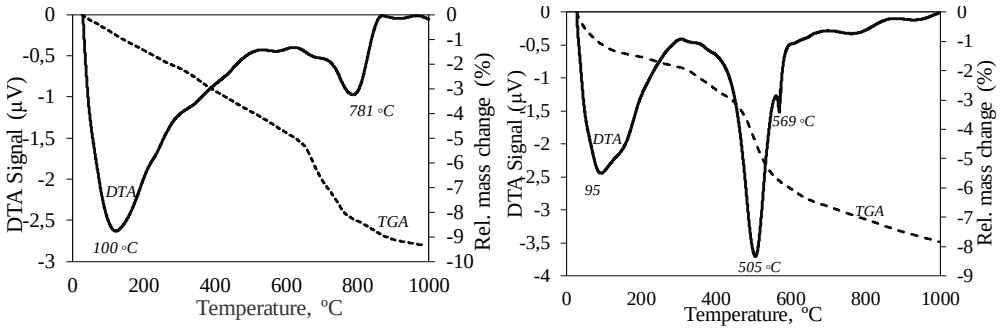

Fig. 3.23. DTA and TGA curves of bottom ash **(a)** and clay **(b)**.

The situation is similar for the DTA and TGA curves of the bottom ash. The DTA curve for the ash residue has two pronounced endothermic peaks at 100°C and 781°C. The TGA curve of the first peak shows a 1.55% weight loss at 100°C and a 3.33% weight loss between 110–620°C. The TGA second peak curve shows a weight loss of 3.47% between 669–750°C and a 15% loss between 620–760°C. The total weight loss was 9.39%. The endothermic peak and weight loss in the temperature range of 100–200°C are due to the removal of residual moisture. In the 300–500°C, organic inclusions burned out, and "crystallisation" water was removed. The well-defined endothermic peak and weight loss at 790°C are due to the decomposition of carbonates, accompanied by the release of CO_2[51].

Almost all clay samples fired at 900 and 1000°C did not have swelling and cracking defects. A typical colour change was observed in the fired specimens. Colour saturation intensified with increasing BA addition. It should be noted that in some samples (with the addition of 40% BA) fired at a temperature of 1000°C, small dark grey cores were observed in the form of dots. This can be explained by the fact that during firing (800–1000°C), calcium and magnesium carbonates actively interact with decomposition products of clay minerals, amorphous silica (SiO_2) and alumina (Al_2O_3). The release of CO_2 accompanies the course of such reactions.

The decrease in the volume of the material occurs due to the forces of surface tension of the formed melt, called fire shrinkage. Shrinkage during drying of the

samples without adding BA was 5.15%; shrinkage during firing at 900°C was 6.2%, and at 1000°C was 7.1%. From the data obtained, it can be concluded that the shrinkage of products during firing depends on the amount of added BA.

There is little difference between the morphology and appearance of clay brick surfaces without and with 10% ash added. The microstructure of the samples is dense, with a small number of pores evenly distributed throughout the sample. The microstructure of the fired samples with a BA of 20% differs from those previously described: the surface is less uniform, with a predominance of pores of different sizes. Pore formation occurs due to the intensive removal of carbon dioxide as a result decomposition of $CaCO_3$ during the firing. The amount of carbon in the samples increases (with the addition of BA) is confirmed by the SEM-EDS analysis data.

The microstructure of samples with 30% BA is different in comparison with samples without BA, with 10 and 20% BA: larger pores of various shapes appear, which are the result of intensive removal of crystalline water and removal of gas components during the interaction of $CaCO_3$, $MgCO_3$ and the decomposition of colourful oxides (Fe_2O_3).

The formation of a durable product occurs due to the adhesion of solid particles of clay and BA by the resulting melt during thermal firing. In this case, the decrease in the volume of the material occurs due to the surface tension forces of this melt, called fire shrinkage. The maximum shrinkage of the samples during drying without adding a BA was 5.15%; the maximum shrinkage during firing at 900°C was 6.25%, and at 1000°C, the shrinkage was 7.14%. The data obtained show that the shrinkage of products during firing depends on the amount of BA added.

Clay samples with the addition of 30% BA and fired at 1000°C had a compressive strength of 14.5 MPa and, as a result, can be used to construct buildings and structures (**Fig. 3.24**). At the same time, samples with the same percentage of BA fired at a temperature of 900°C had a compressive strength of 10.6 MPa. Burnout of adhesive additives, dehydration of clay minerals and chemical transformations inside the sintered ceramic mass lead to a decrease in the compressive strength of the samples.

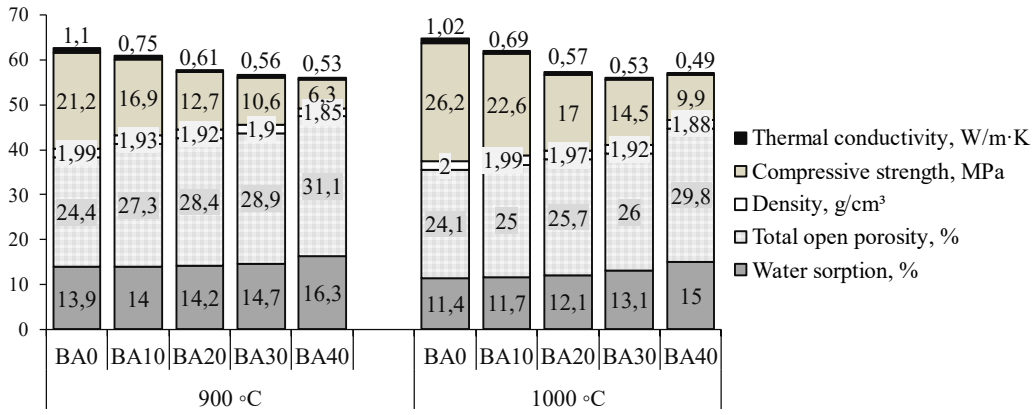

Fig. 3.24. Properties of clay bricks samples.

The compressive strength of clay bricks prepared under laboratory conditions

for testing should be at least 20 MPa[52, 53]. The EU does not define minimum compressive strength values for clay bricks. Therefore, each manufacturer must declare the compressive strength of finished products, and according to these data, designers must consider these values when designing buildings and structures.

Open porosity and water sorption depend on the number, size and distribution of pores in the product and are important. There was a difference in water sorption and open porosity for clay bricks at firing temperatures of 900 and 1000°C.

The lowest water sorption and open porosity values were observed for samples without adding BA and fired at 1000°C. With the addition of BA and its increase, water sorption and open porosity of clay brick samples were increased. Clay samples fired at 900°C had water sorption and open porosity values higher than samples fired at 1000°C.

Requirements for water sorption of clay brick samples are not established by the standard LST EN 771-1:2011+A1:2015. Based on this, manufacturers must specify the water absorption values for their products according to the LST EN 772-21:2011 standard. Permissible water sorption of clay bricks should be from 12 to 20%. Water sorption below 12% can lead to poor adhesion between mortar and clay brick. In our case, such samples include samples without adding BA and with its addition of 10% and fired at a temperature of 1000°C.

Frost resistance is a mandatory stage of the study. Formed, dried and fired clay brick samples were subjected to freeze-thaw testing and visual evaluation. The sample without the addition of BA and the samples with the addition of BA 10, 20 and 30% and fired at 900°C passed 25 cycles of freezing and thawing (the cycle consists of one freezing phase at -18°C and one thawing phase at +18°C). Samples with the addition of 40% BA and fired at 900°C passed only 23 cycles of freezing and thawing. All samples without and with the addition of BA fired at a temperature of 1000°C, passed 25 cycles of freezing and thawing. According to LST EN 771-1:2011+A1:2015, clay bricks can be used in passive and moderately aggressive environments.

Thermal conductivity analysis was carried out on samples of clay bricks without and with the addition of BA (10–40%) and fired at 900 and 1000°C. The relationship between thermal conductivity and porosity of clay bricks with BA addition can be seen in **Fig. 3.24**. An increase in the content of BA causes an increase in the porosity of the samples and, as a result, causes a low thermal conductivity of the samples. This occurs due to the increase in air volume during the interaction of clay minerals with BA, which leads to the formation of pores inside the samples, making them poor heat conductors and, as a result, good insulators. The results show that the thermal conductivity value is directly related to porosity. Based on the ASTM D 78896 standard, it can be argued that adding BA to clay during clay brick production does not impair the technical properties of finished products.

The infrared spectra of clay bricks without the addition of BA and with its addition (10–40%) and fired at 900 and 1000°C are shown in **Fig. 3.25**.

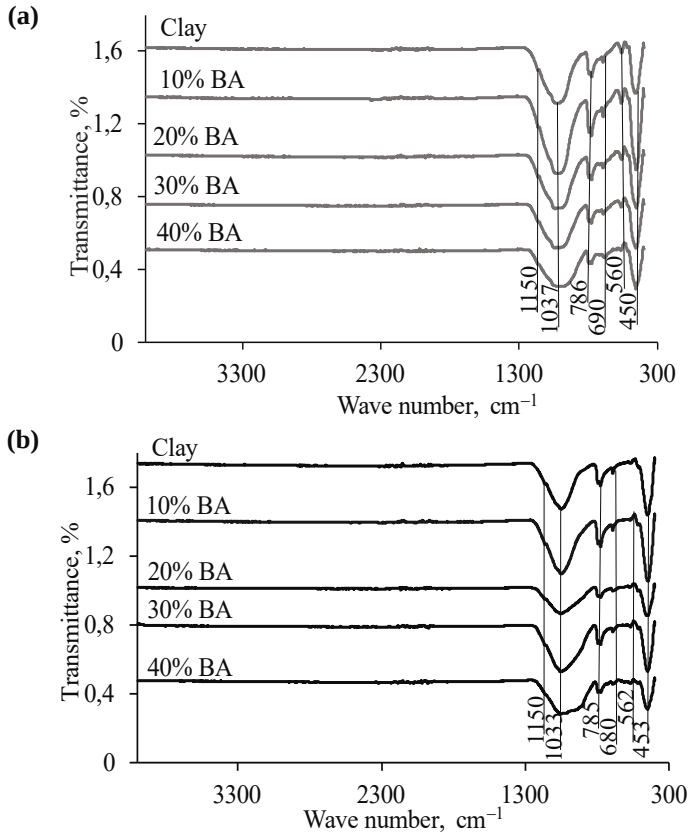

Fig. 3.25. FTIR analysis for clay bricks with the additive of BA fired at 900 °C **(a)** and 1000 °C **(b)**.

The characteristic of clay bricks fired at 900°C was next: the band at 1150 cm^{-1} corresponds to the SO_4 tetrahedron stretching vibration modes, and the bands at 1033 and 1037 cm^{-1} refer to Si-O bonds. In samples fired at 1000°C, a doublet at 792 and 778 cm^{-1} and 798 and 774 cm^{-1} for samples at a firing temperature of 900°C is attributed to quartz vibrations. Quartz peaks with different Si-O and Si-O-Al(Mg) vibrations are found near 690 and 680 cm^{-1}, bands near 560 and 562 cm^{-1} indicate typical elongation of Si-O-Mg, and bands near cm^{-1}, the Si-O-Al bond is observe[54].

Powder diffraction is a widely used analytical method for characterising solid materials. The XRD-Rietveld refinement method can be used for phase identification, quantisation, cell parameter determination, or complete crystal structure analysis. **Fig. 2.26** shows the results of the X-ray diffraction analysis of clay bricks with Rietveld refinement for samples fired at 900 and 1000°C without and with the addition of BA. All fired samples presented quartz, illite, muscovite 2M1, anorthoclase, microcline, cristobalite, wollastonite, akermanite, melilite, gelenite, rutile hematite, labradorite and diopside but in different amount depending on the part of additive and temperature firing.

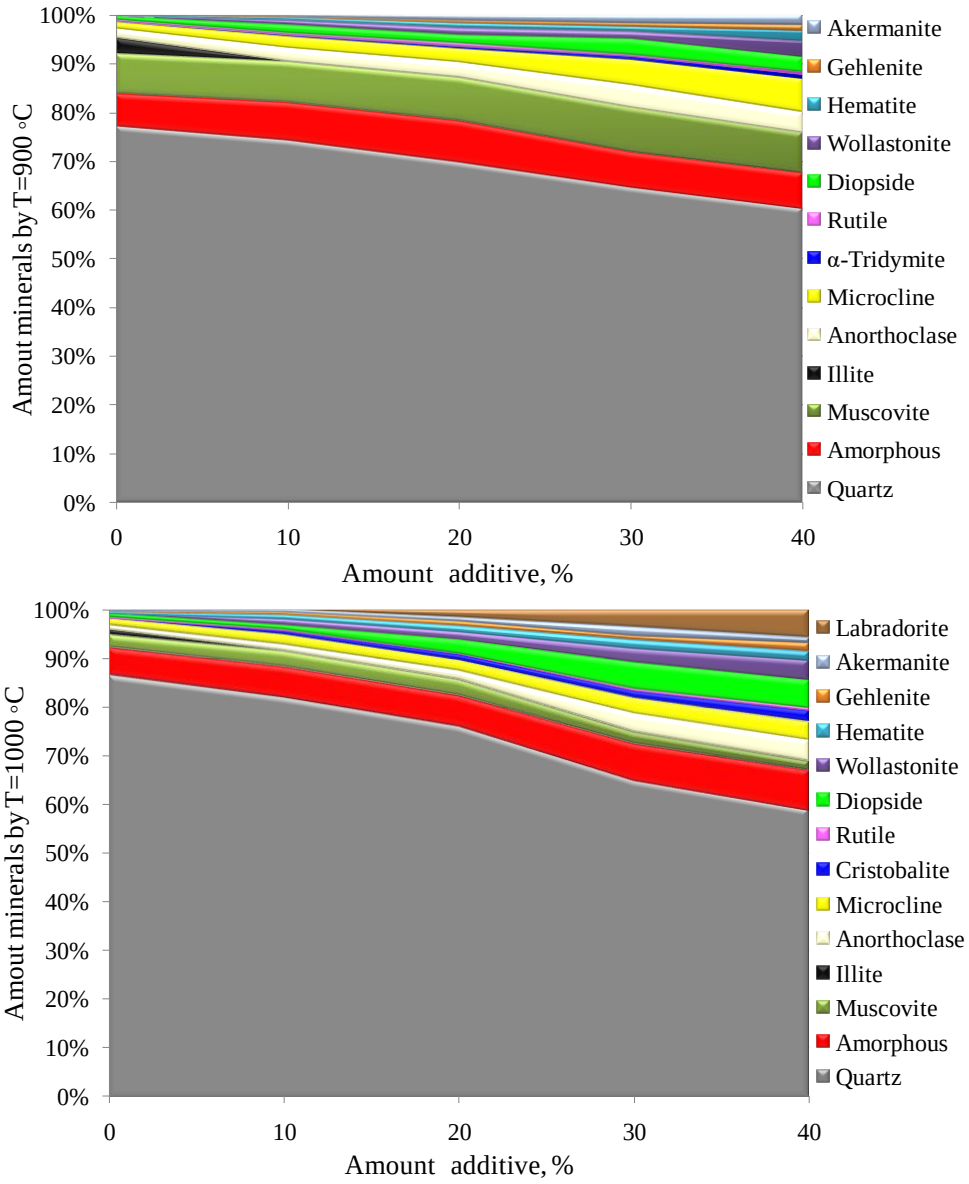

Fig. 3.26. Results of XRD Analysis by Rietveld refinement of clay bricks.

The structure of materials is formed at the stages of crystallisation and consists of isolated or interconnected pores with the same or different shapes and sizes. According to the international union of pure and applied chemistry (IUPAC) classification, the pore sizes of the samples of clay bricks fired at 900 and 1000°C belong to type II isotherms (non-porous or macroporous materials), and the hysteresis loop of the samples classifies the samples as H3 and is characterised by slit-like pores. The H3 hysteresis desorption curve contains a slope associated with the force on the hysteresis loop due to the effect of tensile strength[55]. Studies of the pore size

distribution show a different trend when BA is included in the clay from 10 to 40% and at firing temperatures of 900 and 1000°C. The BET-based method was performed using nitrogen as the adsorbate at 77.35 K. The relationship between pore diameter and surface area was determined by the DFT method (**Fig. 3.27**).

In **Fig. 3.27**, it can be seen that mesopores dominate in samples fired at 900°C, while micropores predominate in samples with and without the addition of BA and fired at 1000°C. Surface area and adsorption were obtained from the adsorption isotherm and calculated using the BET method.

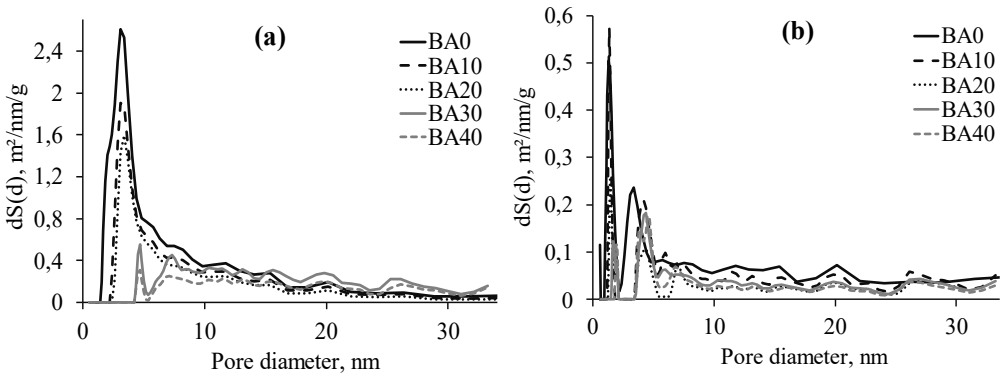

Fig. 3.27. Pore size distribution analysis for clay bricks by N_2 adsorption: **(a)** samples fired at 900 °C, **(b)** fired at 1000°C.

Using the DFT method, the total pore volume and the average pore diameter were estimated (**Fig. 3.28**).

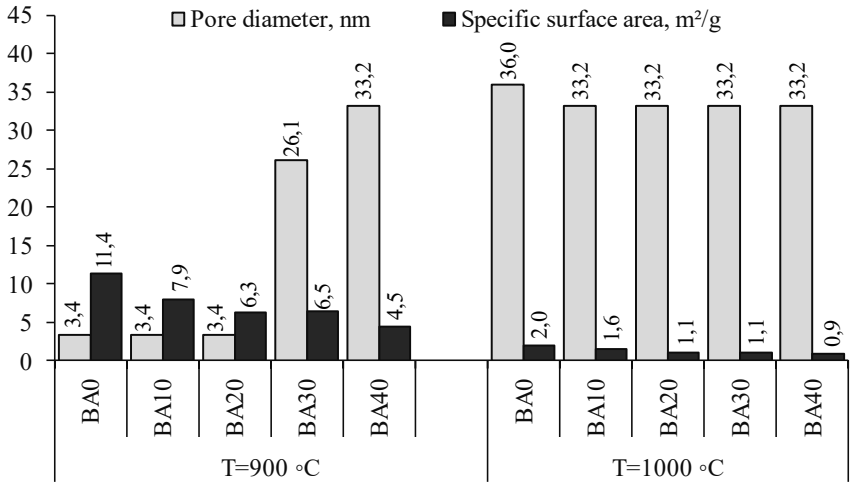

Fig. 3.28. N_2 adsorption measurements for clay bricks (DFT method).

It was established that the average pore diameter of specimens without adding BA 10 and 20% and fired at 900°C is constant (3.4 nm). However, with an increase of BA (30 and 40%) and at the same firing temperature, the average pore diameter of the samples increased and amounted to 26.1 and 33.2 nm, respectively. Samples fired

at 1000°C had a different dependence on the average pore diameter. The samples' pore diameter without adding BA was 36 nm. Adding BA to clay (10, 20, 30, and 40%) decreased pore diameter and amounted to 33.2 nm.

The formation of cylindrical pores and increased pore diameter resulted from adding BA (30 and 40%) and fired at 900°C. A denser structure of the fired samples characterises this. Slit-like pores were revealed in samples without adding BA and samples with its addition (10 and 20%) and fired at 1000°C. This porosity was increased in fired samples by adding 30 and 40% BA.

Cylindrical pores are isolated and characteristic of the BA material, and the slit porosity of the samples is related to the porosity of the clay. According to LST EN 772-22:2019, formed clay bricks containing 10 and 20% BA in their composition and fired at 900 and 1000°C belong to class F1 and can be used in moderately aggressive environments. However, samples containing 30% BA fired at 1000°C can be used in passive-aggressive environments. Such samples may be used for internal use. When used outdoors, at sub-zero temperatures, such specimens may be damaged by frost if an impervious cladding or plaster does not protect them.

It has been established that thermal conductivity values directly depend on the amount of the additive and, as a consequence, on the porosity of the samples. According to ASTM D 78896, it has been established that the addition of BA in the production of clay bricks does not impair the technical properties of the fired samples. According to the data obtained, it can be argued that it is possible to produce clay bricks with the addition of BA of up to 30%. The production of this type of building materials with the additive will reduce accumulated waste after the incineration of not a recyclable fraction of MSW at landfills.

3.4. Justification of the possibility of using ash after gasification of biomass-sludge waste as a partial substitute in materials based on cement (Paper 4)

The potential application of solid ash residue obtained after gasification of SS with wood, in binary compositions with silica fume, to utilise solid wastes was investigated[56].

In this study, materials such as Portland cement type CEM II/A-LL 42.5 N (Lithuania), micro silica with a particle size of 0.1–0.45 μm (RW-Füller, RW silicon GmbH) and sand with a particle size 0–2 mm (Sakret, Lithuania). As a replacement component, waste is obtained from gasification (from now on, "Residue") in the thermal treatment of granular woody biomass with sewage sludge in a down flow gasifier connected to a secondary thermoplasma reactor. The average particle size of the residue was 7.95 μm. After ball milling, the residue was examined by SEM. **Fig. 3.29** shows the morphology of the pulverised residue after gasification.

The surface of the particles is almost smooth, without visible pores, and the shape of the particles is inhomogeneous, from lamellar to rectangular. The SEM-EDS analysis of elemental composition confirmed that the main chemical elements are carbon (72.2%), oxygen, calcium, iron, silicon, phosphorus, zinc, magnesium, aluminium, and sulphur are present in smaller amounts; their amount does not exceed three wt.%.

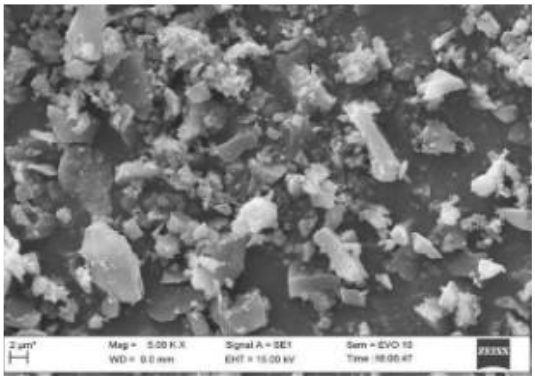

Fig. 3.29. SEM image of gasification residue after ball milling.

Although Zn is included in the list of environmentally harmful elements, based on the waste acceptance criteria[57], its small amount (<1 $\%_{wt}$) can be interpreted as inert.

Thermal analysis was conducted to investigate the influence of both substitutes in cement hydration. Thermogravimetric and differential thermogravimetric curves are shown in **Fig. 3.30**. Comparison of plain and blender cement pastes used after hydration for 28 days is shown in **Fig. 3.30-a**. In turn, the influence of the hydration time of the cement paste with micro-silica and gasification residues (pSFR) is shown in **Fig. 3.30-b**.

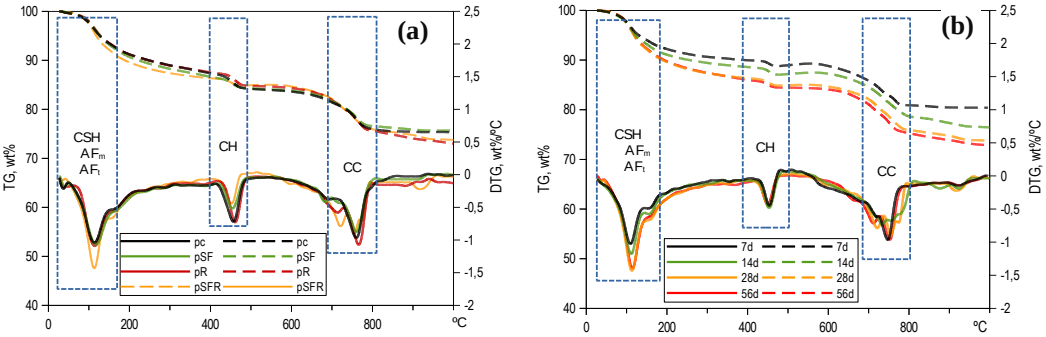

Fig. 3.30. TG and DTG curves for plain and blended cement pastes four weeks of hydration **(a)**, and pSFR cement paste hydrated at various hydration periods **(b).**

Fig. 3.30 shows that all curves contain three prominent temperature peaks. According to[37,38,58], dehydration of calcium silicate hydrate (*CSH*), ettringite (*AFt*), calcium monosulfo-, hemicarboaluminate or calcium monocarboaluminate (all phases are designated as *AFm*) appear up to 200ºC. Dehydroxylation of portlandite (*CH*) occurs at 400–500°C and decarbonises calcium carbonates (*CC*) – at 700–800°C. It is difficult to distinguish the phases *AFt* and *AFm* in the DTG curves since their decomposition temperature ranges are very narrow and can overlap.

For the reference paste, a prominent peak at about 110°C corresponds to the decomposition of *CSH* and is most intense for the pSFR paste (**Fig. 3.30-a**). The second distinct peak is at 160°C, which corresponds to the formation of AFm compounds[59]. The third peak at about 450°C can be *CH* dehydration, much lower for

pastes with micro silica (samples pSF and pSFR). This is logical since micro silica is a highly reactive pozzolan that can react with *CH* in the presence of water and form *CSH* compounds. But in the temperature range from 710°C to 780°C, the decomposition of calcium carbonate, mainly from raw cement, with various polymorphic or less crystalline carbonates occurs. In the blended pastes, slight peaks of 720°C and above may indicate the decomposition of compounds that are part of the waste or micro silica crystallisation occurs (**Fig. 3.30**). Generally, samples prepared with residual cement have the highest weight loss. On the other hand, for pc and pSF pastes, the TG curves have almost the same shape. An increase in hydration time significantly affects weight loss, which leads to a more intense increase in the peak of *CSH* (and *AFm*) than *CH* and *CC* (**Fig. 3.30-b**).

If we compare the TG data, then **Fig. 3.31** shows the amounts of bound water (*wb*) and portlandite *CH* (normalised). Usually, a certain amount of *wb* indicates the volume of reaction products (*CSH*, *AFt*, *AFm* and *CH*) formed during cementing and hydration. However, the amount of normalised *CH* can be represented as an indicator of the change in the complex of reaction products (*CH* consumption during the formation of additional *CSH*). **Fig. 3.31-a** shows that the *wb* content increases for all compositions with increasing hydration time.

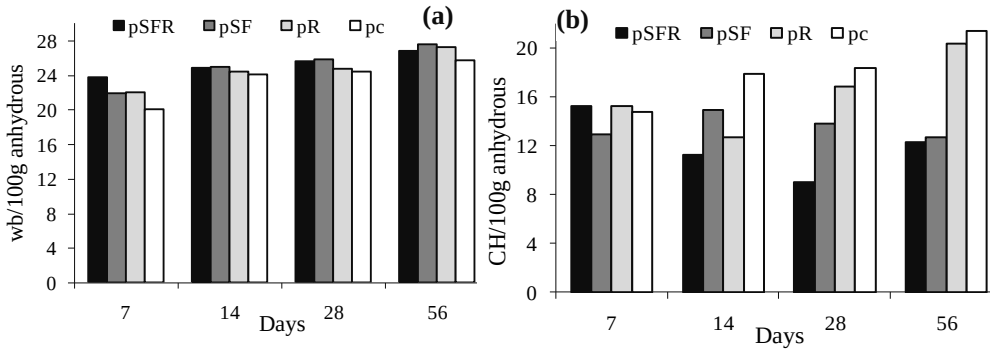

Fig. 3.31. Evolution of normalised to 100 g anhydrous amount of **(a)** bound water (w_b) and **(b)** portlandite (*CH*).

For the paste containing a substitute, the *wb* values are higher than the reference paste. During the first seven days, the value of bound water is highest for the sample with both substitutes (pFPS), and after 14 days, a higher content of *wb* is found in the paste with micro-silica (pF). Increased hydration in the early stages is due to the filler's effect, but dissolution-precipitation's chemical reactions begin later. Concerning the reference paste, the cement-residue-replacement sample (pR) was characterised by more bound water and less *CH* content. At the same time, replacing the cement with both substitutes (pSFR) increases the reactivity of the cement paste and leads to faster consumption of *CH* than in the pSF sample. However, the *wb* value is almost the same or less. The recovery of normalised *CH* for the pSFR paste is faster than for the pSF sample. Such a change may indicate that the filler effect contributed to the reactivity of micro-silica.

SEM images of the surfaces of the fractions of the reference and blended cement pastes after hydration for 56 days are shown in **Fig. 3.32.** The elemental composition

is also presented with the analysis of crystals. After two months of hydration (**Fig. 3.32**), the portlandite crystals are quite small in the micro-silica paste, without clearly defined edges, due to their partial absorption by the pozzolana. However, massive *CH* crystals are present in the reference paste and the past with the gasification residue (**Fig. 3.32-a, c**). However, acicular hydrates of different thicknesses (*AFt*) were mainly found in mixtures with a residue and were absent in the reference paste. The formation of *AFt* is related to the ash's high content of sulphates (≈23%).

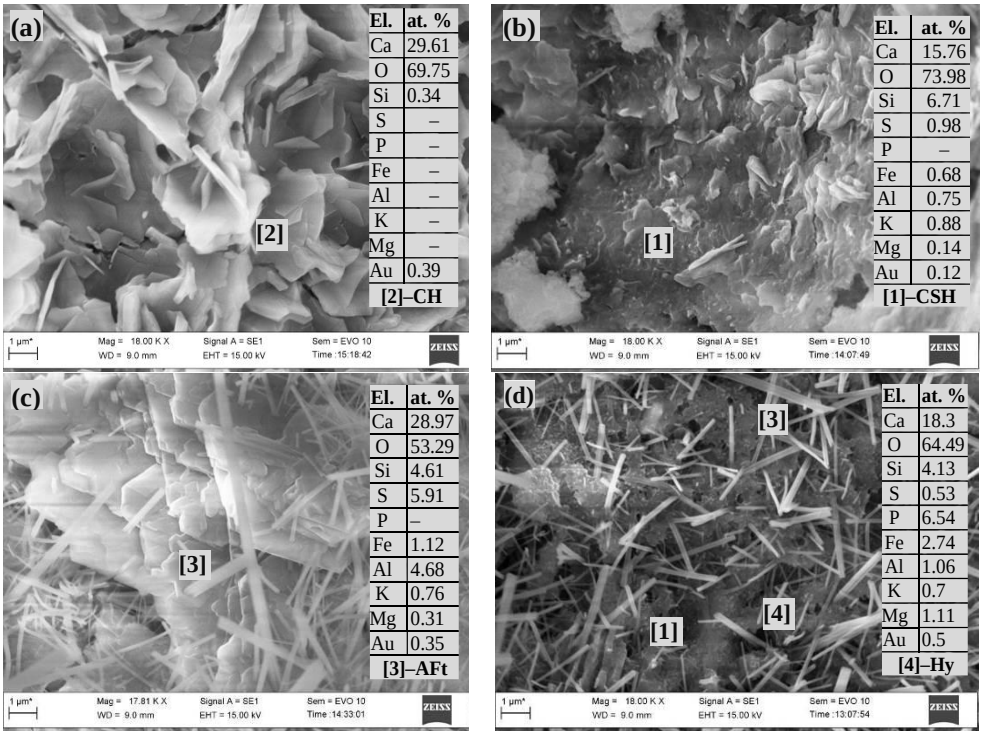

Fig. 3.32. SEM images of blended cement pastes hydrated for 56 days **(a)** PC, **(b)** pSF, **(c)** pR and **(d)** pSFR.

After 56 days, systems containing sewage sludge ash showed precipitation of *AFt* crystals, most likely due to the dissolution of the amorphous phase of the ash and the presence of chemically bound water. In our case, the gasification residue did not contain many sulphates; however, for the pSFR formulation, ettringite crystals were expected to precipitate in the reference paste samples. A more detailed analysing of the crystals showed that some acicular hydrates contain enough phosphorus content to suggest the possible formation of calcium phosphate (*Hy*) hydrates.

The formation of calcium-containing phosphate compounds (with the addition of sewage sludge ash) can increase the compressive strength of the compositions. Amorphous phase and acicular hydrates were found in pSFR samples. However, the phase's elemental composition was similar to the *CSH* gels; its visual shape and overall porosity differed from those observed in the pSF system.

Fig. 3.33 showed X-ray diffraction patterns of pastes (simple and mixed) that

were hydrated for 56 days. The main difference between the patterns is the *CH* intensity (2Θ=18°), which is much lower in micro silica pastes and quite objectively agrees with the results of thermal analysis (**Fig. 3.33**). A small peak of ettringite (2Θ=9º) is less noticeable in the pSF paste, the intensity of other peaks is identical. The peak intensity varies between samples; however, there is one wide peak at 31º2Θ, which the presence of gasification residues can explain.

There was used the gasification residue contained an amorphous phase. Because of phosphates, this amorphous phase can become a reactive fraction that will initiate the formation of weakly crystalline hydroxyapatite ($Ca_5(PO_4)_3OH$) with reinforcing properties. The SEM-EDS analysis showed the presence of acicular crystals with high phosphorus content. The main peak of hydroxyapatite was located at 32º2Θ and was overlapped by peaks of other cement products. From this, it turns out that due to the presence of calcite, a peak at 31º2Θ (**Fig. 3.33**) can be detected, which is characteristic of samples with a gasification residue. The formation of hydroxyapatite could have occurred in the amorphous phases that were in the gasification residue.

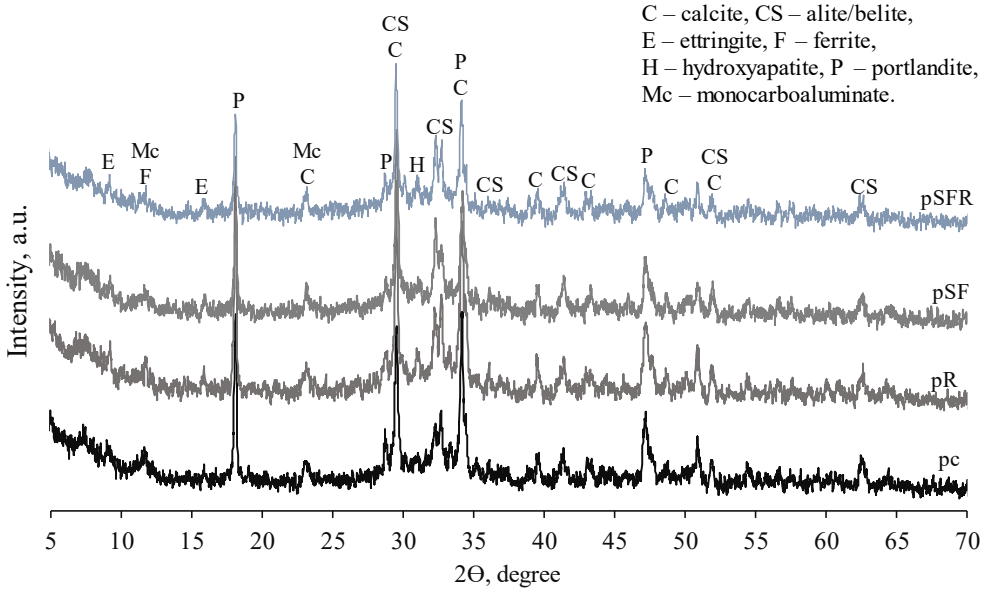

Fig. 3.33. XRD analysis result for hydrated pastes.

The studies of the microstructures of cement-based materials by nitrogen porosimetry are functional since various models can be used to obtain the pore size distribution in the ranges of microporosity (<2 nm) and mesoporosity (2–50 nm)[60]. Pores smaller than 10 nm as CSH gel pores, from 10 to 50 nm as medium or microcapillaries, and pores up to 10 μm as large capillary pores. The presence of gel pores is associated with pozzolanic reactions and the rate of hydration, while medium and large capillary pores affect the permeability and strength of the structure. A comparative evaluation of the effect of cement substitutes on the development of pore volume during hydration showed that the pore volume in pSFR paste decreases quite rapidly to 28 days in the pore size range of more than 12 nm. A more extended

hydration period mainly affects the pore region up to 20 nm, which is sensitive to the formation of hydration products and packing density. The percentage of relative pore volume for blended compositions with silica fume was found to have higher values than for the reference paste. Thus, a decrease in the pore volume indicates a refinement of the pore structure, which may occur due to the ability of the pozzolan or the reactive phase complex to fill the pore space with hydration products. The highest consumption of portlandite in the pSFR system with excessive formation of acicular hydrates for 56 days confirms these statements.

Two methods, DFT and BJH, were applied to obtain the pore size distribution for the adsorption branch of the isotherms. The DFT method obtained the distribution of pores in the range up to 35 nm, characteristic of the *CSH* gel and microcapillary pores (**Fig. 3.34**). For the distribution of larger capillary pores, it is better to use the BJH method (**Fig. 3.35**).

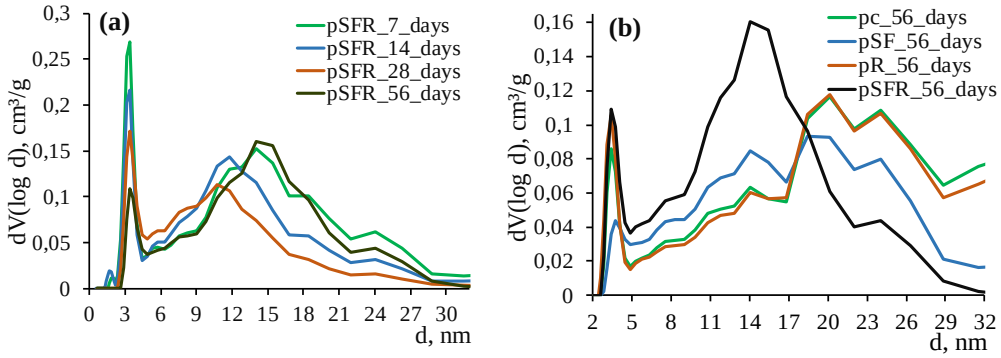

Fig. 3.34. Results of study for pore size distribution by DFT method: impact of hydration time **(a)** and additives **(b)**.

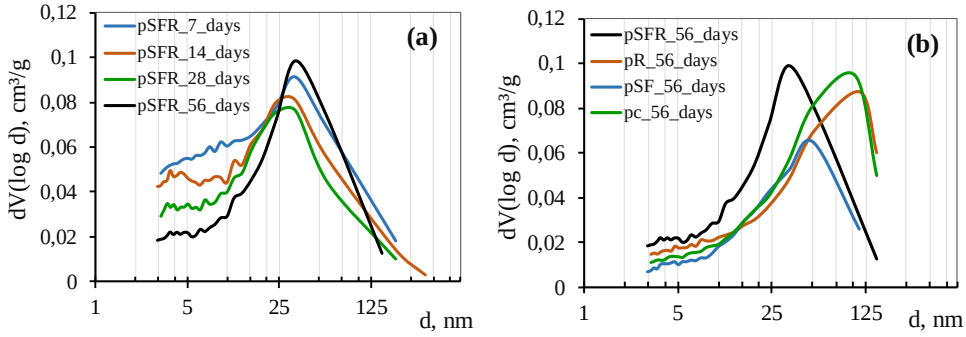

Fig. 3.35. Results of study for pore size distribution by BJH method: impact of hydration time **(a)** and additives **(b)**.

When using the BJH method, distinct peaks are practically invisible in the range of up to 10 nm. This range corresponds to the region of the *CSH* gel. But when using the DFT method, one can observe two narrow peaks between 2 nm and 3.5 nm (**Fig. 3.34-a**). The most prominent peak at 3.5 nm decreases with increasing hydration time; smaller peaks at 2 nm disappear after 14 days of hydration, which is associated with filling the pore space with hydration products, mainly *CSH* gel.

The tendency to decrease the size of the peaks is also observed when using the BJH method. In the mesoporous range (10–50 nm), using the BJH method, one clear peak was detected (**Fig. 3.35-a**), while with the DFT method (**Fig. 3.34-a**), several distinct peaks can be seen. The magnitude of clear peaks varies depending on the time of hydration.

After seven days of hydration, four peaks were found in the range of 12, 14, 18, and 28 nm (**Fig. 3.34-a**). A decrease in the volume of pores with a size of 18 and 25 nm was found with an increase in the hydration time. However, two other peaks were found to be shifted to a smaller size, which borders on the *CSH* gel region. On the 56th day of hydration, pores with a diameter of 15 nm predominate in the pSFR system; it most likely indicates significant changes in pore bonds. In other compositions hydrated in the same period, peaks were established a pore range of 20–24 nm and 30–150 nm for both methods (**Fig. 3.34-b, 3.35-b**). When comparing the results obtained using both methods, it was found that after 56 days of hydration, the pSF system contains the smallest number of pores ranging from 2 to 100 nm (**Fig. 3.34-b, 3.35-b**). A larger pore volume was found in the reference paste sample (pc) and the sample with cement substituted by residue (pR). Among all samples, the most significant pore volume is formed in the pSFR paste; however, the maximum value is shifted towards a smaller pore of 15 nm and 34 nm (**Fig. 3.35-b**). This suggests that the pSFR paste contains more purified, and most likely water-filled, capillary pores available for the precipitation of hydration products. The highest consumption of *CH* and the formation of hydration products (crystalline and amorphous) confirm that the introduction of both substitutes contributes to the hydration of the cement. This is due to the increased reactivity of micro silica since it can act as both filler and a pozzolana. The formation of additional hydration products promotes pore refinement and a more compact structure.

The water absorption rate during capillary absorption reflects the flow of water into the capillary pores (10–50 nm). The most extensive water absorption corresponds to the reference mortar sample, and the smallest – to the SF10 solution sample. Water absorption results for samples with gasification residues are low compared to the data of the reference sample and the SF10 sample. However, sample SF10R2 has the most insufficient moisture absorption, almost identical to sample SF10. The sorption coefficient has decreased with increasing hydration time and at a minimum R/SF ratio. The effect of cement substitution on the value of sorption capacity is evident. In mortar compositions, at a constant amount of silica fume, the degree of cement substitution increased from 10% to 12% due to an increase in the residue content. When comparing the data R/SF=0.7 and 1.0, it was found that a higher percentage of the content of the gasification residue leads to a decrease in sorption capacity by almost 8%. However, there are exceptions; these include samples SF10 and SF10R2 (R/SF=0 and 0.2), for which the sorption capacity increased by 6% due to the inclusion of the residue. Other results were obtained for water absorption when the samples were immersed entirely (differences are insignificant). According to the data obtained, it was found that the water absorption of all samples is lower than that of the reference paste. This is explained by the fact that replacing cement with micro silica with a residue affects the size and distribution of capillary pores. The pSFR cement paste

showed a pore volume lower than the reference paste and significantly higher than the micro silica paste.

The results in **Fig. 3.36-a, b** show that the blended compositions had higher mechanical strength than the reference sample throughout the hydration period. The compressive strength of the samples tended to increase with decreasing R/SF ratio.

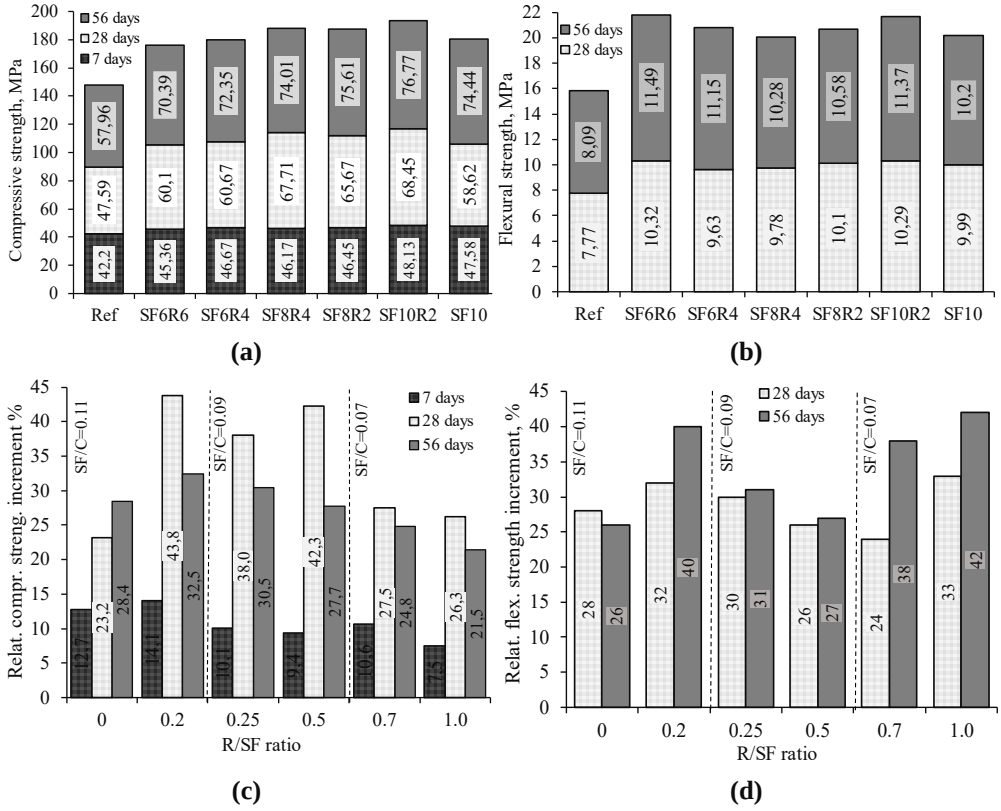

**SF/C – silica fume-to-cement ratio, R/SF – gasification residue-to-silica fume ratio

Fig. 3.36. Compressive **(a)** and flexural **(b)** strength results (average) for mortar samples; comparison of compressive **(c)** and flexural **(d)** strength increments relative to the reference mortar.

This trend is not as pronounced for flexural strength, as the best performance was obtained with an R/SF ratio of 0.2 and 1.0, corresponding to the highest and lowest SF/C content. **Fig. 3.36-c, d** shows the change in mechanical strength (increment or reduction) compared to the reference paste. For compositions for which the ratio R/SF>0.2, the increase in compressive strength is 7–14%, 26–44% and 22–32% after 7, 28 and 56 days, respectively (**Fig. 3.36-c, d**). The exception is the sample without residue (R/SF=0), the strength index of which increases evenly both with the time of hydration (**Fig. 3.36-a, b**) and relative to the reference paste (**Fig. 3.36-c, d**). However, unlike formulations containing sediment, the SF_{10} solution showed relatively moderate strength.

The data presented in **Fig. 3.36 a-d** show that among all the samples, the

compositions with R/SF ratios of 0.2, 0.25 and 0.5 showed the highest compressive strength results. The sample SF10R2 (R/SF=0.2) proved to be not only strong but also showed increased resistance to bending when compared with sample R/SF>0.7, especially after prolonged hydration (**Fig. 3.36-c, d**). It has been established that introducing a more significant amount of residue (R/SF≥0.7) decreases compressive strength by only 5%, resulting in lower water absorption with moderate sorption capacity. The results indicate that combined with the gasification residue, the level of micro silica can be reduced from 10 to 6% without significant loss of functional properties.

When converting cement-based waste into materials, consideration should be given to the environmental impact. Based on this, the CO_2 emission estimate is chosen as the main parameter for assessing the potential for waste generation. It was found that the micro silica used in the study was quite expensive, which led to an increase in the cost of mixed samples by 6% compared to the reference sample. Ultimately, the cost value was reduced by 3% due to increased residual content.

It was found that the inclusion of both types of waste reduced CO_2 emissions by 10–15%. CO_2 emissions were lower for samples with a cement replacement level of 12% compared to 10%. The effectiveness of the selected number of mineral additives was evaluated, combining the environmental impact with mechanical strength. The compositions mixed with the residue give the same emission as those with cement replacement with micro silica only (R/SF=0). In addition, it was found that due to the low scatter of data between samples with cement replacement levels of 10% and 12%, an R/SF ratio of 0.5–1.0 could be considered a good number of substitutes from an environmental and engineering point of view. Despite the improvement in strength, the low level of water absorption obtained for compositions with an R/SF>0.5 suggests the possibility of processing gasification residues in combination with silica fume to produce rain screens or cement-based boards.

The potential use of two types of waste, sewage sludge, biomass gasification residues and micro silica, was studied to replace cement. Their synergistic effects on hydration and properties of building materials were analysed. Estimated costs and CO_2 emission results showed that the total cement replacement rate could be increased up to 12%, within the 4–6% range covered by gasification residues, without compromising mechanical strength values. At the same time, reducing the amount of micro silica (up to 6%) would also save resources.

4. CONCLUSIONS AND RECOMMENDATIONS

4.1. Conclusions

1. The main characteristics of RDF were determined, and it was established that RDF can only be used for combustion in CPP to generate heat and energy. It was found that by the classification characteristics, SRF has better quality than RDF, belongs to Class III and can be used as a replacement fuel instead of coal during the clinker firing process. It has been proven that the ash obtained after the incineration of SRF has a crystalline structure and consists of clinker-forming minerals. The productivity of the developed SRF production line amounted to 4.47 t/h. During the SRF production process, the humidity of materials decreased by 85% and the volume of the finished product by 18%. It proved the economic and environmental efficiency of using SRF in a cement kiln by up to 25%.
2. Research demonstrated the feasibility of extracting energy-intensive materials from landfills by developing a two-stage mechanism of separation LMRs and SRF production process. It was revealed that the LMRs coarse fraction includes burnable fractions such as plastics, wood, paper, rubber and other burnable components and can be extracted up to a depth of 10 m. The ash from obtained SRF has a crystalline structure and, by the elemental and oxide composition, corresponds to the oxide's composition of the finished clinker.
3. Clay brick samples with up to 20% BA as replacement components and fired at 900°C can be utilised in moderately aggressive environments and belong to the F1 class. Clay bricks with 30% BA instead of the clay and fired at 1000°C can be used in passively aggressive environments and belong to the F0 class. Using 30% of BA as a replacement component in clay bricks production will make it possible to produce 1000 standard size pieces of clay bricks without deteriorating their quality and reduce the consumption of natural resources in the amount of 1,31 tons.
4. It was established that the composition of the mortar with the replacement of cement with the mixing of 6% AR and 6% SF seems beneficial, as it will reduce the resource of Portland cement and silica fume. Estimated costs and CO_2 emission results indicated that the total cement substitution level might increase to 12%, within 4–6%, covered by AR, and 6% of SF without deteriorating mechanical strength.

4.2. Recommendations

1. Recommended removing prohibited materials (Cl- and Hg-containing) from the MSW stream for high-quality SRF production
2. Using inertial screens is recommended at the first extraction stage, not a drum sieve. This type of sieve ensures the classification and simultaneous transport of the material through the sieve.
3. In the process of clay brick production, it is recommended to use clays with low calcium content. The bottom ash has a relatively high calcium content that negatively impacts the quality of the finished product.
4. Using gasification ash residue as a replacement component in the 4–6% range is recommended.

5 SANTRAUKA

5.1. Motyvacija ir problemos aktualumas

Pasaulyje susidarančių atliekų kiekis per pastarąjį dešimtmetį išaugo ir toliau didėja. Pasaulio banko[1] duomenimis, iki 2050 metų atliekų susidarymas pasaulyje padidės 70,4 %, t. y. iki 3,4 mlrd. tonų. Bendras ES susidarančių atliekų kiekis 2005–2020 m. padidėjo 19,8%, o 2020 m. vienam gyventojui susidarė 505 kg kietųjų komunalinių atliekų. Ši tendencija rodo, kad būtina imtis rimtų ir konkrečių veiksmų, siekiant sumažinti atliekų susidarymą ir padidinti jų perdirbimą.

Atliekų tvarkymas ir šalinimas šiandien yra viena iš aktualiausių pasaulinių problemų. Tinkamas kietųjų komunalinių atliekų (KKA) valdymas yra prioritetas siekiant ES tvaraus vystymosi tikslo sumažinti neigiamą poveikį aplinkai ir žmonių sveikatai[2]. Pagrindiniai patobulinimai šioje srityje buvo pasiekti įdiegus mechaninį-biologinį apdorojimą (MBA) ir kogeneracines jėgaines (KJ). Tačiau nemažas atliekų kiekis vis dar išvežamas į sąvartynus, o tai rodo, kad atliekų šalinimo problema lieka neišspręsta[3,4]. Kai kuriose šalyse daugiau kaip 50 proc. buitinių atliekų perdirbama, kompostuojama ir anaerobiškai skaidoma[5].

Kaip ir kitose šalyse, kur atliekų susidarymas sumažėjo, Norvegijoje, Čekijoje, Slovakijoje ir Islandijoje 2020 m. buitinių atliekų susidarymas vienam gyventojui buvo didžiausias, o per 15 metų jis vis didėjo. Kaip parodyta **1 pav**., Lietuva yra tarp tų šalių, kuriose nuo 2005 m. KKA susidarymas didėjo.

Atliekų susidarymo mažinimas ir žiedinės ekonomikos sukūrimas yra strateginiai ES tikslai[6]. Žiedinė ekonomika yra atsinaujinanti sistema, kurioje sulėtinant, uždarant ir siaurinant energijos ir medžiagų naudojimo ciklus sumažinami išteklių sunaudojimas atliekų susidarymas, emisijos į aplinką ir energijos nuostoliai. Tai galima pasiekti naudojant tvarų dizainą, priežiūrą, pakartotinį naudojimą, visišką atnaujinimą ir perdirbimą. Svarbiausi ES aplinkos politikos komponentai yra aplinkai nekenksmingas atliekų tvarkymas ir perdirbtos medžiagos.

Šiame kontekste atliekų tvarkymo sektorius turėtų tapti atsakingu padaliniu, apimančiu naujų verslo modelių kūrimą, orientuojantis į buitinių atliekų prevenciją, kryptingą monitoringą, atliekų susidarymo prognozavimą, skaitmeninių technologijų diegimą ir išteklių gavybą iš sąvartynų. Perdirbimas ir pakartotinis naudojimas bus ypač svarbūs siekiant tvarios aplinkos apsaugos tikslų.

Išsivysčiusios ir besivystančios šalys stengiasi pasiekti atliekų šalinimo sąvartyne minimumą. Tai, savo ruožtu, lemia didėjantį buitinių atliekų deginamą, perdirbimą ir kompostavimą. Energijos atgavimas iš atliekų kogeneracinėse jėgainėse (KJ) yra tvaresnis atliekų tvarkymo būdas nei šalinimas sąvartynuose. Naudodama išrūšiuotas ir degias atliekas kaip kurą elektros gamybai ir centralizuotam šildymui, KJ veikia sinergijoje su žiedine ekonomika ir skatina atsakingą atliekų tvarkymą. Per metus Lietuvoje susidaro $1{,}34 \cdot 10^6$ t atliekų, iš kurių šiuo metu Lietuvos KJ sudeginama apie $203 \cdot 10^3$ t, tai yra ≈15,15 %[7–9]. Šiuo metu Lietuvos teritorijoje yra trys KJ: Vilniuje, Kaune ir Klaipėdoje (**2 pav.**).

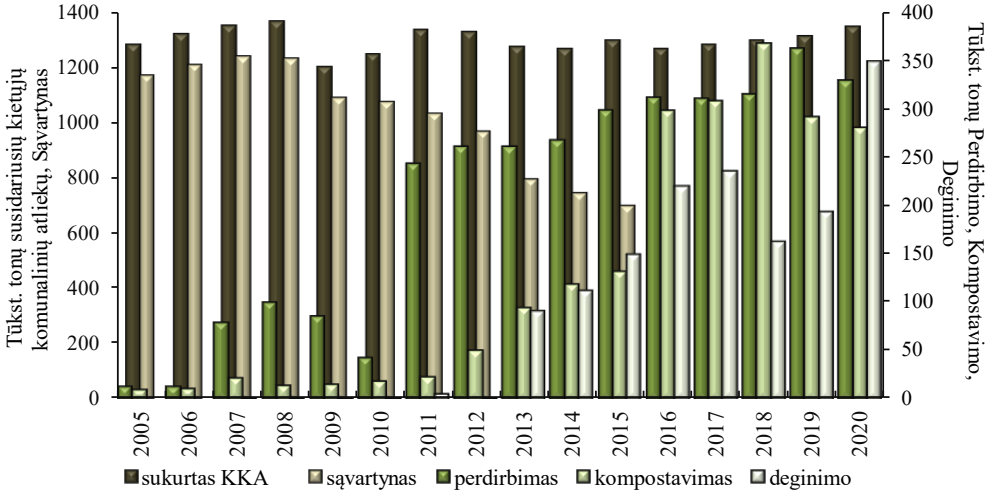

1 pav. Kietųjų komunalinių atliekų susidarymas ir tvarkymas Lietuvoje

Deginant atliekas išgaunama šiluma arba elektros energija; šalutinis produktas – dugno pelenai (DP) – sudaro apie 11 proc. nuo deginamų atliekų kiekio. Išgavus metalus, DP išvežami šalinimui į sąvartyną. Tačiau yra reali galimybė susidariusius pelenų likučius panaudoti statybų pramonėje. DP fizikinių ir mechaninių charakteristikų tyrimai parodė, kad jie gali būti tinkami statybų inžinerijai, ypač kelių tiesimui ir molinių plytų bei čerpių gamybai[10–12].

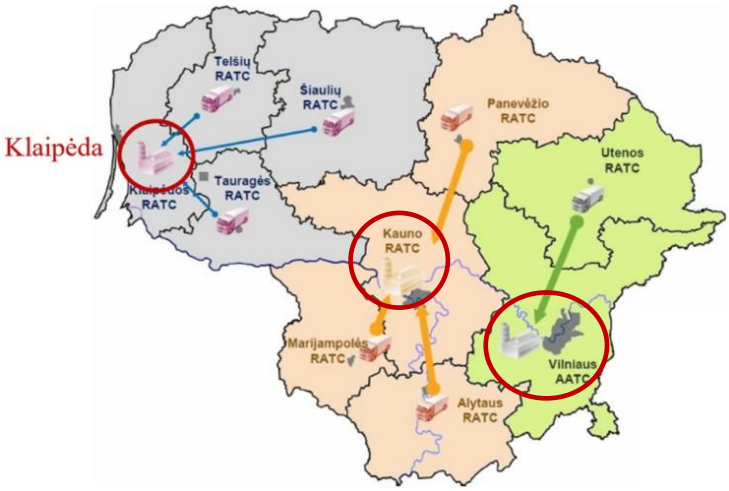

2 pav. Kogeneracinių jėgainių Lietuvoje vietos ir atliekų tiekimo šilumos ir energijos gamybai kryptys.

Sutinkant su autorių[13] teiginiu, kad geriausias būdas atsikratyti atliekų ir priartėti prie žiedinės ekonomikos yra pakartotinis naudojimas ir šilumos bei energijos gamyba, būtina atsižvelgti ir į tai, kad atliekos gali būti naudojamos kaip pakaitinis kuras, skirtas daug energijos vartojančioms pramonės šakoms, pavyzdžiui, cemento pramonei. Autoriai[14–16] taip pat mano, kad atliekos ir medžiagos gali būti tvarūs

energijos šaltiniai. Tokia strategija leis įmonėms sutaupyti lėšų, užtikrins kontroliuojamą atliekų šalinimą ir sumažins neatsinaujinančių gamtinių energijos išteklių vartojimą.

Iš atliekų pagamintas kuras tampa perspektyvia ir populiaria iškastinio kuro alternatyva. Šis kuro tipas skirstomas į dvi pagrindines kategorijas: iš atliekų gautas kuras (AGK) (angliškai *refuse derived fuel* – RDF) ir kietasis atgautasis kuras (KAK) (angliškai *solid recovered fuel* – SRF). AGK yra terminas, reiškiantis atliekas, kurios nebuvo tinkamai apdorotos. AGK nėra standartizuotas, jo funkcijos neapibrėžtos, o gatavo produkto kokybė negali būti garantuota. KAK – tai kuras, gaunamas rūšiuojant, džiovinant ir smulkinant kietąsias atliekas. KAK paprastai sudaro degūs komponentai, gauti iš kietųjų komunalinių atliekų. Paprastai jis gaminamas iš KKA, pramoninių ir komercinių atliekų arba statybos ir griovimo atliekų (SGA). Tipinė KAK gamybos schema parodyta **3 pav.** pagal Europos atgautojo kuro organizaciją (angliškai *European Recovered Fuel Organi*sation – ERFO)[17].

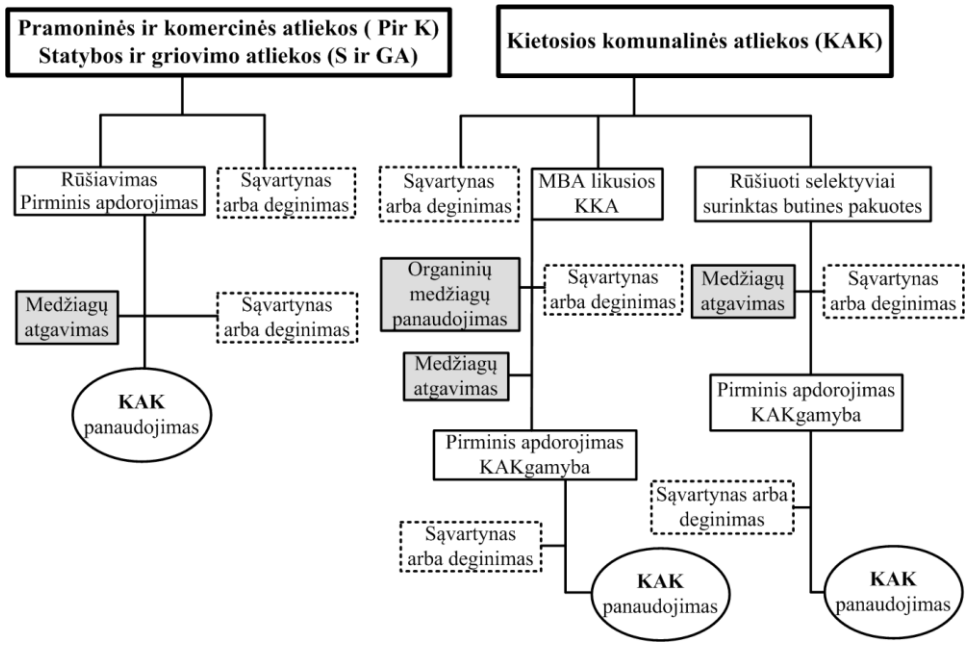

3 pav. Kietojo atgautojo kuro (KAK) gamybos procesas.

Tačiau pažymėtina, kad pastaruoju metu aktualus tapo alternatyvių energijos šaltinių, naudojant ne gamtinius energijos išteklius, bet sąvartynų atliekas, kurios kažkada buvo išvežtos šalinimui, klausimas. Sąvartynų kasyba yra terminas, dažniausiai vartojamas išteklių gavybai iš sąvartynų apibūdinti[18–19]. Sąvartynų kasyba turėtų būti suprantama kaip integruota išteklių gavybos ir išsaugojimo veikla, kurios metu iš sąvartynų atliekų atgaunami ištekliai (metalai, plastikai, kuras ir statybinės medžiagos), sprendžiamos filtrato panaudojimo problemos ir kitos su sąvartynais susijusios aplinkosaugos problemos[18,20]. Kai atliekos iškasamos iš sąvartyno, tai jas perdirbant atlaisvinama daugiau vietos, todėl nebereikia statyti naujų sąvartynų. Svarbiausia medžiagų atgavime iš sąvartynų yra tai, kad anksčiau sąvartyne pašalintos

medžiagos bus naudingesnės kitur. Atgaunant išteklius iš sąvartynų, atliekoms, patekusioms į sąvartynus, suteikiama nauja galimybė kilti atliekų hierarchijoje aukštyn link energijos atgavimo, perdirbimo ar pakartotinio naudojimo. Taigi iš sąvartyno iškastas atliekas galima perdirbti į alternatyvų kurą. KAK gamyba nėra konkuruojantis perdirbimo procesas, bet neatsiejama jo dalis. KAK Lietuvoje yra žinomas bet mažai naudojamas, tačiau tai esminis atliekų tvarkymo elementas. Cemento krosnyse klinkerio degimo procese galima naudoti tik KAK. Naudojant iš atliekų pagamintą kurą klinkerio deginimo procese, sumažės neatsinaujinančių gamtos energijos išteklių sunaudojimas ir šiltnamio efektą sukeliančių dujų emisijos.

Taigi atliekų šalinimas gaminant aukštos kokybės alternatyvųjį kurą ir jo panaudojimas cemento krosnyje klinkerio deginimo procese turi ekonominę ir aplinkosauginę naudą ir yra itin svarbus siekiant žiedinės ekonomikos tikslų. KAK gamyba taip pat sąlygos mažesnę priklausomybę nuo neatsinaujinančių gamtinių energijos išteklių, mažesnį anglies pėdsaką ir pastovų „kokybiško“ kuro tiekimą už santykinai stabilią kainą.

Remiantis pateiktais atliekų susidarymo ir tvarkymo duomenimis, buvo nustatyta, kad atliekų tvarkymo srityje tiek pasaulyje, tiek Lietuvoje esama realių problemų. Pasaulio bendruomenė siekia žiedinės ekonomikos tikslų, ne išimtis ir Lietuva. Šiame darbe siūlomi galimi žingsniai kuriant alternatyvią kuro rūšį, taip pat pasiūlytas mechanizmas, kaip šalinti likutinius pelenus, susidariusius deginant atliekas. Vykdomi tyrimai ir siūlomi mechanizmai priartins Lietuvą prie žiedinės ekonomikos tikslų įgyvendinimo.

5.2. Darbo tikslas ir uždaviniai

Disertacinio darbo tikslas yra ištirti galimybę panaudoti atliekas gaminant kietąjį atgautąjį kurą energijai imlioms pramonės šakoms ir naudojant šalutinius produktus kaip pakaitinius komponentus keraminių plytų ir cemento pagrindo medžiagų gamyboje.

Tyrimo uždaviniai

1. Nustatyti pagrindines AGK, KAK ir pelenų, gautų sudeginus KAK, charakteristikas ir sukurti KAK gamybos linijos koncepciją.
2. Nustatyti galimybę iš sąvartyno kasti atliekas ir gaminti alternatyvų kurą.
3. Įvertinti KAK pelenų kaip pakaitinio komponento panaudojimo molio plytų gamyboje aplinkosauginį pagrįstumą.
4. Įrodyti pelenų, susidariusių dujofikuojant biomasės atliekas su nuotekų dumblu, kaip dalinio pakaitalo cemento pagrindo medžiagose panaudojimo galimybę.

Ginamieji **teiginiai**

1. Kauno regione susidarančių mišriųjų komunalinių atliekų mechaninio apdorojimo produktas iš atliekų gautas kuras (AGK) yra tinkama žaliava kietajam atgautajam kurui, kurio panaudojimas cemento pramonėje padidina pastarosios tvarumą.
2. Kietųjų komunalinių atliekų sąvartynai yra kokybiško KAK gamybai tinkamų medžiagų šaltiniai.

3. KAK dugno pelenų, kaip dalinio molio pakaitalo, naudojimas plytų gamybos procese lemtų atliekų kiekio mažėjimą ir nepablogintų gaunamo produkto kokybės.
4. Likutiniai KAK dujinimo pelenai gali iš dalies pakeisti cemento pagrindą sudarančias medžiagas ir sumažinti gamtinių išteklių naudojimą.

Mokslinis **naujumas**

1. Sukurta kietojo atgautojo kuro (KAK) gamybos iš AGK linijos koncepcija ir parinktos optimalios sąlygos alternatyvaus kuro gamybai Kauno regiono sąlygomis.
2. Sukurtas dviejų pakopų sąvartynų kasybos produktų (SKP) išgavimo ir tolesnės KAK gamybos mechanizmas.
3. Pasiūlyta tvaresnė molio plytų gamybos technologija, pakeičiant dalį molio KAK dugno pelenais su mažu kalcio kiekiu.
4. Remiantis KAK ir nuotekų dumblo mineralinės sudėties panašumu, nustatyti ir patvirtinti optimalūs KAK dujinimo likutinių pelenų, kaip hibridinio užpildo cemento pagrindo medžiagoms, naudojimo parametrai.

5.3. Tyrimų metodologija

KAK gamybos linijos koncepcija buvo sukurta numatant draudžiamų medžiagų pašalinimą iš AGK, smulkinimą, džiovinimą ir įvertinant KAK panaudojimo cemento pramonėje ekonominį ir aplinkosauginį pagrįstumą (**1 straipsnis**). AGK charakteristikos Kauno MBA gamykloje buvo tiriamos keturis sezonus (2020–2021 m.). Konkreti AGK sudėtis buvo pasiekta pašalinant biologiškai skaidžias frakcijas iš KKA srauto. Toliau tokio pavidalo AGK buvo persijotas per tris sietus su kvadratinėmis 80, 40 ir 20 mm skersmens akutėmis. Gautos granuliometrinės frakcijos buvo pasvertos ir nustatyta jų morfologinė sudėtis rūšiuojant rankiniu būdu. Papildomas atliekų frakcijos 40 mm>d>20 mm rūšiavimas buvo praktiškai neįmanomas, nes buvo sunku vizualiai atskirti medžiagas. Tuo pačiu metu vizualinis rūšiavimas buvo neįmanomas mažoms frakcijoms d<20 mm. Po morfologinės analizės kiekviena ARD granuliometrinė frakcija buvo pasverta, sudėta į konteinerius ir vežama į laboratoriją tolesniam tyrimui ir KAK ruošimui. Draudžiamos medžiagos (turinčios chloro ir gyvsidabrio) buvo pašalintos anksčiau. KAK frakcija buvo ruošiama susmulkinant SM 300 malūne. Paruošto KAK pagrindinės charakteristikos (drėgmė ir pelenų kiekis, aukštutinis šilumingumas, chloro ir gyvsidabrio kiekis) buvo nustatytos pagal ES standartus. Pelenų elementinė sudėtis (%) buvo nustatyta naudojant skenuojančią elektroninę mikroskopiją (SEM). Kristalinių medžiagų (KAK ir nuotekų dumblo pelenuose) struktūra ir fazinė sudėtis nustatyta naudojant rentgeno difrakciją (XRD), kuriai KAK ir nuotekų dumblo (ND) mėginiai buvo paruošti per valandą deginant mufelinėje krosnyje 950 °C temperatūroje.

KAK srautas gamybos linijoje apskaičiuotas naudojant šias formules:

$$S_{KAK} = S_{AGK} - X - Y - Z - S_{DK} \quad (5.1)$$

$$X = (S_{AGK} \cdot x) / 100\% \quad (5.2)$$

$$Y = [(S_{AGK} - X) \cdot y] / 100\% \quad (5.3)$$

$$Z = [(S_{AGK} - Y)\cdot z] / 100\% \quad (5.4)$$

$$S_{DK} = [(S_{AGK} - Z)\cdot DK_P] / 100\%, \quad (5.5)$$

kur S_{KAK} yra KAK srautas gamybos procese (t/val.), SG_{AGK} yra MBA apdorotų atliekų degios frakcijos (iš atliekų gauto kuro) srauto greitis, *X, Y* ir *Z* yra iš AGK kiekvienoje proceso stadijoje pašalintų medžiagų (inertinių, juodųjų metalų, spalvotųjų metalų) srautai (t/val.), *x, y* ir *z* yra pašalintų medžiagų kiekiai AGK (inertinių, juodųjų metalų, spalvotųjų metalų) kiekvienoje proceso stadijoje (%), DK_P yra iš AGK pašalintos drėgmės kiekis, S_{DK} yra pašalintos drėgmės srautas (t/val).

KAK panaudojimo cemento pramonėje ekonominės ir aplinkosauginės galimybės buvo apskaičiuotos naudojant 1 priede nurodytus metodus.

Buvo sukurtas sąvartynų kasybos produktų (SKP) išgavimo mechanizmas, nustatytos jo charakteristikos ir taikymo galimybės.

Buvo tiriamos KAK gamybos iš SKP gamybos ir panaudojimo cemento pramonėje galimybės (**2 straipsnis**). Šių tyrimų objektas buvo Kauno regiono nepavojingų atliekų sąvartynas. Sąvartyną sudaro trys sekcijos. Mėginių paėmimas buvo vykdomas darant gręžinius viso sąvartyno sekcijose. Buvo gręžiama naudojant 15 cm skersmens grąžtą, mėginiai buvo imami iš kiekvieno 2 m storio sluoksnio iki 20 m gylio. I sekcijoje gręžimas buvo vykdomas iki 10 m, II iki 14 m, III iki 20 m. Gręžimo gylį lėmė jo vykdymo metu susiklosčiusios aplinkybės. Gręžimo sudėtingumą lėmė anksčiau sąvartyne pašalintos šarvuotos transporto priemonės. Neapdorotų SKP morfologinė sudėtis buvo nustatyta rankinio rūšiavimo būdu po gręžimo ir kasimo. Tyrimai atlikti pagal Standartinį neapdorotų kietųjų komunalinių atliekų sudėties nustatymo metodą ASTM D5231-92 (2016). Iškastos medžiagos sijojimo būdu buvo perskirtos į smulkiąją (<20 mm) ir stambiąją (>20 m) frakcijas. Smulkioji frakcija buvo sugrąžinta į sąvartyną. Stambioji frakcija buvo rūšiuojama. Toliau iš stambiosios frakcijos išskirtos degios medžiagos (pvz., plastikas, mediena ir kitos) buvo smulkinamos, maišomos tais pačiais santykiais kaip ir SKP ir iš jų formuojamas KAK, toliau nustatant jo savybes pagal jam keliamus reikalavimus.

Toliau buvo ištirtos dugno pelenų (DP), gaunamų sudeginant KAK, panaudojimo molio plytų gamyboje galimybės (**3 straipsnis**). Tam tikslui buvo panaudoti panašių savybių Kauno kogeneracinėje jėgainėje susidarantys AGK deginimo dugno pelenai. Jų bandiniai tyrimui buvo paimti po keturių mėnesių sendinimo atmosferoje. Plytų bandiniams formuoti naudotas molis „Technik-3“ buvo iškastas didžiausiame Ukrainos telkinyje Andrejevsky, netoli Družovkos Donecko regione. Abi medžiagos buvo džiovinamos 105±5 °C temperatūroje, smulkinamos, sijojamos per 0,63 mm sietą ir tiriamos prieš plytų bandinių formavimą. Bandiniai buvo suformuoti iš molio ir DP, prieš tai džiovinant iki pastovios drėgmės. Komponentai buvo maišomi sausomis sąlygomis, į mišinį pridedant 8 % vandens. Paruoštuose molio plytų bandiniuose DP pakeitė nuo 10 iki 40% molio. Bandiniai buvo formuojami esant 120 kg/cm^2 slėgiui, džiovinami ir išdegami 900 ir 1000 °C temperatūrose. Išdeginti bandiniai buvo aušinami krosnyje iki aplinkos temperatūros. Suformavus, išdžiovinus ir išdegus bandinius buvo vertinamos (tvirtinamos ar atmetamos) DP panaudojimo kaip pakaitinės medžiagos molio plytų gamyboje galimybės.

Vertinant KAK pelenų, gaunamų dujofikacijos procese, panaudojimo

galimybes, buvo panaudoti nuotekų dumblo (ND) ir medienos mišinio dujofikacijos pelenai, sumaišyti lygiu santykiu su mikrosilicio dioksido dalelėmis (**4 straipsnis**). Tyrimai buvo atliekami panaudojant pramonines medžiagas, tokias kaip komercinis cementas „Portland“, mikrosilicio dioksidas ir cemento gamybai naudojamas smėlis. Dujofikacijos pelenai buvo paimti iš pasrovinio dujofikatoriaus, prijungto prie antrinio plazminio reaktoriaus, po granuliuotos medienos biomasės su nuotekų dumblu terminio apdorojimo. Ruošiant kiekvieną mėginių partiją, visi rišantieji komponentai (cementas, mikrosilicio dioksidas ir dujofikavimo liekanos) buvo sausai maišomi iki homogeninės būsenos prieš pridedant reikiamą kiekį vandens. Šviežia skiedinio masė buvo supilama į formas ir paliekama 24 val. Toliau iš formos išimti bandiniai kurį laiką buvo laikomi (21±2)ºC temperatūros ir 95% santykinės drėgmės sąlygomis. Skiedinio, kuriame rišiklio ir smėlio santykis buvo 2,5, o vandens ir rišiklio santykis 0,4. Įvairūs mikrosilicio dalelių ir dujofikavimo liekanų santykiai buvo panaudoti pakeičiant 10% ir 12% cemento pagal masę. Kiekvienam skiedinio variantui buvo panaudota 0,8 g sauso superplastifikatoriaus „Gaia“ (pH=5, ρ=1.15 g/mL). Aštuoniems kubo ir trims prizmės pavidalo kiekvienos kompozicijos mėginiams po jų suformavimo buvo atliekami atsparumų gniuždymui ir lenkimui matavimai.

5.4 Svarbiausi darbo rezultatai

5.4.1. Pagrindinių AGK, KAK ir KAK deginimo pelenų charakteristikų nustatymas ir KAK gamybos linijos koncepcijos sukūrimas (1 straipsnis)

Šiame bandomajame tyrime buvo kuriama KAK gamybos iš AGK linijos koncepcija remiantis Kauno MBA gamyklos infrastruktūra. Taip pat buvo įvertinti KAK panaudojimo klinkerio degimo procese energetinis potencialas, ekonominiai ir aplinkosauginiai aspektai[21].

Nustatyta, kad šilumingų frakcijų procentas svyruoja priklausomai nuo sezono. Morfologinės analizės rezultatai rodo, kad AGK dominuojančios medžiagos yra plastikai, popierius, tekstilė ir kitos degios medžiagos (**4 pav.**).

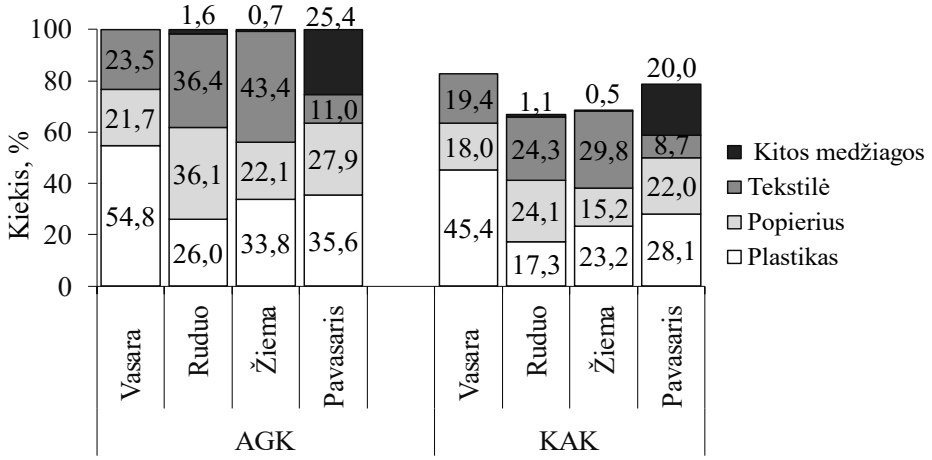

4 pav. Iš atliekų gauto kuro ir kietojo atgautojo kuro (KAK) sezoninė morfologinė sudėtis.

KAK morfologinės charakteristikos skyrėsi nuo AGK dėl draudžiamų medžiagų (chloro turintys plastikai, gyvsidabrio turinčios medžiagos) pašalinimo, taip pat ir dėl medžiagų praradimo išgaunant, sijojant, smulkinant ir džiovinant. Darbe nuotekų dumblas buvo lyginamas su gaminamo KAK charakteristikomis, kadangi šiuo metu nuotekų dumblas naudojamas kaip pakaitinis kuras klinkerio deginimo procese.

Buvo nustatytos pagrindinės AGK charakteristikos (**5 pav.**) ir nustatyta, kad pagal savo charakteristikas AGK gali būti naudojamas tik deginimui kogeneracinėse jėgainėse gaminant šilumą ir elektrą. Nustatytas KAK energetinis potencialas ir pagrįsta galimybė naudoti KAK kaip pakaitinį kurą klinkerio deginimui.

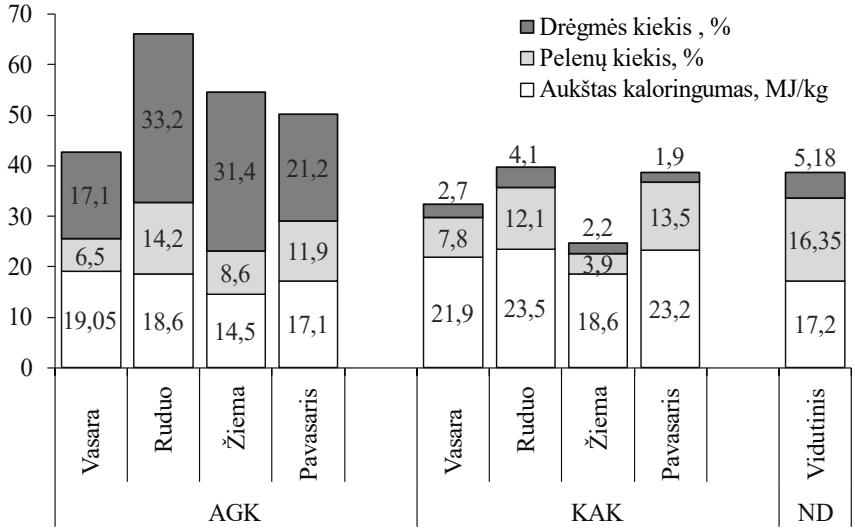

5 pav. AGK, kietojo atgautojo kuro (KAK) ir nuotekų dumblo (ND) sezoninių tyrimų rezultatai.

Pagaminto KAK drėgnis neviršija leistinų ribų, nustatytų kurui iš atliekų (1,9–4,1%). KAK šilumingumas yra gana didelis ir gali konkuruoti su kietuoju kuru. Nuotekų valymo įrenginių dumblas, paruoštas naudoti kaip pakaitinis kuras, yra gana aukšto šilumingumo (17,2 MJ/kg), drėgmės kiekis – 5,18%, pelenų kiekis aukštas, lyginant su KAK (16,35%).

Chloro ir gyvsidabrio kiekis taip pat yra esminis veiksnys, kuris turi būti nuolat stebimas dėl aplinkosauginių ir techninių priežasčių. Chloro kiekis AGK mėginiuose svyravo nuo 1,18 iki 1,04%; paruoštame KAK chloro kiekis buvo daug mažesnis ir siekė 0,16–0,53% (**6 pav.**). Palyginti mažą chloro kiekį pagamintame KAK lemia tai, kad kure nėra draudžiamų chloro turinčių plastikų. Gyvsidabrio kiekis AGK mėginiuose svyravo nuo 0,26 iki 0,4 mg/kg^{-1}, priklausomai nuo sezono ir atitinkamai nuo tam tikru sezonu susidarančių atliekų morfologinės sudėties. Gyvsidabrio kiekis pagamintame KAK buvo mažesnis nei AGK ir svyravo nuo 0,22 iki 0,3 mg/kg^{-1}.

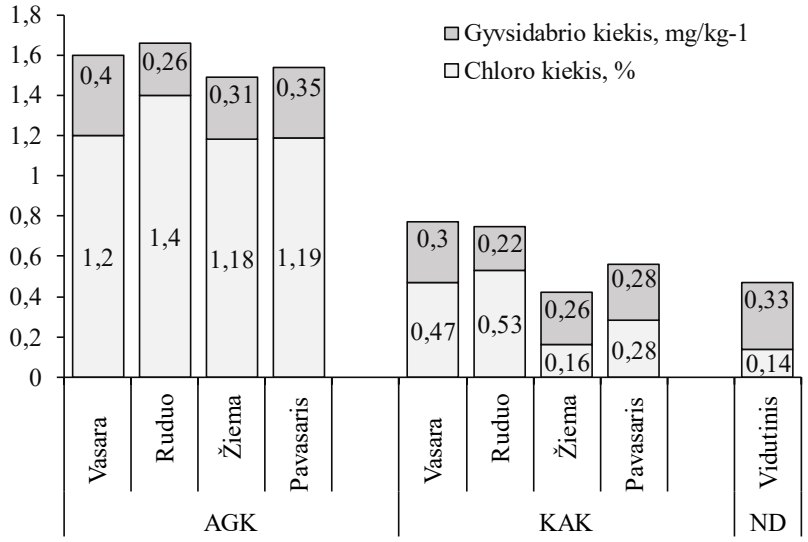

6 pav. Chloro ir gyvsidabrio kiekis iš atliekų gautame kure ir kietajame atgautajame kure.

Remiantis tyrimų, atliktų siekiant nustatyti pagrindines alternatyvaus kuro cemento pramonei charakteristikas, rezultatais buvo nustatyta, kad:

– Kauno MBA gautas AGK turi šiluminių ir energetinių savybių ir gali būti naudojamas deginti kogeneracinėje jėgainėje. Degioji AGK frakcija gali būti naudojama tik šilumai ir elektrai gaminti ir negali būti naudojama kaip alternatyvus kuras daug energijos naudojančiose pramonės šakose, nes joje yra daug drėgmės, chloro ir gyvsidabrio;

– pagamintas KAK, pašalinant draudžiamas medžiagas, smulkinant, sijojant ir džiovinant yra kokybiškesnis nei AGK. Pagamintas KAK įvertintas pagal standartą EN 15359 ir gali būti naudojamas kaip pakaitinis kuras cemento pramonėje. Nustatyta, kad KAK gamybos metu medžiagų drėgnumas sumažėja 85%, o gauto produkto tūris – 18%.

Į esamą MBA liniją papildomai įvedus šešis įrangos blokus, galima sukurti KAK gamybos iš AGK technologinę liniją, apskaičiuojant jos našumą, kuris siektų 4,47 tonos per valandą (**7 pav.**).

Pasiūlytoje KAK gamybos linijoje būtų šeši papildomi įrenginiai. Biologiškai skaidi ir smulki inertinė frakcija bus pašalinama pirmajame būgniniame siete. Po to degioji frakcija bus smulkinama (d<40 mm); stambesnės medžiagos, kurios nėra susmulkintos, keliauja į antrą būgninį sietą homogenizavimui ir degumo savybių pagerinimui. Toks dvigubas sijojimas būgno sietuose užtikrina reikiamą KAK dydį, nes didesnės dalelės siunčiamos į gamybos linijos pradžią. Siekiant sumažinti metalų buvimą KAK, susmulkintos medžiagos praeina per separatorius metalų atgavimui. Paskutiniame gamybos linijos etape medžiaga yra išdžiovinama būgninėje kameroje.

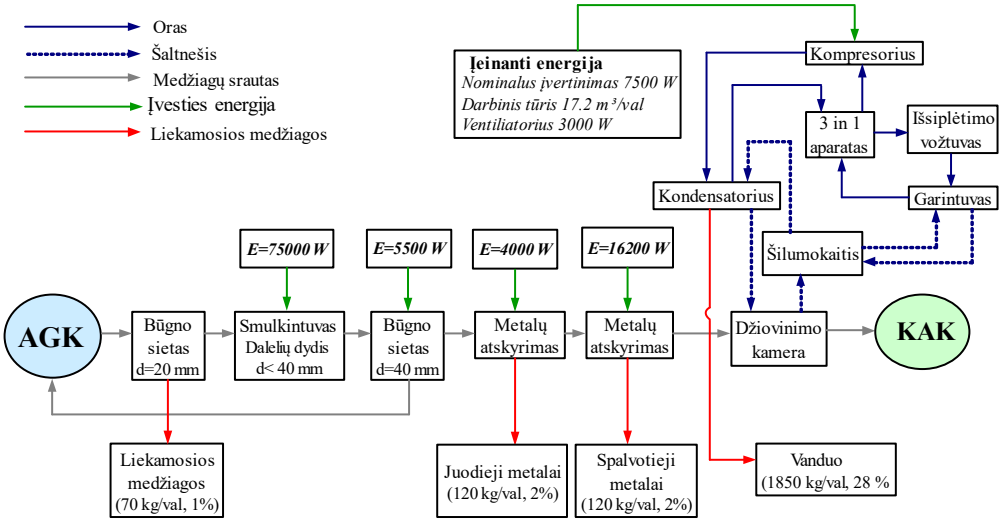

7 pav. Kietojo atgautojo kuro (KAK) gamybos linija.

KAK naudojimas kartu su šiuo metu naudojamu nuotekų dumblu, kuris elementinės ir oksidų sudėties požiūriu atitinka gauto klinkerio oksidų sudėtį, yra pagrįstas. Eksperimentiškai įrodyta, kad pelenai, gauti deginant KAK ir nuotekų dumblą, yra kristalinės struktūros ir susideda iš natrio, kalcio, kalio, geležies ir silicio turinčių fazių **(1 lentelė).**

1 lentelė. Elementų oksidų analizė (%, pelenuose), pagrįsta SEM-EDS matavimais

Oksidai / **Produktai**	**CaO**	**Fe_2O_3**	**SiO_2**	**P_2O_5**	**Al_2O_3**	**SO_3**	**MgO**	**Na_2O**	**TiO_2**	**K_2O**	**Cr_2O_3**	**CuO**	**MnO**	**ZnO**
Nuotekų dumblas	32,8	19,3	12,6	20,2	3,8	4,3	2,2	0,9	0,8	1,2	0,1	0,2	1,7	
KAK	30,5	8,8	35,5	1,3	8,7	2,6	3,7	5,5	1,6	0,7	0,1	0,4		0,6
Klinkeris	65,5	3,0	23,0	0,2	6,0	0,2	2,8	0,3	0,2	0,3				

Dominuojantys elementai Si ir Ca yra du pagrindiniai elementai klinkerio gamyboje. Taip pat pastebėti Al, Fe, Mg ir kiti cemento pramonei svarbūs elementai. Tačiau reikia pažymėti, kad oksidų procentas KAK, nuotekų dumble ir klinkeryje skyrėsi. Galima daryti išvadą, kad KAK gali būti naudojamas kaip kuras gaminant klinkerį ir nuotekų dumblą, tačiau tam tikra dalimi. Taip yra todėl, kad kai kurių oksidų (Al, Fe, Na, P) kiekis turi būti griežtai kontroliuojamas.

Siekiant įvertinti SRF naudojimo ekonominę naudą, buvo pasiūlytos keturios KAK naudojimo kaip pakaitinio ir pridėtinio kuro galimybės. Ekonominiam KAK priedo prie pagrindinio kuro (anglies) vertinimui buvo pasirinkti įvairūs variantai: 10, 15, 20 ir 25 proc. Naudojant KAK vietoj anglies, sumažinamos jos sąnaudos ir iškastinių išteklių naudojimas bei šiltnamio efektą sukeliančių dujų emisijos. Pasaulio banko duomenimis, naudojant 10 proc. KAK kaip pakaitinį kurą klinkerio degimo proceso metu, Lietuva gali pasiekti tokį CO_2 išmetimo lygį kaip Estija (10175,4 kt). Tačiau naudojant 25 proc. KAK vietoj akmens anglių, Lietuva gali priartėti prie Latvijos išmetamo CO_2 kiekio (7569,2 kt).

5.4.2. Atliekų iškasimo iš sąvartyno ir KAK gamybos iš jų galimybių vertinimas (2 straipsnis)

Šiais tyrimais buvo įvertintos energijos gamybai tinkamų žaliavų atgavimo iš sąvartynų galimybės ir sukurta KAK, skirto naudoti kaip kuro pakaitalas cemento pramonėje, gamybos linijos koncepcija. Moksliniais tyrimais įrodyta, kad energijos gamybai tinkamas žaliavas iš sąvartynų galima išgauti sukūrus ES standartą atitinkantį KAK gamybos mechanizmą. KAK gamybai siūloma naudoti dviejų stadijų mechanizmą: pirmoji stadija gali būti vykdoma sąvartyno teritorijoje (smulkios frakcijos, inertinių medžiagų ir stambiagabaričių atliekų pašalinimas pirminio sijojimo būdu), o antroji stadija gali būti vykdoma naudojant MBA esančią įrangą, kurioje antrinio sijojimo būdu papildomai pašalinamos smulkios ir draudžiamos medžiagos, išskiriamas metalas, smulkinamos ir džiovinamos degiosios frakcijos **(8 pav.)**.

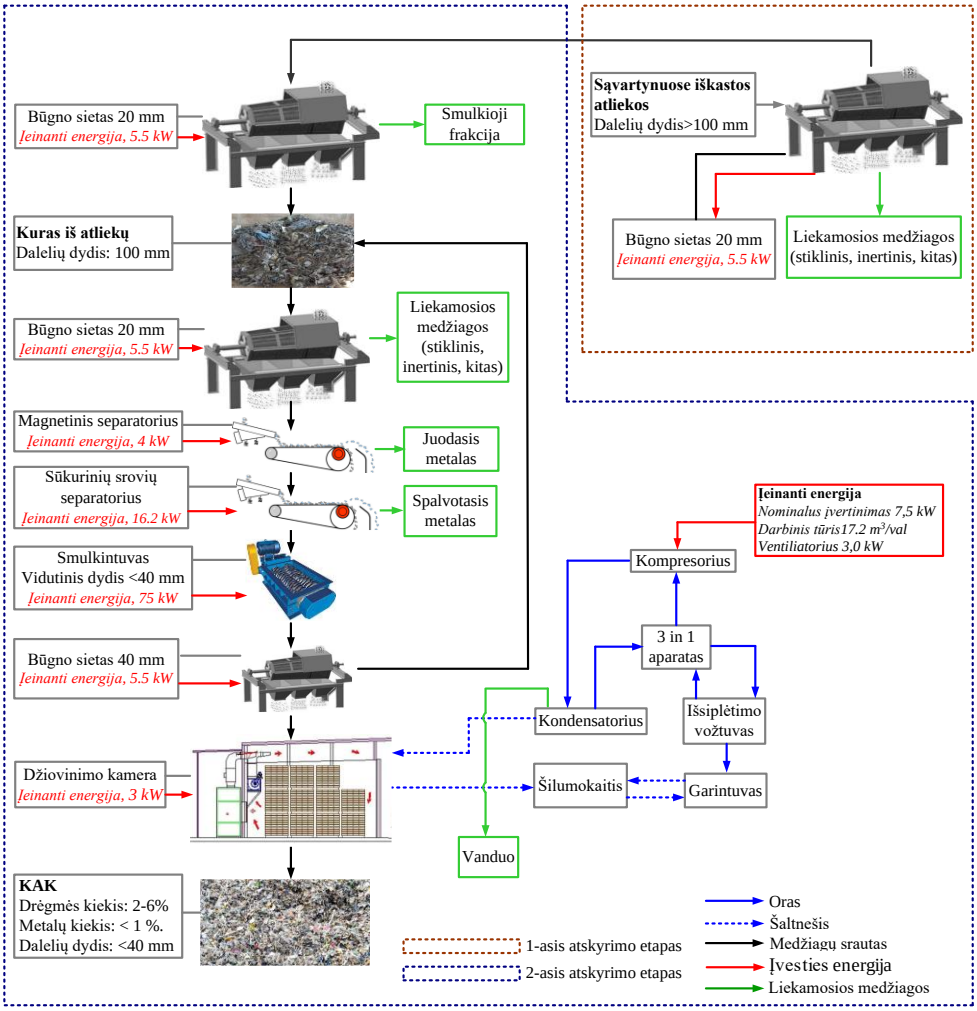

8 pav. KAK gamybos linija.

Sukurtą atliekų iškasimo iš sąvartyno ir KAK gamybos mechanizmo koncepciją sudaro dvi stadijos. Pirmojoje būgniniu sietu (sąvartyno teritorijoje) atskiriamos didžiosios inertinės medžiagos ir smulkioji frakcija. Nuo iškastų atliekų atskirtos smulkios frakcijos kiekis buvo 43%. Antrojoje paskutinėje KAK gamybos stadijoje Kauno MBA teritorijoje siūloma atskirti likutinę smulkiąją frakciją antriniu sijojimu pašalinant dar 50% smulkios frakcijos. Antrojo etapo pabaigoje smulkios dalelės tesudaro 1,3%. Antrasis etapas apima šešias papildomas įrangos dalis, kurių kiekviena atlieka svarbų vaidmenį.

Nustatyta, kad sąvartyno kasybos produktų (SKP) stambiąją frakciją sudaro tokios įprastos degios frakcijos kaip minkštasis plastikas, mediena, kietasis plastikas, popierius, guma ir kiti degūs komponentai, kurie gali būti išgaunami iki 10 m gylyje **(9 pav.)**.

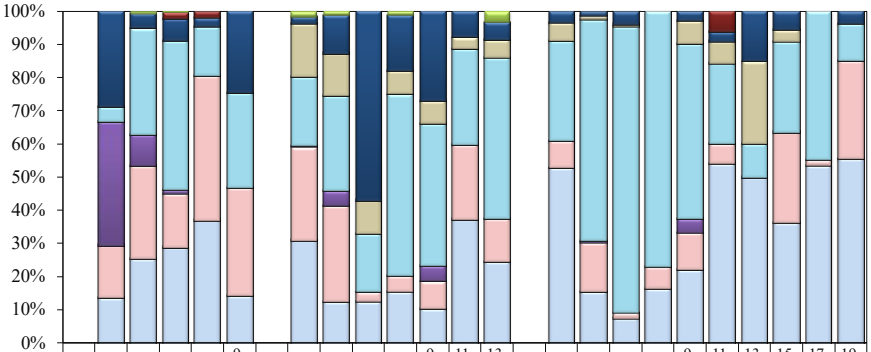

	I	1-2	3-4	5-6	7-8	9-10	II	1-2	3-4	5-6	7-8	9-10	11-12	13-14	III	1-2	3-4	5-6	7-8	9-10	11-12	13-14	15-16	17-18	19-20
Daugiasluoksniai kompozitai			0,6	0,3				1,6	1,1		1,1			3,3											
Kitos				1,8	2,0																6,0				
Mediena		28,6	4,5	6,6	2,6	24,6		2,1	11,4	56,8	16,8	26,9	7,7	5,3		3,3	1,3	3,7		2,8	3,0	15,0	5,5	0,0	3,7
Popierius								16,1	12,8	10,2	7,0	6,7	3,5	5,3		5,7	1,1	0,9		6,9	6,6	25,0	3,6	0,0	0,0
Tekstilė		4,7	32,0	44,9	14,9	28,4		20,9	28,7	17,4	54,7	43,0	28,9	48,6		30,1	66,6	86,0	76,9	52,8	24,1	10,0	27,3	44,6	11,1
Guma		37,2	9,6	1,3				0,3	4,5			4,7					0,7			4,2					
Kietasis plastikas		15,8	28,0	16,1	43,5	32,6		28,0	29,0	2,9	4,9	8,3	22,5	13,1		8,1	14,8	1,9	6,6	11,1	6,0		27,3	1,8	29,6
Minkštas plastikas		13,7	25,4	28,9	37,1	14,4		31,1	12,5	12,7	15,4	10,4	37,3	24,5		52,8	15,5	7,5	16,5	22,2	54,2	50,0	36,4	53,6	55,6

9 pav. Sąvartyno degiosios frakcijos sudėtis.

Gautas KAK pagal pagrindinius parametrus (šilumingumas, chloro ir gyvsidabrio kiekis) priklausys III klasei. Gamybos linijos gale gaunamas alternatyvus kuras, kurio charakteristikos nurodytos **10 pav**. Smulkios frakcijos, drėgmės kiekio (DK), peleningumo (P), lakiosios dalies (LD ir žemutinio šilumingumo (ŽŠ) vertės atitinkamai lygios 1,3% (pagal masę), 2,5% (pagal masę), 44,3% (pagal masę), 8% (pagal masę) masės ir 16 MJ/kg. Gauti duomenys rodo, kad smulkiosios frakcijos atskyrimas dvigubai sijojant žymiai pagerina gaunamo KAK charakteristikas.

Kuras – tai angliavandenilių mišinys, turintis anglies (C), vandenilio (H) ir tam tikrą kiekį sieros (S), azoto (N), deguonies (O) ir mineralų, kuriame C dalis yra nuo 20 iki 70% pagal masę, H – nuo 3 iki 8% pagal masę ir N – nuo 1 iki 1 iki 5% pagal masę. Kaip matyti 15 pav., pagamintas KAK yra geras C, H ir N santykių derinys degimui. Kalbant apie sierą, sieros dalis analizuojamose medžiagose buvo įprastas bet kokiam kurui nuo 0,2 iki 1% pagal masę.

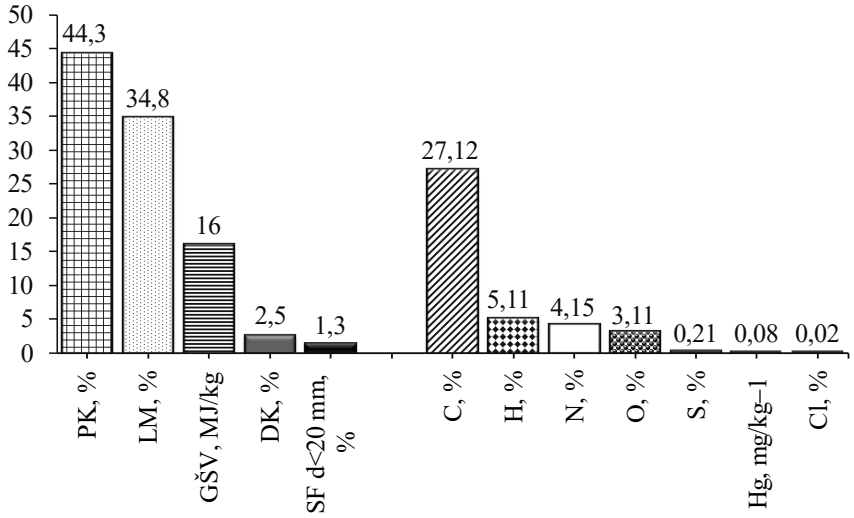

10 pav. Pagaminamo KAK charakteristikos.

Kalbant apie halogenus, nustatyta chloro dalis buvo 0,02% pagal masę, o gyvsidabrio kiekis neviršijo leistinų kurui iš atliekų ribų ir atitiko priimtinus naudojimo cemento krosnyse standartus.

KAK deginimo metu gauti pelenai yra kristalinės struktūros, juose yra Ca, Na, K, Fe ir Si turinčių fazių, kas atitinka klinkerį formuojančius mineralus **(11 pav.).** Medžiagų struktūra ir granuliometrinės charakteristikos yra susijusios su pelenų kristalinės struktūros ypatumais. Morfologija suteikia informacijos apie mineralų susidarymo sąlygas ir naudojama joms nustatyti. Mūsų atveju pelenų dalelių atspalvis įvairiai kinta nuo šviesiai pilkos iki tamsiai pilkos ir joms būdinga lamelinė-kristalinė forma. Pelenų dalelių dydis kinta nuo 1 iki 20 μm ir nėra tolygiai pasiskirstęs.

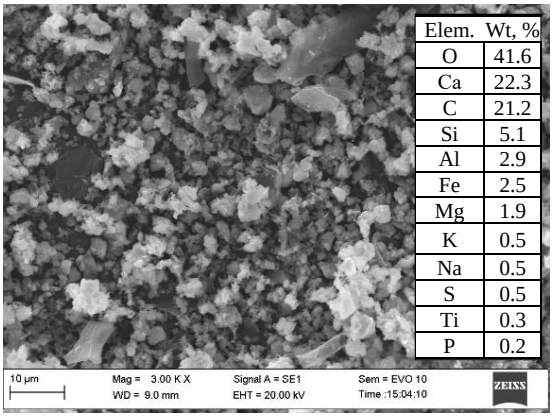

11 pav. Pelenų po KAK deginimo SEM vaizdas ir EDS analizė.

Pelenų, gautų sudeginus iš sąvartyno iškastas atliekas, rentgeno struktūrinė analizė patvirtino klinkerį formuojančių mineralų buvimą visose pasirinktose sąvartyno sekcijose ir gyliuose **(12 pav.)**. Rentgeno struktūrinės analizės būdu rasta kvarco (SiO_2), akermanito ($Ca_2Mg(SiO_2O_7)$, perovskito ($CaTiO_3$), hematito (Fe_2O_3),

mikroklino ($KAlSi_3O_8$), diopsido ($CaMg(Si_2O_6)$), volastonito 1A ($CaSiO_3$), anhidrito $CaSO_4$, lisetito ($CaNa_2Al_4Si_4O_{16}$), augito ($Ca_xMg_yFe_z)(Mg_{y1}Fe_{z1})\cdot SiO_6$) ir anortito ($Ca(Al_2Si_2O_8)$).

Išsamiai ištyrus Kauno regioninio sąvartyno atliekų sudėtį, buvo apskaičiuotas tirtų sąvartyno sekcijų energetinis potencialas. Remiantis tyrimų rezultatais, atliekas rekomenduojama kasti iš sąvartyno, kurio gylis yra iki 10 m imtinai. Atliekų kasyba iš didelio gylio nėra pagrįsta ir neturi teigiamų perspektyvų. Nagrinėjamų sąvartyno dalių energetinio potencialo skaičiavimai siekė 196,700 GJ.

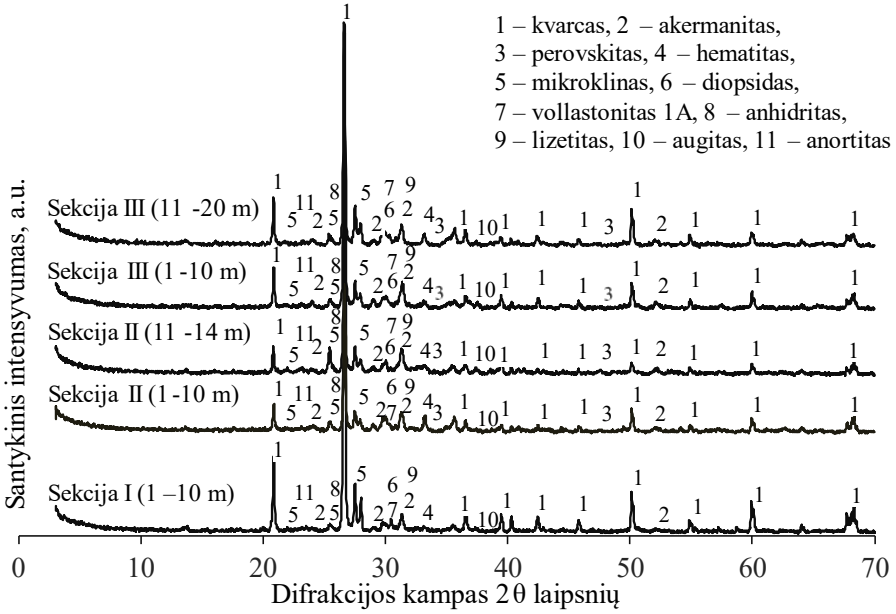

12 pav. KAK deginimo pelenų XRD analizė.

Patvirtintas KAK kaip pakaitinio kuro naudojimo klinkerio deginimo procese ekonominis ir aplinkosauginis pagrįstumas. Alternatyvaus kuro gamyba ir naudojimas energijai imliose pramonės šakose priartins Lietuvą prie žiedinės ekonomikos tikslų, naudojant anksčiau sąvartynuose pašalintas medžiagas ir paverčiant jas energijos ištekliais.

5.4.3. Dugno pelenų kaip pakaitinio komponento panaudojimo molio plytų gamyboje galimybių vertinimas (3 straipsnis)

Ištirta KAK deginimo dugno pelenų (DP) panaudojimo molio plytų gamybai galimybė.

Nustatyta, kad molyje ir DP esantys cheminiai elementai didelės grėsmės aplinkai nekelia, nes juose nėra sunkiųjų metalų. **13 pav**. pateikti DP ir molio kiekybinės elementinės analizės rezultatai. Dugno pelenai priskiriami nepavojingoms atliekoms ir gali būti naudojami kaip priedas plytų gamyboje.

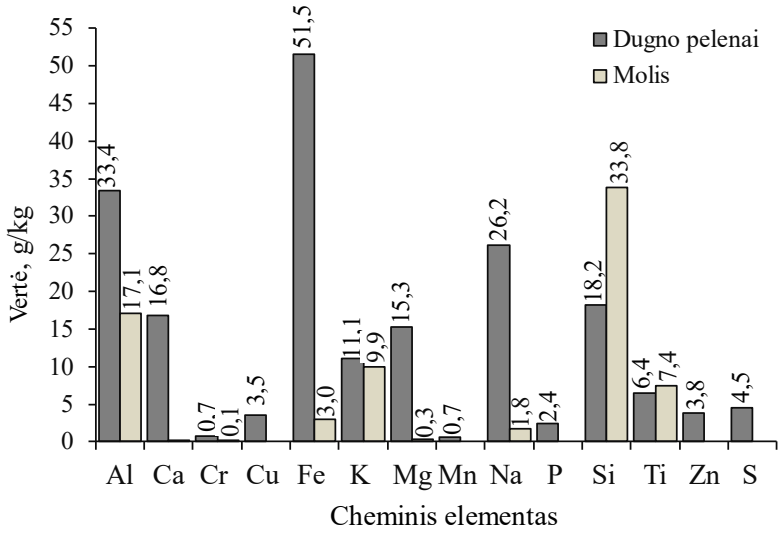

13 pav. Dugno pelenų ir molio elementinės kiekybinės analizės rezultatai (*reikšmė dauginama iš 10).

Ištirta DP įtaka molinių plytų fizikinėms ir mechaninėms savybėms, mėginių mikro- ir struktūrai, atsparumui užšalimui ir atšildymui, poringumui, vidutiniam porų dydžiui ir porų dydžio pasiskirstymui **(14 pav.).**

Dėl DP priedo pakito molinių plytų fizinės ir mechaninės savybės: sumažėjo susitraukimas, tankis ir gniuždymo stipris, padidėjo vandens įgeriamumas ir atviras poringumas. Įvertinti molinių plytų atvirojo poringumo pokyčiai pridedant DP.

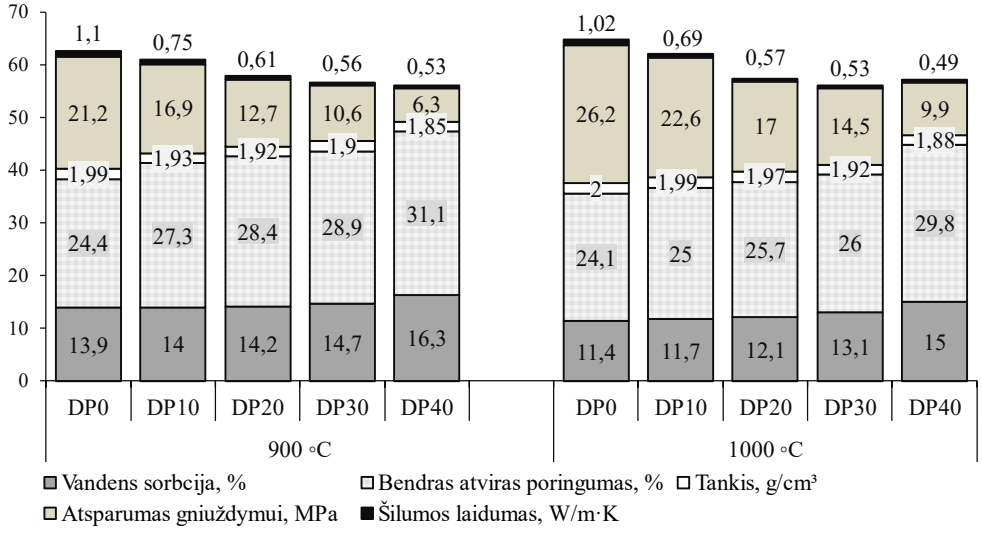

14 pav. Molio plytų pavyzdžių savybės.

Rentgeno struktūrinėje analizėje taikant Rietveldo patikslinimo metodą 900 ir 1000 °C temperatūrose iškaitintiems mėginiams su ir be DP priedu, buvo nustatyti kvarcas, ilitas, muskovitas 2M1, anortoklazė, mikroklinas, kristobalitas, volastonitas,

akermanitas, melilitas, gelenitas, rutilas, hematitas, labradoritas ir diopsidas, kurių skirtingus kiekius lemia priedo kiekis ir degimo temperatūros.

Plytų medžiagos struktūra susiformuoja kristalizacijos stadijose. Šią struktūrą sudaro izoliuotos arba tarpusavyje sujungtos vienodų arba skirtingų formų ir dydžių poros. Pagal IUPAC klasifikaciją molinių plytų, degintų 900 ir 1000 °C temperatūrose, porų dydžiai atitinka II tipo izotermes (neakytos arba makroporingos medžiagos), o pagal mėginių histerezės kilpą mėginiai klasifikuojami kaip H3 ir jiems būdingos į plyšį panašios poros. H3 histerezės desorbcijos kreivė turi nuolydį, susijusį su atsparumo tempimui histerezės kilpa[43]. Porų dydžio pasiskirstymo tyrimai rodo skirtingą tendenciją, kai DP molyje yra nuo 10 iki 40%, o degimo temperatūros yra 900 ir 1000 °C. BET metodu pagrįsti tyrimai buvo atlikti naudojant azotą kaip adsorbatą 77,35 K temperatūroje. Porų skersmens ir paviršiaus ploto santykis buvo nustatytas DFT metodu **(15 pav.)**.

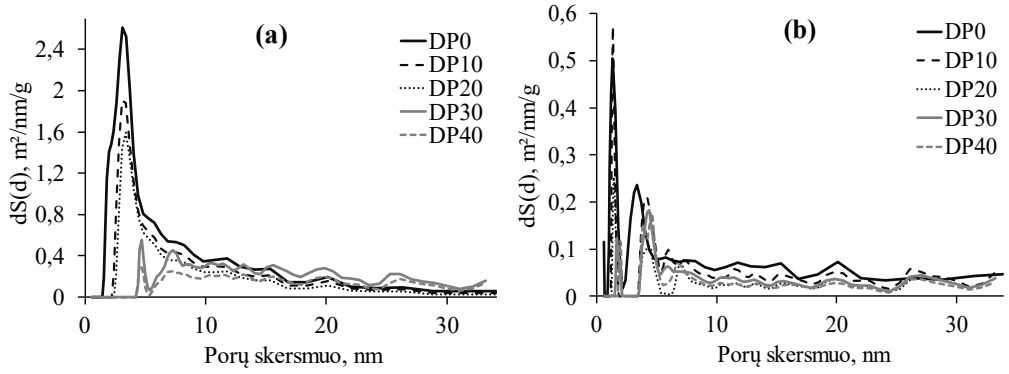

15 pav. Porų dydžio pasiskirstymo analizė pagal N_2 adsorbciją: **(a)** bandiniai išdeginti 900 °C temperatūroje, **(b)** išdeginti 1000 °C temperatūroje.

Nustatyta, kad bandiniuose, išdegintuose 900 °C temperatūroje, vyrauja mezoporos, o išdegintuose 1000 °C temperatūroje ir nesant DP priedo – mikroporos.

Nustatyta, kad 900 °C temperatūroje išdegintų bandinių be 10 ir 20% DP priedo vidutinis porų skersmuo yra pastovus (3, 4 nm). Tačiau padidinus DP priedą (30 ir 40 %) ir esant tokiai pačiai išdegimo temperatūrai, vidutinis mėginių porų skersmuo padidėjo ir sudarė atitinkamai 26,1 ir 33,2 nm. Mėginiai, išdeginti 1000 °C temperatūroje, turėjo skirtingą priklausomybę nuo vidutinio porų skersmens. Mėginių be DP priedo porų skersmuo buvo 36 nm. Dėl DP priedo prie molio (10, 20, 30 ir 40 %) porų skersmuo sumažėjo ir sudarė 33,2 nm.

30 ir 40% DP priedas ir išdeginimas 900°C temperatūroje lemia cilindrinių porų susidarymą ir padidėjusį porų skersmenį. Tai parodo tankesnė išdegtų mėginių struktūra. Plyšio formos poros buvo nustatytos išdegus 1000 °C temperatūroje išdegtuose mėginiuose be DP priedo ir su 10 bei 20% priedu. Porėtumas buvo didesnis išdegintuose mėginiuose su 30 ir 40% DP priedu **(16 pav.)**.

Tokiu būdu buvo eksperimentiškai patvirtinta galimybė molį iš dalies pakeisti 10–20% DP, išdeginant 900 °C temperatūroje arba 10–30% DP, išdegant 1000 °C temperatūroje.

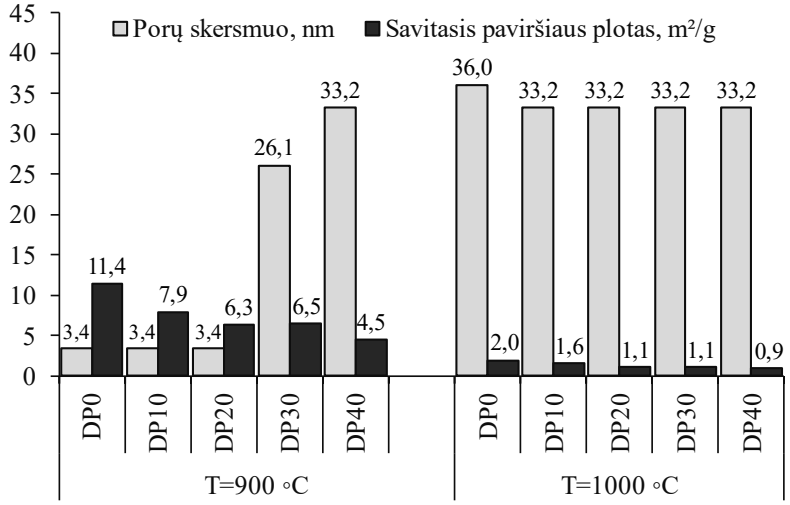

16 pav. N_2 adsorbcijos matavimų DFT metodu molio plytoms rezultatai.

Pirmojo tipo molio plytos gali būti naudojamos vidutiniškai agresyvioje aplinkoje, o antrojo – pasyviai agresyvioje aplinkoje (pagal atsparumo šalčiui matavimą). DP panaudojimas molinių plytų gamyboje leis gaminti molines plytas nepakenkiant jų kokybei ir iki 30% sumažinant gamtos išteklių sunaudojimą. Gaminant tokio tipo statybines medžiagas su priedu, sumažės po deginimo susikaupusių atliekų – neperdirbamos KKA dalies šalinimas sąvartynuose.

5.4.4. Biomasės ir dumblo dujofikavimo pelenų kaip dalinio cemento pagrindo medžiagų pakaitalo panaudojimo galimybių pagrindimas (4 straipsnis).

Ištirtos pelenų liekanų, gautų dujofikuojant nuotekų dumblo su biomase, dvikomponenčių mišinių su mikrosilicio dioksido dalelėmis, kaip pakaitinio rišiklio komponento cemento pagrindo medžiagose panaudojimo galimybės.

Nustatyta, kad cemento pakeitimas abiem pakaitalais padidina hidratacijos produktų kiekį ir lemia ankstesnį *CH* sunaudojimą, nei kompozicijose, kuriose kaip pakaitalas naudojamas tik mikrosilicio dioksidas **(17 pav.).**

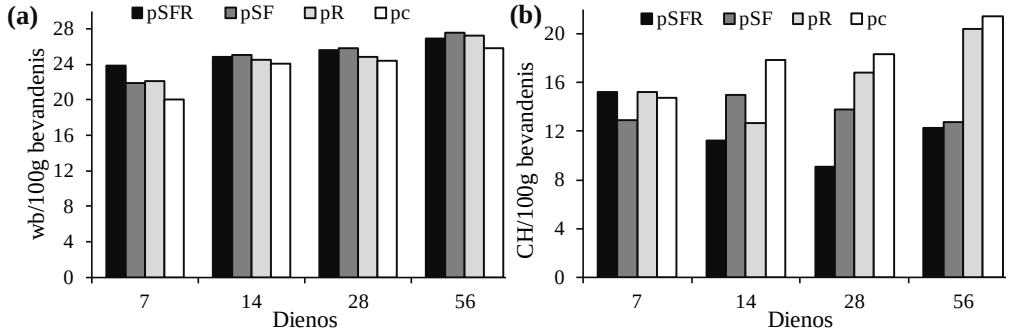

17 pav. Normalizuoto iki 100 g bevandenio kiekio **(a)** surišto vandens (*wb*) ir **(b)** portlandito (*CH*) išsiskyrimas.

Abiejų pakaitalų įvedimas paskatino amorfiškesnės *CSH* fazės, sumaišytos su adatų formos hidratais (etringitu ir kalcio fosfatu), susidarymą. Etaloninių ir sumaišytų cemento pastų frakcijų paviršių SEM vaizdai po 56 dienų hidratacijos pateikti **18 pav**. Elementinė sudėtis taip pat pateikiama kartu su kristalų analizės rezultatais. Po dviejų hidratacijos mėnesių (**18 pav**.) portlandito kristalai mikrosilicio dioksido pastoje yra gana maži, be aiškiai apibrėžtų kraštų, nes pucolanas juos iš dalies sugeria. Masyvūs *CH* kristalai matomi etaloninėje pastoje ir pastoje su dujinimo liekanomis. (**18 a, c pav.**).

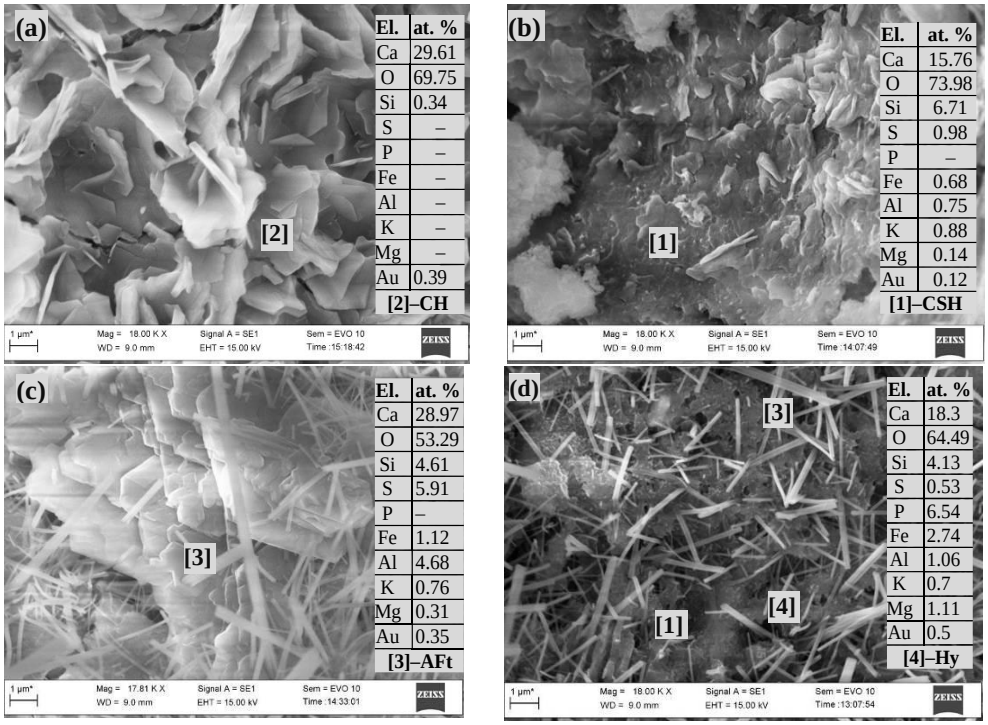

18 pav. Sumaišytų cemento pastų, hidratuotų 56 dienas, SEM vaizdai **(a)** PC, **(b)** pSF, **(c)** pR ir **(d)** pSFR.

Tačiau įvairaus storio (*AFt*) adatų formos hidratai daugiausia buvo randami mišiniuose su liekanomis ir jų nebuvo etaloninėje pastoje. *AFt* susidarymas susijęs su dideliu sulfatų kiekiu pelenuose (≈23%). Po 56 dienų nuotekų dumblo pelenų turinčiose sistemose dėl ištirpusios amorfinės pelenų fazės ir chemiškai surišto vandens iškrito *AFt* kristalai. Kalcio turinčių fosfatų junginių susidarymas (pridedant nuotekų dumblo pelenų) gali padidinti kompozicijų atsparumą gniuždymui. pSFR mėginiuose buvo rasta amorfinė fazė ir adatų formos hidratai. Tačiau fazės elementinė sudėtis buvo panaši į *CSH* gelių sudėtį; jos vizualinė forma ir bendras poringumas skyrėsi nuo tų, kurie buvo stebimi pSF sistemoje.

Mikrosilicio dioksido ir liekanų sinergija labiausiai lemia mikro- ir mezoporų (iki 40 nm), atspindinčių *CSH* struktūrą, bei mažų kapiliarinių porų gausumą. Gelio porų buvimas yra susijęs su pucolaninėmis reakcijomis ir hidratacijos greičiu, o vidutinės ir didelės kapiliarinės poros turi įtakos struktūros pralaidumui ir stiprumui.

Lyginamasis cemento pakaitalų poveikio porų tūrio kitimui hidratacijos metu įvertinimas parodė, kad porų tūris pSFR pastoje mažėja gana greitai 28 dienų laikotarpiu, kai porų dydis yra didesnis nei 12 nm. Ilgesnis hidratacijos laikotarpis daugiausia paveikia porų sritį iki 20 nm, kuri yra jautri hidratacijos produktų susidarymui ir pakavimo tankiui. Nustatyta, kad mišriųjų kompozicijų su silicio dioksido dūmais santykinio porų tūrio vertės yra didesnės nei etaloninės pastos. Taigi, porų tūrio sumažėjimas rodo porų struktūros pagerėjimą, kas yra įmanoma dėl pucolano arba reaktyviosios fazės komplekso gebėjimo užpildyti porų erdvę hidratacijos produktais. Šiuos teiginius patvirtina didžiausias portlandito sunaudojimas pSFR sistemoje, kai per 56 dienas susidarė per daug adatos formos hidratų.

Patvirtinta, kad kapiliarinio vandens sugertis priklauso nuo bendro cemento pakeitimo lygio ir hidratacijos laiko, o ne nuo liekanų ir mikrosilicio dioksido (R/SF) santykio. Įvedus abu pakaitalus, sorbcijos pajėgumas sumažėja nuo 24 iki 56%. Nustatyta, kad skiedinių atsparumas gniuždymui mažėja didėjant R/SF santykiui, o atsparumas lenkimui mažiau priklauso nuo pakaitalų balanso **(19 pav.)**.

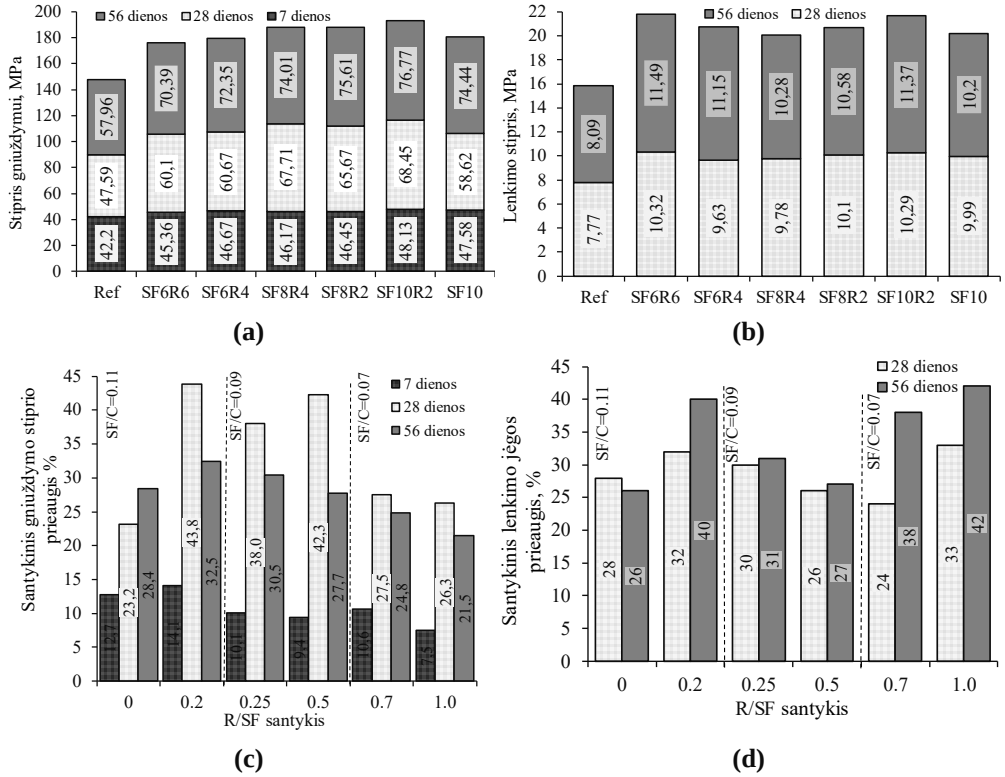

**SF/C – silicio dioksido dūmų ir cemento santykis, R/SF – dujinimo likučio ir silicio dioksido dūmų santykis

19 pav. Skiedinio mėginių gniuždymo **(a)** ir lenkimo **(b)** stiprumo rezultatai (vidutinis); gniuždomojo **(c)** ir lenkimo **(d)** stiprumo padidėjimo palyginimas su etaloniniu skiediniu.

Cemento pagrindu susidariusias atliekas paverčiant medžiagomis, reikia atsižvelgti į poveikį aplinkai. Remiantis tuo, CO_2 emisijos įvertis pasirenkamas kaip pagrindinis atliekų susidarymo potencialo vertinimo parametras. Nustatyta, kad tyrime naudotas mikrosilicio dioksidas buvo gana brangus, todėl mišrių mėginių kaina, palyginti su etaloniniu mėginiu, padidėjo 6%. Galiausiai dėl padidėjusio liekanų kiekio savikainos vertė sumažėjo 3%.

Nustatyta, kad įvedus abiejų rūšių atliekas CO_2 emisija sumažėjo 10–15 proc. CO_2 emisija buvo mažesnė mėginiams, kuriems cemento pakeitimo lygis buvo 12%, lyginant su 10%. Buvo įvertintas pasirinktų mineralinių priedų efektyvumas, derinant poveikį aplinkai su mechaniniu atsparumu. Kompozicijos, sumaišytos su liekanomis, skleidžia tik tokias pat emisijas kaip ir cemento pakeitimas mikrosilicio dioksidu (R/SF=0). Be to, nustatyta, kad dėl mažo duomenų išbarstymo mėginiams, kuriuose cemento pakeitimo lygis yra 10% ir 12%, R/SF santykis 0,5–1,0 gali būti laikomas gera pakaitalų charakteristika aplinkosauginiu ir inžineriniu požiūriais. Nepaisant pagerėjusio atsparumo, žemas vandens sugėrimo lygis, gautas naudojant kompozicijas, kurių R/SF>0,5, rodo, kad dujofikavimo liekanas kartu su silicio dioksido dūmais galima taip apdoroti, kad jos būtų tinkamos lietaus grotelių arba cemento pagrindo plokščių gamybai.

Ištirtas dviejų rūšių atliekų, nuotekų dumblo ir biomasės dujinimo liekanų ir mikrosilicio dioksido, panaudojimo cementui pakeisti potencialas. Išnagrinėtas jų sinerginis poveikis hidratacijai ir statybinių medžiagų savybėms. Apskaičiuotos sąnaudos ir nustatytos CO_2 emisijos parodė, kad bendras cemento pakeitimo santykis gali būti padidintas iki 12%, kur 4–6% sudaro dujinimo liekanos, nesumažinant mechaninio atsparumo. Tuo pačiu sumažinus mikrosilicio dioksido kiekį (iki 6 proc.) būtų sutaupomi ir ištekliai. Apibendrinant galima teigti, kad skiedinio sudėtis, pakeičiant cementą 6% liekanų ir 6% mikrosilicio dioksido mišiniu, atrodo naudinga, nes sumažintų portlandcemenčio ir mikrosilicio dioksido išteklius.

5.5. Išvados ir rekomendacijos

5.5.1. Išvados

1. Nustačius pagrindines MBA proceso metu išskiriamo iš atliekų gauto kuro (AGK) charakteristikas, paaiškėjo, kad AGK gali būti deginamas tik kogeneracinėse jėgainėse šilumos ir elektros gamybos tikslais. Buvo nustatyta, kad, remiantis klasikiniais reikalavimais, iš AGK gaunamas KAK yra geros kokybės ir gali būti panaudojamas kaip pakaitinis kuras klinkerio išdegimo procese. Pagamintas KAK pagal ES standartus priklauso III kategorijai. Buvo nustatyta, kad KAK deginimo pelenai yra kristalinės struktūros ir turi klinkerio formavimo mineralas. Buvo sukurta KAK gamybos linijos koncepcija ir apskaičiuotas jos produktyvumas, kuris siektų 4,47 t/val. Buvo nustatyta kad KAK gamybos proceso metu medžiagų drėgmė sumažėja 85%, o galutinio produkto tūris – 18%. Įvertinta, kad KAK kaip pakaitinio kuro cemento krosnyje panaudojimo ekonominis ir aplinkosauginis efektyvumas yra iki 25 %.
2. Tyrimais įrodyta, kad energijos gamybai tinkamų medžiagų atgavimas iš sąvartynų yra įmanomas sukūrus KAK gamybos iš sąvartynų kasybos produktų (SKP) mechanizmą. Buvo pasiūlytas dviejų etapų KAK gamybos mechanizmas:

pirmasis etapas gali būti vykdomas sąvartyno teritorijoje, antrasis – panaudojant MBA įrangą. Tapo akivaizdu, kad SKP stambiojoje frakcijoje esama degių subfrakcijų, tokių kaip plastikas, mediena, popierius, guma ir kitos, kurios gali būti atgaunamos gylyje iki 10 m. Gauto KAK pelenai turi kristalinę struktūrą ir, remiantis elementine ir oksidų sudėtimi, atitinka pagaminto klinkerio sudėtį.

3. Molio plytų pavyzdžiai, kuriuose yra iki 20% KAK dugno pelenų (DP) kaip pakaitinio komponento ir kurie išdegami 900 °C temperatūroje, gali būti naudojami vidutiniškai agresyvioje aplinkoje ir priklauso F1 klasei. Molio plytos su 30% tų pačių DP vietoj molio, kurios išdegamos 1000 °C temperatūroje, gali būti naudojamos pasyviai agresyvioje aplinkoje ir priklauso F0 klasei. Molio plytų gamyboje naudojant 30% DP kaip pakaitinį komponentą, bus galima pagaminti 1000 vienetų standartinio dydžio molio plytų nepabloginant jų kokybės ir sunaudojant 1,31 tonos mažiau gamtinių išteklių.
4. Buvo nustatyta, kad yra naudinga skiedinio sudėtyje cementą pakeisti 6% KAK dujinimo liekanomis ir 6% mikrosilicio dalelėmis, nes tai sumažintų cemento „Portland“ ir mikrosilicio dulkių kaip žaliavos naudojimą. Sąnaudų ir CO_2 emisijų apskaičiavimo rezultatai rodo, kad bendras cemento pakeitimo lygis gali padidėti iki 12%, 4–6%, padengtas dujinimo liekanomis ir 6% mikrosilicio dulkėmis, nepabloginant mechaninio atsparumo.

5.5.2. Rekomendacijos

1. Norint iš AGK pagaminti aukštos kokybės KAK, rekomenduojama iš kietųjų komunalinių atliekų pašalinti chloro ir gyvsidabrio turinčias medžiagas. Tai galima padaryti tik pašalinant Cl- ir Hg- turinčias medžiagas iš kietųjų komunalinių atliekų srauto.
2. Pirmajame smulkiosios frakcijos išskyrimo etape (sąvartyno teritorijoje) rekomenduojama naudoti inercinius sietus, o ne būgninį sietą. Tokio tipo sietai užtikrina medžiagos rūšiavimą ir tuo pačiu metu jos pernešimą per sietą.
3. Molio plytų gamyboje, dalį molio pakeičiant dugno pelenais, rekomenduojama naudoti mažai kalcio turinčius molius. Dugno pelenų sudėtyje yra palyginti didelis kalcio kiekis, kuris turi neigiamos įtakos galutinio produkto kokybei.
4. Kaip pakaitinį komponentą rekomenduojama naudoti 4–6% dujinimo dumblo.

REFERENCES

1. KAZA, S., YAO, L.C., BHADA-TATA, P., WOERDEN, F.V. What a Waste 2.0: A Global Snapshot of Solid Waste Management to 2050. Technical Report. World Bank. 2018. URL: http://hdl.handle.net/10986/30317.
2. ABDEL-SHAFY, H.I., MANSOUR, M.S.M. Solid Waste Issue: Sources. Composition. Disposal. Recycling. and Valorization. Egyptian Journal of Petroleum. 2018, 27(4), 1275–1290. https://doi.org/10.1016/j.ejpe.2018.07.003.
3. KHANDELWAL, H., DHAR, H., THALLA, A.K., KUMAR, S. Application of Life Cycle Assessment in Municipal Solid Waste Management: A Worldwide Critical Review. Journal of Clean. Prod. 2019, 209, 630–654. https://doi.org/10.1016/j.jclepro.2018.10.233.
4. OECD. 2020. Environment at a glance: Climate Change. https://www.oecd.org/environment/environment-at-a-glance/Circular-Economy-Waste-Materials-Archive-Jan uary-2020.pdf.Accessed: June 18, 2021.
5. Eurostat. 2021. Municipal Waste Statistics. https://ec.europa.eu/eurostat/statisticsexplained. Accessed: July 5. 2021.
6. LEE, P., SIMS, E., BERTHAM, O., SYMINGTON, H., BELL, N., PFALTZGRAFF, L., SJOGRE, P. Towards a Circular Economy – Waste Management in the EU. 2017. Technical Report. European Parliamentary Research Service. https://www.google.ru/url?sa=t&rct=j&q=&esrc=s&source=web&cd=&ved=2ahUKEwjn4t-Hzeb6AhUSgP0HHcjbBIEQFnoECAoQAQ&url=https%3A%2F%2Fwww.europarl.europa.eu%2FRegData%2Fetudes%2FSTUD%2F2017%2F581913%2FEPRS_STU%25282017%2529581913_EN.pdf&usg=AOvVaw3czn3OtXWlX6nu7Xfa52xy.
7. Vilnius cogeneration power plant https://vkj.lt/en/about-us/eu-funding/147.
8. Kaunas cogeneration power plant https://kkj.lt/en/about-us/power-plant/93.
9. Klaipeda cogeneration power plant https://gren.com/lt/.
10. CHO, B. H., NAM, B. H., AN, J., YOUN, H. Municipal Solid Waste Incineration (MSWI) Ashes as Construction Materials-A Review. Materials. 2020, 13(14), 3143. https://doi:10.3390/ma13143143.
11. TAURINO, R., KARAMANOVA, E., BARBIERI, L., ATANASOVA-VLADIMIROVA, S., at all. New fired bricks based on municipal solid waste incinerator bottom ash. Waste Management & Research. 2017, 35(10), 1–9. https://doi:10.1177/0734242X17721343.
12. SALEH, A. M., RAHMAT, M. N. Potential use of municipal solid waste ash (MSWA) as sustainable construction bricks. Materials Science and Engineering. 2019, 620, 012073. https://doi:10.1088/1757-899X/620/1/012073.
13. MENÉNDEZ, P., PARRA MARTÍN, R., VARELA-CANDAMIO, A., GARCÍA-ÁLVAREZ, L. An enhanced techno-economic analysis of LCOE: public incentives vs private investment. Technol. and Econ. Development of Economy. 2021, 27(1), 1–23. https://doi.org/10.3846/tede.2020.11259.
14. STRIUGAS, N., PEDISIUS, N., PRASPALIAUSKAS, M. Elemental migration and transformation from sewage sludge to residual products during the pyrolysis process. Energy Fuels. 2018, 32(4), 5199–5208. https://doi.org/10.1021/acs.energyfuels.8b00196.
15. NEEHAUL, N., JEETAH, P., DEENAPANRAY, P. Energy recovery from municipal solid waste in Mauritius: Opportunities and challenges. Environmental Development. 2020, 33, 100489. https://doi.org/10.1016/j.envdev.2019.100489.
16. AL-HAMAMRE, Z., SAIDAN, M., HARARAH, M., RAWAJFEH, K.,

ALKHASAWNEH, H., AL SHANNAG, M. Wastes and biomass materials as sustainable-renewable energy resources for Jordan. Renewable and Sustainable Energy Reviews. 2017, 67, 295–314. https://doi.org/10.1016/j.rser.2016.09.035.

17. ERFO. The Role of SRF in a Circular Economy. Retrieved from 1048. Available online: https://www.erfo.info/images/PDF/The_role_of_SRF_in_a_Circular_Economy.pdf (accessed on 29 April 2019).
18. KROOK, J. N., SVENSSON, M. Eklund. Landfill mining: A critical review of two decades of research. Waste Management. 2012, 32(3), 513–520. https://doi.org/10.1016/j.wasman.2011.10.015.
19. JONES, P. T., GEYSEN, D., TIELEMANS, Y., VAN PASSEL, S., PONTIKES, Y., BLANPAIN, B., QUAGHEBEUR, M., HOEKSTRA, N. Enhanced Landfill Mining in view of multiple resource recovery: a critical review. Journal of Cleaner Production. 2013, 55, 45–55. https://doi.org/10.1016/j.jclepro.2012.05.021.
20. FRÄNDEGÅRD, P., KROOK, J., SVENSSON, N., EKLUND, M. A novel approach for environmental evaluation of landfill mining. J. of Cleaner Production. 2013, 55, 24–34. https://doi.org/10.1016/j.jclepro.2012.05.045.
21. ARINA, D., BENDERE, R. Waste as Energy Source in EU Action Plan for the Circular Economy. Environmental Research, Engineering and Management. 2018, 74/1, 43–49. https://doi.org/10.5755/j01.erem.74.1.19779.
22. CAETANO M., GÓIS, J., LEITÃO, A. Challenges and perspectives of greenhouse gases emissions from municipal solid waste management in Angola. Energies reports 6, 2020, 364–369. https://doi.org/10.1016/j.egyr.2019.08.074.
23. S. HASHEM, F., A. RAZEK, T., A. MASHOUT, H. Rubber and plastic wastes as alternative refused fuel in cement industry. Construction and Building Materials. 2019, 212, 275–282. https://doi.org/10.1016/j.conbuildmat.2019.03.316.
24. SAKRI, A., AOUABED, A., NASSOUR, A., NELLES, M. Refuse-derived fuel potential production for co-combustion in the cement industry in Algeria Waste Management & Research: The Journal for a Sustainable Circular Economy. 2021, 39(9), 1174–1184. https://doi.org/10.1177/0734242X20982277.
25. GERASSIMIDOUA, S., VELISHTTPS, C. A., WILLIAMSB, P. T., CASTALDIC, M. J., BLACKA, L., KOMILIS D. Chlorine in waste-derived solid recovered fuel (SRF), co-combusted in cement kilns: A systematic review of sources, reactions, fate and implications Critical Reviews in Environmental Science and Technology. 2021, 51(2), 140–186. https://doi.org/10.1080/10643389.2020.1717298.
26. VICZEK, S.A., ALDRIAN, A., POMBERGER, R., SARC, R. Determination of the material-recyclable share of SRF during co-processing in the cement industry. Resources, Conservation and Recycling. 2020, 156, 104696. https://doi.org/10.1016/j.resconrec.2020.104696.
27. GHINEA, C., DRAGOU, E. N., COMANITA, E-D., GAVRILESCU, M., CAMPEAN, T., CURTEANU S., GAVRILESCU, M. Forecasting municipal solid waste generation using prognostic tools and regression analysis Journal Environmental management, 2016, 182, 80–93. https://doi.org/10.1016/j.jenvman.2016.07.026.
28. HEMIDAT, S., SAIDAN, M., AL-ZU'BI, S., IRSHIDAT, M., NASSOUR, A., NELLES, M. Potential Utilization of RDF as an Alternative Fuel to be Used in Cement Industry in Jordan Sustainability. 2019, 11(20), 5819. https://doi.org/10.3390/su11205819.
29. PECORINI, I., IANNELLI, R. Characterization of Excavated Waste of Different Ages in

View of Multiple Resource Recovery in Landfill Mining. Sustainability. 2020, 12, 1780. https://doi.org/10.3390/su12051780.

30. GARCÍA, J., DAVIES, S., VILLA, R., GOMES, D.M., COULON, F., WAGLAND, S.T. Compositional analysis of excavated landfill samples and the determination of residual biogas potential of the organic fraction. Waste Manag. 2016, 55, 336–344. https://doi.org/10.1016/j.wasman.2016.06.003.
31. CHEELA, V.R., JOHN, M., DUBEY, B. Quantitative determination of energy potential of refuse-derived fuel from the waste re-covered from Indian landfill. Sustain. Environ. Res. 2021, 31, 1–9. https://doi.org/10.1186/s42834-021-00097-5.
32. CHIOU, I.-J., CHEN, C.-H. Municipal solid waste landfill age and refuse-derived fuel. Waste Manag. Res. 2020, 39, 601–606. https://doi.org/10.1177/0734242X209618.
33. WOLFSBERGER, T., ALDRIAN, A., SARC, R., HERMANN, R., HÖLLEN, D., BUDISCHOWSKY, A., at all. Landfill mining: Resource potential of Austrian Landfills-Evaluation and quality assessment of recovered municipal solid waste by chemical analyses. Waste Manag. & Res.: J. Sustain. Circ. Econ. 2015, 33, 962–974. https://doi.org/10.1177/0734242X15600051.
34. DOU, X., REN, F., QUAN NGUYEN, M., AHAMED, A., YIN, K., PING CHAN, W., WEI-CHUNG CHANG, V. Review of MSWI bottom ash utilization from perspectives of collective characterization. treatment and existing application. Renewable and Sustainable Energy Reviews. 2017, 79, 24–38. https://doi.org/10.1016/j.rser.2017.05.044.
35. VAN PRAAGH, M., JOHANSSON, M., FAGERQVIST, J., GRÖNHOLM. R., HANSSON, N., SVENSSON, H. Recycling of MSWI-bottom ash in paved constructions in Sweden-A risk assessment. Waste Management. 2018, 79, 428–434. https://doi:10.1016/j.wasman.2018.07.025.
36. SORMUNEN, L. A., KOLISOJA, P. Construction of an interim storage field using recovered municipal solid waste incineration bottom ash: Field performance study. Waste Manag. 2017, 64, 107–116. https://urn.fi/URN:ISBN:978-952-15-4019-6.
37. STEPKOWSKA, E. T., BLANES, J. M., FRANCO, F., REAL, C., PÉREZ-RODRIGUEZ, J. L. Phase transformation on heating of an aged cement paste. Thermochimica Acta. 2004, 420, 79–87. https://doi.org/10.1016/j.tca.2003.11.057.
38. VANCE, K., AGUAYO, M., OEY, T., SANT, G., NEITHALATH, N. Hydration and strength development in ternary Portland cement blends containing limestone and fly ash or metakaolin. Cement Concrete Composites. 2013, 39, 93–103. https://doi.org/10.1016/j.cemconcomp.2013.03.028.
39. PITAK, I., RINKEVIČIUS, D., KALPOKAITĖ-DIČKUVIENĖ, R., BALTUŠNIKAS, A., DENAFAS, G. The strategy for conservation non-renewable natural resources through producing and application solid recovery fuel in the cement industry: a case study for Lithuania. Environmental Science and Pollution Research. 2022, 29, 69618–69634. https://doi.org/10.1007/s11356-022-20793-y.
40. Council Decision 2003/33/EC establishing criteria and procedures for the acceptance of waste at landfills pursuant to article 16 of an Annex II to Directive 1999/31/EC. https://www.ecolex.org/details/legislation/council-decision-200333ec-establishing-criteria-and-procedures-for-the-acceptance-of-waste-at-landfills-pursuant-to-article-16-of-and-annex-ii-to-directive-199931ec-lex-faoc039228/. Accessed 19 December 2002.
41. KARA, M. Environmental and economic advantages associated with the use of RDF in cement kilns. Resources Conservation and Recycling. 2012, 68, 21–28. https://doi.org/10.1016/j.resconrec.2012.06.011.

42. PITAK, I., DENAFAS, G., BALTUŠNIKAS, A., PRASPALIAUSKAS, M., LUKOŠIŪTĖ, S. I. Proposal for implementation of extraction mechanism of raw materials during landfill mining and its application in alternative fuel production. Sustainability. 2023, 15(5), 4538. https://doi.org/10.3390/su15054538.
43. ROTHEUT, M., QUICKER, P. Energetic utilisation of refuse derived fuels from landfill mining. Waste Manag. 2017, 62, 101–117. https://doi.org/10.1016/j.wasman.2017.02.002.
44. Council Decision 2003/33/EC Establishing Criteria and Procedures for the Acceptance of Waste at Landfills Pursuant to Article 16 of an Annex II to Directive 1999/31/EC. Available online: https://www.ecolex.org/details/legislation/council-decision-200333ec-establishing-criteria-and-procedures-for-the-acceptance-of-waste-at-landfills-pursuant-to-article-16-of-and-annex-ii-to-directive-199931ec-lex-faoc039228/(accessed on 19 December 2002).
45. 2014/955/EU: Commission Decision of 18 December 2014 amending Decision 2000/532/EC on the list of waste pursuant to Directive 2008/98/EC of the European Parliament and of the Council Text with EEA relevance. Available online: https://eur-lex.europa.eu/legal-content/EN/TXT/PDF/?uri=OJ:L:2014:370:FULL&from=EN (accessed on 30 December 2014).
46. PITAK, I., BALTUŠNIKAS, A., KALPOKAITĖ-DIČKUVIENĖ, R., KRIUKIENE, R., DENAFAS, G. Experimental study effect of bottom ash and temperature of firing on the properties. microstructure and pore size distribution of clay bricks: a Lithuania point of view. Case Studies in Constr. Mate. 2022, 17, e01230. https://doi.org/10.1016/j.cscm.2022.e01230.
47. SUTCU, M., ERDOGMUS, E., GENCEL, O., GHOLAMPOUR, A., ATAN, E., OZBAKKALOGLU, T. Recycling of bottom ash and fly ash wastes in eco-friendly clay brick production. Journal of Cleaner Production. 2019, 233, 753–764. https://doi.org/10.1016/j.jclepro.2019.06.017.
48. HOOI CHO, B., HYUN NAM, B., AN, J., YOUN, H. Municipal Solid Waste Incineration (MSWI) Ashes as Construction Materials–A Review. Materials. 2020, 13, 3143. https://doi:10.3390/ma13143143.
49. VESCO holds the leading position among the global producers and exporters of ball clays. https://www.vesco.com.ua/en/production.
50. REZENDE, J.C.T., RAMOS, V.H.S., OLIVEIRA, H.A., OLIVEIRA, R.M.P.B., JESUS, E. Removal of Cr(VI) from Aqueous Solutions Using Clay from Calumbi Geological Formation. N. Sra. Socorro. SE State. Brazil. Materials Science Forum. 2018, 912, 1–6. https://doi.org/10.4028/www.scientific.net/MSF.912.1.
51. CONCONI, M. S., MOROSI, M., MAGGI, J., ZALBA, P.E., CRAVERO, F., RENDTORFF, N. M. Thermal behavior (TG-DTA-TMA). sintering and properties of a kaolinitic clay from Buenos Aires Province. Argentina. Cerâmica. 2019, 65, 227–235. https://doi.org/10.1590/0366-69132019653742621.
52. ALIU, I. Comparative analysis of the compressive strengths of clay and sandcrete blocks for low-cost housing. Journal of Engineering and Architecture. 2021, 4(2):19, 19.
53. https://www.gobrick.com/docs/default-source/read-research-documents/technical-notes/9a-specifications-for-and-classification-of-brick.pdf/.
54. LOUATI, S., BAKLOUTI, S., SAMET, B. Geopolymers Based on Phosphoric Acidand Illito-Kaolinitic Clay. Advances in Materials Science and Engineering. 2016, 7, 1–7. http://dx.doi.org/10.1155/2016/2359759.

55. ALOTHMAN, Z. A Review: Fundamental Aspects of Silicate Mesoporous Materials. Materials. 2012, 5(12), 2874–2902. https://doi.org/10.3390/ma5122874.
56. KALPOKAITĖ-DIČKUVIENĖ, R., PITAK, I., BALTUŠNIKAS, A., LUKOŠIUTĖ, S. I., DENAFAS, G., ČESNIENĖ, J. Cement substitution by sludge-biomass gasification waste: the synergy with silica fume. Construction and building materials. 2022, 326, 126902. https://doi.org/10.1016/j.conbuildmat.2022.126902.
57. 2003/33/EC: Council Decision of 19 December 2002 establishing criteria and procedures for the acceptance of waste at landfills pursuant to Article 16 of and Annex II to Directive 1999/31/EC. 2003. Official J European Comm. 46, 27–49.
58. GABROVŠEK, R., VUK, T., KAUČIČ, V. Evaluation of the hydration of Portland cement containing various carbonates by means of thermal analysis. Acta Chim. Slov. 2006, 53, 159–165.
59. MEJDI, M., SAILLIO, M., CHAUSSADENT, T., DIVET, L., TAGNIT-HAMOU, A. Hydration mechanisms of sewage sludge ashes used as cement replacement. Cem. Concr. Res. 2020, 135, 106–115. https://doi.org/10.1016/j.cemconres.2020.106115.
60. SING, K.S.W., EVERETT, D.H., HAUL, R.A.W., MOUSCOU, I., PIEROTTI, R.A., ROUQUEROL, J., SIEMIENIEWSKA, T. Reporting physisorption data for gas/liquid systems with special reference to the determination of surface area and porosity. Pure Appl. Chem. 1985, 57, 603–619.
61. Akmenės cementas. Description of cement production technology. 2021. Available online: https://cementas.lt/en/production/description-of-cement-production-technology/ (accessed on 12 August 2014).
62. CMI. Coal Marketing International. Coal Basics. Available online: http://www.coalmarketinginfo.com/coal-basics (accessed on 5 November 2012).
63. Directive 2000/76/EC of the European Parliament and of the Council on the incineration of waste. Available online: https://eur-lex.europa.eu/eli/dir/2000/76/oj (accessed on 31 December 2020).
64. DEL ZOTTO, L., TALLINI, A., DI SIMONE, G., MOLINARI, G., CEDOLA, L. Energy Enhancement of Solid Recovered Fuel within Systems of Conventional Thermal Power Generation. Energy Procedia. 2015, 81, 319–338. https://doi.org/10.1016/j.egypro.2015.12.102.
65. Organization for Economic Co-Operation and Development. Effective Carbon Rates. Available online: https://www.oecd.org/tax/tax-policy/effective-carbon-rates-2021-highlights-brochure.pdf (accessed on 5 May 2021).

CURRICULUM VITAE

Name. Surname: Inna Pitak
E-mail: inna.pitak@lei.lt

Education

1998-2002
Bachelor's Degree in Environmental Science. National Technical University "Kharkiv Polytechnic Institute". Faculty of Chemical Engineering

2002-2004
Master's Degree in Environmental Science. National Technical University "Kharkiv Polytechnic Institute". Faculty of Chemical Engineering

2019-2023
PhD studies in Environmental Engineering. Lithuanian Energy Institute. Laboratory of Materials Research and Testing

Work experience

March 15. 2021 – August 13. 2021
Project: "Model of resource recovery from landfills assessment and its testing in Lithuanian conditions". Kaunas University of Technology. Department of Environmental Technology

April 19. 2021 – December 31. 2021
Project: "Possibilities and sustainability model of recovery of energy resources from landfills (ISLAND)". Lithuanian Energy Institute. Laboratory of Materials Research and Testing

January 03. 2022 – May 31. 2022
Project: "Model of resource recovery from landfills assessment and its testing in Lithuanian conditions". Kaunas University of Technology. Department of Environmental Technology

January 01. 2022 – April 30. 2024
Project: "Innovation in concrete design for hazardous waste management applications (ICONDE)". Lithuanian Energy Institute. Laboratory of Materials Research and Testing

April 01.2023 – March 31.2026
Project: "Theory, technology and circularity of material recovery from multilayer composite waste by simultaneous delamination and leaching (SIMULARITY)" Lithuanian Energy Institute. Laboratory of Materials Research and Testing

LIST OF PUBLICATIONS

1. **Inna Pitak**; Darius Rinkevičius; Regina Kalpokaitė-Dičkuvienė; Arūnas Baltušnikas; Gintaras Denafas. The strategy for conservation non-renewable natural resources through producing and application solid recovery fuel in the cement industry: a case study for Lithuania // Environmental science and pollution research. Heidelberg: Springer. ISSN 0944-1344. eISSN 1614-7499. 2022, vol. 29, p. 69618–69634. https://doi.org/10.1007/s11356-022-20793-y [Science Citation Index Expanded (Web of Science); Scopus; MEDLINE] [IF: 5,190; AIF: 6,309; IF/AIF: 0,822; Q2 (2021, InCites JCR SCIE)] [CiteScore: 6,60; SNIP: 1,154; SJR: 0,831; Q1 (2021, Scopus Sources)] [Field: T 004] [Input: 0,5].
2. **Inna Pitak**; Gintaras Denafas; Arūnas Baltušnikas; Marius Praspaliauskas; Stasė Irena Lukošiūtė. Proposal for implementation of extraction mechanism of raw materials during landfill mining and its application in alternative fuel production // Sustainability. Basel: MDPI. ISSN 2071-1050. 2023, vol. 15(5), 4538, p. 1–22. https://doi.org/10.3390/su15054538 [Science Citation Index Expanded (Web of Science); Scopus; DOAJ] [IF: 3,889; AIF: 6,732; IF/AIF: 0,577; Q2 (2021, InCites JCR SCIE)] [Field: T 004, T 008] [Input: 0,5].
3. **Inna Pitak**; Arūnas Baltušnikas; Regina Kalpokaitė-Dičkuvienė; Rita Kriukiene; Gintaras Denafas. Experimental study effect of bottom ash and temperature of firing on the properties. microstructure and pore size distribution of clay bricks: a Lithuania point of view // Case Studies in Construction Materials. Elsevier BV. ISSN 2214-5095. 2022, vol. 17, p. e01230. https://doi.org/10.1016/j.cscm.2022.e01230 [Science Citation Index Expanded (Web of Science); Scopus] [IF: 4.934; AIF: 4.885; IF/AIF: 1.010; Q1 (2021, InCites JCR SCIE)] [CiteScore: 5.2; SNIP: 1,932; SJR: 1.01; Q1 (2021, InCites JCR SCIE)] [Field: T 004, T 008] [Input: 0,7].
4. Regina Kalpokaitė-Dičkuvienė; **Inna Pitak**; Arūnas Baltušnikas; Stasė Irena Lukošiutė; Gintaras Denafas; Jūratė Česnienė. Cement substitution by sludge-biomass gasification waste: the synergy with silica fume // Construction and Building Materials. Oxford: Elsevier BV. ISSN 0950-0618. 2022, vol. 326, 126902, p. 1–14. https://doi.org/10.1016/j.conbuildmat.2022.126902. [Science Citation Index Expanded (Web of Science); Scopus] [IF: 7,693; AIF: 5,545; IF/AIF: 1,387; Q1 (2021, InCites JCR SCIE)] [Cite Score: 10.6; SNIP: 2.362; SJR: 1.777; Q1 (2021, InCites JCR SCIE)] [Field: T 004, T 008] [Input: 0,2]

Attendance of international conferences:

1. **Pitak, Inna**; Baltušnikas, Arūnas; Denafas, Gintaras. Analysis of separated waste for the preparation of solid recovered fuels // 1st International conference Strategies toward Green Deal Implementation Water & Raw Materials. December 14-16. Cracow. Poland: 2020.
2. **Pitak, Inna**; Denafas, Gintaras; Lukošiūte, Stasė Irena. Analysis of MSW fraction after separation with the goal to have solid recovery fuel // Linnaeus

Eco-Tech 2020. November 23-25. Kalmar. Sweden: 2020.

3. **Pitak, Inna;** Mumladze, Tamari; Šleiniūtė, Agne; Denafas, Gintaras. Recyclability of separate collected municipal solid waste fractions: case study for Kaunas. Lithuania // Materials of the winter session of the International Carpathian School "Protection of Vulnerable Ecosystems in the Pandemic and Climate Change". Scientific Society named after T. G. Shevchenko. February 25-27. Kosiv. Ukraine: 2021.
4. **Pitak, Inna**; Denafas, Gintaras; Kriūkienė, Rita. About solid recovered fuel: chemical characteristics and role in the waste management system // 9th European Young Engineers Conference. April 19-21. Warsaw. Poland: 2021.
5. **Pitak, Inna**; Kalpokaite-Dičkuvienė, Regina; Denafas, Gintaras. Extraction of high calorific fraction from municipal solid waste during the mechanical biological treatment process // 17th International conference of young scientists on energy and natural sciences issues. May 24-28. Kaunas. Lithuania: 2021.
6. Matiženok, Gytis; **Pitak, Inna**; Baltušnikas, Arūnas; Kriūkienė, Rita; Lukošiūtė, Stasė Irena; Denafas, Gintaras. Properties and recycling feasibilities of municipal solid waste incineration residues: issues for Kaunas waste incineration plant. Lithuania // XXII International Science Conference "Ecology. Human. Society". May 20-21. Kyiv. Ukraine: 2021.
7. **Pitak, Inna**; Baltušnikas, Arūnas; Čėsnienė, Jūratė; Denafas, Gintaras. Opportunity production of solid recovered fuel from refuse-derived fuel and use as an alternative fuel for the cement industry of Lithuania // 2nd International conference strategies toward green deal implementation water and raw materials. December 08-10. Cracow. Poland: 2021.
8. **Pitak, Inna**; Baltušnikas, Arūnas; Denafas, Gintaras. The feasibility of using SRF in the cement industry //18th International conference of young scientists on energy and natural sciences issues. May 24-27. Kaunas. Lithuania: 2022.
9. Denafas, Gintaras; **Pitak, Inna**; Kruopienė, Jolita; Streikus, Dionizas; Romaneckas, Kęstutis; Jasinskas, Algirdas. Comparison of stored and renewable energy potentials in landfill conditions: a case study for Kaunas waste management region. Lithuania // Sixth Symposium on circular economy and urban mining. May 18-20. Capri. Italy: 2022.
10. **Pitak, Inna**; Denafas, Gintaras; Lukošiūte, Stasė Irena. Characteristics and feasibilities to use waste from landfill to produce energy: case study for Lithuania. Linnaeus Eco-Tech 2022. November 21-23. Kalmar. Sweden: 2022.

Environmental Science and Pollution Research (2022) 29:69618–69634
https://doi.org/10.1007/s11356-022-20793-y

RESEARCH ARTICLE

The strategy for conservation non-renewable natural resources through producing and application solid recovery fuel in the cement industry: a case study for Lithuania

Inna Pitak[1] · Darius Rinkevičius[2] · Regina Kalpokaitė-Dičkuvienė[1] · Arūnas Baltušnikas[1] · Gintaras Denafas[1,2]

Received: 3 November 2021 / Accepted: 9 May 2022 / Published online: 16 May 2022

Abstract
This pilot study aimed to develop a production line for SRF production from RDF by extracting prohibited materials, grinding, and drying, and the energy potential for using SRF in the cement industry as an alternative fuel was evaluated. This paper defined the main characteristics of RDF, which were obtained after the separation of the biological fraction from MSW at an MBT plant. According to its characteristics, RDF can only be used for incineration in the CPP to obtain heat and energy. The produced SRF meets the requirements for fuel from waste and can be used as an alternative fuel for clinker firing. A technological process line for SRF production from RDF has been developed by adding technical units to the existing MBT line. The SRF production line yield was calculated as 4.47 t/h. At the end of the SRF production process, the moisture content of the finished product decreased by 85%, and the volume decreased by 18%. The obtained SRF had a high calorific value, low moisture content, and a permissible value of chlorine and mercury. It was proposed that the produced SRF and sewage sludge (already used during the clinker firing process) be utilized as alternative fuels since they correspond to the oxide composition of the finished clinker in elemental and oxide composition. A calculation to assess the economic and environmental efficiency of the use of SRF in the cement kiln was conducted. The result showed that using 10% SRF as a substitute fuel for coal used in clinker roasting at 1.92 t/h would save 601.7 USD/h coal costs. This use of SRF will emit 3.7 t/h CO_2 and achieve net savings of 754.7 USD/h.

Keywords Resource recovery · SRF production · Energy sources · Sewage sludge · Cement industry · CO_2 emissions

Abbreviations

AC	Ash content
CEN	European Standards Organization
Cl	Chlorine content
CPP	Cogeneration power plant
EU	European Union
Hg	Mercury content
MBT	Mechanical biological treatment
MC	Moisture content
MSW	Municipal solid waste
NCV	Net calorific value
NIR	Near-infrared radiation
PVC	Polyvinyl chloride
RDF	Refuse derived fuel
SEM	Scanning electron microscopy
SEM–EDS	Scanning electron microscopy-energy dispersive X-ray spectroscopy
SRF	Solid recovery fuel
XRD	X-ray diffraction

Responsible Editor: Philippe Garrigues

✉ Inna Pitak
inna.pitak@lei.lt

Darius Rinkevičius
darius@kaunoratc.lt

Regina Kalpokaitė-Dičkuvienė
regina.kalpokaite-dickuviene@lei.lt

Arūnas Baltušnikas
arunas.baltusnikas@lei.lt

Gintaras Denafas
gintaras.denafas@ktu.lt; gintaras.denafas@lei.lt

[1] Laboratory of Materials Research and Testing, Lithuanian Energy Institute, Breslaujos st. 3, 44403 Kaunas, Lithuania

[2] Department of Environmental Technology, Kaunas University of Technology, Radvilėnų pl. 19, 50254 Kaunas, Lithuania

Introduction

Scientific and technological progress has made it possible for humans to improve their quality and conditions of life and achieve independence from nature. To develop the economy and improve the well-being and quality of life of humans, the extraction of natural resources is increasing. However, it should be noted that most extracted resources are used inefficiently and are returned to the environment in the form of waste. The diversity and danger of waste pose a threat to humanity. The share of a useful social product does not exceed 10%, and the remaining 90% of the substance enters the environment in the form of waste.

The rapid growth of waste generation is forcing scientists and governments to look for ways to solve this problem. To date, waste that cannot be reused is sent for incineration or sent to a landfill. However, depositing waste in landfills is the lowest step in the waste management system since the disposal of waste in landfills entails an environmental problem in the foreseeable future. Reducing the nonrecyclable fraction of waste in developed and developing countries has been partially resolved. The nonrecyclable fraction of waste is sent for incineration at a cogeneration station where heat and energy can be obtained. However, this is not an ideal option since fly and bottom ash are formed after incinerating waste. It is also necessary to seek opportunities for reuse and disposal of these materials if needed. However, attention should be given to waste as an alternative fuel for energy-intensive industries such as cement production. The use of prepared fuel from waste in clinker firing will reduce the consumption of non-renewable natural resources and greenhouse gas emissions. The cement industry is a significant ecological reserve with all the possibilities for efficiently managing nonrecyclable materials. The advantage of the cement kiln lies in the high applied temperatures (up to 1450 °C). In a kiln at these temperatures, it is possible to burn various wastes and at the same time ensure the decomposition of organochlorine compounds (furans, dioxins, etc.), which brings both the production process and its final product into full compliance with environmental standards.

Therefore, waste disposal by high-quality alternative fuel production and using it in a cement kiln during the clinker firing process have economic and environmental benefits and are of crucial importance.

The aim of this study was to investigate the characteristics of SRF produced from RDF and use it during the clinker firing process as an alternative fuel for the Lithuania cement plant by developing an SRF production line including prohibited material extraction, shredding, and drying stages. The use of the produced SRF as an alternative fuel during clinker firing is a relevant and relatively new application, but in practice, this material is not used to its full extent. To achieve this goal, it is necessary to perform the following tasks: determine the main characteristics of the SRF and compare them with those of the RDF and sewage sludge; prove that the ash obtained after the incineration of SRF and sewage sludge contains crystalline phases; propose a variant of the SRF production line that will produce an alternative fuel meeting the EU standard, taking into account the operation of the existing CPP; and conduct economic and environmental justification for the feasibility of the production and use of SRF in the cement industry.

Literature review

The increase in prosperity and quality of human life has caused a rise in generated waste. According to author statements (Apergis et al. 2021; Calvo and Valero 2021; Aslan and Altinoz 2021; Kulkarni 2020), natural resource consumption, waste generation, greenhouse gas emissions, and climate change are amongst the most severe environmental problems that humanity has faced.

The generation of waste in the European Union has increased over the past few decades and continues to increase, as shown by data from the European Commission. In accordance with municipal waste statistics (2020), in EU countries, in 2020, the amount of municipal waste generated per person amounted to 505 kg, 4 kg per person more in 2019, and 38 kg per person more than in 1995.

In accordance with a previously published statement (Liu et al. 2021), waste generated should be considered an inevitable product of human activity. This paper focuses on the relevance and correctness of the choice of waste disposal method. An incorrect waste disposal method can lead to serious environmental problems, especially for waste that is deposited in landfills. The forecasting of waste generation is considered, and advice is given on the optimal placement of waste at the landfill; however, issues related to minimizing waste that is sent to the landfill remain unresolved. However, according to Di Lonardo et al. (2016), there is legislation on waste disposal that establishes a hierarchy of available technologies. According to the waste management hierarchy, in the EU, landfilling is the least preferable option and should be limited. If the waste cannot be recycled, it may be sent to a landfill, but it must comply with Directive 2018/850 on landfills. According to the above statements of the authors, it can be concluded that the formation and disposal of waste are a complex problem.

According to the authors (Menéndez et al. 2021), the best way to dispose of waste and move closer to a circular economy is to reuse and produce heat and energy. The authors also argue that the amount of waste from which heat and

energy can be obtained is considerable. The authors (Arina and Bendere 2018) say that technologies for collecting and processing materials improve the quality and quantity of materials that can be reused. According to the authors (Striugas et al. 2018; Neehaul et al. 2020; Al-Hamamre et al. 2017), waste and materials can be used as sustainable energy sources. This strategy can save companies a large amount of money, ensure controlled waste disposal, and reduce the consumption of non-renewable natural resources. The authors (Dianda and Mahidin Munawar 2018) emphasize that the landfilling of waste leads to other environmental problems, such as leachate generation and landfill gas production. The prerequisites for producing alternative fuel from waste, which contains a biological fraction, are outlined. The authors proposed using this type of fuel in energy-intensive industries. However, this paper does not consider the issue of extracting the biological fraction of the waste since it is this fraction that makes a relatively significant contribution to the increase in humidity and decreases in calorific value and harms the operation of cement kilns. According to the authors (Danish and Ulucak 2021; Kulokas et al. 2021), there is increasing interest in burning the nonrecyclable, high-calorie fraction of the waste to generate electricity. The reasons discussed to explain the demand for waste incineration are increased waste generation, climate change, depletion of natural resources, and reduced dependence on imported energy sources. However, the difficulties an enterprise may face due to deciding to use waste as an alternative fuel have not been considered.

The authors (Caetano et al. 2020) consider the quality of the finished product, energy consumption, and the reduction in greenhouse gas emissions. Reducing the consumption of natural energy resources will thus reduce CO_2 emissions. According to the authors' information (S. Hashem et al. 2019; Birnstengel et al. 2015), the cement industry is an energy-intensive industry and is a leader in the consumption of natural energy resources and greenhouse gas emissions. Energy consumption and greenhouse gas emissions are also discussed in the authors' work (Sakri et al. 2021). The paper notes that one ton of cement production releases approximately 800 kg of carbon dioxide. Reducing the amount of natural resources, global warming, and rising energy prices are forcing the leaders of cement enterprises to use alternative fuels. According to the authors (Gerassimidoua et al. 2021), SRF production and its use in the cement industry as an additive to the main fuel will reduce the amount of waste sent to landfill, the production of greenhouse gas emissions, energy consumption, and material consumption. The authors also note that it is necessary to control the chlorine content in the supplied fuel since chlorine negatively affects the work and design of cement kilns. The authors found that SRF mainly (50–60%) consists of biogenic components, followed by a mixture of plastics. According to Viczek et al. (2020) and COM (2019), the coincineration of various wastes with fossil fuels provides economic and environmental benefits. According to Wang (2021), Usón et al. (2013), and Prabhakaran et al. (2020), up to a 10% reduction in greenhouse gas emission intensity from cement production by 2050 will reduce CO_2 emissions by 0.4 Gt, which will significantly slow climate change.

According to the statement (Hemidat et al. 2019), when SRP is burned during the clinker burning process, no byproduct is formed, and no additional harmful emissions are emitted. However, the issues of SRF production and the possibility of combining it with other types of waste, such as sewage sludge, remain unresolved.

Based on analysing the existing problem of increasing waste generation and ways to solve this problem, the following can be distinguished. Even though using SRF in cofiring with the main fuel has been sufficiently studied, it is not used in Lithuania from a practical point of view. The issues of SRF production and technological capabilities remain unresolved, resulting in high-quality fuel from waste obtained, which will meet the European standard and which can be used when cocombusted with coal in the clinker burning process. Economic and environmental benefits will be achieved through savings on solid fuel imports, reducing the consumption of non-renewable natural resources, reducing greenhouse gas emissions, and reducing the amount of waste sent to the landfill.

Materials and methods

The research area was the Kaunas MBT plant located in Kaunas city, Lithuania, and referred to the Kaunas region waste management centre. During four seasons, 2020–2021, morphological and granulometric studies of the RDF were carried out in the property of the Kaunas MBT plant. The SRF was prepared in the laboratory. The sewage sludge was obtained from the cement plant "Akmenės cementas." This research was based on data from the Kaunas MBT facility, sample analysis of RDF fractions, cement plant data, scientific articles, and our studies. Representative samples were prepared for laboratory analysis and detection of the parameters of the analysed materials within the laboratories of the Lithuanian Energy Institute. The scheme of the study is presented in Fig. 1.

Sample preparation

The RDF composition obtained after mechanical–biological treatment of MSW at Kaunas MBT was analysed for further calculations. To analyse the size materials in RDF, sieves of 80 mm, 40 mm, and 20 mm were used. The material fraction was passed through three sieves with square holes

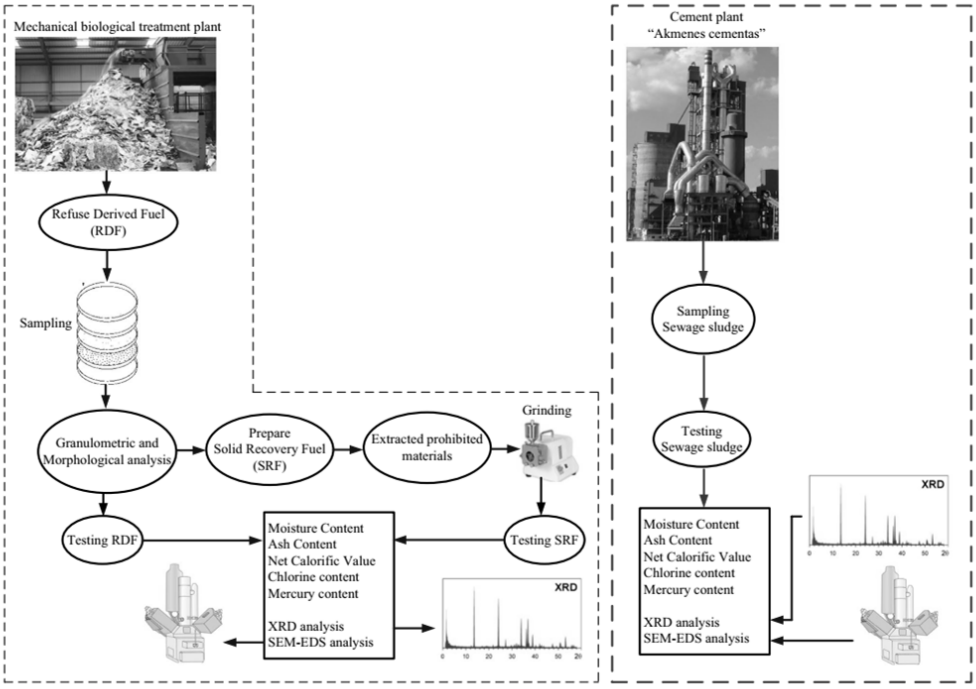

Fig. 1 Protocol for RDF, SRF, and sewage sludge extraction, preparation, and testing

80, 40, and 20 mm in diameter. Granulometric fractions $d > 80$ mm and $80\ \text{mm} > d > 40$ mm were further subdivided into subfractions. Additional waste sorting of the particle size fraction $40\ \text{mm} > d > 20$ mm was practically impossible since it was difficult to separate the materials visually. Moreover, visual sorting was not possible for small fractions $d < 20$ mm. Each subfraction was weighed, and the fine fraction particle size and morphological composition were calculated from the weight data. Morphological separation was performed by hand. After morphological analysis was carried out, each fraction was weighed, placed in containers, and transported to the laboratory for further research.

To prepare SRF, we used PDF obtained after the mechanical–biological separation of MSW at the Kaunas MBT plant. Preliminary, the prohibited materials (chlorine and mercury content) were extracted. The fraction of SRF was ground in an SM 300 mill. After preparing SRF, the main characteristics (moisture and ash contents, high calorific value, and chlorine and mercury contents) were determined according to EU standards.

The elemental composition (%, in ash) was determined by applying scanning electron microscopy (SEM), and the structure and phase composition of crystalline materials were determined by X-ray diffraction (XRD), for which SRF and sewage sludge samples were prepared by combustion in a muffle furnace at a temperature of 950 °C for an hour. In the clinker firing process, according to the technological scheme, sewage sludge was fed into a vertical (static) furnace and then into a calciner, where the temperature was 900–1000 °C. Therefore, to obtain ash in the laboratory, the precise temperature range of 900 and 1000 °C was used. After passing through the first firing stage, the materials entered a horizontal furnace where the final firing stage occurred at the temperature of 1400–1500 °C.

Testing RDF, SRF, and sewage sludge

After carrying out morphological and granulometric analyses, SRF samples were prepared from RDF. The main characteristics of RDF, SRF, and sewage sludge were determined according to the EN 15,359:2011:

– Moisture content (MC)—EN 15,414–3:2011;
– Ash content (AC)—EN 15,403:2011;

– Chlorine content (Cl)—EN 15,408:2011;
– Mercury content (Hg)—EN 15,411:2011;
– Net calorific value (NCV)—EN 15,400:2011.

To prove the above, elemental analysis of sewage sludge and SRF was performed by scanning electron microscopy and X-ray diffraction. SEM observation was performed on a ZEISS EVO MA10 microscope at an accelerating voltage of 20 kV.

Calculations of the percentage fraction of SRF produced from RDF

For calculations of the percentage fraction of SRF after RDF treatment, Eqs. 1 and 2:

$$SRF_{fr} = C \times RDF_{fr}, \tag{1}$$

where SRF_{fr} is the amount of SRF produced from RDF (%),RDF_{fr} is the amount of each material in the RDF composition plastic, paper, textile, and other) (%), and C is the ratio of conversion. This value was calculated by using Eq. 2:

$$C = \frac{100\% - MC_{RDF}}{RDF_{fr}}, \tag{2}$$

where MC_{RDF} is the moisture content of RDF (%).

Development and calculation of flow rates of the SRF production line

To produce SRF from RDF, RDF must go through several stages of preparation: a substantial amount of moisture must be removed; the materials must be ground to the necessary size ($d < 20$ mm); and metals and prohibited materials must be extracted to achieve the requirements for fuel production from waste.

To achieve SRF production in accordance with EU standards, developing an additional SRF production line is needed. The SRF production line was based on Pomberger and Sarc's (2014) data and the current waste management situation in Kaunas MBT. No recyclable waste after separation at the MBT plant is sent to produce heat and energy to the Kaunas CPP. Moreover, it is impossible to convert all incinerated waste into additive fuel for the cement industry. Otherwise, it will disrupt the operation of the CPP. Calculating the required RDF for Kaunas CPP and SRF for the cement plant is necessary. To avoid disturbing the process of the Kaunas CPP, the amount of waste for the cement plant should be approximately 50% of the incinerated waste (6.6 t/h). The flow rates of the SRF production line were calculated using Eqs. 3–24 and information from Fig. 2:

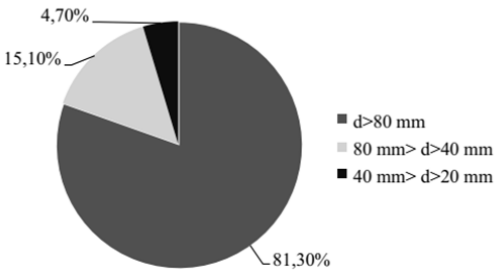

Fig. 2 Average granulometric composition of the RDF fraction

$$FR_{SRF} = FRP_{RDF} - X - Y - Z - FR_{W}| \tag{3}$$

$$X = \frac{\left(FRP_{RDF} \times a\right)}{100\%} \tag{4}$$

$$Y = \frac{[(FRP_{RDF} - X) \times b]}{100\%} \tag{5}$$

$$Z = \frac{[(FRP_{RDF} - Y) \times c)}{100\%} \tag{6}$$

$$FR_{W} = \frac{[(FRP_{RDF} - Z) \times MC_{L}]}{100\%} \tag{7}$$

where FR_{SRF} is the flow rate of the SRF production process (t/h); FRP_{RDF} is the flow rate of some part of incinerated waste (6.6 t/h); X, Y, and Z are the flow rates of RDF after extraction materials (inert, ferrous, nonferrous metal) (t/h); a, b, and c are the amount of extraction materials at each stage of separation (%); MC_L is the amount of moisture lost (%); and FR_W is the flow rate of RDF after moisture loss (t/h).

Environmental and economic assessment

We proposed using the produced SRF from RDF in the current technological scheme to produce cement clinker. Currently, sewage sludge is used as an alternative fuel during the clinker firing process. From an economic perspective, it is inadvisable to produce SRF in the property of a cement plant. Therefore, in this work, using SRF production at the MBT plants was proposed.

Some research shows that variations in potential environmental benefits and effects are related to SRF production and use in cement kilns. SRF production has a positive impact on the environment by reusing materials and energy. Replacing traditional non-renewable material fuels with SRF in industry facilities leads to energy recovery and reduced gas emissions

(Reza et al. 2013; Garces et al. 2017). This stage of work was an opportunity for producing SRF as an alternative fuel in the cement industry. Our task was to confirm or deny the economic and environmental feasibility of incinerating the SRF as an alternative fuel during clinker firing. Parameters and limit values, which need calculation, are presented in Table 1.

To calculate the economic efficiency of using the SRF during clinker firing, Eqs. 8–24 were used. The calculation assumed four options that were present due to the addition of the SRF as a substitute for the primary fuel, coal. Variants of this calculation were based on literature data, internet resources, actual data, and technical requirements obtained at the cement plant "Akmenes cementas." The proportion of carbon dioxide in greenhouse gas emissions was calculated and analysed, and the energy requirements were determined by replacing coal with SRF. The perspectives of reducing greenhouse gas emissions were studied, and the amount of carbon dioxide emissions upon partial replacement of coal by the SRF was calculated. Below is a methodology for calculating the environmental and economic assessment of the use of SRF in the cement industry.

The energy consumption of coal to produce clinker tons per day, kcal/kg (E):

$$E = KP \times 1000 \times Ec, \tag{8}$$

The coal energy consumption savings by using the replacement ratio of SRF, kcal/kg (Es):

$$Es = E \times RR \tag{9}$$

The SRF amount to be replaced per hour to achieve the required energy, ton/h (A_{SRF}):

$$A_{SRF} = \left(\frac{Es}{HCV_{SRF}}\right)/1000/24 \tag{10}$$

The coal amount per hour required to achieve the energy, ton/h (C_{coal}):

$$C_{coal} = \left(\frac{RE}{CV_{coal}}\right)/1000/24 \tag{11}$$

where RE is the required energy to produce 1 kg of clinker taking into account the replacement ratio of SRF (kcal/kg):

$$RE = KP \times Ec_{calc} \times RR \times 1000 \tag{12}$$

where Ec_{calc} is calculation energy required to produce 1 kg of clinker (kcal/kg):

$$Ec_{calc} = (Ec \times AC)/100 \tag{13}$$

where AC is the coal consumption (t/h) and was calculated by Eq. 14:

$$AC = C^0{}_{coal} - C_{coal} \tag{14}$$

where C_{coal} is the coal consumption calculated by different replacement ratios of SRF (t/h).

The amount of SRF required for replacing 1 ton of coal (Q_{SRF}) was

$$Q_{SRF} = \frac{A_{SRF}}{AC} \tag{15}$$

Using SRF as a replacement fuel, the annual coal savings, t/year (AS_{coal}), were calculated using Eq. 16:

$$AS_{coal} = AC \times OD \times 24 \tag{16}$$

The annual income in coal savings, USD/year (AI), was calculated by Eq. 17:

$$AI = AS_{coal} \times P_{coal} \tag{17}$$

The annual consumption of SRF, t/year (AC_{SRF}), was calculated using Eq. 18:

$$AC_{SRF} = A_{SRF} \times OD \times 24 \tag{18}$$

Table 1 Parameters for calculation

№	Parameters	Limit value	Symbol	Sources
1	Daily kiln production quantity	3056 ton/day	KP	Akmenės cementas (2021)
2	Number of total operating day	360 day/year	OD	
3	Emission factor of coal	85%	CA_{CO2}	
4	Energy required to produce 1 kg of clinker	840 kcal/kg	Ec	Hemidat et al. (2019)
5	The calorific value of coal	7400 kcal/kg	HCV_{coal}	CMI (2021)
6	Price 1 ton of coal	137 USD	P_{coal}	Directive 2000/76/EC
7	The cost price of one-ton SRF	25 USD	P_{SRF}	Del Zotto et al. (2015)
8	The calorific value of SRF	5000 kcal/kg	CV_{SRF}	Determined
9	Emission cost of 1 ton CO_2	58 USD	P_{CO2}	OECD (2021)
10	Replacement ratio of SRF	10%, 15%, 20%, 25%	RR	
11	Coal consumption by initial situation	16.1 t/h	$C^0{}_{coal}$	

By Eq. 19, the annual costs of SRF, USD/year (C_{SRF}), were calculated:

$$C_{SRF} = AC_{SRF} \times P_{SRF} \quad (19)$$

The actual financial savings, USD/year (FS), were calculated using Eq. 20:

$$FS = AI - C_{SRF} \quad (20)$$

The annual CO_2 emission savings for the cement plant using coal, USD/year (CS_{CO2}), were calculated by Eq. 21:

$$CS_{CO2} = AC \times CA_{CO2} \times OD \times 24 \quad (21)$$

Reducing CO_2 emissions from coal, USD/year (ES_{CO_2}), was calculated using Eq. 22:

$$ES_{CO_2} = CS_{CO_2} \times P_{CO_2} \quad (22)$$

Loss of efficiency taking into account the use of SRF, % (EL), was calculated by Eq. 23:

$$EL = 0.20 \times RR \times 100 \quad (23)$$

The net cost savings was calculated according to Eq. 24:

$$NS = \frac{(AI + ES_{CO2} - C_{SRF}) \times (100 - EL)}{100} \quad (24)$$

The given calculation results in Table 4 illustrate the savings gained by SRF utilization in the cement kilns. The results in Table 4 presented four scenarios using SRF as replacement fuel with 10%, 15%, 20%, and 25% replacement rates. It is accepted that 1 kg of coal emits 85% of the CO_2 emitted at "Akmenės cementas."

Results

The world faces challenges considering municipal solid waste treatment and its environmental impact. One of the solutions to these challenges is to reuse some waste as viable material, which can be used as an alternative to fossil fuels in energy-demanding industries, such as the cement industry.

RDF, SRF, and sewage sludge properties

The studies were carried out throughout four seasons. At the Kaunas MBT, RDF was obtained after separating biological fractions from MSW. For conducting granulometric analysis of RDF, sieves with dimensions $d > 80$ mm, 80 mm $> d > 40$ mm, and 40 mm $> d > 20$ mm were used. It was found that 81.3% of the material was $d > 80$ mm, 15.1% was 80 mm $> d > 40$ mm, and 4.7% was 40 mm $> d > 20$ mm, which was difficult to separate and recognize. Figure 2 shows the average granulometric composition of the RDF fraction.

From the $d > 80$ mm fraction, samples of materials were taken for the analysis of waste through manual sorting and for laboratory research. On average, for four trials (seasons), the main components of the RDF were plastics (37.55%), textiles (28.56%), paper (26.95%), and other materials that were difficult to visualize (6.92%) (Table 2).

The SRF fraction obtained from RDF was calculated using Eqs. 1 and 2. The calculation results of fractions SRF are presented in Table 2. The annual average results of fraction SRF are the following: plastics (28.51%), textiles (19.81%), paper (20.55%), and other materials (5.39%). More detailed information on each season is presented in Table 2. As detailed in Table 2, the amount of produced SRF differed with RDF origin. The difference in the results is explained by the fact that during the production of SRF, the

Table 2 RDF, SRF, and sewage sludge testing results

Composition of RDF/SRF (%)						Sewage sludge (%)
Fraction	1 Summer	2 Autumn	3 Winter	4 Spring	Annual average	
Plastic (%)	54.82/45.45	25.95/17.33	33.82/23.20	35.63/28.08	37.55/28.51	
Paper (%)	21.72/18.1	36.05/24.08	22.12/15.17	27.94/22.02	26.95/19.81	
Textile (%)	23.46/19.45	36.4/24.32	43.4/29.77	11.0/8.67	28.56/20.55	
Other (%)	–	1.6/1.07	0.66/0.45	25.43/20.04	6.92/5.39	
Total	**100/82.90**	**100/66.80**	**100/68.60**	**100/78.80**	**100/74.28**	
Moisture content (%)	17.1/1.9	33.2/4.1	31.4/2.2	21.2/2.7	25.7/2.7	5.18
Ash content (%)	7.5/5.8	14.2/9.1	8.6/3.9	11.9/6.5	11.9/6.3	16.35
Chlorine content (%)	1.2/0.47	1.4/0.53	1.18/0.16	1.19/0.28	1.27/0.36	0.14
Mercury content (mg/kg)	0.4/0.3	0.26/0.22	0.31/0.26	0.35/0.28	0.33/0.265	0.33
Net calorific value, MJ/kg	19.05/21.9	18.6/23.5	14.5/18.6	17.1/23.2	17.3/21.7	17.2

prohibited materials are extracted from the RDF, and during grinding, some moisture is lost.

Moisture significantly reduces the calorific value of fuel. As the humidity of the RDF increased, the calorific value tended to decrease. The moisture content of the RDF varied from 17.1 to 33.2% throughout the year and strongly depended on the season. The average moisture content during the four seasons of RDF was 25.7%. The moisture content value of SRF produced from RDF was lower than RDF and was in the range of 1.9 to 4.1%, depending on the season, and the average per year was 2.7% (Table 2). It was found that the moisture content of SRF depended on the moisture content of the RDF and the season.

The NCV was determined in two subsamples. The samples were tested in pellet form. The prepared samples were pressed with a hydraulic press at a force of approximately 10 t, having a diameter of approximately 13 mm and a mass of (1.0 ± 0.2) g. The calorific value was determined in an automatic bomb calorimeter IKA C6000 in adiabatic mode. The net calorific value of the RDF produced at the MBT was on average 17.3 MJ/kg. Due to the high moisture content (25.7%) and chlorine content in the materials, the RDF can be used only as fuel to produce heat or energy at the cogeneration power plant. Pretreated and prepared SRF had a relatively low moisture content (2.7%), a relatively high NCV (21.7 MJ/kg), and an acceptable chlorine content and can be used as an additive fuel (replacement fuel) in the cement industry.

It was found that the ash content in RDF produced at Kaunas MBT ranged from 7.5 to 14.2% (annual average 10.6%); for SRF, the ash content ranged from 3.9 to 9.1%, and the average yearly content was 6.3%.

Chlorine content has also been a limiting factor for fuel quality, not only for environmental but also for technical reasons. The chlorine concentration for RDF samples was in the range of 1.18–1.04% by weight. This result is most likely related to the presence of different types of plastics. However, the chlorine content in SRF samples was less than that in RDF and was 0.53–0.16%. A lower chlorine content is associated with the absence of prohibited materials in the fuel, especially chlorine-containing plastics.

The mercury content in the RDF varied seasonally and depended on the mercury-containing wastes. The mercury content of the RDF ranged from 0.26 to 0.4 mg/kg^{-1} and averaged 0.33 mg/kg^{-1}. The content of mercury in the prepared SRF had a lower value and was in the range from 0.22 to 0.3 mg/kg^{-1}, and the annual average content was 0.265 mg/kg^{-1}.

In summary, we determined the following from this study of fuel production from waste. The RDF obtained at the Kaunas MBT plant has stable thermal and energy properties, and it can be used for heat and energy production. However, due to its high moisture chlorine and mercury contents, the RDF is not recommended as a replacement fuel in the cement industry.

Nonetheless, after pretreatment of the RDF, after extracting prohibited materials (chlorine and mercury-containing), screening, and shredding, SRF was produced, and it had significantly better results than RDF. The SRF had lower humidity, higher calorific value, and lower chlorine and mercury contents than the RDF. From the data we obtained, we can summarize the following: SRF obtained from RDF has higher quality characteristics and can be used in the cement industry as replacement fuel according to EN 15,359.

During the treatment of municipal wastewater, a large amount of sewage sludge is formed, and its use is limited. One of the most promising ways to use municipal sewage sludge is to use it as fuel in clinker production. Such a technological solution is necessary due to the presence of prohibited materials in sewage sludge, which is not applicable for other uses. At high temperatures during clinker firing, various chemical and thermal transformations occur, which ultimately do not lead to deterioration of the clinker quality and exceed the maximum permissible concentrations of heavy metals. Today, the cement plant uses sewage sludge from all city wastewater treatment plants in the country. Sewage sludge has a sufficiently high calorific value and contains clinker-forming minerals. Therefore, it can be used as an alternative fuel at cement plants. The characteristics of sewage sludge obtained in our study are presented in Table 2. The characteristics of sewage sludge are within acceptable limits to use this waste in clinker production as an alternative fuel. The moisture content is 5.18%, which is a permissible moisture content value in clinker production. The ash content of sewage sludge is higher than the SRF ash content and is 16.35%. The calorific value is 17.2 MJ/kg, which is sufficient to be used as an additive with coal. Concerning the mercury and chlorine contents, the obtained values are in the acceptable ranges and are 0.33 mg/kg^{-1} and 0.14%, respectively.

Characterization and calculation of the SRF production line

Significant waste management is already conducted, as, at the Kaunas MBT, there are NIR separators, shredders, drum sieves, and manual separation processes, as seen in Fig. 3. However, these processes are not sufficient for the final product (RDF) to be usable in clinker production since it contains prohibited materials and metals and has a high moisture content. However, with the help of existing NIR separators, chlorine (PVC plastics) can be removed during MSW treatment; thus, additional NIR separators are not required in the SRF production line. We proposed supplementing the existing waste processing scheme with several additional operations and equipment.

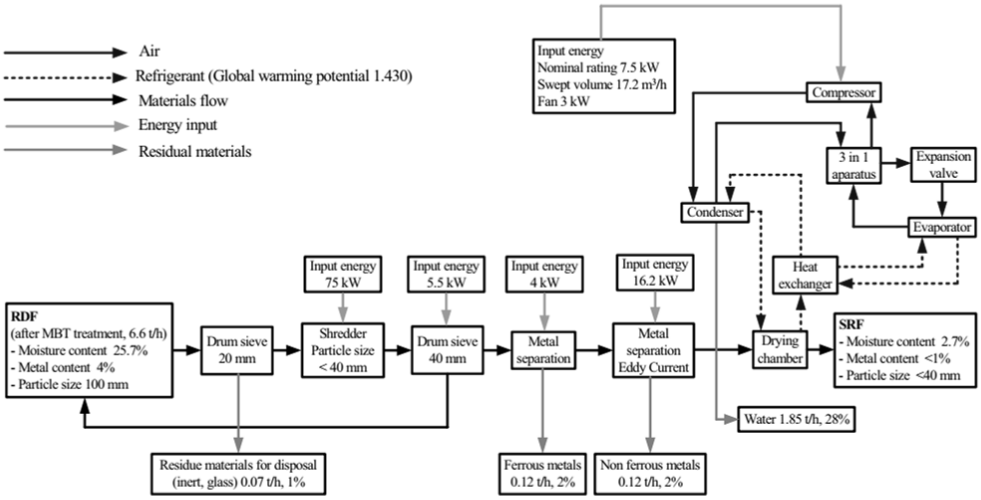

Fig. 3 SRF production line

As seen in Fig. 3, the production line of the SRF consists of six additional units of equipment. Each part of the equipment plays a vital role in preparing and improving fuel quality from waste. The first stage in preparing fuel from waste begins with a first drum sieve. At the first drum, the sieve produces fractions mainly composed of food and inert materials such as dust, stones, and glass. The drum sieve rotates the material diagonally down, and due to 20-mm-wide gaps in the wall of the drum, it separates large and small fractions. Waste is shredded down to 40-mm-sized particles, which are later passed through a second drum sieve to make the material homogeneous and improve its combustible properties. The second drum sieve ensures the required size of the SRF, as larger particles are directed back to the beginning position of the production line.

As the fuel becomes homogeneous depending on the particle size, it is necessary to lower the content of the metal, prohibited materials (plastics such as PVC), and moisture content in the material, as they reduce the quality of the product. First, ferrous metal separation is used at the line. In the next stage of the utilization of waste, these metals can be sold and recycled. Then, in the SRF production line, nonferrous metals are separated with an eddy current separator based on induced circular electric currents that occur in a moving piece of nonferrous metal scrap. At the end of the production line of SRF, there is a thermally treated stage with a drum dryer. Drying in the drum is optimal because it has a low maintenance cost, is simple to operate, and can proceed with large amounts of production. The SRF was obtained by applying all necessary technological operations with the separation and extraction stages and is presented in Fig. 4.

Today, waste, after treatment at the Kaunas MBT, is sent to the cogeneration power plant to produce heat and energy. Because some waste is incinerated in the Kaunas cogeneration power plant, it is not practically possible to fully convert all of the incinerated waste (RDF) into SRF. The amount of waste for producing power in the Kaunas CPP and the amount of waste for the cement plant at "Akmenės cementas" must be balanced. Some of the waste, approximately half, is incinerated, with a maximum of 6.6 t/h; this waste can be converted into SRF production. This amount of SRF will be sufficient to use in co-firing with coal and will not degrade the quality of the clinker produced. The material flow rates in the SRF production line were calculated based on the data above. The calculation of the flow rate of the SRF production line was conducted with Eqs. 3–24 and amounted to 4.47 t/h. The flow rate of the SRF production line will depend on the extracted materials at each stage of the separation line.

The next stage of studying fuel from waste was calculating the percentage fractions of SRF obtained after RDF treatment. From RDF-extracted food, glass, and metals to meet the requirements to fuel from waste, some of the moisture is lost during treatment. The moisture content in the final product was less than 1%. The calculation of the SRF fraction produced from RDF was conducted with Eqs. 1 and 2, and the results are presented in Table 2. The percentage

Fig. 4 SRF produced from RDF

RDF

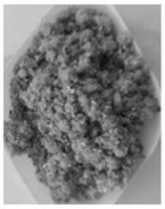

SRF summer

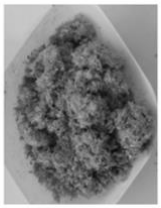

SRF autumn

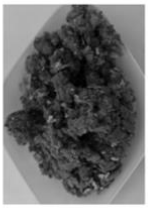

SRF winter

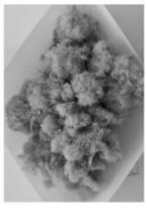

SRF spring

of a particular faction strictly depends on the season, human behaviour, and certain circumstances, such as holidays.

SRF in the cement industry

Currently, "Akmenes cementas" use coincineration sewage sludge with limestone, clay, sand, and iron ore. Approximately 10% of the fuel used in the company is tires. Figure 5 shows the clinker production line with tires and sewage sludge as additional fuel. Whole tires are transferred to the middle part of the kiln through the transporter system through a special supply line. According to data from the cement enterprise, an advantage of cement production kilns is that no additional waste products remain when burning waste (the temperature is 1300–1400 °C at the waste feeding point). All ash that forms during the burning process compounds into a clinker without affecting product quality.

As mentioned above, we proposed using the obtained SRF in the current technological line of clinker production. The essential characteristics of SRF and sewage sludge can be summarized as follows: the calorific value, moisture, ash, and chlorine content of this waste allow for its use as a fuel in the cement industry. The importance of these parameters may change depending on the season, but these changes will be within acceptable limits and will not degrade the quality of the product. Ash was obtained after incinerating SRF and sewage sludge in a muffle furnace. Both ashes are presented in Fig. 6.

The elemental oxide analysis (%, in ash) obtained by SEM–EDS and presented in Table 3 confirms that the oxide composition of SRF and sewage sludge corresponds to the oxide composition of the finished clinker. From the available data, the dominating elements are Si and Ca, two of the main elements in clinker production. Additionally, Al, Fe, Mg, and other elements that play important roles in the cement industry were observed. However, it should be noted that the percentage of oxides in SRF, sewage sludge, and clinker differed. It can be concluded that SRF can be used as a fuel in clinker production and sewage sludge but in a particular proportion. Because there are some oxides, the amount must be strictly controlled.

The italicized elements in Table 3 are foundational in the chemical composition of the clinker. For the contents of chromium, copper, and manganese did not exceed 3%; at high temperatures of 1200–1450 °C and above, these elements do not pose any danger to the clinker. Although Zn has been added to the list of environmentally harmful elements, its relatively low content (less than one percent), based on waste acceptance criteria (Council Decision 2003/33/EC 2003), can be interpreted as inert.

X-ray studies of sewage sludge and SRF in Fig. 7 show that the main minerals are quartz (SiO_2), iron oxide (Fe_2O_3), monalbite ($NaAlSi_3O_8$), whitlockite ($Ca_{18.53}Fe_4Mg_{1.6}(PO_4)_{14}$), calcite ($Ca(CO_3)$), microcline ($KAlSi_3O_8$), cristobalite ($SiO_2$), akermanite ($(Ca_{1.53}Na_{.51})(Mg_{.39}Al_{.41}Fe_{.16})(Si_2O_7)$), albite ($Na(AlSi_3O_8)$), perovskite ($CaTiO_3$), brushite ($CaPO_3(OH)_2H_2O$), and monetite ($CaHPO_4$).

XRD analysis presented in Fig. 8 shows that the residue contains crystalline calcium-, sodium-, potassium-, iron-, and silicon-bearing phases. The presence of the crystalline phase has favourable effects on the production of

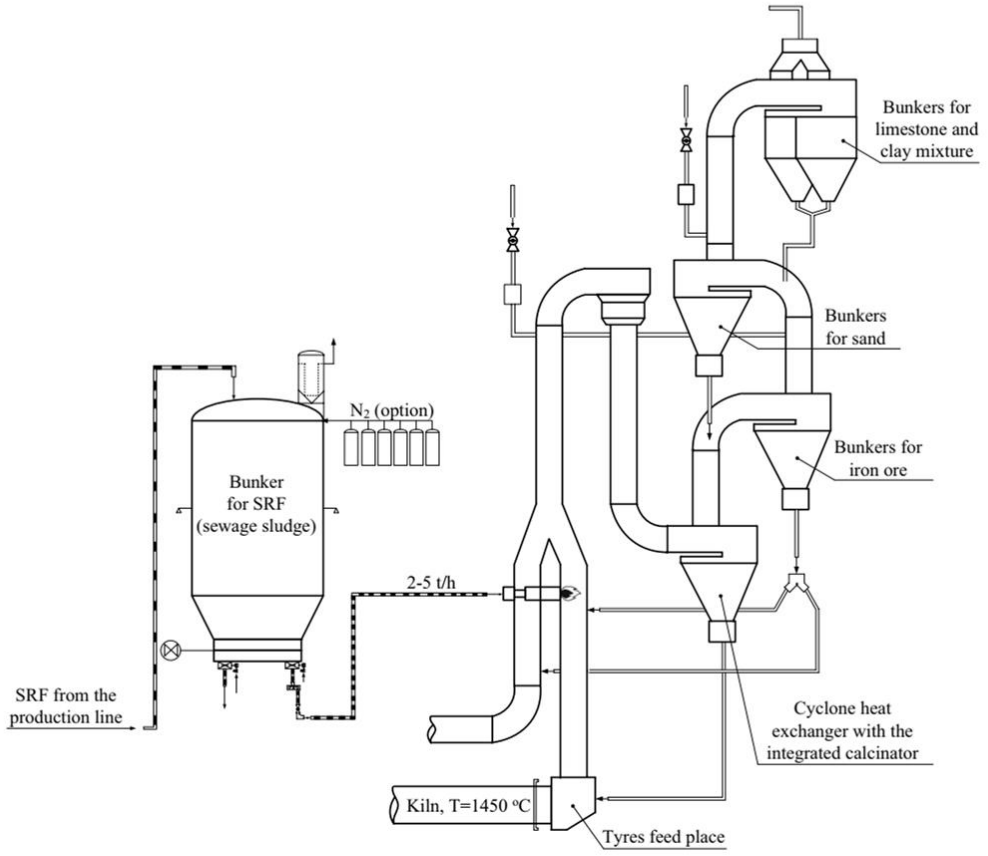

Fig. 5 Flow sheet of clinker production

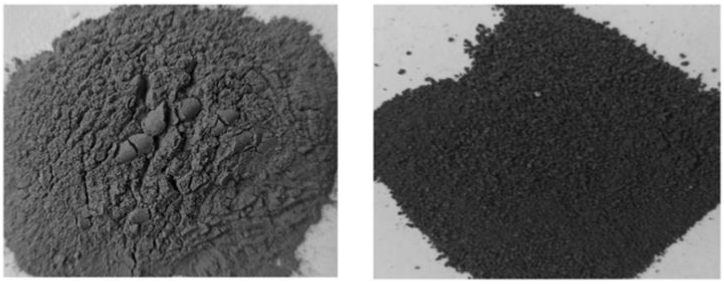

Fig. 6 Images of ash after incineration of SRF (left), sewage sludge (right)

Table 3 Elemental oxide analysis (%, in ash) based on SEM–EDS measurements

Elements	CaO	Fe_2O_3	SiO_2	P_2O_5	Al_2O_3	SO_3	MgO	Na_2O	TiO_2	K_2O	Cr_2O_3	CuO	MnO	ZnO	**Total**
Sewage sludge	***32.82***	***19.27***	***12.62***	***20.16***	***3.81***	***4.30***	***2.15***	***0.86***	***0.75***	***1.20***	0.09	0.19	1.72	–	**100**
SRF	***30.46***	***8.83***	***35.53***	***1.26***	***8.68***	***2.62***	***3.71***	***5.48***	***1.62***	***0.67***	0.09	0.38	–	0.61	**100**

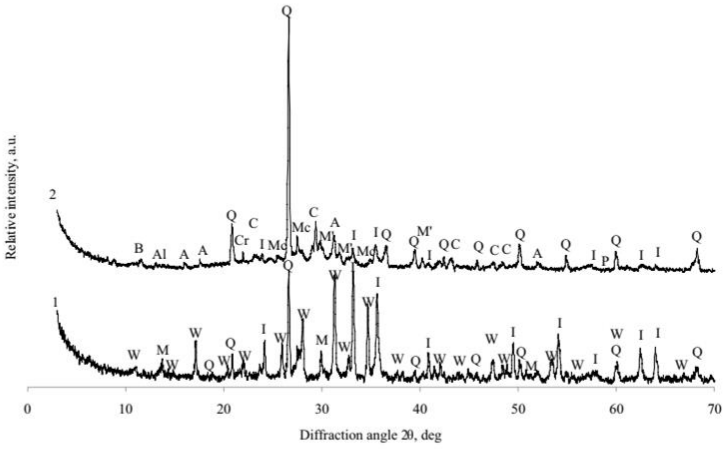

Fig. 7 The X-ray diffraction pattern of sewage sludge (1) and SRF (2) ash: Q quartz, I iron oxide, M monalbite, W whitlockite, C calcite, Mc microcline, A akermanite, Cr cristobalite, Al albite, P perovskite, B brushite, M′ monetite

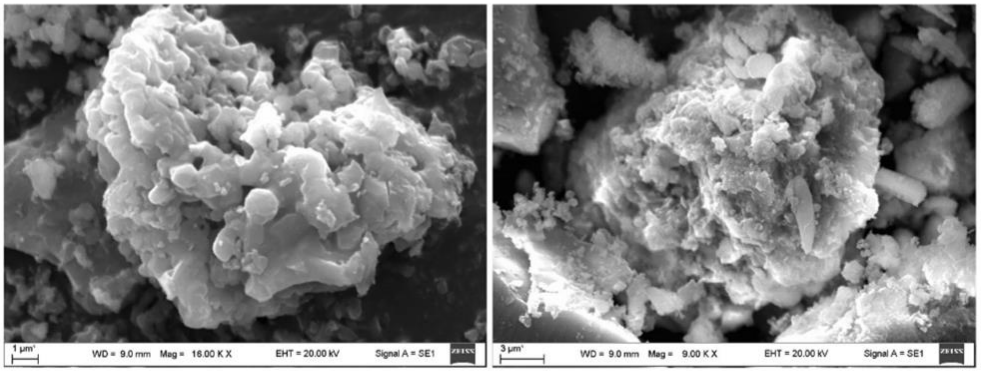

Fig. 8 SEM image of the ash of sewage sludge (left) and SRF (right)

building materials. The elemental composition obtained by SEM–EDS analysis, XRD analysis, and X-ray diffraction patterns of sewage sludge and SRF after incineration at 950 °C confirmed the presence of crystalline phases in the obtained materials, confirming the possibility of using SRF in the production of cement.

Table 4 shows the calculation results on the possibility of utilizing SRF in clinker firing. According to the data in Table 4, the feed rate of the SRF is 3.5 t/h when the SRF is used at a rate of 25%. Moreover, with the coincineration of sewage sludge and SRF, the total waste feed rate will be

Table 4 The calculation for the use and saving coupled with SRF and coal

Parameter	Initial situation	Scenario 1	Scenario 2	Scenario 3	Scenario 4
SRF replacement ratio (%)	0	10	15	20	25
Coal consumption ratio (%)	100	90	85	80	75
Coal consumption, C_{coal} (t/h)	16.1	11.7	10.4	9.3	8.1
SRF consumption, A_{SRF} (t/h)	0	1.92	2.72	3.42	4.0
Replacement ratio to substitute 1 t of coal, RR	0	1:0.43	1:0.48	1:0.5	1:0.51
Coal savings, AS_{coal} (t/year)	0	37,948	48,876	59,178	68,857
Coal savings, AI (USD/year)	0	5,198,978	6,696,013	8,107,504	9,433,449
CO_2 emission saving in coal, CS_{CO2} (t/year)	0	32,256	41,544	50,302	58,528
CO_2 emission saving in coal, ES_{CO2} (USD/year)	0	1,870,873	2,409,587	2,917,517	3,394,664
Net saving, NS (USD/year)	0	6,520,911	8,260,971	9,874,286	11,363,651

five tons per hour, which does not exceed the permissible value for clinker quality.

Economic and environmental benefits of using SRF in the cement industry

According to the cement plant, adding up to 25% of nonhazardous waste as an additional fuel in cement production does not impair the quality of clinker and does not lead to the formation of other emissions of flue gases into the atmosphere. According to the Directive, 2000/76, approximately 3.52 MJ is needed to obtain 1 kg of clinker. Some studies (Hemidat et al. 2019) have shown potential environmental and economic benefits associated with SRF production and its use as a fuel in clinker firing. On the one hand, SRF production has an advantageous effect on the environment by reducing the use of non-renewable energy sources. On the other hand, replacing traditional fossil fuels with SRF at industrial facilities leads to energy recovery and reduced emissions (Reza et al. 2013). The possibility of using the produced SRF as an additive for fuel during clinker firing was assessed. This calculation included analysing the share of CO_2 in greenhouse gas emissions and determining the energy needed for firing clinker by replacing coal with an SRF.

Clinker production generated a vast amount of CO_2. Carbon dioxide is a product of the chemical conversion (calcinations) process that occurs in clinker production. During the cement production process, calcium carbonate ($CaCO_3$) is heated in a cement kiln to a temperature of approximately 1300–1450 °C to form calcium oxide and carbon dioxide—a calcination process. The calcination process releases a large amount of CO_2 into the atmosphere. The resulting lime reacts with silicon dioxide, aluminium, and other materials to form clinker. Then, a small amount of gypsum is added to the clinker materials to produce Portland cement.

To assess the economic benefits of SRF utilization and calculation, four options resulting from adding SRF as a replacement fuel were proposed. The variants for this calculation were based on previous publications (Kara 2012; Hemidat et al. 2019) and actual data. Four distinct options were for the economic assessment of the addition of SRF to the primary fuel (coal) at ratios of 10%, 15%, 20%, and 25%. The calculation was carried out according to Eqs. 8–24. The calculation results of the four scenarios are presented in Table 4.

Calculations of the net savings in total operating costs and carbon dioxide emissions from the addition of SRF as a fuel to replace the coal currently used in the cement plant are detailed in Table 4. Calculations were performed using Eqs. 8–24 for four scenarios for replacing coal with SRF.

Discussion

Human activities always produce large amounts of waste, and generation rates increase with population expansion and economic growth. This raises the problem of waste recycling and disposal. The problem of recycling waste is quite acute in Europe and worldwide. Bright disposable packaging and new fashion clothes pose a severe danger to the ecosystems of industrialized countries, not to mention the fact that a considerable amount of energy and raw materials is spent on their production.

The primary legal documents according to which it is possible to recycle waste without harming humans and the environment are Directive (EU) 2018/850 and Directive (EU) 2000/76. According to these documents, waste disposal sent to landfills must be significantly reduced by 2030. This reduction will prevent negative impacts on human health and the environment, lead to maximum recycling waste, and achieve a circular economy. In addition to the directive, landfills should remain exceptional, not the norm. According to Directive 2000/76, waste can be incinerated to generate energy or produce material products, where waste is used as regular or additional fuel. This applies to all nonhazardous wastes, including sewage sludge, tires, and other

nonhazardous waste. Based on these two directives, studies have been carried out on the possible disposal of waste with maximum benefits and without harming humans and the environment.

The cement industry increasingly often tries to use alternative fuels with maximum benefits and minimum capital costs. Therefore, SRF can provide an immense benefit because reuse as an alternative fuel can decrease the cost of disposal. By using alternative fuels, cement companies reduce the consumption of non-renewable minerals and, at the same time, help to avoid the traditional disposal of waste materials through landfilling or incineration. Increased use of alternative fuels can influence the cement company's direct carbon dioxide emissions because the alternative fuel emission factors differ from those of traditional fuels (CSI 2011; You and Kakinaka 2021). In addition to the direct effects, the use of alternative fuels in the cement industry generally reduces GHG (greenhouse gas) emissions from landfills and incinerators. Such indirect emissions can be higher than direct CO_2 emissions from the combustion of alternative fuels, depending on the type of waste. The combination of the direct and indirect impacts of emissions and resource efficiency makes substituting non-renewable natural resources an effective way to reduce global GHG emissions (CSI 2011; Rehman et al. 2021).

This paper investigated SRF production from RDF and the feasibility of its utilization in the cement industry. Additionally, sewage sludge characteristics that are currently used as additional fuel during clinker firing were studied. The data obtained indicate that after separating the biological fraction, a nonrecyclable fraction (RDF) is sent to the Kaunas CPP for incineration to produce heat and energy. The granulometric analysis made it possible to determine that the bulk of the nonrecyclable material has a size $d > 80$ mm and 80 mm $> d > 40$ mm (81.3 and 15.1%, respectively). According to the results of morphological analysis, it was established that the main fractions present in the waste are plastics, paper, and textiles (37.55, 26.95, and 28.56%, respectively). To achieve the goals set in Directive 2018/850 and Directive (EU) 2000/76, an SRF production line for the production of alternative fuel for the cement industry was developed. The main characteristics that play an essential role in using waste as fuel have been studied.

Figure 9 shows the moisture contents of the RDF and SRF, which strongly depend on the season and waste composition, and also shows the measurements of the net calorific value. The presented results show that the RDF obtained at the MBT plant can only be used for energy production since this type of fuel is not regulated and does not comply with the EN 15,359 standard. RDF has reasonably high humidity and lower calorific value in comparison with the characteristics of the prepared SRF. The moisture content is a good indicator to use the fuel from waste as an additional fuel in

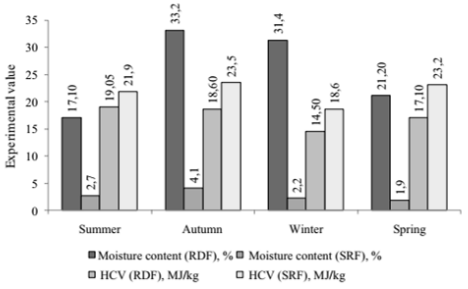

Fig. 9 Moisture content and net calorific value of the RDF and SRF

clinker production. The moisture content of the produced SRF is 2.7%, which is a satisfying value for use in clinker production. The net calorific value (average annual value) of the SRF (21.7 MJ/kg) has a higher indicator than the calorific value of the RDF (17.3 MJ/kg).

In parallel with the study of RDF and SRF, the characteristics of sewage sludge were investigated. Currently, sewage sludge is used as an additional fuel in clinker firing since sewage sludge is classified as nonhazardous waste following Directive 2000/76. Today, the humidity of sewage sludge used as additional fuel in clinker production is 10–12%; the ash content and net calorific values are 16.35% and 17.2 MJ/kg, respectively. In the course of this research, it was found that the ash obtained from the combustion of sewage sludge and SRF in a muffle furnace at a temperature of 950 °C in terms of oxide composition and phase composition corresponds to the chemical composition of clinker but in different percentages amount. The ash presents crystalline calcium-, sodium-, potassium-, iron-, and silicon-bearing phases. This result proves the fact that the SRF produced by us can be used as an additional fuel in the production of clinker.

This paper proposes and calculates a technological line for the production of SRF. The flow rate of the SRF production line for the Kaunas MBT plant was calculated to be 4.5 tons per hour. There was a proposal to locate the production SRF line on the property of the MBT plant since the bulk of the equipment for the extraction of metals, glass, and other prohibited materials is already available. A method for calculating the resulting fraction of SRF from RDF was proposed. This paper presents a calculation method that confirms the feasibility of using SRF in the cement industry as additional fuel from an economic and ecological point of view. The development of Scenario 4 (maximum option 25% replacement ratio) will achieve 9,433,449 USD/year annual coal savings after adding 34,655 t/year SRF to traditional fuel. The net cost saving calculation, which takes CO_2 cost savings and SRF cost and efficiency losses into

account, shows that the net annual saving is approximately 11,363,651 USD/year with a maximum fuel replacement fraction of 25%.

This work shows that SRF as an alternative fuel has potential for the Lithuanian cement industry. Today, for the production of one ton of clinker, 843 kg of CO_2 is emitted into the atmosphere. The results confirmed that using SRF as an alternative fuel during the clinker firing process will significantly reduce greenhouse gas emissions.

It should be noted what difficulties can be encountered during the SRF production process. The first thing to note is the method of extracting prohibited materials. Today, at the MBT plant, the extraction of prohibited materials is carried out manually. Consideration should be given to installing separators to recover these materials. It is also necessary to minimize the production of chlorine and mercury content materials and collect them at a particular point.

The disadvantage of the SRF production process is the constant monitoring of compliance with the morphological composition, and in the case of deviation from the norm, the replacement coefficient should be adjusted. Additionally, the disadvantage should include the installation of additional equipment. However, such capital investments will be one time.

Conclusions

In this study, a production line for SRP production from RDF was developed. After extracting prohibited materials from RDF, shredding, and drying, the SRF was obtained. Then, the energy potential of SRF and the possibility of its use as an alternative fuel during clinker firing were studied. The main characteristics of fuel from waste were determined and compared with the European standard. The morphological and granulometric composition of the fractions made it possible to determine that the percentage of high-calorie fractions varies depending on the season. After the separation of the biological fraction from MSW, the size of the RDF consisted of 81.3% $d > 80$ mm and 15.1% 80 mm $> d > 40$ mm. The produced SRF had the following characteristics: NCV = 21.7 MJ/kg, Cl = 0.36%, and Hg = 0.265 mg/kg^{-1}. This material can be used as additional fuel for clinker firing. The RDF produced at the MBT plant by its characteristics can only be used in CPP to generate heat or power. Today, clinker kilning in a cement plant uses sewage sludge as an alternative fuel. The main characteristics of sewage sludge were determined as follows: NCV = 17.2 MJ/kg, Cl = 0.14%, and Hg = 0.33 mg/kg^{-1}. It has been established that the sewage sludge and the SRF produced correspond to the European standard in terms of the main characteristics required for fuels from waste and can be used in clinker firing as an alternative fuel.

It has been experimentally proven that the ash obtained after the combustion of SRF and sewage sludge has a crystalline structure and consists of sodium-, calcium-, potassium-, iron-, and silicon-bearing phases. Elemental analysis using the SEM–EDS method confirmed that the oxide composition of the SRF and sewage sludge consists of clinker-forming oxides but with a different percentage of oxides.

This paper proposed a line for the production of SRF. The consumption of the production line was calculated to be 4.47 t/h. The SRF production line was developed so not to disturb the operation of the CPP. It is substantiated that the SRF line is best located on the property of the MBT plant with the installation of additional equipment for the extraction of prohibited materials, grinding, and drying. At the end of the SRF production process, the volume of the finished product decreased by 18%. This paper proposes to use the supply of the produced SRF to the existing clinker firing line in addition to sewage sludge. Currently, the enterprise uses sewage sludge (1.5 t/h) as a replacement fuel; however, the capacity of the SRF line can supply an alternative fuel of 7.5 t/h without compromising the quality of the resulting clinker.

This paper calculated the economic feasibility of using SRF as a replacement fuel for clinker firing. Thus, when using 10% of the SRF as additional fuel to coal, which is 16,634 t/year, it will save 37,948 t/year of coal and 5,198,978 USD/year from the cost of coal imports and 1,870,873 USD/year from greenhouse gas emissions, and the net savings will be 6,520,911 USD/year. Calculations show that replacing coal with SRF at 10% to 25% will reduce the consumption of fossil resources, reduce greenhouse gas emissions, and bring Lithuania closer to a circular economy.

Acknowledgements We acknowledge Marius Praspaliauskas, Senior research associate, Laboratory of Heat-Equipment Research and Testing, Lithuanian Energetic Institute (LEI) for helping in preparing materials for the experiment. We would like to say our great gratitude to the staff of the Center for Hydrogen Energy Technologies, LEI for helping with research. We acknowledge the staff of Kaunas regional waste management centre and "Akmenes cementas" for helping with research and informational support.

Author contribution IP: conceptualization, data curation, formal analysis, methodology, resources, software, supervision, writing—original draft, review, and editing; DR: data curation, software; AB: formal analysis, methodology, software; RK-D: formal analysis, software; GD: conceptualization, data curation, formal analysis, review, and editing.

Data availability The datasets used and/or analysed during the current study are available from the corresponding author on reasonable request.

Declarations

Ethics approval and consent to participate Not applicable.

Consent for publication Not applicable.

Competing interests The authors declare no competing interests.

References

Akmenės cementas (2021) Description of cement production technology.https://cementas.lt/en/production/description-of-cement-production-technology/. Accessed August 2014

Al-Hamamre Z, Saidan M, Hararah M, Rawajfeh K, Alkhasawneh H, Al Shannag M (2017) Wastes and biomass materials as sustainable-renewable energy resources for Jordan. Renew Sustain Energy Rev 67:295–314. https://doi.org/10.1016/j.rser.2016.09.035

Apergis N, Gozgor G, Lau CK (2021) Globalization and environmental problems in developing countries. Environ Sci Pollut Res 28:33719–33721. https://doi.org/10.1007/s11356-021-14105-z

Arina D, Bendere R (2018) Waste as energy source in EU action plan for the circular economy. Environ Res Eng Manag 74(1):43–49. https://doi.org/10.5755/j01.erem.74.1.19779

Aslan A, Altinoz B (2021) The impact of natural resources and gross capital formation on economic growth in the context of globalization: evidence from developing countries on the continent of Europe, Asia, Africa, and America. Environ Sci Pollut Res 28:33794–33805. https://doi.org/10.1007/s11356-021-12979-7

Birnstengel B, Alwast H, Häusler A, Vogt R, Giegrich J, Baumann W (2015) Resource savings and CO_2 reduction. https://doi.org/10.13140/RG.2.1.1910.6721

Caetano M, Góis J, Leitão A (2020) Challenges and perspectives of greenhouse gases emissions from municipal solid waste management in Angola. Energies Reports 6:364–369. https://doi.org/10.1016/j.egyr.2019.08.074

Calvo G, Valero A (2021) Strategic mineral resources: availability and future estimations for the renewable energy sector. Environmental Development Online: 100604. https://doi.org/10.1016/j.envdev.2021.100640

Coal marketing international CMI (2021) Coal marketing international. Coal basics. http://www.coalmarketinginfo.com/coal-basics/. Accessed 2012

Council Decision 2003/33/EC establishing criteria and procedures for the acceptance of waste at landfills pursuant to article 16 of an Annex II to Directive 1999/31/EC. https://www.ecolex.org/details/legislation/council-decision-200333ec-establishing-criteria-and-procedures-for-the-acceptance-of-waste-at-landfills-pursuant-to-article-16-of-and-annex-ii-to-directive-199931ec-lex-faoc039228/. Accessed 19 December 2002

Cement Sustainability Initiatives (CSI) (2011) CO_2 accounting reporting standard for the cement industry, the cement CO_2 protocol. http://docs.wbcsd.org/2011/05/CSI-CO2-Protocol.pdf. Accessed 26 May 2011

Danish UR, Ulucak R (2021) Renewable energy, technological innovation and the environment: a novel dynamic auto-regressive distributive lag simulation. Renew Sustain Energy Rev 150:111433. https://doi.org/10.1016/j.rser.2021.111433

Del Zotto L, Tallini A, Di Simone G, Molinari G, Cedola L (2015) Energy enhancement of solid recovered fuel within systems of conventional thermal power generation. Energy Procedia 81:319–338. https://doi.org/10.1016/j.egypro.2015.12.102

Di Lonardo MC, Franzese M, Costa G, Gavasci R, Lombardi F (2016) The application of SRF vs. RDF classification and specifications to the material flows of two mechanical-biological treatment plants of Rome: comparison and implications. Waste Manag 47B:195–205. https://doi.org/10.1016/j.wasman.2015.07.018

Dianda P, MahidinMunawar E (2018) Production and characterization refuse derived fuel (RDF) from high organic and moisture contents of municipal solid waste (MSW). IOP Conf Ser: Mater Sci Eng 334:012035. https://doi.org/10.1088/1757-899X/334/1/012035

Directive (EU) 2018/850 of the European Parliament and of the Council amending Directive 1999/31/EC on the landfill of waste. https://eur-lex.europa.eu/eli/dir/2018/850/oj. Accessed 30 May 2018

Directive 2000/76/EC of the European Parliament and of the Council on the incineration of waste. https://eur-lex.europa.eu/eli/dir/2000/76/oj. Accessed 31 Dec 2020

EN 15359 (2011) Solid recovered fuels—specifications and classes. https://standards.iteh.ai/catalog/standards/cen/cb0123b1-6835-45e7-9257-12016bb1db42/en-15359-2011. Accessed 09 Nov 2011

Communication from the commission to the European parliament, the council, the European economic and social committee and the committee of the regions COM (2017) The role of waste-to-energy in the circular economy. Brussels, 26.1.2017 34 final. https://eur-lex.europa.eu/legal-content/EN/TXT/PDF/?uri=CELEX:52017DC0034

Garces D, Diaz E, Sastre H, Ordonez S, González-LaFuente JM (2017) Evaluation of the potential of different high calorific waste fractions for the preparation of solid recovered fuels. Full Text Links Waste Manag 47(Pt B):164–173. https://doi.org/10.1016/j.wasman.2015.08.029

Gerassimidoua S, Velishttps CA, Williamsb PT, Castaldic MJ, Blacka L, Komilis D (2021) Chlorine in waste-derived solid recovered fuel (SRF), co-combusted in cement kilns: a systematic review of sources, reactions, fate and implications. Crit Rev Environ Sci Technol 51(2):140–186. https://doi.org/10.1080/10643389.2020.1717298

Hashem FS, Razek TA, Mashout HA (2019) Rubber and plastic wastes as alternative refused fuel in cement industry. Constr Build Mater 212:275–282. https://doi.org/10.1016/j.conbuildmat.2019.03.316

Hemidat S, Saidan M, Al-Zu'bi S, Irshidat M, Nassour A, Nelles M (2019) Potential utilization of RDF as an alternative fuel to be used in cement industry in Jordan. Sustainability 11(20):5819. https://doi.org/10.3390/su11205819

Kara M (2012) Environmental and economic advantages associated with the use of RDF in cement kilns. Resour Conserv Recycl 68:21–28. https://doi.org/10.1016/j.resconrec.2012.06.011

Kulkarni BN (2020) Environmental sustainability assessment of land disposal of municipal solid waste generated in Indian cities—a review. Environ Dev 33:100490. https://doi.org/10.1016/j.envdev.2019.100490

Kulokas M, Praspaliauskas M, Pedišius N (2021) Investigation of buckwheat hulls as additives in the production of solid biomass fuel from straw. Energies 14(2):265. https://doi.org/10.3390/en14020265

Liu D, Zhang W, Wang X et al (2021) Greenhouse gas emissions and mitigation potential of hybrid maize seed production in northwestern China. Environ Sci Pollut Res. https://doi.org/10.1007/s11356-021-16990-w

Menéndez P, Parra Martín R, Varela-Candamio A, García-Álvarez L (2021) An enhanced techno-economic analysis of LCOE: public incentives vs private investment. Technol Econ Dev Econ 27(1):1–23. https://doi.org/10.3846/tede.2020.11259

Municipal waste statistics (2020) Eurostat statistics explained. https://ec.europa.eu/eurostat/statistics-explained/index.php?title=Municipal_waste_statistics. Accessed Feb 2021

Neehaul N, Jeetah P, Deenapanray P (2020) Energy recovery from municipal solid waste in Mauritius: opportunities and challenges. Environ Dev 33:100489. https://doi.org/10.1016/j.envdev.2019.100489

Organization for economic Co-operation and development OECD (2021) Effective carbon rates. https://www.oecd.org/tax/

tax-policy/effective-carbon-rates-2021-highlights-brochure.pdf. Accessed 2021

Pomberger R, Sarc R (2014) Use of solid recovered fuels in the cement industry. https://www.vivis.de/wp-content/uploads/WM4/2014_wm_471_488_pomberger.pdf. Accessed 2014

Prabhakaran SP, Swaminathan S, Viraj G, Joshi V (2020) Energy conservation—a novel approach of co-combustion of paint sludge and Australian lignite by principal component analysis, response surface methodology and artificial neural network modeling. Environ Technol Innov 20:101061. https://doi.org/10.1016/j.eti.2020.101061

Rehman A, Ma H, Ozturk I et al (2021) Sustainable development and pollution: the effects of CO_2 emission on population growth, food production, economic development, and energy consumption in Pakistan. Environ Sci Pollut Res. https://doi.org/10.1007/s11356-021-16998-2

Reza B, Soltani A, Ruparathna R, Sadiq R, Hewage K (2013) Environmental and economic aspects of production and utilization of RDF as alternative fuel in cement plants: a case study of Metro Vancouver Waste Management. Resour Conserv Recycl 81:105–114. https://doi.org/10.1016/j.resconrec.2013.10.009

Sakri A, Aouabed A, Nassour A, Nelles M (2021) Refuse-derived fuel potential production for co-combustion in the cement industry in Algeria. Waste Manag Res: J Sustain Circ Econ 39(9):1174–1184. https://doi.org/10.1177/0734242X20982277

Striugas N, Pedisius N, Praspaliauskas M (2018) Elemental migration and transformation from sewage sludge to residual products during the pyrolysis process. Energy Fuels 32(4):5199–5208. https://doi.org/10.1021/acs.energyfuels.8b00196

Usón AA, Lopez-Sabirón AM, Ferreira G, Sastresa EL (2013) Uses of alternative fuels and raw materials in the cement industry as sustainable waste management options. Renew Sustain Energy Rev 23:242–260. https://doi.org/10.1016/j.rser.2013.02.024

Viczek SA, Aldrian A, Pomberger R, Sarc R (2020) Determination of the material-recyclable share of SRF during co-processing in the cement industry. Resour Conserv Recycl 156:104696. https://doi.org/10.1016/j.resconrec.2020.104696

Wang Z (2021) Greenhouse data acquisition system based on ZigBee wireless sensor network to promote the development of agricultural economy. Environ Technol Innov 24:101689. https://doi.org/10.1016/j.eti.2021.101689

You V, Kakinaka M (2021) Modern and traditional renewable energy sources and CO_2 emissions in emerging countries. Environ Sci Pollut Res. https://doi.org/10.1007/s11356-021-16669-2

sustainability

MDPI

Article

Proposal for Implementation of Extraction Mechanism of Raw Materials during Landfill Mining and Its Application in Alternative Fuel Production

Inna Pitak [1,*], Gintaras Denafas [1], Arūnas Baltušnikas [1], Marius Praspaliauskas [2] and Stasė-Irena Lukošiūtė [1]

[1] Laboratory of Materials Research and Testing, Lithuanian Energy Institute, Breslaujos st. 3, LT-44403 Kaunas, Lithuania
[2] Laboratory of Heat-Equipment Research and Testing, Lithuanian Energy Institute, Breslaujos st. 3, LT-44403 Kaunas, Lithuania
* Correspondence: inna.pitak@lei.lt

Abstract: New approaches to waste management and the demands of the circular economy have changed the management of landfills. Over time, the decomposition of buried waste primarily determines the amount of recyclable and combustible materials. This pilot study attempted to assess the feasibility of extracting and recovering energy-intensive raw materials from landfills by developing a waste extraction mechanism and creating a solid recovered fuel (SRF) production line for use as a replacement fuel in the cement industry. The proposed mechanism consisted of two stages. The first stage was recommended to be carried out on the landfill territory by screening out the fine fraction and extracting inert materials and bulky waste. The second stage should be on the mechanical biological treatment (MBT) plant's territory by adding additional technological equipment to the MBT line. The productivity of the SRF production line was calculated and was 4.9 t/h. The mechanism proposed in the work was tested at the operating test site in Lithuania. The composition of Landfill Mined Residues (LMRs) was studied, and the energy potential of the studied part of the landfill was calculated, which was 196,700 GJ. It has been found that the SRF produced complies with the European Union (EU) standard and, according to its classification characteristics, belongs to class III and can be used as a replacement fuel in the clinker firing process. An environmental and economic efficiency assessment was conducted using SRF in the cement kiln. The calculation result showed that using 10% SRF as a replacement fuel for coal used in clinker firing at 2.51 t/h would save 1274 USD/h in coal costs. This use of SRF will emit 3.64 t/h CO_2 and achieve a net savings of 1355 USD/h. The mechanism proposed in this work aimed at reducing waste in landfills by converting materials into energy resources will help achieve the circular economy's goals.

Keywords: landfill mining; mechanism; renewable energy; alternative fuel production; properties; cement industry

Citation: Pitak, I.; Denafas, G.; Baltušnikas, A.; Praspaliauskas, M.; Lukošiūtė, S.-I. Proposal for Implementation of Extraction Mechanism of Raw Materials during Landfill Mining and Its Application in Alternative Fuel Production. *Sustainability* **2023**, *15*, 4538. https://doi.org/10.3390/su15054538

Academic Editor: Rajesh Kumar Jyothi

Received: 25 January 2023
Revised: 24 February 2023
Accepted: 28 February 2023
Published: 3 March 2023

1. Introduction

In recent years, the waste management industry has experienced rapid development, setting increasingly ambitious environmental goals for the future and working towards the rational use of waste as a resource, especially as an energy resource [1].

The waste management hierarchy indicates the order of preference for actions to reduce and manage waste and aims to extract the maximum practical benefit. In the waste hierarchy, prevention, minimization, recycling and energy recovery are preferred over landfills, which remain the last option in waste management [2]. According to the statements of Eurelco [3], by 2030, at least 65% of household waste should be recycled, and waste disposal in landfills should be reduced to 10% or less by 2035. While the waste landfilling will be minimal in the near future, huge amounts of various materials are accumulated in the operating and closed landfills over the long term. We must consider

options to extract resources from the anthroposphere. Landfill mining (LFM) will ensure that material and energy recovery goals are met throughout the life cycle of a landfill. This concept of LFM is supported by several organizations [4]. In the field of LFM research, several problems can be faced, such as technological, the need to address the conditions for implementation and the development of a standardized framework for assessing economic and environmental indicators [5]. Mining existing and future landfills can lead to secondary materials and energy flow, reducing the area it covers [6–8]. The above shows that landfill mining corresponds with the EU Roadmap for a Resource Efficient Europe, which provides no land acquisition by 2050.

According to the authors' statements [9–11], LFM is presented as a process that provides additional materials and energy sources. However, LFM has recently become a topical subject for research resource potential [12], technical [13] and economic aspects [14]. While the number of LFM projects is relatively small, a fair amount of data about the composition of landfills and recoverable resources has been collected and presented in recent years [15–17]. Currently, the discussion of the feasibility of the LFM and the search for the optimal use of resources continues, moving from the conceptual stage to the modeling stage by building different models, conducting a comparative assessment of alternatives and finally choosing the optimal option and implementation of it "in life". Physical investigations of the composition of the landfill are mandatory and serve as a form of input or verification of available data, as in the study of Hossain and DeVries [18]. Material flows are an essential component of the economic evaluation of LFM. The economic value of the LFM process can have positive and negative effects, such as in the results of Kieckhäfer et al. [19]. However, financial analysis alone cannot be decisive in assessing the economic feasibility of applying LFM. The innovative development of the LFM has highlighted the relevance of several aspects, such as biochemical flows, management, business dynamics, infrastructure and markets [20]. For the LFM, economic system and material flow models were developed, and life cycle assessments were created and calculated to assess the impact of the LFM process on the environment. Emphasis was placed such that the feasibility of the LFM would be most effective if separation methods were improved, the need for land development increased and resources became in short supply.

Based on the early-developed models and strategies, considering the lack of energy resources, there is an increasing discussion of using LFM as a tool for extracting energy resources and their use as an alternative fuel in energy-intensive industries. There are results of many researchers who also considered the issue of producing alternative fuels for the cement industry. Mustafa Kara [21] considered the production of refuse-derived fuel (RDF) from the non-recyclable waste fraction and studied its potential as a replacement fuel in the cement industry. Hemidat et al. [22] studied the production and disposal of RDF obtained from mixed waste using bio-drying and subsequent use of the produced fuel in the Jordanian cement industry. Dase et al. [23] explored the potential of the RDF in terms of waste generated and the amount of landfill waste. Garces et al. [24] investigated the potential of various landfill wastes and the possibility of extracting Landfill Mined Residues (LMRs) and SRF production. All the described studies pursue one goal—disposing of newly generated waste and recovering energy resources.

The characterization of LMRs strongly depends on the type of waste disposed (domestic or industrial), the climate zone and the landfill's age [25,26]. Since the raw material extracted from the landfill is specific, non-standard technology must be developed for the extraction LMRs. Moreover, it must be prepared before raw materials can be used as an energy resource.

This study focused on developing a mechanism for extracting LMRs, studied the possibilities of producing alternative fuel and its characteristics and used it in the cement industry as a replacement fuel during the clinker firing process. It also determined the composition and the main characteristics of the LMRs at various depths of the landfill and established the optimal depth from which LMRs can be extracted. Moreover, the article calculates the energy potential of the studied part of the landfill. It developed

the technological line for SRF production, studied ash after the incineration of SRF and established that it contains the inorganic component, clinker-forming minerals and crystal structure. The developed mechanism will contribute to extracting, from LMRs, a high-calorific fraction and producing alternative fuel for energy-intensive industries.

2. Materials and Methods

2.1. Study Area

The Kaunas regional non-hazardous waste landfill (Figure 1) was established in 1973. It covers an area of 37.4 hectares. The landfill utilizes mixed domestic waste for Kaunas city and other municipalities in the country (Lithuania).

Figure 1. Sections of landfill: —Section I; —Section II; —Section III.

Waste is accepted to the landfill based on the waste management agreement. The landfill territory consists of a waste disposal zone (landfill), a service zone and a prospective zone for leachate collection and treatment. The landfill itself consists of three sections. Section I (N 54°59′47″ E 24°01′51″) is the oldest and is decommissioned and reclaimed; Section II (N 54°99′65″ E 24°03′08″) is in operation and consists of five sections for waste disposal, separated from each other by barriers 2.4 m high. Section III (N 54°99′79″ E 24°02′80″) is reclaimed and has a separate site for the disposal of asbestos-containing waste with an area of 0.25 ha.

2.2. Test Instrument

The composition of unprocessed LMRs was determined through manual sorting after drilling and excavating. The studies were conducted according to the Standard Test Method for Determining the Composition of Unprocessed Municipal Solid Waste (ASTM D5231-92(2016). Excavated materials were sieved to fine (<20 mm) and course (>20 mm) fractions. The fine fraction was backfilled. The coarse fraction was sorted. Afterwards, the coarse fraction was processed for material recovery whenever possible (e.g., plastic, wood, rubber and others) and used as materials to produce alternative fuels.

The drillings were carried out at the landfill with a 15cm drill on the landfill sections; waste samples were taken every two meters at a depth of 1 to 20 m. In Section I, drilling was carried out up to 10 m, in Section II, up to 14 m, and in Section III, up to 20 m. The drilling depth was determined on-site at the time of the study. The difficulty in drilling was that there used to be a dump of armored vehicles on the territory of the current landfill. This place had a huge ravine, which eventually turned into the largest landfill.

2.3. Testing LMRs

After drilling, the material was obtained and subsequently subjected to research to prove the feasibility of extracting LMRs from the landfill and using it as an alternative fuel. The samples of LMRs were shredded and mixed and, after these manipulations, tested. The samples were heterogeneous, and their composition may have fluctuated. The following studies have been carried out:

- Moisture content (MC)—CEN/TS 15414-2:2010 [27];
- Ash content (AC)—EN ISO 21656:2021 [28];
- Volatile matter (VM)—EN ISO 18123:2015 [29];
- Net calorific value (NCV)—EN ISO 21654:2021 [30];
- Chlorine content (Cl)—EN 15408:2011 [31];
- Mercury content (Hg)—EN 15411:2011 [32];
- SEM-EDS analysis of ash;
  - XRD–Rietveld refinement analysis was carried out on a BRUKER D8 ADVANCE diffractometer with CuKα radiation at 40 kV in a 2Θ (5°÷70°) interval at a scanning step 0.02° and with the Topas program;
  - The ash morphology and elemental analysis were investigated using scanning electron microscopy equipped with an energy-dispersive spectroscopy detector (SEM-EDS). The analyzed samples were passed through sieves and then dried at 40 °C. Before the morphological observation, the ash specimens were coated using gold (Au) to obtain SEM images. SEM observation of samples was performed on a ZEISS EVO MA10 microscope at an accelerating voltage of 20 kV. The Bruker AXSX Flash 6/10 Detector can display all elements present in the specimen at an overall accuracy of about 1% and detection sensitivity down to 0.1% by weight;
  - The quantity element analysis of LMRs was performed using an ICP-OES, Optima 8000 (Perkin Elmer). The samples (0.4–0.5 g) were mineralized with 8 mLof concentrated nitric acid, 1 mLof hydrofluoric acid and 3 mLof hydrogen peroxide at 800 W, 6 MPa and pRate: 50 kPa · s^{-1} (Multivalve 3000). After the mineralization, the solution was poured into 50 mL flasks and diluted to 50 mL using deionized water. A quantitative analysis mode was used for the data acquisition of the samples. The scanning of every sample during element analysis was repeated three times to gather reasonably good results. Analysis was made in four replicates of each sample.

2.4. Energy Potential of Combustible Fractions

The energy potential of LMRs depended on the moisture content and chemical composition and was calculated based on Equations (1)–(4). In this work, we recommend calculating the energy potential of the waste fraction using Dulong's equation [33]. The first thing to do is calculate *HCV* for each waste fraction, according to Equation (1):

$$HCV_i = 338 \cdot C + 1442 \cdot [H - (O/8)] + 94 \cdot S \quad (1)$$

where HCV_i—high calorific value of each fraction of dry waste; *C*, *H*, *O*, *S*—content of chemical elements in the waste fraction, %.

The chemical composition of the waste fractions was calculated from the elemental composition based on the data of Reinhart D.R. [34].

The lower calorific value (LCV_i) of the dry waste fraction was calculated by subtracting the amount of energy required to evaporate water from each fraction of waste [35]:

$$LCV_i = HCV_i - [24.41 \cdot (18.015/2.015) \cdot MC_i] \quad (2)$$

where LCV_i—lower calorific value of each fraction of waste, kJ/kg; MC_i—moisture content of fraction of waste, %; *24.41*—coefficient based on the "secret" heat of vaporization of

water, where l = 2441 kJ/kg at 25 °C; *18.015*—the molar mass of water, g/mol; *2.015*—molar mass of hydrogen, g/mol.

The lower calorific value of the wet waste of each fraction was calculated according to [35]:

$$LCV_{i(wet)} = LCV_i \cdot [(100 - MC_i)/100] - 24.41 \cdot (100 - MC_i)/100] \quad (3)$$

where $LCV_{i(wet)}$—lower calorific value of each wet fraction of waste, kJ/kg.

The total energy potential of a combustible fraction of LMRs was calculated according to the data of the World Bank [35]:

$$E = [\Sigma LCV_{i(wet)} \cdot SW_i] \cdot \eta \cdot 0.278 \cdot 10^{-6} \quad (4)$$

where η—energy efficiency when burning excavated combustible materials for heat production is 85%; SW_i—the amount of the incinerated waste fraction of each fraction, kg; *0.278*—conversion factor from MJ to kWh (1 MJ = 0.278 kWh).

2.5. Development and Calculation of SRF Production Line

Based on the data obtained from the drilling at the landfill, the SRF production line was developed, and the flow rate was calculated. To produce SRF from the LMRs, they must undergo several stages of preparation so that the resulting alternative fuel meets the EU standard and can be used in energy-intensive industries. The main stages of SRF production are extracting prohibited materials, metals, inert materials, glass and fine fractions. The moisture contained in the waste must be removed; combustible materials must be crushed (d < 20 mm). The flow rate of the SRF production line was calculated using Equations (5)–(10), considering parameters from the SRF production line that we developed.

$$FR_{SRF} = \Sigma LMR - F_1 - F_2 - F_3 - F_4 - W_{lost} \quad (5)$$

$$F_1 = (\Sigma LMRs \cdot Q_1)/100\% \quad (6)$$

$$F_2 = [(\Sigma LMRs - F_1) \cdot Q_2]/100\% \quad (7)$$

$$F_3 = [(\Sigma LMRs - F_2) \cdot Q_3]/100\% \quad (8)$$

$$F_2 = [(\Sigma LMRs - F_3) \cdot Q_4]/100\% \quad (9)$$

$$W_{lost} = [(\Sigma LMRs - F_4) \cdot MC_{LMR}]/100\% \quad (10)$$

where FR_{SRF} is the estimated consumption of the production line of the *SRF* production (t/h); $\Sigma LMRs$ is the flow rate of waste after drilling from a landfill (14.2 t/h); F_1, F_2, F_3 and F_4 are the flow rate $\Sigma LMRs$ after the extraction of metals (ferrous and non-ferrous), inert materials, glass and a fine fraction (t/h); Q_1, Q_2, Q_3 and Q_4 are the quantity of extracted materials at each stage of separation (%); MC_{LMRs} is the quantity of moisture contained in *LMRs* (%); W_{lost} is the *LMRs* flow after moisture loss (t/h).

3. Results

3.1. Granulometric and Morphological Analysis

According to the data obtained in the course of research (as a result of drilling), the granulometric characteristic of the LMRs was obtained (Figure 2). In all sections of the landfill (I–III), a fine fraction predominates, regardless of the depth of the waste.

For Section I (up to 10 m), the size of the coarse fraction (d > 80 mm) was from 0.09 to 27.34%. The less coarse fraction of LMRs (80 > d > 40 mm) was from 2.75 to 16.02%, and the size of 40 > d > 20 mm was from 5.43 to 10.2%. Depending on the depth, a total fraction of more than 20 mm for Section I ranged from 3 to 47%. The minimum amount of the coarse fraction and the predominance of the fine fraction in this section refer to the upper layer of the landfill and are explained by the fact that this section of the landfill is re-claimed.

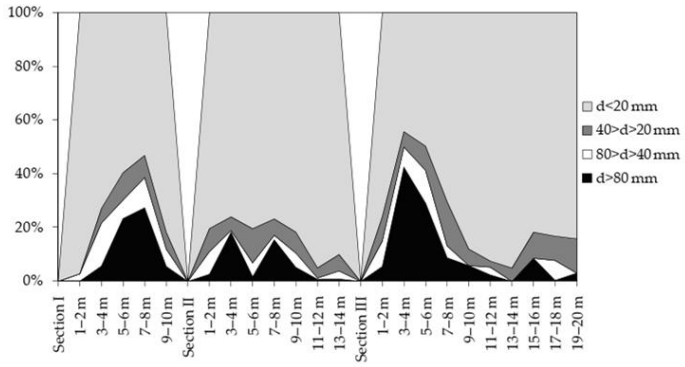

Figure 2. Granulometric analysis of landfill.

Section II is currently active (up to 10 m) comprising LMR fraction sizes of more than 20 mm from 0.72 to 15.47%. Therefore, for a depth of 11 to 14 m, the coarse fraction was less than that at a drilling depth of up to 10 m. The quantity of the coarse fraction (diameter of more than 20 mm) ranged from 0.5 to 6.12%.

For Section III (up to 10 m), along with the fine fraction, there is also a coarse fraction; however, its amount is much less than that of the fine fraction, and its value was in the range of 4.4 to 42.44%. The fraction size distribution of LMRs changed with an increased drilling depth. Thus, the fine fraction dominated for depths from 11 to 20 m; a coarse fraction presented but in a lower amount than that at a depth of up to 10 m and was from 0.37 to 12.77%. Such a granulometric composition of the considered sections of the landfill is due to the composition of the waste taken to the landfill for deposition and the residence time of this waste at the landfill. Obtained results about the granulometric composition and amount of fine fraction of LMRs correspond to the research study [36,37].

The LMR characterization is based on the methodology of the European Commission [38]. LMRs were divided into 12 primary categories. Regardless of the drilling depth, the composition of the LMRs from all landfill sections showed that the fine fraction predominated. Based on the methodology of EN 15415-1:2011 [39], obtained results of compositions of LMRs are presented in Figure 3.

The results of the analysis show that the total waste composition for Section I consisted of plastics by up to 5.87%, rubber by up to 2.28%, textiles by up to 16.64%, wood by up to 3.07%, metals by up to 6.59%, glass up to 0.84% and inert materials up to 1.47%, and the content of the fine fraction at some depths was up to 97.16%.

A similar situation occurred with the composition of the LMRs for Section II. The composition of the waste was as follows: plastics up to 10.03%, rubber up to 0.6%, textiles up to 9.16%, paper up to 2.73%, wood up to 9.58%, metal up to 17.4%, glass up to 1.77% and inert materials and fine fraction up to 1.99% and 94.98%, respectively.

For Section III, the composition was as follows: plastics up to 16.13%, rubber up to 0.44%, textiles up to 39.84%, paper up to 1.21%, wood up to 1.73%, metal up to 9.14%; the amount of glass, inert materials and the fine fraction were up to 1.08%, 5.55% and 95.07%, respectively.

Based on the results of the morphological analysis of LMRs, it is possible to trace the trend in the commissioning of the MBT plant.

Figure 3 shows the general characteristic of the LMRs with fine and coarse fractions. According to it, we can conclude that the predominant material is the fine fraction for all three sections (wells), and the presence of textiles in the studied samples ranks second. Soft, hard plastics and metal occupy the third, fourth and fifth places in terms of content in the material under study. The investigated fraction also was observed to have multilayer

composites, rubber, paper, wood, glass, inert materials and other burnable fractions. Their amount in the studied material did not exceed 5%. After extracting the fine fraction from LMRs, a combustible fraction, RDF, was obtained. Figure 4 shows the amount of the total combustible fraction. The research results correlate with the data [40,41] obtained in studies of landfills in European countries.

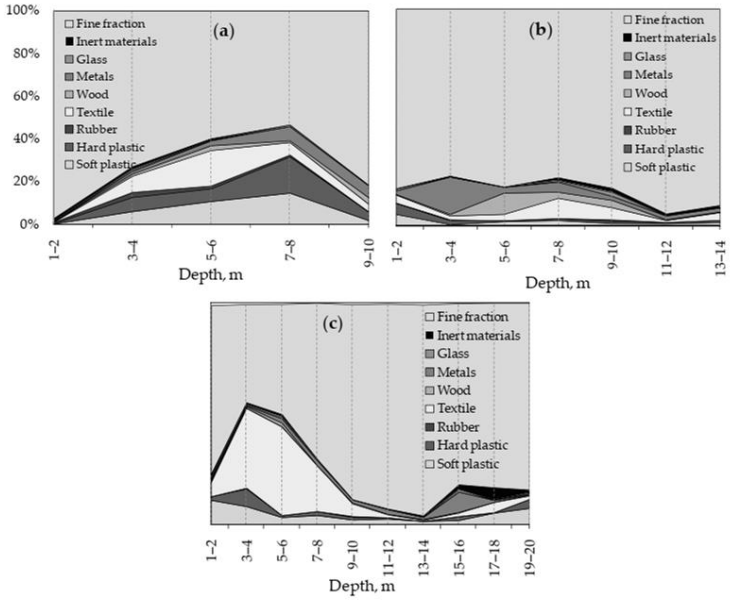

Figure 3. Total morphological composition of landfill: (**a**) Section I, (**b**) Section II, (**c**) Section III.

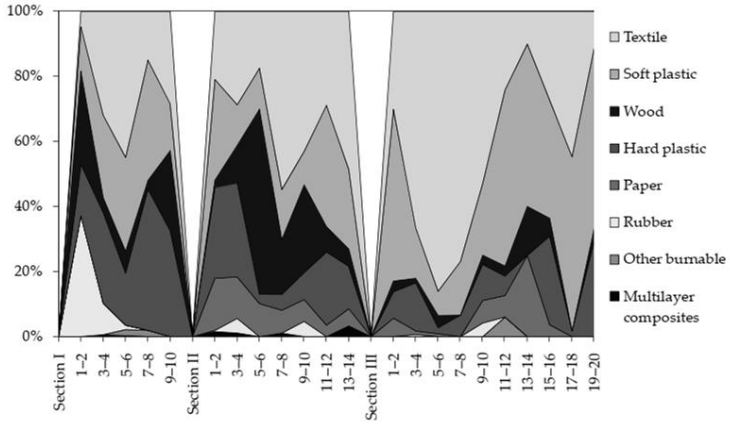

Figure 4. Composition of the combustible fraction of RDF.

The primary materials that make up the combustible fraction are plastics (soft and hard), rubber, textiles, paper, wood, multilayer composites and other materials. The combustible fraction was mainly represented by textiles and contains the least multilayer composites. The results allowed us to consider the landfill a "potential energy object".

3.2. *Physicochemical Properties of Potential Fuel*

After extracting the fine fraction and large inert materials from the LMRs, the resulting potentially combustible fraction will be called RDF. It is a non-defined term and refers to waste that has not undergone proper processing. RDF is not standardized, and features (composition, contaminants, calorific value) are undetermined [42]. This combustible fraction (RDF) had high humidity and contained prohibited materials (chlorine-containing plastics, inert materials, metals, e.i.). In such conditions, the RDF cannot be used as an alternative fuel in the intensive-energy industries. RDF can be used only for incineration to obtain heat or energy. The combustible fraction after extraction of the fine fraction from LMRs had the same characteristics for developed and developing EU countries [10].

After carrying out several technical operations with RDF, we will be able to obtain SRF. SRF is fuel from waste produced and tested according to EU standards. Its features are well specified, and following that, SRF is classified. SRF is produced under the producer's regime of a quality assurance scheme [42]. Stages for preparing SRF from RDF, which meet the EU standard, should include the following stages: extraction of prohibited materials, metals, inert materials, shredding and drying.

Moreover, the first thing you need to start analyzing fuel from waste should be measuring the main calorific characteristics. Based on these results, we can conclude the possibility of using this fuel as an alternative. The results of the main properties of RDF that were obtained after extracting the fine fraction from LMRs are presented in this section. First, MC, AC and NCV were measured and are illustrated in Figure 5, with the results of determining Cl- and Hg- content in Table 1.

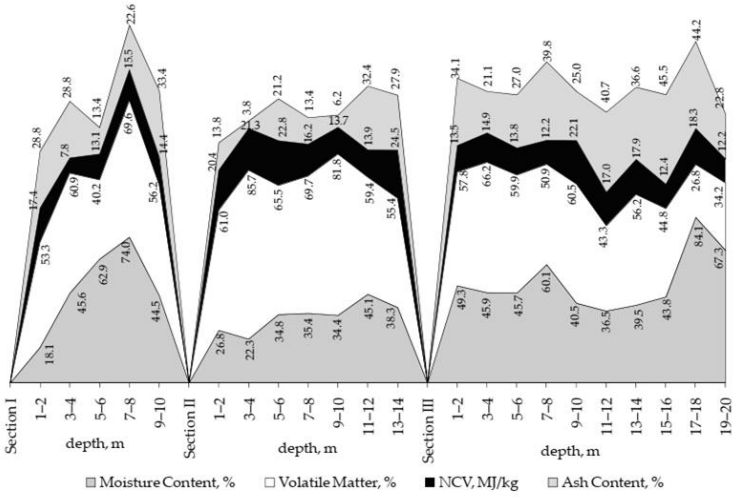

Figure 5. Characteristics of RDF.

Table 1. Results of determining chlorine and mercury content of RDF.

Parameters	Sections Landfill																				
	Section I					Section II							Section III								
	Depth of Drilling, m																				
	1–2	3–4	5–6	7–8	9–10	1–2	3–4	5–6	7–8	9–10	11–12	13–14	1–2	3–4	5–6	7–8	9–10	11–12	13–14	15–16	17–18	19–20
Cl, %	1.87	0.25	0.24	4.32	0.96	0.33	0.31	1.8	0.25	0.16	0.25	0.94	0.469	0.4	0.07	0.09	0.29	0.11	0.96	1.46	0.09	0.27
Hg, mg/kg^{-1}	0.02	0.03	0.11	0.05	0.09	0.02	0.02	0.02	0.02	0.02	–	–	0.30	0.07	0.04	0.03	0.02	–	–	–	–	–

The main properties of any waste, especially those representing energy potential, are in Section 2.3 and are moisture content (MC), ash content (AC), volatile mater (VM) and net calorific value (NCV). These properties depend on the waste's morphological composition, the year's season, and many other conditions.

The MC of RDF significantly influences the choice of recycling to SRF technology and depends on many factors, including the RDF composition. The MC of RDF at the entire considered depth of the landfill was measured. Thus, for Section I, at a depth of 1 to 10 m, the MC of the materials ranged from 18.05 to 74.01%. For Section II, at a depth of 1 to 10 m, it ranged from 22.32 to 35.38%, and a depth of 11 to 14 m, it ranged from 38.34 to 45.06%. For Section III, at the considered depth from one to 10 m, it went from 40.48 to 60.14%, and at a depth of 11 to 20 m, it ranged from 36.53 to 84%. From the presented results of the study, it can be concluded that with an increase in the depth of the waste, the MC of the excavated LMRs and, consequently, the obtained RDF also increase by the possible retention of moisture in deeper layers of the landfill.

The AC represents the fireproof component remaining after a sample is combusted. In this analysis, one gram of the sample was put into a crucible and placed in a furnace. The furnace was heated to 950 °C, and the samples were kept for one hour. Further, after cooling and weighing, the AC was calculated according to EU standards and presented in Figure 5. In addition to the oxidation of organic matter, in this temperature range during combustion, chemical reactions occur in minerals, such as the hydration and decomposition of carbonates, sulfates and other sulfur compounds. The amount of ash depends on the content of organic and inorganic substances and possible impurities. The AC varied following the presence of materials that were part of the studied fraction. Therefore, for Section I at a depth of 1 to 10 m, the AC ranged from 13.4 to 33.38%; for Section II at a depth of 1 to 10 m, it was from 3.77 to 21.22%; for the same section of the landfill, but a depth of 11 to 14 m, it ranged from 27.89 to 32.42%. Section III was considered at depths from 1 to 10 m and 11 to 20 m; the AC for these depths was 21.07 to 39.81% and 22.78 to 45.48%, respectively. Based on the results, we can say that the AC of RDF strongly depends on the AC of landfilled materials, the nature and time of their decomposition in the landfill and particles of the fine fraction stuck on the excavated LMR surface.

The VM is the part of organic matter that is transformed into gas when heated, such as hydrocarbons, hydrogen, oxygen, carbon oxide and other non-combustible gases resulting from the thermal decomposition of materials. The VM of RDF has a high value because of the increased oxygen, which can be seen in Figure 5. For landfill Section I, the VM value ranged from 40.22 to 69.56% at a depth of 1 to 10 m. For Section II, for the considered drilling depth (from 1 to 14 m), the VM was in the range of 55.42 to 85.7%. For Section III, at a depth of 1 to 10 m, the VM ranged from 50.9 to 66.15%; for depths of 11 to 20 m, it went from 26.83 to 56.23%. Fuel containing a large amount of VM is unfavorable because it releases more tar, which condenses at ambient temperature and causes problems in equipment operation.

The NCV of fuel depends upon the nature of the fuel and the relative proportions of the elements present. Figure 5 shows that the NCV of the RDF directly depends on the materials of the considered fraction at a certain depth. There were presented measurements of NCV for RDF: Section I ranged from 7.76 to 17.43 MJ/kg; Section I went from 13.69 to

24.48 MJ/kg. For Section III, at a depth of 1 to 10 m, the NCV consisted of 12.22 to 14.94 MJ/kg, and at a depth of 11 to 20 m, it was from 12.21 to 18.3 MJ/kg. It can be concluded that the main factors affecting the calorific value of RDF are the humidity and burnable part of the landfilled waste.

The *chlorine content* was quantitatively investigated in three landfill sections at different depths and presented in Table 1. Thus, for Section I, the chlorine content at a depth of 1 to 10 m was 0.54 to 4.32%. For Section II, at a depth of 1 to 14 m, the chlorine content was 0.16 to 1.8%. The considered Section III of the landfill had the following values of chlorine content: at a depth of 1 to 10 m, from 0.072 to 0.469%; the value of the chlorine content for a depth of 11 to 20 m was in the range from 0.091 to 1.459%. The presented data indicate that the chlorine content directly depends on the materials included in the RDF that were taken to the landfill for disposal and did not depend on the depth of the waste.

Managing Hg *emissions* for incinerators is essential since more than 78% of municipal solid waste (MSW) is incinerated today. The total Hg content in waste samples obtained from Section I of the landfill from a depth of 1 to 10 m shows that the Hg content does not depend on the depth of the waste and relies on the presence of Hg-containing materials in the waste and was in the range from 0.02 to 0.106 mg/kg^{-1}. For Section II, the mercury content was 0.02 mg/kg^{-1} at the depth under consideration. For Section III, the Hg content in the RDF obtained during drilling at a depth of 1 to 10 m had a value of 0.02 to 0.304 mg/kg^{-1}. Nevertheless, with an increasing depth, the Hg content at 11 to 20 m was less than 0.02 mg/kg^{-1}. The characteristics of RDF practically had the same value as the characteristics of municipal solid waste from one of the largest landfills in Kazakhstan [43].

Powder diffraction is a scientific method using X-ray, neutron or electron diffraction to determine the *structural characteristics* of materials. The XRD–Rietveld refinement method was used for phase identification, quantitative analysis and complete crystal structure analysis. X-ray diffraction analysis of the RDF ash from different landfill sections and depths was carried out, and the obtained X-ray patterns were deciphered using the Diffract Eva program. The results of the XRD analysis are presented in Figure 6.

Figure 6 shows an X-ray pattern (2θ = 5°–70°) of control samples of ash obtained after incinerating RDF from landfill sections. The X-ray diffraction analysis of ash based on the Rietveld refinement method (using the Topas program) is presented in Table 2.

Table 2. Results of XRD analysis by Rietveld refinement.

№	Minerals	Section Landfill				
		№1	№2		№3	
		Drilling Depth, m				
		1–10	1–10	11–14	1–10	11–20
		Value, %				
1	Quartz	72.23	36.32	38.66	45.77	49.40
2	Akermanite	5.35	9.21	7.23	7.77	11.28
3	Perovskite	-	1.87	0.54	1.26	0.99
4	Hematite	0.60	1.85	13.39	3.11	1.51
5	Microcline	3.19	5.44	4.63	6.60	2.74
6	Diopside	2.12	3.21	9.44	1.53	2.06
7	Wollastonite	0.54	5.85	3.63	1.94	1.09
8	Anhydrite	1.43	6.68	2.35	2.37	1.61
9	Lisetite	4.85	3.42	3.20	3.19	3.76
10	Augite	1.20	3.97	4.53	10.84	6.28
11	Anorthite	1.73	4.92	2.74	8.84	8.53
	Amorphous	6.75	17.26	9.66	6.78	10.96

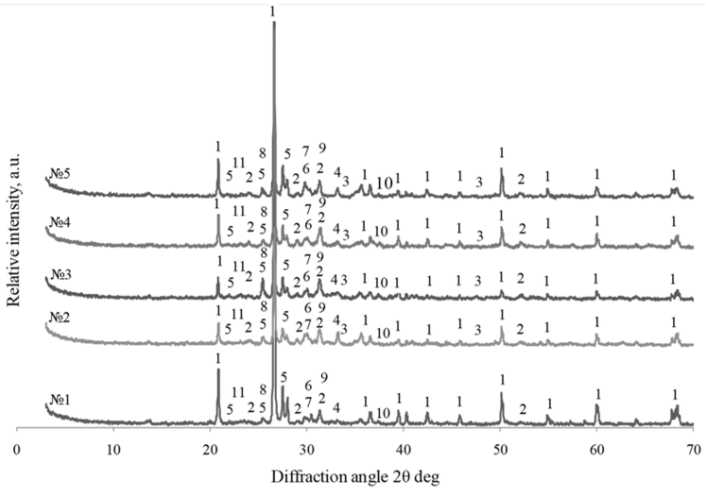

Figure 6. XRD analysis of ash after incineration of RDF: (**№1**)—Section I (1–10 m), (**№2**)—Section II (1–10 m), (**№3**)—Section II (11–14 m), (**№4**)—Section III (1–10 m), (**№5**)—Section III (11–20 m): 1—quartz (SiO_2), 2—akermanite ($Ca_2Mg(SiO_2O_7)$, 3—perovskite ($CaTiO_3$), 4—hematite (Fe_2O_3), 5—microcline ($KAlSi_3O_8$), 6—diopside ($CaMg(Si_2O_6)$), 7—wollastonite 1A ($CaSiO_3$), 8—anhydrite ($CaSO_4$), 9—lisetite ($CaNa_2Al_4Si_4O_{16}$), 10—augite ($Ca_xMg_yFe_z)(Mg_{y1}Fe_{z1}) \cdot SiO_6$), 11—anorthite ($Ca(Al_2Si_2O_8$).

According to the data in Figure 6 and Table 2, it can be seen that 11 compounds found during the analysis were present in all studied sections of the landfill, except for Section I. In this section, no perovskite compound was found. The found compounds differed in quantitative composition. The data from X-ray diffraction analysis allowed us to conclude that the ash obtained after the combustion of RDF contains minerals that are part of the clinker. Moreover, these data will enable us to consider RDF as a resource for obtaining alternative fuel that meets the EU standard. Results of mineralogical analysis of compositions showed similarity for some minerals, quartz and microcline anorthite, with results of Daniel Vollprecht et al. [44].

Elemental oxide analysis, based on SEM/EDS measurements, is presented in Table 2. SEM/EDS analysis of ash made it possible to determine chemical elements and calculate the composition of the oxides. Data from Table 2 prove that ash consists of the inorganic part, and the oxide composition of ash corresponds to the oxide composition of the clinker, but in different quantities [45].

According to Table 3, it was found that the oxides of Ca, Fe, Si, Al and Mg are dominant in the oxide composition of the ash; their amount was more than one wt.%. The content of Na-, S-, K-, Ti-, and Mg oxides in the ash was less than one wt.%. Thus, according to [46], the ash obtained by combusting RDF does not contain prohibited oxides and gives us the prerequisites for creating an alternative fuel that will be prepared and, in the end, will comply with the EU standard.

Table 3. Elemental oxide analysis of ash based on SEM/EDS measurements.

Oxides	CaO	CO_2	SiO_2	Al_2O_3	Fe_2O_3	MgO	K_2O	SO_3	TiO_2	Na_2O	P_2O_5	Mn_2O_3	Cr_2O_3	ZnO
Quantity in ash, %	**Section I, depth 1–10 m**													
	23.02	57.33	8.05	4.04	2.63	2.32	0.44	0.92	0.36	0.49	0.33	-	-	-
	Section II, depth 1–10 m													
	32.82	25.64	18.97	3.53	4.08	5.22	0.59	3.69	3.45	1.06	0.9	-	-	-
	Section II, depth 11–14 m													
	33.08	16.24	22.13	8.75	11.55	2.94	0.23	1.47	1.47	1.19	0.9	-	-	-
	Section III, depth 1–10 m													
	22.28	23.0	25.5	9.28	10.4	3.93	0.54	1.36	0.21	1.59	0.62	0.11	0.13	-
	Section III, depth 11–20 m													
	30.32	7.49	24.49	17.19	7.6	4.4	0.61	1.53	2.21	2.06	1.4	-	-	0.63
Quantity in clinker, %	42.5	34.5	14.0	3.5	1.8	1.0	0.7	0.5	0.2	0.1	0.08	0.05	-	-

3.3. Development of Concept for SRF Production Line

Based on the obtained results, the concept for an SRF production line was developed and presented in Figure 7. The flow rate of the SRF production line was calculated with Equations (5)–(10) and amounted to 4.9 t/h.

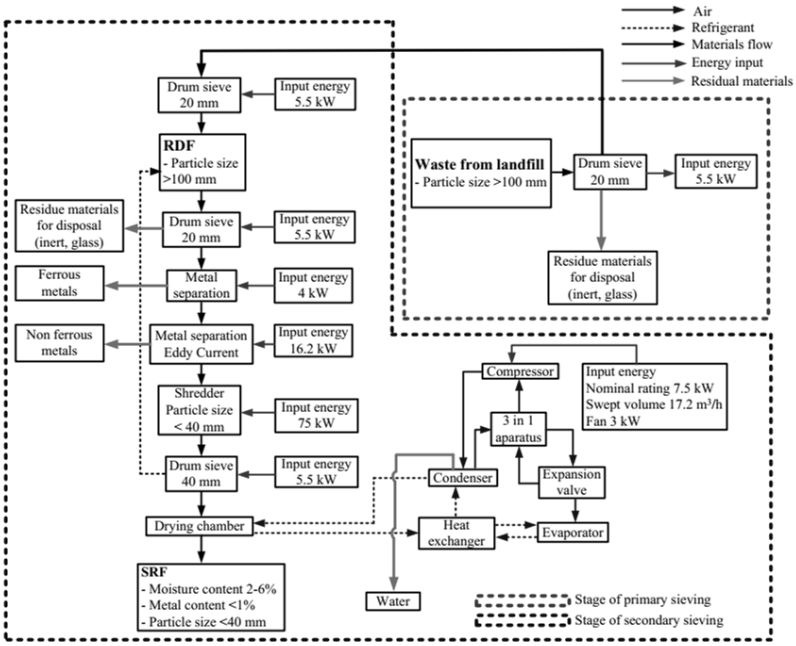

Figure 7. Proposed mechanism of extraction of LMRs and SRF production.

The LMRs extraction and SRF production mechanism we developed consisted of two stages. The first stage involves extracting inert, huge materials and the fine fraction on the landfill territory using a drum sieve. The amount of the fine fraction separated from the LMRs is 43%. In the second and final stage, re-extraction of the fine fraction and SRF production is proposed to be carried out on the territory of the Kaunas MBT to reduce capital costs. In the second stage of SRF production, another 50% part of the fine fraction is removed via secondary sieving. At the end of the second stage, the fine fraction content was 1.3%. The second stage will contain six additional units. Each unit plays an important role.

After removal of fine fraction extraction and coarse inert material, the materials are sent for the extraction of ferrous and non-ferrous metals. With a magnetic separator, ferrous metals were extracted, and an eddy current separator was used for non-ferrous metals. After the extractionof metals, the material is shredded up to 40 mm until a homogeneous material is obtained. After the shredding stage, the material is sent to a repeated drum sieve to homogenize and detect large particles. Material more extensive than 40 mm is sent for shredding to achieve the required size. At the end of the shredding stage, the moisture content of the material decreased by 86.7% and amounted to 2.5%.

A drying chamber is provided at the end of the production line. Tumble-drying is the optimal method, as it has low capital costs, is easy to operate and allows one to produce large volumes of products. Characteristics of the produced SRF are shown in Figure 8. The amount of the fine fraction, MC, AC, VM and NCV amounted to 1.3 wt.%, 2.5 wt.%, 44.3 wt.%, 34.8 wt.% and 16 MJ/kg, respectively. The data obtained indicate that separating the fine fraction through double sieving significantly improves the characteristics of the obtained SRF.

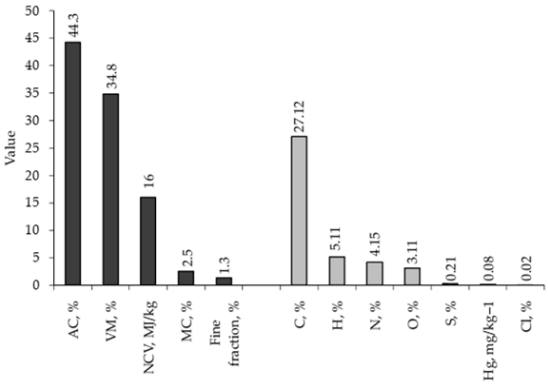

Figure 8. Characteristics of obtained SRF.

According to data [47,48], fuels are hydrocarbons comprised primarily of the following elements: carbon and hydrogen and some sulfur, nitrogen, oxygen and mineral matter in the next interval, with the C content from 20 to 70 wt.%, H from 3 to 8 wt.% and N from 1 to 5 wt.%. As seen in Figure 8, the SRF is a favorable combination of the C, H and N content for combustion. As for sulfur, the sulfur content in the analyzed materials was within the usual range for this element (0.2–1 wt.%). Regarding the halogen elements, a chlorine concentration was measured and amounted to 0.02 wt.%. The Hg-content in produced SRF was within acceptable limits for this fuel and complied with the allowable limits for use in cement kilns.

It was also found that the ash obtained after incinerating SRF had a crystalline structure and contained crystalline calcium-, sodium-, potassium-, iron- and silicon-bearing phases. The crystalline phase in materials is favorable for clinker production (Figure 9).

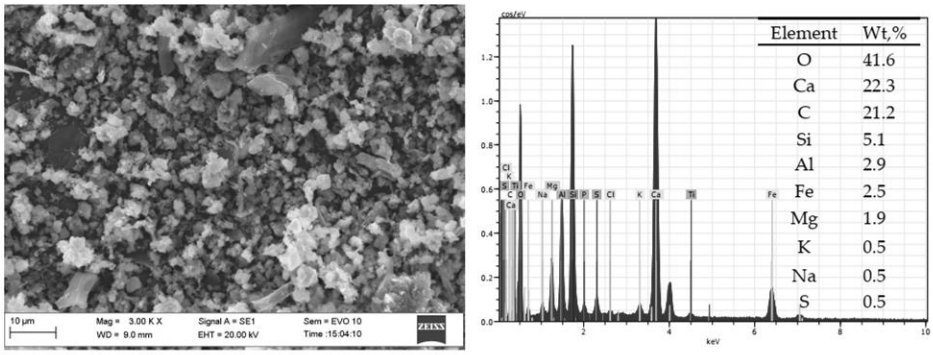

Figure 9. SEM image (**left**) and EDS analysis (**right**) of the ash after incineration of SRF.

Material morphology and particle size characteristics are associated with their crystal structure features. In our case, the ash particles had a different color, changed with depth from light grey to dark grey and had a lamellar and crystal shape. Ash particles had a size range of 1–20 µm and were not steadily distributed.

Quantity element analysis of RDF (obtained via extraction of the fine fraction and huge inert materials from LMRs) and SRF obtained through re-extraction of the fine fraction, inert and prohibited materials showed that metals consisted of 14 elements: Al, Ca, Cd, Cr, Cu, Fe, K, Mg, Mn, Na, P, Si, Ti, Zn (Figure 10). The dominant elements were Si, Ca, Fe, K, Na and Mg. The predominant presence of these elements is due to the composition of the waste once taken to the landfill.In their study, the authors of Jagodzinska et al. [49] also found chemical elements, such as K, Na, P, Cd, Cr, Mn and Ti.

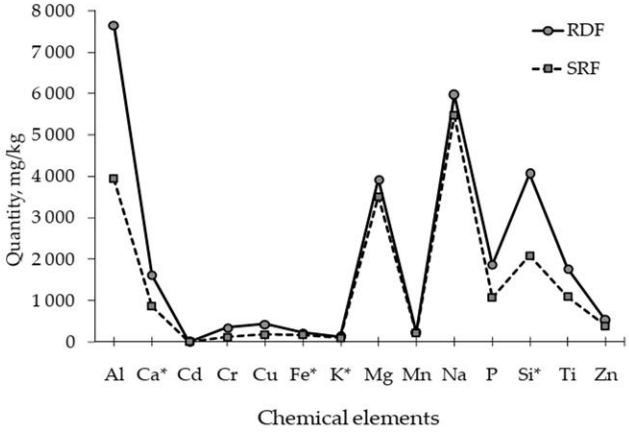

Figure 10. Quantity element analysis of RDF and SRF. * The value must be multiplied by 10^2.

Silicon is a dominant element in the ash. The quantity of silicon in the RDF was 406,861 mg/kg, and in SRF, it was 208,655 mg/kg. From the obtained data, we can see that the amount of silicon in SRF decreased to 48.7%; the double extraction of the fine fraction conditions this decrease. Calcium was in second place, containing chemical elements in the ash. The quantity of calcium in RDF amounted to 162,031 mg/kg, and in SRF, it

was 86,575 mg/kg. The iron was in third place in terms of its content in the prepared SRF. The quantity of iron in SRF decreased to 21.8% compared with the RDF content and amounted to 17,435 mg/kg. The amount of potassium in the SRF decreased by 26.5% and amounted to 9448 mg/kg. Sodium was also present in the prepared SRF but at a lower concentration than silicon. As a result of the re-extraction of the fine fraction, sodium in the ready SRF decreased by 8.4% and amounted to 5474 mg/kg. Sufficiently high magnesium concentrations in SRF indicate the presence of ceramics, inert materials and garden waste. The magnesium content in SRF decreased by 10.7% and amounted to 3516 mg/kg.

As for the other elements present in the obtained SRF, their amount was reduced through double extraction of the fine fraction. The amount of aluminum decreased by 48.5%, chromium decreased by 65.3%, copper decreased by 57.9%, manganese decreased by 10.9%, phosphorus decreased by 42.5%, titanium decreased by 38.1% and zinc decreased by 25.4%. The amount of cadmium in the SRF before and after separation remained the same.

The actual composition of the waste at the Kaunas regional landfill in Lithuania was studied, and the energy potential of the considered landfill sections was calculated. From our point of view, according to the conducted studies, extracting waste from the landfill to a depth of up to 10 m inclusive is advisable. According to available data, waste extraction from greater depths does not have a positive outlook. Calculations of the energy potential of the considered part of the landfill amounted to 196,700 GJ.

4. Discussion

Based on the analysis of the existing waste generation and accumulation problem, a lack of energy resources and increase in greenhouse gas emissions, the following was determined. The use of waste previously taken to the landfill as an alternative fuel for energy-intensive industries, particularly the cement industry, is a relatively new and relevant area but is practically not used. It is known that the production of cement, namely the clinker firing process, is one of the largest energy resource consumers and contributes significantly to the pollution of atmospheric air with greenhouse gases. In this regard, the question arises of producing viable fuel from LMRs that meets EU standards by developing a mechanism for excavating LMRs and a process line for SRF production.

The use of the non-recyclable waste fraction as an alternative fuel in energy-intensive industries has been well studied. It has been established that it is possible to produce an alternative fuel that will meet EU standards, subject to the development of a technological line for the production of SRF. However, it should be considered that producing SRF will use the LMRs. This type of waste has specific properties since it is subject to various transformations and changes over time. After some stages of preparation, obtained SRF will have a high quality. After incinerating SRF, the ash will contain a crystalline phase, its oxide composition will consist of clinker-forming minerals and the developed two-stage technological line will ensure the uninterrupted production of SRF.

The results of drilling studies at the landfill found that the main fraction of the LMRs consists of a fine fraction (d < 20 mm) and amounted to 44.27 to 97.16% depending on the section of the landfill and depth. The obtained data correspond to the results of other authors [50,51]. The LMR composition of the considered landfill sections at various depths was mainly represented by plastics (hard and soft), textiles, wood and metals. The LMRs had the typical characteristics of most countries regarding high moisture content and the fine fraction with an increasing depth. These indicators contribute to environmental pollution through the formation of landfill gases and leachate and the presence of an unpleasant smell. Waste composition varies with the socio-economic status within a particular community.

The limiting values of MC, AC and the content of combustible components (carbon and hydrogen) are essential characteristics of MSW as a fuel. The limits of fluctuations of the considered parameters are vast and differ depending on the depth of the waste at the landfill and its composition. The MC of LMRs ranged from 18.05% to 84.09%, the value of VM components ranged from 34.17 to 85.7% and the AC, in turn, ranged from

3.77 to 45.48%. Compared to solid fuels, such as coal (VM is up to 44%), fuel from waste containing biomass has a higher amount of VM (up to 87%). The biomass content in the samples under consideration, especially in Section 2, was traced. These results confirm the previously stated information that Section 2 is in operation, and in the relatively recent past (before the commissioning of the MBT plant), waste was taken to the landfill without any technological operations. The amount of volatile substances strongly depends on the nature of the material, combustion conditions, temperature and heating rate. It increases with increased amounts of hydrogen and decreases with the MC present in the fuel. The results obtained regarding the composition of the LMRs and their main characteristics are typical for landfills and correspond with the data obtained by the authors [36,50–53], who were engaged in similar studies.

In general, LMRs have all the necessary properties that make it possible to consider them as fuel: good chemical activity ensures the possibility of combustion in atmospheric oxygen; continuous reproduction allows us to consider their reserves sufficient for industrial use; the energy value is comparable to the energy value of low-calorie fuel used in the energy sector, as evidenced and by the data obtained by the researchers who worked in this direction [26,54–56].

The NCV of the considered sections of the landfill does not correlate with the depth of the waste but directly depends on the waste that is part of the landfill. Similar data were obtained during studies in Korea [55,57,58]. Chlorine is a crucial element causing high-temperature corrosion and low efficiency in waste-to-energy plants and its thermal behavior. To prevent operational problems, the quantity control of chlorine-containing materials in the composition is necessary. The chlorine content in the considered RDF does not correlate with the depth of occurrence and is related to the results of Hölzle, I. [58]. The chlorine content depends on chlorine-containing materials, mainly plastics, which were taken to the landfill for disposal at one time. The mercury content in the studied fuel had the same trend as chlorine and depended on the origin of the waste taken to the landfill. The mercury content in the produced SRF was shallow and corresponded to the data obtained [59] on the landfill Opolskie Voivodeship. However, the maximum value of mercury content was found in Section III in the top layer and consisted of 0.304 mg/kg^{-1}.

X-ray diffraction analysis of the ash obtained after incinerating RDF and SRF confirmed the presence of clinker-forming minerals in all sections and depths under consideration but in different percentages. The fact that the ash, after combusting RDF, contains clinker-forming minerals was confirmed by the studies of the authors Pitak et al. [60].

Quartz is the main mineral in samples [61]. Quartz content varies by landfill section and depth from 36.32 to 72.23%. Wollastonite is an industrial mineral comprised of calcium, silicon and oxygen. In the studied samples, the amount of wollastonite did not depend on the depth but on waste composition (0.54–5.85%). Akermanite is a mineral of the melilite group [62], also named a technogenic mineral. Akermanite is more durable than wollastonite. The akermanite content, as well as the content of wollastonite, did not depend on the depth of the waste location (5.35–11.28%). Hematite [63,64] is a relatively common and durable mineral. The hematite content in the samples did not tend to increase or decrease depending on the depth but relied only on the composition. The presence of hematite results in a slight change in the color of samples of ash (0.6–13.39%). Microcline is an important raw material for industries [65]. The microcline content in samples was in the range of 2.74 and 6.60%. According to [61,66], diopside is a pyroxene mineral. It promotes the formation of an iron oxide melt, which acts as a flux and participates in the sintering of the material. The diopside content in the ash samples ranged from 1.53 to 9.44%, depending on the section of the landfill. The presence of the minerals perovskite, anhydrite, lisetite, augite and anorthite in the compositions of ash is typical for this type of ash and, like the previous minerals, does not depend on the depth of the waste location at the landfill but depends only on the composition of the waste that was excavated and combustible.

The SRF production line for the production of replacement fuel for the cement industry was developed and calculated. The production line consisted of two stages. The first

consisted of extracting the fine fraction and huge inert materials at the landfill territory. The second involved developing the production line with six additional pieces of equipment, including the secondary extraction of the fine fraction by passing the material through a sieve. It is recommended to install a production line on the territory of the current MBT since it is here that there is already equipment that can be used in the production of SRF. Considering the composition of the LMRs and based on Equations (5)–(10), the SRF production line's productivity was calculated, which amounted to 4.9 t/h. The energy potential of a combustible fraction of excavated waste up to 10 m in depth was calculated. The calculation was performed according to Equations (1)–(4) and was 196,700 GJ. After analyzing the data obtained during the research, we can conclude that the optimal depth from which LMRs can be extracted and produce SRF is 10 m. Waste located deeper than 10 m is not advisable for alternative fuel production. Wastes at such a depth have a strongly altered structure and high humidity and are a black lump of material that is difficult to recognize with an unpleasant odor.

After passing through all stages of alternative fuel production, as indicated in the production line, SRF was obtained. The characteristics of the produced SRF are shown in Figure 7. The fine fraction content in the production of SRF decreased by 96.75%, humidity decreased by 86.7%, AC decreased by 43.3%, VM components increased by 48.8% and NCVs increased by 65.6%. According to the gaseous characteristics of the fuel, the percentage of carbon increased by 51.8%; hydrogen, nitrogen and sulfur increased by 64.3%, 77.1% and 52.3%, respectively. However, oxygen and mercury decreased by 62% and 25%, respectively. The characteristics of the produced SRF are typical of those for fuel from waste. Thus, Hervy et al. [67] studied the fuel they obtained from waste, and their results correlate with our data. Ash content values are almost identical, with significantly different values for oxygen content, and minor differences can be seen in the content of C and H. The chlorine content in the studied materials did not change and amounted to 0.02%. It must be taken into account that the high chlorine content in the fuel causes the corrosion of metals and air pollution caused by the formation of HCl, Cl_2, dioxins, furans and PCBs (polychlorinated biphenyls). The characteristics of the obtained SRF comply with the EN15359 standard and, according to the classification characteristics, correspond to class III.

Quantity element analysis of the studied SRF is very important for the presence or absence of heavy metals. The elemental analysis showed 14 chemical elements present, and the same elements were represented in RDF but in other concentrations. The predominant elements are Si, Ca, Fe, K, Na and Mg, and their amount was more than 1 mg/kg. As shown in Figure 9, during the production of SRF from RDF, the mass amount of elements decreased by the following: Si 48.1%, Ca 46.5%, Fe 21.8%, K 26.5%, Na 8.44% and Mg 10.7%. Such quantitative changes occurred at the expense of the two-stage sifting and extractionof thefine fraction and the separation of prohibited materials, which should not be in the SRF.

The SEM image and elemental analysis confirmed the earlier assumptions that the ash, after the incineration SRF, has a crystalline structure and contains clinker-forming oxides. The element-oxide analysis of the ash based on SEM/EDS measurements confirmed the presence of clinker oxides. The oxide content of aluminum, iron, sodium and phosphorus must be strictly controlled during the clinker firing process. The content of iron and aluminum oxides should not exceed 5 to 7%. An increase in the content of these oxides leads to deterioration in the quality of the finished product. Although Zn and Cr oxides are on the list of environmentally harmful elements, their relatively small amount (less than one wt. %) can be considered inert based on acceptance criteria [68].

The calculation results (Table S1) confirm the feasibility of using SRF in the cement industry as replacement fuel from economic and ecological aspects. A 20% replacement ratio will achieve 17,319,514 USD/year annual coal savings after adding 38,697 t/year SRF to traditional fuel. The net cost-saving calculation, which considers CO_2 cost savings and SRF cost and efficiency losses, shows that the net annual saving will be 17,699,517 USD/year with a maximum fuel replacement of 20%.

The advantages of the proposed mechanism for extracting raw materials from landfill are conserving non-renewable energy resources by using recycled materials, reducing the burden on the environment by reducing greenhouse gas emissions and increasing the land area occurring at the expense of landfill reclamation and producing alternative fuel (SRF) that will meet the EU standard. The disadvantage of the LFM process is the increased noise, dust and unpleasant odors in extracting and producing the fuel. The complexity of the LFM process lies in the fact that the raw material from the landfill is demanding and specific and requires additional precautions during sieving due to the content of inert materials and large-size materials. However, we can overcome such disadvantages by using the proposed mechanism. Ultimately, we will have an alternative fuel (SRF) that can compete with coal, gas or oil in terms of its characteristics.

The recommendations for future research work can be the following: conduct an environmental impact assessment compared to coal and gas; conduct tests on the combustion of the resulting fuel in real conditions. In our research, we propose to carry out the second stage of extraction of the fine fraction at the MBT plant and then the production of SRF. In the future, consideration should be given to recovering LMRs and producing SRF at the landfill without transporting materials to the MBT plant.

5. Conclusions

The obtained research results described in this paper allowed us to make the next valuable conclusions from a scientific and practical point of view:

(1) The extracting of energy-intensive raw materials from landfills is feasible, and it allows us to develop a mechanism for SRF production, which complies with the EU standard;
(2) The mechanism for the production of SRF may, in principle, consist of two technological stages.
(3) the first stage can be performed at the territory of the landfill, including the removal of the fine fraction, inert materials and bulky waste via primary sieving;
(4) The secondary stage can be performed by using an existing MBT facility and may include the additional removal of the fine fraction and prohibited materials via secondary sieving, extraction of metals, shredding and drying;
(5) The LMR coarse fraction includes combustible fractions, such as soft plastics, wood, hard plastics, paper, rubber and other burnable components, representing the total combustible fraction;
(6) Extracting LMRs for SRF production is suitable for up to a 10 m landfill depth;
(7) Obtained SRF by classification characteristics (caloricity, chlorine and mercury content) will belong to class III based on the main parameters;
(8) Based on X-ray diffraction analysis results, the ash, which can beobtained after the incineration of the produced SRF, has a crystalline structure and contains Ca-, Na-, K-, Fe- and Si-bearing phases and corresponds to the clinker-forming minerals; it was confirmed that this SRF can be used as replacement fuel during the clinker firing process;
(9) The use of obtained SRF as a replacement fuel in the cement industry would be economically feasible and more environmentally friendly due to reductions (10–20%) in coal import with a subsequent saving of costs and greenhouse emissions;
(10) This would bring Lithuania closer to a circular economy by using formerly disposed materials at landfills and converting them into energy resources.

Supplementary Materials: The following supporting information can be downloaded at: https://www.mdpi.com/article/10.3390/su15054538/s1. Table S1: Parameters, methodology and results of calculation of economic efficiency of the use of the SRF during clinker firing. References [69–73] are citied in the Supplementary Materials.

Author Contributions: Conceptualization, Data curation, Formal analysis, Methodology, Resources, Software, Writing—original draft, review and editing, I.P.; Conceptualization, Data curation, Formal analysis, Review, Supervision, G.D.; Investigation, Formal analysis, Methodology, Validation, A.B.; Methodology, Formal analysis, Software, M.P.; Conceptualization, Resources, Supervision, S.-I.L. All authors have read and agreed to the published version of the manuscript.

Funding: This research received no external funding.

Institutional Review Board Statement: Not applicable.

Informed Consent Statement: Not applicable.

Data Availability Statement: Not applicable.

Acknowledgments: We acknowledge Laboratory of Heat-Equipment Research and Testing, Lithuanian Energetic Institute (LEI) for help in preparing materials for the experiment. We would like to express our great gratitude to the staff of the Centre for Hydrogen Energy Technologies, LEI for helping with the research. We acknowledge the staff of the Kaunas mechanic biological treatment plant for helping in providing material for research and informational support.

Conflicts of Interest: The authors declare no conflict of interest.

Abbreviations

AC	Ash content
Cl	Chlorine content
EU	European Union
Hg	Mercury content
LFM	Landfill mining
LMRs	Landfill Mined Residues
LFM	Landfill mining
MBT	Mechanical biological treatment
MC	Moisture content
MSW	Municipal solid waste
NCV	Net calorific value
RDF	Refuse-derived fuel
SEM	Scanning electron microscopy
SEM-EDS	Scanning electron microscopy-energy dispersive X-ray spectroscopy
SRF	Solid recovered fuel
VM	Volatile matter
XRD	X-Ray diffraction

References

1. EU Council Directive 1999/31/EC of 26 April 1999 on the Landfill of Waste. Available online: http://eur-lex.europa.eu/legal-content/EN/TXT/?uri=celex:31999L0031 (accessed on 8 November 2017).
2. EC, Waste Policy Review-Environment-European Commission. Available online: http://ec.europa.eu/environment/waste/target_review.htm (accessed on 8 November 2017).
3. Eurelco, European Parliament Votes YES to Include ELFM in the EU Landfill Directive Eurelco. Available online: https://www.eurelco.org/single-post/2017/03/15/European-Parliament-votes-YES-toinclude-Enhanced-Landfill-Mining-in-the-EU-Landfill-Directive (accessed on 2 May 2017).
4. COST Mining the European Anthroposphere (MINEA). Available online: http://www.cost.eu/COST_Actions/ca/CA15115 (accessed on 8 November 2017).
5. Ragazzi, M.; Fedrizzi, S.; Rada, E.C.; Ionescu, G.; Ciudin, R.; Cioca, L.I. Experiencing Urban Mining in an Italian Municipality towards a Circular Economy vision. *Energy Procedia* **2017**, *119*, 192–200. [CrossRef]
6. Singh, A.; Chandel, M.K. Effect of ageing on waste characteristics excavated from an Indian dumpsite and its potential valorization. *Process Saf. Environ. Protec.* **2020**, *134*, 24–35. [CrossRef]

7. Yi, S. Resource recovery potentials by landfill mining and reclamation in South Korea. *J. Environ. Manag.* **2019**, *242*, 178–185. [CrossRef] [PubMed]
8. Lokahita, B.; Samudro, G.; Huboyo, H.S.; Aziz, M.; Takahashi, F. Energy recovery potential from excavating municipal solid waste dumpsite in Indonesia. *Energy Procedia* **2019**, *158*, 243–248. [CrossRef]
9. Johansson, N.; Krook, J.; Eklund, M. The institutional capacity for a resource transition—A critical review of Swedish governmental commissions on landfill mining. *Environ. Sci. Policy* **2017**, *70*, 46–53. [CrossRef]
10. Parrodi, J.C.H.; Höllen, D.; Pomberger, R. Case study on enhanced landfill mining at Mont-Saint Guibert landfill in Belgium: Mechanical processing of fine fractions for material and energy recovery. *Detritus* **2019**, *8*, 62–78. [CrossRef]
11. Takeda, C.M.; Leme, M.A.D.G.; Romeiro, D.C.; Silva, K.G.; Miguel, M.G. Variation of the Gravimetric Composition of Landfilled Municipal Solid Waste Over the Time in a Developing Country. *Int. J. Environ. Res.* **2022**, *16*, 83. [CrossRef]
12. Jagodzińska, K.; Zaini, I.N.; Svanberg, R.; Yang, W.; Jönsson, P.G. Pyrolysis of excavated waste from landfill mining: Characterisation of the process products. *J. Clean. Prod.* **2021**, *279*, 123541. [CrossRef]
13. Márquez, A.J.C.; Filho, P.C.C.; Rutkowski, E.W.; Isaac, R.D.L. Landfill mining as a strategic tool towards global sustainable development. *J. Clean. Prod.* **2019**, *226*, 1102–1115. [CrossRef]
14. Dino, G.A.; Rossetti, P.; Perotti, L.; Alberto, W.; Sarkka, H.; Coulon, F.; Wagland, S.; Griffiths, Z.; Rodeghiero, F. Landfill mining from extractive waste facilities: The importance of a correct site characterisation and evaluation of the potentialities. a case study from Italy. *Resour. Policy.* **2018**, *55*, 50–61. [CrossRef]
15. Frank, R.R.; Cipullo, S.; Garcia, J.; Davies, S.; Wagland, S.T.; Villa, R.; Trois, C.; Coulon, F. Compositional and physicochemical changes in waste materials and biogas production across 7 landfill sites in UK. *Waste Manag.* **2017**, *63*, 11–17. [CrossRef] [PubMed]
16. López, C.G.; Ni, A.; Hernández Parrodi, J.C.; Küppers, B.; Raulf, K.; Pretz, T. Characterization of landfill mining material after ballistic separation to evaluate material and energy recovery potential. *Detritus* **2019**, *8*, 5–23. [CrossRef]
17. Zhang, P.; Chai, J.; Cao, J.; Qin, Y.; Dang, M.; Wang, T. Analysis of the existence form of landfill leachate water level and its development pattern under the condition of considering internal source water: A case study. *Environ. Sci. Pollut. Res.* **2022**, *30*, 9820–9840. [CrossRef] [PubMed]
18. Hossain, S.; DeVries, B. Resource Recovery and Sustainable Material Management through Landfill Mining. In Proceedings of the 3rd Global Landfill Mining Conference and Exhibition, London, UK, 17–18 November 2014; p. 30.
19. Kieckhäfer, K.; Breitenstein, A.; Spengler, T.S. Material flow-based economic assessment of landfill mining processes. *Waste Manag.* **2017**, *60*, 748–764. [CrossRef] [PubMed]
20. Krook, J.; Baas, L. Getting serious about mining the technosphere: A review of recent landfill mining andurban mining research. *J. Clean. Prod.* **2013**, *55*, 1–9. [CrossRef]
21. Kara, M. Environmental and economic advantages associated with the use of RDF in cement kilns. *Resour. Conserv. Recycl.* **2012**, *68*, 21–28. [CrossRef]
22. Hemidat, S.; Saidan, M.; Al-Zu'bi, S.; Irshidat, M.; Nassour, A.; Nelles, M. Potential Utilization of RDF as an Alternative Fuel to be Used in Cement Industry in Jordan. *Sustainability* **2019**, *11*, 5819. [CrossRef]
23. Dace, E.; Blumberga, D. An assessment of the potential of refuse-derived fuel in Latvia. *Manag. Environ. Qual.* **2012**, *23*, 503–516. [CrossRef]
24. Garces, D.; Diaz, E.; Ordonez, S.; Gonzalez-LaFuente, J.M. Evaluation of the potential of different high calorific waste fraction for the preparation of solid recovered fuels. *Waste Manag.* **2016**, *47*, 164–173. [CrossRef]
25. Somani, M.; Datta, M.; Ramana, G.V.; Hölzle, I.; Sundaram, R.; Sreekrishnan, T.R. Effect of depth of landfill on the characteristics of soil-like material of aged waste: A case study of Bhalswa dumpsite, India. *J. Mater. Cycles Waste Manag.* **2022**, *24*, 1902–1912. [CrossRef]
26. Cheela, V.R.; John, M.; Dubey, B. Quantitative determination of energy potential of refuse-derived fuel from the waste recovered from Indian landfill. *Sustain. Environ. Res.* **2021**, *31*, 1–9. [CrossRef]
27. *CEN/TS 15414-2:2010*; Solid Recovered Fuels—Determination of Moisture Content Using the Oven Dry Method—Part 2: Determination of Total Moisture Content by a Simplified Method. Management Centre: Brussels, Belgium, 2010. Available online: https://standards.iteh.ai/catalog/standards/sist/58032711-f7e5-46ea-a696-4e4bbe46e359/sist-ts-cen-ts-15414-2-2010 (accessed on 12 March 2004).
28. *EN ISO 21656:2021*; Solid recovered fuels—Determination of Ash Content. CEN-CENELEC Management Centre: Brussels, Belgium, 2021. Available online: https://standards.iteh.ai/catalog/standards/sist/49d4536a-b804-4991-833d-cd8aa8e87ae1/sist-en-iso-21656-2021 (accessed on 12 March 2004).
29. *EN ISO 18123:2015*; Solid BioFuels—Determination of the Content of Volatile Matter (ISO 18123:2015). CEN-CENELEC Management Centre: Brussels, Belgium, 2015. Available online: https://standards.iteh.ai/catalog/standards/sist/3e8c87a2-6cf4-412a-9512-b56b10a054fb/sist-en-iso-18123-2016 (accessed on 12 March 2004).
30. *EN ISO 21654:2021*; Solid Recovered Fuels—Determination of Calorific Value. CEN-CENELEC Management Centre: Brussels, Belgium, 2021. Available online: https://standards.iteh.ai/catalog/standards/sist/059c7d2c-79e2-4a57-89a6-8d50a6f3d3b2/sist-en-iso-21654-2021 (accessed on 12 March 2004).
31. *EN 15408:2011*; Solid Recovered Fuels—Methods for the Determination of Sulphur (S), Chlorine (Cl), Fluorine (F) and Bromine (Br) Content. Management Centre: Brussels, Belgium, 2011. Available online: https://standards.iteh.ai/catalog/standards/sist/230b887f-d469-4668-8ffedce61f6f1431/sist-en-15408-2011 (accessed on 12 March 2004).

32. *EN 15411:2011*; Solid Recovered Fuels—Methods for the Determination of the Content of Trace Elements (As, Ba, Be, Cd, Co, Cr, Cu, Hg, Mo, Mn, Ni, Pb, Sb, Se, Tl, V and Zn). Management Centre: Brussels, Belgium, 2021. Available online: https://standards.iteh.ai/catalog/standards/sist/6c0486af-f647-499d-8d40-a00375df5c67/sist-en-15411-2011 (accessed on 12 March 2004).
33. Eboh, F.C.; Ahlström, P.; Richards, T. Estimating the specific chemical energy of municipal solid waste. *Energy Sci. Eng.* **2016**, *4*, 217–231. [CrossRef]
34. Reinhart, D.R. *Determining the Chemical Composition of Solid Waste Problem Statement*; Georgia Institute of Technology: Atlanta, Georgia, 2004.
35. The World Bank. *Municipal Solid Waste Incineration*; The World Bank: Washington, DC, USA, 1999.
36. Jani, Y.; Kaczala, F.; Marchand, C.; Hogland, M.; Kriipsalu, M.; Hogland, W.; Kihl, A. Characterisation of excavated fine fraction and waste composition from a Swedish landfill. *Waste Manag. Res.* **2016**, *34*, 1292–1299. [CrossRef] [PubMed]
37. Quaghebeur, M.; Laenen, B.; Geysen, D.; Nielsen, P.; Pontikes, Y.; van Gerven, T.; Spooren, J. Characterization of landfilled materials: Screening of the enhanced landfill mining potential. *J. Clean. Prod.* **2013**, *55*, 72–83. [CrossRef]
38. European Commission. Methodology for the Analysis of Solid Waste (SWA-Tool) User Version. In Project: SWA-Tool, Development of a Methodological Tool to Enhance the Precision & Comparability of Solid Waste Analysis Data: SWA-Tool Consortium. Available online: https://www.wien.gv.at/meu/fdb/pdf/swa-tool-759-ma48.pdf (accessed on 12 March 2004).
39. *EN 15411:2011*; Solid Recovered Fuels—Determination of Particle Size Distribution—Part 1: Screen Method for Small Dimension Particles. Management Centre: Brussels, Belgium, 2021. Available online: https://standards.iteh.ai/catalog/standards/sist/f5ff81d1-a55c-4ea4-b69e-971e75839527/sist-en-15415-1-2011 (accessed on 12 March 2004).
40. Pecorini, I.; Iannelli, R. Characterization of Excavated Waste of Different Ages in View of Multiple Resource Recovery in Landfill Mining. *Sustainability* **2020**, *12*, 1780. [CrossRef]
41. García, J.; Davies, S.; Villa, R.; Gomes, D.M.; Coulon, F.; Wagland, S.T. Compositional analysis of excavated landfill samples and the determination of residual biogas potential of the organic fraction. *Waste Manag.* **2016**, *55*, 336–344. [CrossRef]
42. ERFO. The Role of SRF in a Circular Economy. Retrieved from 1048. Available online: https://www.erfo.info/images/PDF/The_role_of_SRF_in_a_Circular_Economy.pdf (accessed on 29 April 2019).
43. Abilmagzhanov, A.Z.; Ivanov, N.S.; Kholkin, O.S.; Adelbaev, I.E. Assessment of the Energetical and Biological Characteristics of Municipal Solid Waste from One of the Largest Landfills in Kazakhstan. *Recycling* **2022**, *7*, 80. [CrossRef]
44. Vollprecht, D.; Hernández Parrodi, J.C.; Lucas, H.; Pomberger, R. Case study on enhanced landfill mining at montsaintguibert landfill in Belgium: Mechanical processing, physico-chemical and mineralogical characterisation of fine fractions <4.5 mm. *Detritus* **2020**, *10*, 26–43. [CrossRef]
45. Council Decision 2003/33/EC Establishing Criteria and Procedures for the Acceptance of Waste at Landfills Pursuant to Article 16 of an Annex II to Directive 1999/31/EC. Available online: https://www.ecolex.org/details/legislation/council-decision-2003 33ec-establishing-criteria-and-procedures-for-the-acceptance-of-waste-at-landfills-pursuant-to-article-16-of-and-annex-ii-to-directive-199931ec-lex-faoc039228/ (accessed on 19 December 2002).
46. 2014/955/EU: Commission Decision of 18 December 2014 amending Decision 2000/532/EC on the list of waste pursuant to Directive 2008/98/EC of the European Parliament and of the Council Text with EEA relevance. Available online: https://eur-lex.europa.eu/legal-content/EN/TXT/PDF/?uri=OJ:L:2014:370:FULL&from=EN (accessed on 30 December 2014).
47. Neehaul, N.; Jeetah, P.; Deenapanray, P. Energy recovery from municipal solid waste in Mauritius: Opportunities and challenges. *Environ. Dev.* **2020**, *33*, 100489. [CrossRef]
48. Acha, E.; Lopez-Urionabarrenechea, A.; Delgado, C.; Martinez-Canibano, L.; Perez-Martinez, B.B.; Serras-Malillos, A.; María Caballero, B.; Unamunzaga, L.; Dosal, E.; Montes, N.; et al. Combustion of a Solid Recovered Fuel (SRF) Produced from the Polymeric Fraction of Automotive Shredder Residue (ASR). *Polymers* **2021**, *13*, 3807. [CrossRef]
49. Jagodzinska, K.; Lopez, C.G.; Yang, W.; Jonsson, P.G.; Pretz, T.; Raulf, K. Characterisation of excavated landfill waste fractions to evaluate the energy recovery potential using Py-GC/MS and ICP techniques. *Res. Conser. Recyc.* **2021**, *168*, 105446. [CrossRef]
50. Goli, V.S.N.S.; Singh, D.N.; Baser, T. A critical review on thermal treatment technologies of combustible fractions from mechanical biological treatment plants. *J. Environ. Chem. Eng.* **2021**, *9*, 105643. [CrossRef]
51. Jones, P.T.; Geysen, D.; Tielemans, Y.; Van Passel, S.; Pontikes, Y.; Blanpain, B.; Quaghebeur, M.; Hoekstra, N. Enhanced Landfill Mining in view of multiple resource recovery: A critical review. *J. Clean. Prod.* **2013**, *55*, 45–55. [CrossRef]
52. Chandana, N.; Goli, V.S.N.S.; Mohammad, A.; Singh, D.N. Characterization and Utilization of Landfill-Mined-Soil-Like-Fractions (LFMSF) for Sustainable Development: A Critical Appraisal. *Waste Biomass-Valorization* **2020**, *12*, 641–662. [CrossRef]
53. Hull, R.M.; Krogmann, U.; Strom, P.F. Composition and characteristics of excavated materials from a New Jersey landfill. *J. Environ. Eng.* **2005**, *131*, 478–490. [CrossRef]
54. Chiou, I.-J.; Chen, C.-H. Municipal solid waste landfill age and refuse-derived fuel. *Waste Manag. Res.* **2020**, *39*, 601–606. [CrossRef] [PubMed]
55. Wolfsberger, T.; Aldrian, A.; Sarc, R.; Hermann, R.; Höllen, D.; Budischowsky, A.; Zöscher, A.; Ragoßnig, A.; Pomberger, R. Landfill mining: Resource potential of Austrian landfills–Evaluation and quality assessment of recovered municipal solid waste by chemical analyses. *Waste Manag. Res. J. Sustain. Circ. Econ.* **2015**, *33*, 962–974. [CrossRef]
56. Rotheut, M.; Quicker, P. Energetic utilisation of refuse derived fuels from landfill mining. *Waste Manage.* **2017**, *62*, 101–117. [CrossRef]
57. Dong, T.T.T.; Lee, B.-K. Analysis of potential RDF resources from solid waste and their energy values in the largest industrial city of Korea. *Waste Manag.* **2009**, *29*, 1725–1731. [CrossRef]

58. Hölzle, I. Analysing material flows of landfill mining in a regional context. *J. Clean. Prod.* **2019**, *207*, 317–328. [CrossRef]
59. Bożym, M.; Klojzy-Karczmarczyk, B. Assessment of the mercury contamination of landfilled and recovered foundry waste—A case study. *Open Chem.* **2021**, *19*, 462–470. [CrossRef]
60. Pitak, I.; Baltusnikas, A.; Kalpokaite-Dickuviene, R.; Kriukiene, R.; Denafas, G. Experimental study effect of bottom ash and temperature of firing on the properties, microstructure and pore size distribution of clay bricks: A Lithuania point of view. *Case Stud. Constr. Mater.* **2022**, *17*, e01230. [CrossRef]
61. Götze, J.; Pan, Y.; Müller, A. Mineralogy and mineral chemistry of quartz: A review. *Miner. Mag.* **2021**, *85*, 639–664. [CrossRef]
62. Yang, L.; Ying, W.; Yuqiong, Z.; Zheng, W.; Yuan, L.; Wuxing, H.; Yongfa, Z. The characteristics of mineralogy, morphology and sintering during co-combustion of Zhundong coal and oil shale. *RSC Adv.* **2017**, *7*, 51036–51045. [CrossRef]
63. Kotowski, J.; Nejbert, K.; Olszewska-Nejbert, D. Rutile Mineral Chemistry and Zr-in-Rutile Thermometry in Provenance Study of Albian (Uppermost Lower Cretaceous) Terrigenous Quartz Sands and Sandstones in Southern Extra-Carpathian Poland. *Minerals* **2011**, *11*, 553. [CrossRef]
64. Muhammad, M.; Fatmaliana, A.; Jalil, Z. Study of hematite mineral (Fe_2O_3) extracted from natural iron ore prepared by co-precipitation method. *IOP Conf. Ser. Earth Environ. Sci.* **2019**, *348*, 012135. [CrossRef]
65. Boulliard, J.-C.; Gaillou, E. Twinning in "anorthoclase" megacrysts from phonolitic eruptions, Erebus volcano, Antarctica. *Eur. J. Miner.* **2019**, *31*, 99–110. [CrossRef]
66. Diopside Mineral Data. Available online: https://www.mindat.org/min-1294.html (accessed on 25 January 2023).
67. Hervy, M.; Remy, D.; Dufour, A.; Mauviel, G. Air-blown gasification of Solid Recovered Fuels (SRFs) in lab-scale bubbling fluidizedbed: Influence of the operating conditions and of the SRF composition. *Energy Convers. Manag.* **2019**, *181*, 584–592. [CrossRef]
68. Locher, F.W. Zement—Grundlagen der Herstellung und Verwendung. Düsseldorf 522. 2000. Available online: https://www.google.ru/url?sa=t&rct=j&q=&esrc=s&source=web&cd=&cad=rja&uact=8&ved=2ahUKEwin_Obn-Lr9AhX4g_0HHYgYD34QFnoECA0QAQ&url=https%3A%2F%2Fdownload.e-bookshelf.de%2Fdownload%2F0003%2F5106%2F68%2FL-G-0003510668-0013613454.pdf&usg=AOvVaw0-HmoVI11qP-j392H6cyQA (accessed on 24 February 2023).
69. Akmenės cementas. Description of cement production technology. 2021. Available online: https://cementas.lt/en/production/description-of-cement-production-technology/ (accessed on 12 August 2014).
70. Coal Marketing International (CMI). Coal Basics. Available online: http://www.coalmarketinginfo.com/coal-basics (accessed on 5 November 2012).
71. Directive 2000/76/EC of the European Parliament and of the Council on the incineration of waste. Available online: https://eur-lex.europa.eu/eli/dir/2000/76/oj (accessed on 31 December 2020).
72. Del Zotto, L.; Tallini, A.; Di Simone, G.; Molinari, G.; Cedola, L. Energy Enhancement of Solid Recovered Fuel within Systems of Conventional Thermal Power Generation. *Energy Procedia* **2015**, *81*, 319–338. [CrossRef]
73. Organization for Economic Co-Operation and Development (OECD). Effective Carbon Rates. Available online: https://www.oecd.org/tax/tax-policy/effective-carbon-rates-2021-highlights-brochure.pdf (accessed on 5 May 2021).

Case Studies in Construction Materials 17 (2022) e01230

Contents lists available at ScienceDirect

Case Studies in Construction Materials

journal homepage: www.elsevier.com/locate/cscm

Experimental study effect of bottom ash and temperature of firing on the properties, microstructure and pore size distribution of clay bricks: A Lithuania point of view

Inna Pitak [a,*], Arūnas Baltušnikas [a], Regina Kalpokaitė-Dičkuvienė [a], Rita Kriukiene [a], Gintaras Denafas [a,b]

[a] Laboratory of Materials Research and Testing, Lithuanian Energy Institute, Kaunas 44403, Lithuania
[b] Department of Environmental Technology, Kaunas University of Technology, Kaunas 51424, Lithuania

ARTICLE INFO

Keywords:
Bottom ash
Recycling
Properties
Structure
Clay bricks

ABSTRACT

The paper studied the feasibility of reusing the bottom ash (BA) in clay bricks production. The study has researched the influence of BA on clay bricks' physical and mechanical properties, the micro-and structure of samples, resistance to freezing and thawing porosity, average pore size and pore size distribution. Clay bricks were made from BA from 10% to 40% and clay (with CaO less than 1%), fired at 900 and 1000 °C. The open porosity of clay bricks developed when a BA was added due to burning a small amount of organic part of clay, decarbonising calcite, and the release of gaseous substances and crystalline moisture. The infrared spectra of clay brick samples fired at 900 and 1000 °C showed the presence of Si-O, Si-O-Mg, and Si-O-Al bond. These results are consistent with the XRD patterns. Clay bricks' physical and mechanical properties changed with the presence of BA: shrinkage, density and compressive strength decreased, water absorption and open porosity increased. It is recommended to add 10% and 20% BA to the clay body and fire at 900 °C, or 10–30% BA and fire at 1000 °C. In freezing and thawing resistance, clay bricks containing BA10 and BA20 fired at 900 and 1000 °C can be utilized in moderately aggressive environments. Samples containing BA30 and fired at 1000 °C can be used in passively aggressive environments. Micropores predominate in clay bricks; however, with an increase in BA, micropores turn into mesopores. The pore diameter of samples changes with BA and the firing temperature. The specific surface area is directly proportional to the amount of added BA. The use of bottom ash in the production of clay bricks will allow producing clay brick without deteriorating its quality and reduce the consumption of natural resources by up to 30%.

1. Introduction

Many countries use the waste incineration process to generate energy. Waste that cannot recycle is sent to a cogeneration power plant (CPP) for incineration. In this case, the incineration process is considered an integral part of the waste management strategy. In waste incineration, we obtain energy, thereby saving non-renewable natural resources and reducing the amount of waste disposed of at the landfill. During the incineration process, the volume of waste is reduced by about 90%. But any technological process has

* Corresponding author.
E-mail addresses: inna.pitak@lei.lt, ipitak5@gmail.com (I. Pitak).

https://doi.org/10.1016/j.cscm.2022.e01230
Received 15 March 2022; Received in revised form 20 May 2022; Accepted 7 June 2022
Available online 10 June 2022

advantages and disadvantages. One of these disadvantages is a significant amount of BA generated due to waste incineration.

As the non-recyclable part of the waste is incinerated, the volumes of BA increase, and there is a need to develop technologies for the disposal of "new" materials [1,2].

The amount of waste generated in Lithuania is 1.34 million tons per year, of which about 203000 tons are currently incinerated at Lithuanian CPP [3–5]. During the waste incineration process (to produce heat or energy), it generated about 11% of BA. After extracting metals, the BA is taken to the landfill and used for dumping. Although, there is a real opportunity to use generated BA in the construction industry. In some European countries such as France, Germany, and the Netherlands, BA is used to construct roads production of clay bricks and tiles [6–8].

Waste Directive 2008/98/EC provides the prevention of waste and the use of waste as a resource. Attempts should be made to recycle, reuse and dispose of waste [9]. The bottom ash is a mixture of slag, metals and other non-incineration materials. Its composition strictly depends on the composition of the waste incinerated [10].

Incineration of waste at a CPP takes in a boiler at 920–990 °C [4]. The efficiency and type of boiler affect the combustion quality. The organic part of the ash mainly consists of unincinerated cellulose and lignin obtained from plant materials contained in municipal solid waste (MSW).

Sintering is a thermal process of converting fine loose particles into a solid, coherent mass by heat and/or pressure without fully melting the particles [11]. This method is used in industry, especially in producing fired ceramic products and composite materials. This type of heat treatment of materials has advantages for industrial waste. During the sintering process, the inorganic part of the ash reacts with the minerals contained in the clays, and, as a result, new safety ceramic products are formed [12].

The solution to the problem associated with the accumulation of BA, an excellent solution is to use it as a substitute component in ceramic production. In works [13–16], it is reported that the ash obtained after incineration of waste can be used to produce silicate bricks, ceramic tiles, glass and glass ceramics.

In this work, the BA characteristics were studied, and mixtures of clay were prepared with various percentages of BA (10–40%) to investigate the possibility of reusing BA in ceramic products. The physical and mechanical properties of clay bricks have been studied; quantitative phase analysis of clay bricks fired at 900 °C and 1000 °C and determined the characteristics of the porous structure of materials, particularly the average pore size and pore size distribution had been completed. FTIR spectroscopy has determined the composition and structure of clay, bottom ash and clay bodies samples fired at a temperature of 900 and 1000 °C to study the interactions of clay minerals with inorganic or organic compounds.

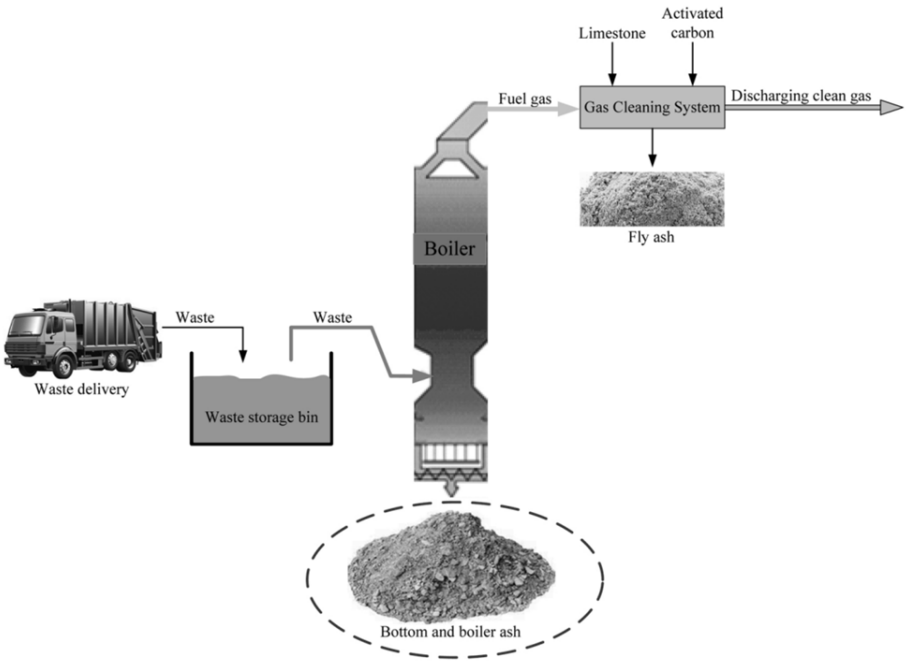

Fig. 1. The schematic process generation of bottom ash.

2. Materials and methods

2.1. Preparation of the test samples

The BA was obtained by incinerating refuse-derived fuel (RDF) at the cogeneration power plant. The waste incineration process occurs at a temperature of 900–950 °C. As a result of the waste incineration process at CPP, electricity is produced at 30%, heat is 60%, and by-products are generated at 10%. The schematic process generation of BA is presented in Fig. 1.

Currently, valuable metals are extracted from this by-product (BA), and the rest is sent to the landfill and used for dumping. After incineration, the generating BA can be disposed of as a replacement component in building materials. The BA samples were obtained from the Kaunas CPP (Lithuania). After four months of BA ageing in the atmosphere, the material samples for investigation had taken.

The clay used to form the samples was mined in the largest Andreevsky deposit in Ukraine, located near the city of Druzhkovka, Donetsk region, Ukraine. Clay Technik-3 has a high dry or fired mechanical strength, white colour after firing, low organic matter content, low water absorption, low drying sensitivity, wide sintering interval and stable quality. The clay humidity is 7%, and organic matter content has a low value of up to 5% [17]. The clay and BA were used in this experimental study. The materials (Fig. 2) have been dried at 105 ± 5 °C, crushed and sieved through a 0.63 mm sieve.

The samples were prepared from the clay and BA, previously dried to constant humidity. The components were mixed under dry conditions; water was added to the mixture (8%). The index of plasticity of the moulding mass practically did not change with the addition of ash residue (Table 1). The plasticity of the clay was determined by the standard Vasiliev cone method. The samples were pressed in steel molds at a pressure of 120 kg/cm^2. After pressed there were obtained small cube bricks 20 × 20 × 20 mm size. The formed samples were dried in an oven (SNOL 58/350) until a constant weight was established (≈24 h).

The dried samples were fired at 900 and 1000 °C for one-hour in the electric muffle furnace (SNOL 8.2/1100). The heating rate that was used during firing samples presented in Fig. 3.

In the temperature range of 25–200 °C, the samples were slowly heated to 75 °C/hour. In this interval, interlayer and partially adsorbed water were removed. In the temperature range of 200–400 °C, the temperature rise rate was 100 °C/hour. Upon reaching 400 °C, an exposure of 15 min was made to remove the evolved gases and equalize the temperature in the kiln space. The temperature range of 400–600 °C is characterized by the hydration of clay minerals and the release of chemically bound water included in the crystal lattice. The rate of temperature rise was 100 °C/hour, and upon reaching 600 °C, an exposure of 20 min was made. Upon reaching 600–800 °C, the rate of temperature rise was 130 °C/hour. In the temperature range of 800–1000 °C, the sintering process began. During sintering, diffusion transfer of matter occurs through chemical interaction of components and new minerals' formation. The rate of temperature rise in such firing was 75 °C/hour. The fired products were cooled down to the ambient temperature in the kiln.

2.2. Test instrument

The BA and clay's morphology and elemental analysis was investigated by applying scanning electron microscopy equipped with an energy dispersive spectroscopy detector (SEM-EDS). The analysed samples were passed through sieves and then subjected to drying at 40 °C. For SEM images the specimens (except powder) were cut into smaller sizes of about 5 × 5 × 5 mm and coated using gold (Au) prior to the morphological observation. SEM, observation of samples was performed on ZEISS EVO MA10 microscope at an accelerating voltage of 20 kV. Bruker AXSX Flash 6/10 Detector can display all the elements present in the specimen at overall accuracy of about 1% and detection sensitivity down to 0.1% by weight.

The properties of bottom ash and clay were determined by the following standards:

- Loss on ignition: LST EN 15935:2012;
- Bulk density: LST EN 13041:2012;

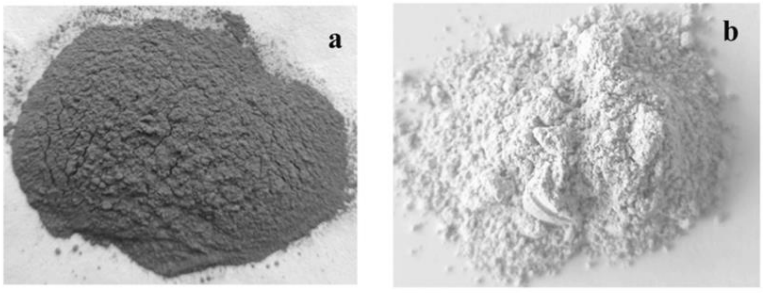

Fig. 2. Bottom ash after incineration of MSW (a) and clay (b).

Table 1
Composition of moulding compounds.

Raw materials	Composition of moulding compounds, %wt				
	BA0	BA10	BA20	BA30	BA40
Clay	100	90	80	70	60
Bottom ash	0	10	20	30	40
Moisture content (optimum)	8	8	8	8	8
Atterberg limits:					
Liquid limit	38	39	40	41	42
Plastic limit	21	23	25	27	30
Plasticity index	17	16	15	14	12

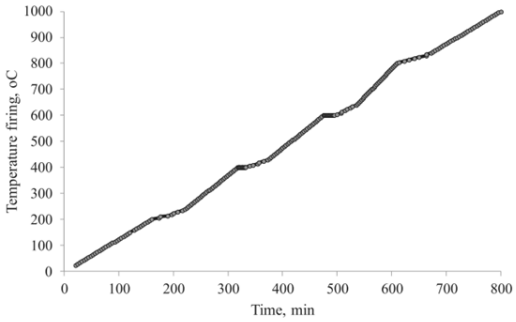

Fig. 3. The heating rate in the kiln.

– Dry solid content: LST EN 15934:2012, method A;
– pH: LST EN 15933:2012

The element analysis of BA and clay to determine metals was performed using an ICP-OES, Optima 8000 (Perkin Elmer). The samples (0.4–0.5 g) were mineralized with 8 ml of concentrated nitric acid, 1 ml of hydrofluoric acid and 3 ml of hydrogen peroxide at 800 W,6 MPa, pRate: 50 kPa·s^{-1} (Multiwalve 3000). After the mineralization, the solution was poured into 50 ml flasks and diluted to 50 ml using deionised water. For the data acquisition of the samples, a quantitative analysis mode was used. The scanning of every single sample during element analysis was repeated three times to gather reasonably good results. Analysis was made in four replicates of each sample.

Differential thermal analysis was done using Simultaneous Thermogravimetry and Differential Scanning Calorimetry (TG-DSC) – High-Pressure ability (STA PT 1600 (TG-DSC).

Fourier Transform Infrared Spectroscopy (FTIR) clay, BA, and clay bodies samples fired at 900 and 1000 °C were carried out. Infrared spectroscopy was conducted through the Fourier transform of adsorbent samples before and after adsorption. Samples were analysed in ALPHA Platinum ATR-FTIR spectrophotometer in the 4000–400 cm^{-1}region.

The physical and mechanical properties of the fired clay bricks were determined by the following standards:

– Density: LST EN 772–13:2003;
– Water sorption: LST EN 772–21:2011;
– The compressive strength: LST EN 772–1:20114;
– Freeze and thaw resistance: LST 1985:2006;
– The thermal conductivity. Hot-wire methods: LST EN 993–14:2001/P: 2006.

The drying and firing shrinkage of clay bodies were calculated according to the Eqs. 1 and 2.

$$S_{drying} = [(S_0 - S_1)/S_0] \cdot 100\% \quad (1)$$

$$S_{firing} = [(S_0 - S_2)/S_0] \cdot 100\% \quad (2)$$

where S_0 — distance between two reference marks in a wet sample, mm; S_1 distance between two reference marks in a dried sample at 105 °C, mm; S_2 — distance between two reference marks in a fired specimen at 900 and 1000 °C, mm.

X-ray diffraction analysis (XRD) of BA, clay and clay bricks were carried out on BRUKER D8 ADVANCE diffractometer with CuKα radiation at 40 kV in 2Θ (3°÷70°) interval at scanning step 0.02°. The obtained X-ray patterns were deciphered using the Diffract Eva program. Rietveld quantitative phase analysis was adopted for the quantitative phase analysis of clay bricks. The measurement

uncertainty was about ± 1 wt%.

Pore size distribution was obtained by the nitrogen adsorption method using the Quenched solid density functional theory (QSDFT), which considers the roughness and heterogeneity of the pore wall surfaces. Some researchers [18,19] use the BJH (Barret, Joyner and Halenda) and the method Mercury Intrusion Porosimetry (MIP) to describe the pore-size distribution, assuming cylindrical pore geometry in the clay materials. According to [20], clays are typical natural nanomaterials with a high sorption capacity. Colloidal forms of sulphides, silica and other compounds take an active part in the sorption of metals. It was decided to use the QSDFT method to consider the pore walls' heterogeneity and reliably characterize mesoporous in the range from 2 to 35 nm. The QSDFT method [21] makes it possible to analyse a broader range of pores.

Two-sided confidence levels with 95% mean values (water sorption, total open porosity, density, linear shrinkage and compressive strength) were calculated, assuming that water sorption, porosity, density, shrinkage and compressive strength usually are fixed random values. The Student's t-distribution was used to calculate the confidence levels.$(M-td,\ (1-\alpha/2)\cdot S/n^{0.5}) \le \mu \le (M+td,\ (1-\alpha/2)\cdot S/n^{0.5})$ of the means measurements, where M is estimates of the mean, S are standard deviation of random variables; n = 6 is the sample size, $td,\ (1-\alpha/2) \approx 2.6$ is $(1-\alpha/2) = 0.97$ quantile of the Student's t-distribution, $\alpha = 0.05$ is a level of significance and degree of freedom d= 5.

3. Results and discussion

The experimental tests by SEM-EDS analysis of clay showed that SiO_2 content is 66.65%, Al_2O_3 +TiO_2 content is 27.64%, CaO content is 0.2%, and the Fe_2O_3 content is 1.51%.

The experimental tests for analyzing the chemical composition of BA showed that SiO_2 content in the BA is 35.53%, Al_2O_3 +TiO_2 content is 10.3%, and the Fe_2O_3 content is 8.83%. The particle size distribution BA and clay showed in Table 2.

The analysis microstructure of clay and BA is presented in Fig. 4. Clay particles had a shape of 1.5–10 μm and were distributed almost evenly. Clay minerals belong to the layered and stratified-strip silicates of aluminium, iron and magnesium. Clay particles are predominantly lamellar, but there are also elongated plates and stripes and tubular and fibrous particles. The morphology and size of particles are associated with the features of their crystal structure. The BA particles were dark grey and had a lamellar and crystal shape. The bottom ash size range from 1 μm to 10 μm.

The main source of clays are feldspars, the destruction of which, under the influence of atmospheric agents, forms silicates of the group of clay minerals. The composition of feldspars is determined by the ratio of the components of the ternary system $NaAlSi_3O_8$-$KAlSi_3O_8$-$CaAl_2Si_2O_8$. There are two series of minerals: alkali-isomorphic mixtures $KAlSi_3O_8$ and $NaAlSi_3O_8$; plagioclase-isomorphic mixtures $NaAlSi_3O_8$ and $CaAl_2Si_2O_8$. At high temperatures, there are continuous series of solid solutions within each series (Fig. 5).

Among plagioclases, there are distinguished ($CaAl_2Si_2O_8$ content in mole %) is indicated in brackets: albite (0−10), oligoclase (10−30), andesine (30−50), labradorite (50−70), bytownite (70−90) and anorthite (90−100). Alkaline feldspars are distinguished ($NaAlSi_3O_8$ content in mole %) is indicated in parentheses: sanidine (0−63), orthoclase (0), microcline (0), which are polymorphic modifications $KAlSi_3O_8$ and anorthoclase (63−90). At low temperatures, solid solutions of alkali feldspars decompose into sodium and potassium phases, and in the $NaAlSi_3O_8$-$CaAl_2Si_2O_8$ system, plagioclases of a complex domain structure are obtained with a $NaAlSi_3O_8$ content of 2–16, 48–58 and 70–90 mol%.

The prevailing minerals in the clay detected by XRD analysis (Fig. 6) are quartz (28.99%), muscovite, titanium oxide (1.45%), kaolinite (3.86%), illite (9.09%), microcline (30.02%) and albite (3.62%) and correspond to the data [23].

The research found that BA content has an inorganic component, and the humidity was 6%. The incineration process of waste transforms organic materials in CO_2 and H_2O but yields inorganic residues from ferrous non-ferrous metals to silicates. X-ray diffraction analysis (Fig. 7) and FTIR spectra (Fig. 9) of BA evidence the presence of inorganic components.

Table 3 presents the results of element quantitative analysis and other properties bottom ash and clay.

According to the analysis results, the chemical elements found in clay and BA does not pose a severe threat to the environment since they do not contain heavy metals in their composition. Thus, according to data [24] and obtained by us, the bottom ash is classified as non-hazardous waste and can be used as an additive in ceramic production.

Fig. 8 shows DTA and TGA curves for clay and bottom ash. The DTA curve for clay has three endothermic peaks. The first one peak at 95 °C, the second one at 505 °C and the third one at 569 °C. The first peak TGA curve shows a weight loss of 1.45% at 120 °C, a 1.38% weight loss between 120 and 405 °C. The second and third peak TGA curve shows a weight loss of 3.12% between 410 and 592 °C. The total mass loss consisted of 7.84%. The endothermic peak and weight loss in the temperature range of 100–200 °C are due to the heating of products and the removal of interlayer and partially adsorbed water. In the temperature range of 200–300 °C, the

Table 2
Chemical and granulometric composition of the clay and BA.

Raw materials	Chemical composition, %											
Clay	SiO_2	Al_2O_3	K_2O	TiO_2	Fe_2O_3	MgO	Na_2O	CaO	SO_3	P_2O_5	other	**Total**
	66.65	25.72	2.8	1.92	1.51	0.66	0.53	0.2	—	—	0.21	**100**
Bottom ash	35.53	8.68	0.67	1.62	8.83	3.71	5.48	30.46	2.62	1.26	1.08	**100**
	Granulometric composition, %											
	> 0.5 mm			0.5–0.063 mm			0.063–0.01 mm			> 0.01 mm		
Clay	0.2			1.8			22.4			75.6		
Bottom ash	0.18			2.5			75.8			21.5		

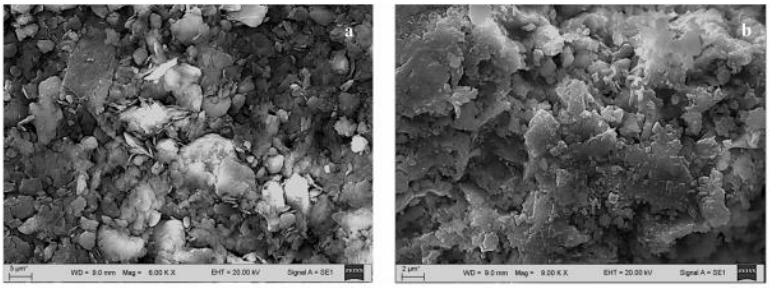

Fig. 4. Microstructure clay (a) and BA (b).

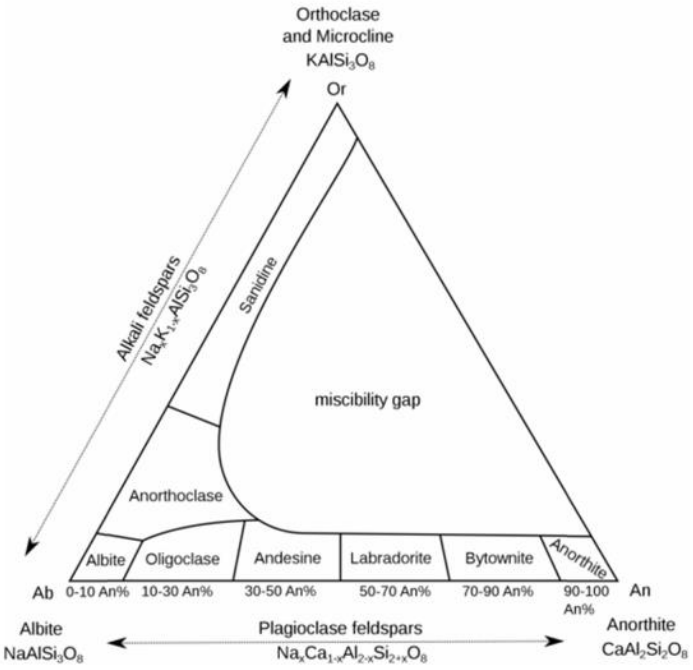

Fig. 5. Ternary phase diagram of the feldspars [22].

removal of bound water is completed, and some of the organic substances are burned. Distinct endothermic peaks and weight loss in the temperature range of 505 and 569 °C are due to the dehydration of clay minerals and the release of chemically bound water included in their crystal lattice [25].

The situation is similar for DTA and TGA curves for bottom ash. The DTA curve for bottom ash has two endothermic peaks at 100 °C and 781 °C. The first peak TGA curve shows a weight loss of 1.55% at 100 °C, a 3.33% loss between 110 and 620 °C. The second peak TGA curve shows a weight loss of 3.47% between 669 and 750 °C and a 15% loss between 620 °C and 760 °C. The total mass loss was 9.39%. The endothermic peak and weight loss in the temperature range of 100–200 °C are due to the removal of residual moisture. In the temperature range of 300–500 °C, there was a burnout of organic inclusions and the removal of "crystallization" water. Distinct endothermic peak and weight loss at 790 °C are due to the decomposition of carbonates, accompanied by the release of carbon dioxide [26]. With the release of gaseous components released during the decomposition of carbonates, cracks can appear on the surface of the matrix and weaken the interaction of particles.

Fig. 9 shows FTIR spectra obtained for clay and BA. Bands of clay at about 3700 and 3400 cm^{-1} are characteristic —OH stretching

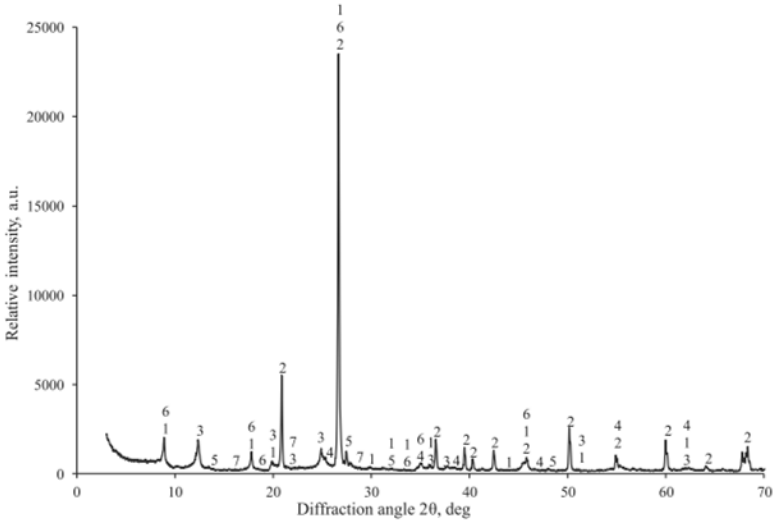

Fig. 6. The clay XRD analysis: 1 – muscovite, 2 – quartz, 3 – kaolinite, 4 – titanium oxide, 5 – microcline, 6 – illite, 7 – albite.

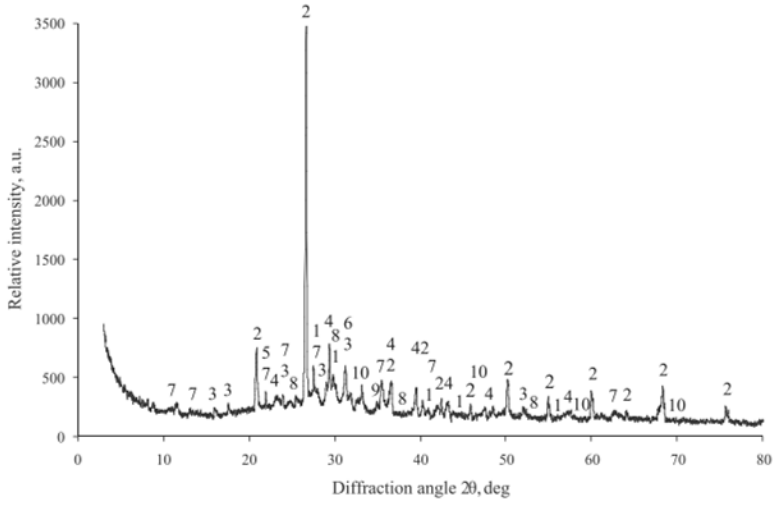

Fig. 7. The bottom ash XRD analysis: 1 – diopside; 2 – quartz; 3 – akermanite; 4 – calcite; 5 – cristobalite; 6 – gehlenite; 7 – albite; 8 – wollastonite; 9 – iron oxide; 10 – perovskite.

regions; these two bands are assigned to the —OH stretching vibration of the structural hydroxyl groups in the clay and the water molecules present in the interlayer, respectively [27] group vibration elongation. The small absorption band for clay and BA at 1630 cm^{-1} are due to adsorbed water presence in clay [25].

The characteristic strong peaks at 876 cm^{-1} and 1430 cm^{-1} correspond to the C–O bonding of $CaCO_3$, which corroborated the presence of $CaCO_3$ in bottom ash. The band attributed to Si-O occurs in the 1035 cm^{-1} region, while 920 cm^{-1} suggests Al-OH-Al [25] deformation vibration. Quartz peaks with different Si-O and Si-O-Al vibrations were detected close to 790 and 690 cm^{-1}, and bands close to 530 and 460 cm^{-1} indicate the typical elongation of the Si-O-Al bond [26].

After firing ceramic specimens at 900 and 1000 °C without adding BA and with adding it, defects such as swelling and cracking

Table 3
Element quantitative analysis and other properties bottom ash and clay.

Species	Results				
	Bottom ash	Standard deviation, %	Clay	Standard deviation, %	Unit of measurement
Silicium (Si)	181625.6	± 16.7	337729	± 15	mg/kg
Calcium (Ca)	168099.8	± 12.7	40.7	± 24.4	mg/kg
Ferrum (Fe)	51532.6	± 9.3	2960.6	± 14.8	mg/kg
Aluminuum (Al)	33396.4	± 4.9	17066.9	± 12.5	mg/kg
Natrium (Na)	26178.5	± 6.6	1774.2	± 14.6	mg/kg
Magnesium (Mg)	15250.4	± 22.9	333.6	± 18.4	mg/kg
Kalium (K)	11128.2	± 9.4	9903.9	± 6.4	mg/kg
Titanium (Ti)	6428.1	± 16.2	7447.3	± 11.8	mg/kg
Sulfur (S)	4487.2	± 6.9	< 1.8		mg/kg
Zincum (Zn)	3762.8	± 26.1	2.0	± 11.3	mg/kg
Cuprum (Cu)	3498.7	± 19.1	28.7	± 12.3	mg/kg
Phosphorus (P)	2400.1	± 14.6	< 3.5		mg/kg
Chromium (Cr)	743.6	± 10	74.6	± 14.4	mg/kg
Manganum (Mn)	668.8	± 11.9	38.4	± 16.5	mg/kg
Dry solid content	977	± 13	946	± 12	g/kg
Bulk density	1101	± 20	1400	± 22	kg/m^3
pH	8.5	± 0.2	7.5	± 0.5	pH value
Loss on ignition	7.75	± 0.5	5.4	±0.5	%

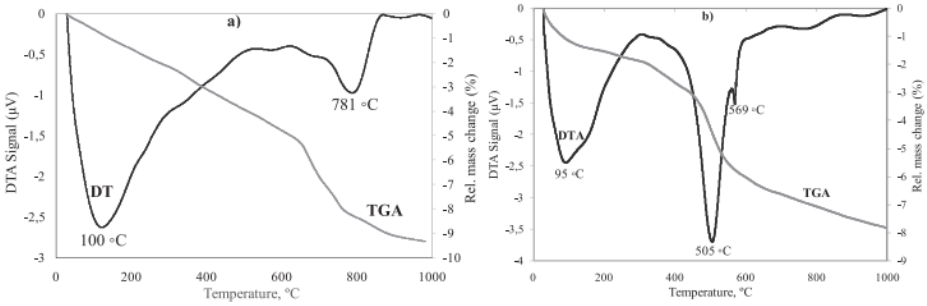

Fig. 8. DTA and TGA curves of bottom ash (a) and clay (b).

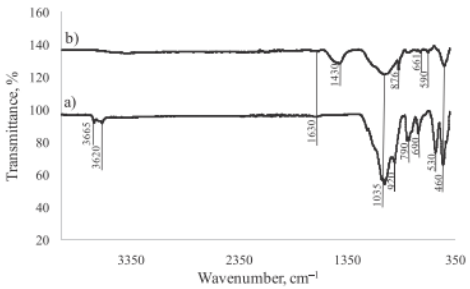

Fig. 9. FTIR spectra for clay (a) and bottom ash (b).

were not observed. A colour change was observed in the finished fired samples. Colour saturation increased with increasing BA addition. In some samples with the BA40 and firing at 1000 °C, small dark-grey coring appeared in the form of a dot. It is known that during firing, at a temperature of 800–1000 °C, calcium $CaCO_3$ and magnesium carbonates $MgCO_3$ actively interact with decomposition products of clay minerals — amorphous silica SiO_2 and alumina Al_2O_3. These reactions proceed with the release of carbon dioxide CO_2. Some colouring oxides — manganese MnO_2, copper CuO, iron Fe_2O_3, decompose during firing, releasing oxygen O_2. Most likely, such chemical transformations could provoke the appearance of such a defect. In the ceramic mixture, when heated, chemical

and physicochemical processes proceed sequentially, leading to a complete and irreversible change in its structure: removal of chemically bound water; decomposition of dehydrated clay into oxides Al_2O_3 and SiO_2; formation of new water-resistant and refractory minerals; formation of a certain amount of melt from low-melting clay.

The formation of a durable product occurs due to the adhesion of solid particles of clay and BA by the resulting melt. In this case, due to the forces of surface tension of this melt, a decrease in the volume of the material occurs, called fire shrinkage. Shrinkage during drying of clay masses without adding ash residue reached 5.15%; the shrinkage during firing at 900 °C was 6.25%, and at 1000 °C, the shrinkage reached 7.14%. The shrinkage of the ceramic products during firing depends on the amount of BA added. Depending on the moulding composition, the shrinkage during firing at 900 °C varies from 5.93% to 5.03% and from 6.69% to 5.55% at 1000 °C (Fig. 10).

Shrinkage occurs due to a decrease in the thickness of the water shells around the clay particles, forming a framework of ash residue minerals and the convergence of particles under the action of capillary pressure forces. This frame prevents the clay particles from coming together during drying. Fire shrinkage during firing occurs as a result of the general effect of all physicochemical processes occurring in the ceramic mass during firing — dehydration of minerals, material transfer due to diffusion, recrystallization and the formation of new minerals, as well as due to the convergence of particles under the action of surface tension forces of liquid phases during sintering. For the samples under consideration, fire shrinkage is relatively small. This occurs due to the formation of new minerals or the recrystallization of the former.

The density of the fired clay samples without the addition of BA varied with the firing temperature. The density of the samples during firing at 900 °C was 1.99 g/cm^3 and at 1000 °C — 2 g/cm^3, respectively. With the addition of 10% BA, the density of the samples decreased and amounted to 1.93 and 1.99 g/cm^3 at the same temperatures. An increase in the additive content in the ceramic mass led to a decrease in the density of the samples. Therefore, with the addition of 40% BA, the density was 1.85 and 1.88 g/cm^3 at temperatures of 900 °C and 1000 °C, respectively (Table 4). The compressive strength of clay samples depends on BA content and the firing temperature. With an increase in the BA content decrease in the density of the samples and the compressive strength.

The clay samples with a BA30 and fired at 1000 °C had a sufficiently high compressive strength of 14.5 MPa and can be used to construct buildings and structures. While ceramic samples with the same percentage of BA, fired at a temperature of 900 °C, had a compressive strength of 10.6 MPa. The compressive strength decreases due to the combustion of adhesive additives, dehydration of clay minerals, and chemical transformations inside the sintered ceramic mass. The main chemical transformation is calcite decarburization. According to [28,29], the compressive strength of a brick prepared under laboratory conditions for testing should not be lower than 20 MPa. The European Union standard does not specify minimum values for compressive strength. Accordingly, each manufacturer must declare compressive strength clay bricks, and according to this data, designers must consider these values when designing structures. However, it is known that the compressive strength of clay bricks must be at least 10 MPa.

Water sorption and open porosity depend on the size, number and distribution of pores in the clay brick and are important for ceramic products. There was a significant difference in water sorption and open porosity values for clay bricks fired at 900 and 1000 °C. The lowest values for water sorption and open porosity had samples fired at 1000 °C without adding BA. These clay brick samples had a water sorption value of 11.4% and an open porosity of 24.1%. With 10% BA, water sorption and open porosity increased to 11.7% and 25%, respectively. With the subsequent addition of 20%, 30% and 40% BA, clay brick samples' water sorption and open porosity increased. Clay samples fired at 900 °C had water absorption and open porosity values higher than samples fired at 1000 °C.

Requirements for water absorption in clay brick samples are not specified by the European Standard LST EN 771–1:2011 +A1:2015. Based on this, manufacturers must indicate the water absorption values for their products in accordance with the standard LST EN 772–21:2011. Permissible water absorption for clay bricks must consist of 12–20%. If the water absorption value is below 12%, it may lead to improper bonding between mortar and bricks.

The physical and mechanical properties presented above are interconnected with the microstructure formed in the samples. It is known that the microstructure, properties and clay bricks depend on the pores, their distribution and interaction with water. The firing process at higher temperatures increases the crystallization process, resulting in intensive sintering of clay minerals, an increase in the volume of the liquid phase, a glass phase increase, a decrease in porosity and closing of the open pores of the samples. Phase and

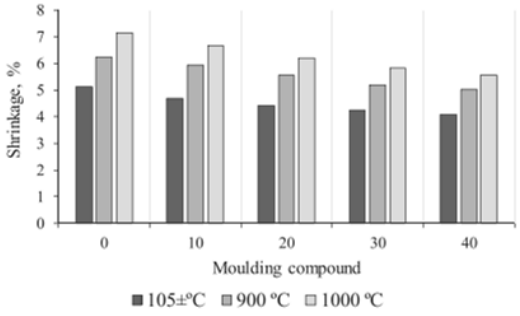

Fig. 10. Linear shrinkage of clay brick specimens.

Table 4
Properties of clay bricks samples.

Properties	Ceramic samples Firing temperature $\frac{900°C}{1000°C}$				
	BA0	BA10	BA20	BA30	BA40
Water sorption, %	$\frac{13.9 \pm 1.1}{11.4 \pm 1.4}$	$\frac{14 \pm 1.5}{11.7 \pm 1.7}$	$\frac{14.2 \pm 1.3}{12.1 \pm 1.5}$	$\frac{14.7 \pm 1.8}{13.1 \pm 2.0}$	$\frac{16.3 \pm 2.0}{15 \pm 2.4}$
Total open porosity, %	$\frac{24.4 \pm 1.8}{24.1 \pm 2.1}$	$\frac{27.3 \pm 2.2}{25 \pm 1.6}$	$\frac{28.4 \pm 1.9}{25.7 \pm 2.0}$	$\frac{28.9 \pm 2.2}{26 \pm 1.9}$	$\frac{31.1 \pm 2.0}{29.8 \pm 1.5}$
Density, g/cm^3	$\frac{1.99 \pm 0.003}{2 \pm 0.002}$	$\frac{1.93 \pm 0.002}{1.99 \pm 0.002}$	$\frac{1.92 \pm 0.002}{1.97 \pm 0.004}$	$\frac{1.90 \pm 0.003}{1.92 \pm 0.002}$	$\frac{1.85 \pm 0.004}{1.88 \pm 0.003}$
Compressive strength, MPa	$\frac{21.2 \pm 0.9}{26.2 \pm 1.21}$	$\frac{16.9 \pm 0.9}{22.6 \pm 1.2}$	$\frac{12.7 \pm 1.2}{17 \pm 1.4}$	$\frac{10.6 \pm 1.1}{14.5 \pm 1.5}$	$\frac{6.3 \pm 1.5}{9.9 \pm 1.4}$
Thermal conductivity, W/m·K	1.1/1.02	0.75/0.69	0.61/0.57	0.56/0.53	0.53/0.49

structural changes in clay samples with the addition of BA lead to a decrease in density, compressive strength, an increase in water absorption and total open porosity [30]. Clay samples with high additive BA have a more significant number of open pores and capillaries formed due to high-temperature transformations of the minerals contained in BA and decarbonisation of calcium carbonate. The resulting pores affect the physical and mechanical properties of clay samples.

There is a little difference between the morphology and appearance of the surfaces of clay bricks BA0 and with BA10. The microstructure of samples is dense with a predominance of a small number of pores. The pores are small and relatively evenly distributed throughout the sample. The microstructure of clay brick sample BA20 has different: the surface is less uniform with a predominance of pores of various sizes. The pores develop due to the intensive removal of CO_2 during the firing and decomposition of calcium carbonate. The fact that the amount of carbon in the samples increases is evidenced by the SEM-EDS analysis of the samples. The thermo chemical transformations of clay minerals and BA occur, as evidenced by the data presented in Fig. 11. These data show that some elements decrease with the addition of ash residue, for example, oxygen, silicon, aluminium, potassium, and some increase.

The microstructure of samples BA30 is different: bigger pores of various shapes predominate, formed due to intensive removal of crystal water and removal of gas components (CO_2, O_2) during the interaction of $CaCO_3$ and $MgCO_3$ the decomposition of colourful oxides (Fe_2O_3). An increase in the content of calcium, magnesium and iron is evidenced by the analysis data.

Frost resistance is an essential step of study that must be carried out without fail [31]. Formed and fired samples of ceramic bricks were subjected to freeze and thaw resistance testing and visual evaluation. The reference sample and samples with BA10–30, fired at 900 °C, completed 25 freezing and defrosting cycles (the cycle consists of one freezing phase at —18 °C and one thawing phase at +18 °C). The samples BA40 and fired at 900 °C completed 23 freezing and defrosting cycles. All samples (control and with the BA) fired at 1000 °C completed 25 freezing and defrosting cycles. Based on LST EN 771–1:2011 +A1:2015, these products can be operated in passive and moderate aggressive environments.

The thermal conductivity analysis was performed on clay brick patterns mixed with BA of 0, 10, 20%, 30% and 40% by weight and fired at 900 and 1000 °C. The relationship between thermal conductivity and porosity of clay bricks with the addition of BA can see in Table 4. An increase in the percentage of BA likely causes an increase in the porosity of the samples. The results show that a higher percentage of BA addition causes low thermal conductivity in the samples. This is a result of the increase in air volume produced by the interaction of clay minerals with BA, which leads to the formation of pores within the samples, making them poor heat conductors and, as a result, good insulators. The results show that thermal conductivity decreases with decreasing density and increasing porosity of fired clay bricks. As a result, the thermal conductivity values directly depend on the porosity. The thermal conductivity values for samples without the addition of BA and with the addition of it were in the range of 0.49–1.1 W/m·K. Based on the ASTM D 78896 standard, it can be argued that the addition of bottom ash during the production of bricks does not impair the technical properties of the fired samples.

The infrared spectra of the clay bodies with BA from 0% to 40% and fired at 900 and 1000 °C are presented in Fig. 12. The clay samples fired at 900 °C characterized the following bands. The characteristics band of 1150 cm^{-1} correspond to the stretching vibration modes of SO_4 tetrahedron.

The other bands at 1033, 1037 cm^{-1} are those of Si—O bonds. The presence of a doublet at 792 and 778 cm^{-1} (for 1000 °C) and 798 and 774 cm^{-1} (for 900 °C) are attributed to the quartz vibrations. Quartz peaks with different Si-O and Si-O-Al(Mg) vibrations were detected close to 690, and 680 cm^{-1}, bands close to 560 and 562 cm^{-1} indicate the typical elongation of the Si-O-Mg and bands close to 450 and 453 cm^{-1} indicate the Si-O-Al bond [32]. This result is in accordance with that of XRD patterns.

Powder diffraction is one of the most widely used analytical techniques for characterizing solid-state materials. The XRD-Rietveld refinement method can be used for phase identification, quantitative analysis, cell parameter determination, or complete crystal structure analysis. Fig. 13 (a) presented the XRD pattern (2θ=5–70°) of control samples of clay bricks with BA10–40 and fired at 900 and 1000 °C. Fig. 13 (b) shows the XRD analysis by Rietveld refinement of clay bricks with BA40 (using the Topas program).

Table 5 shows the data of the XRD Analysis by Rietveld refinement of reference samples and samples with the addition of bottom ash and fired at 900 and 1000 °C. Quartz is the main mineral in fired samples [33]. During the firing of ceramic specimens, the percentage of quartz changes. At the firing of 900 °C, the amount of quartz changed from 76.48% to 60.22% and from 86.71% to 58.97% at 1000 °C, respectively. The clay mineral illite [34–36] is present only in the reference samples and is 3.12% at firing 900 °C and 0.94% at 1000 °C. The presence of muscovite 2M1 [32] is typical in all samples but with different content (from 8.06% to 9.21% at

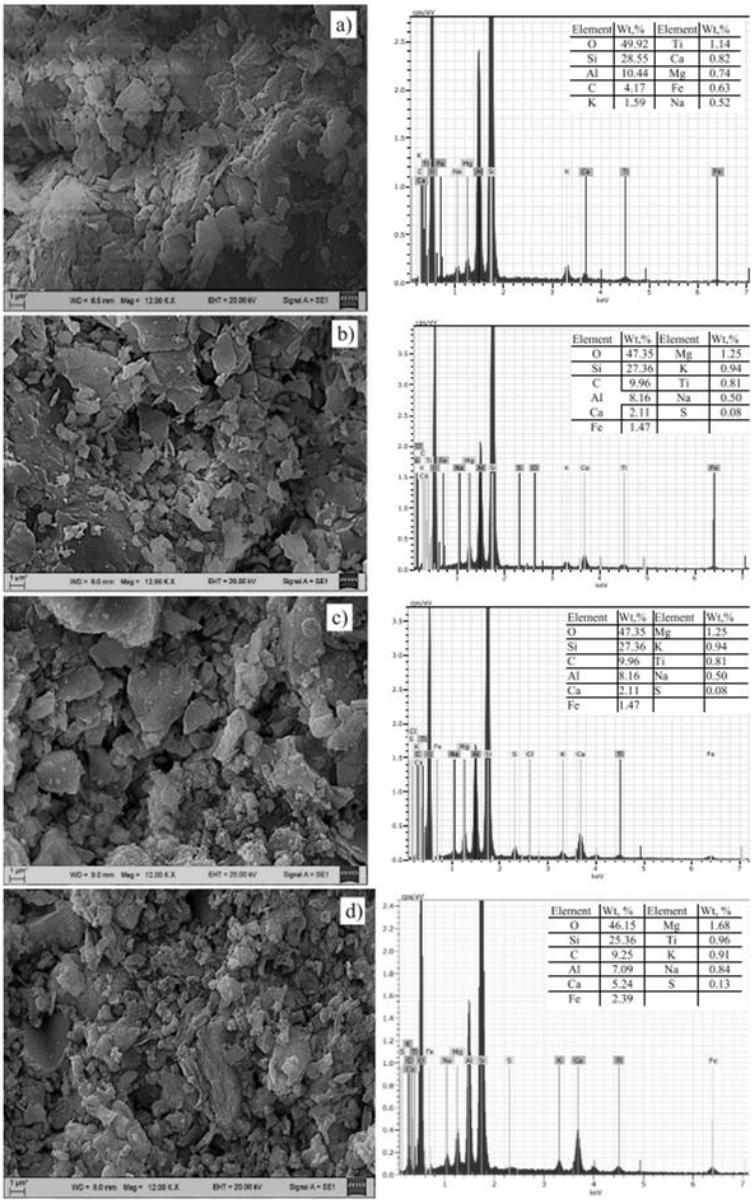

Fig. 11. SEM-EDS analysis of clay brick samples fired at a temperature of 1000 °C: sample BA0 (a), sample BA10 (b), sample BA20 (c), sample BA30 (d).

firing 900 °C and from 1.85% to 3.2% at 1000 °C).

The presence of anorthoclase [37] is characteristic of all samples and increased with the amount of BA and temperature firing (from 1.93% to 4.53% at 900 °C and from 1.32% to 3.62% at 1000 °C). An increase in the percentage of anorthoclase indicates an

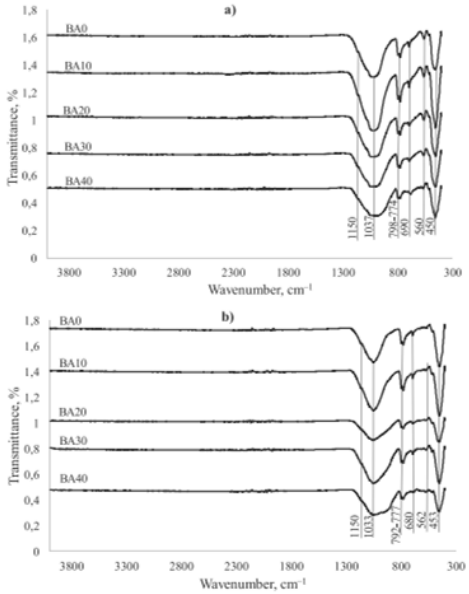

Fig. 12. FTIR spectra for clay bodies samples with different amounts of BA and fired at 900 °C (a) and 1000 °C (b).

improvement in the strength characteristics of clay samples. Microcline is an important raw material for the ceramic industry [36]. The microcline content in fired clay samples increases in proportion to the amount of BA and is from 1.26% to 6.83% at firing 900 °C and from 1.32% to 3.62% at 1000 °C, respectively. It should be noted the presence of cristobalite [38] in fired ceramic samples that contain the addition of BA. Therefore, in the ceramic samples fired at 900 °C, the presence of the.

cristobalite of 0.16–0.85%, at 1000 °C, the samples contending of 0.72–2.18%. According to [33,39,40], wollastonite is an industrial mineral comprised of calcium, silicon and oxygen. In the studied clay brick samples, the amount of wollastonite increases with the rising amount of BA and ranges from 0.85% to 3.1% at firing at 900 °C and from 1.29% to 4.13% at 1000 °C respectively. The samples contain wollastonite 2 M. Akermanite is a mineral of the melilite group [41]; it is also named a technogenic mineral. Akermanite is more durable than wollastonite. The content of akermanite increases with BA content and ranges from 0.24% to 2.06% at firing 900 °C and from 0.43% to 1.79% at 1000 °C. Gehlenite is contained in the fired clay brick samples [41]. It is a mineral of the silicate class, melilite group, forming a series with akermanite, with the same strength as akermanite. The gehlenite content is more than one per cent in samples with BA30 and BA40. In the rest of the samples, the gehlenite content is less than one per cent. In addition, less than one per cent is the mineral rutile [41]. It increases proportionally with the widening in the content of BA in the samples, regardless of the firing temperature.

As for hematite [42,43], this is a relatively common and durable mineral. The hematite content in the samples increases with an increase in the amount of BA from 0.15% to 2.04% at firing 900 °C and from 0.36% to 1.94% at firing 1000 °C. The presence of hematite results in a slight change in the colour of fired items. Labradorite [33,44] is feldspar of the plagioclase series (isomorphic mixture). In the samples under consideration, labradorite is formed in samples fired at 1000 °C beginning from BA20 and constitutes 1.5–5.45%.

According to [33,45], diopside is a mineral belonging to pyroxenes. With an increase in BA content in the samples, the diopside content also is enlarged from 0.67% to 3.23% at firing 900 °C and from 0.76% to 5.67% at 1000 °C. Diopside actively interacts with clay. An increase in diopside in the clay raw material intensifies the sintering process. It promotes the formation of an iron oxide melt, which acts as a flux and participates in the sintering of the material. According to [45], when diopside is presented into the clay mass, it improves the compressive strength and reduces the water absorption of the samples. In our case, this does not happen since, to fulfil such a condition, the content of the diopside must be more than 6%.

The structure of porous materials is usually formed in crystallization or subsequent treatment stages and consists of isolated or interconnected pores that may have similar or different shapes and sizes. Porous materials are characterized by pore sizes derived from gas sorption data [46]. According to IUPAC classification, pore sizes of clay brick samples fired at 900 °C and 1000 °C belong to the II type of isotherms (nonporous or macroporous). According to IUPAC [21], materials of fired clay bricks samples belong to the H3 hysteresis loop and are characterized by slit-shaped pores. The desorption curve of H3 hysteresis contains a slope associated with a force on the hysteresis loop due to the tensile strength effect [47]. Pore size distribution studies obtained from nitrogen adsorption

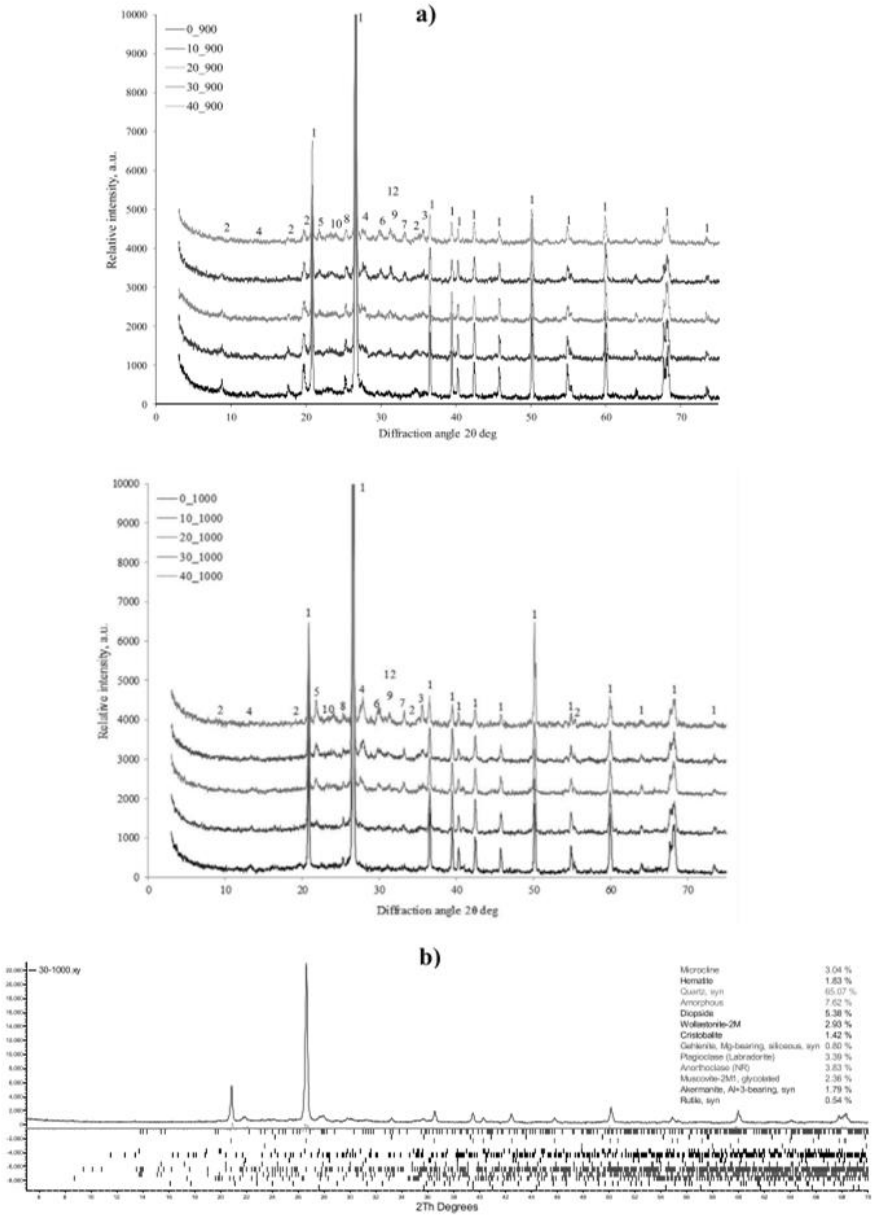

Fig. 13. XRD Analysis by Rietveld refinement of clay bricks: a — X-ray diffraction pattern of clay bricks fired by 900 and 1000 °C (1 – quartz, 2 – muscovite, 3 – hematite, 4 – microcline, 5 – cristobalite, 6 – diopside, 7 – wollastonite, 8 – rutile, 9 – gehlenite, 10 – akermanite, 11 – labradorite, 12 – anorthoclase); b — powder diffraction pattern for clay bricks with BA30 and fired at 1000 °C.

Table 5
Results of XRD analysis by Rietveld refinement.

Parameters	Temperature of firing, 900 °C										Temperature of firing, 1000 °C									
	Amount additive, wt%																			
	0		10		20		30		40		0		10		20		30		40	
Phases	w, %	d-spac., Å	w, %	d-spac., Å	w, %	d-spac., Å	w, %	d-spac., Å	w, %	d-spac., Å	w, %	d-spac., Å	w, %	d-spac., Å	w, %	d-spac., Å	w, %	d-spac., Å	w, %	d-spac., Å
Amorphous	6.68	3.85	7.81	3.8	8.56	3.73	7.37	3.7	7.45	3.64	5.56	3.89	6.25	3.9	6.33	3.81	7.62	3.79	8.31	3.59
Quartz	76.48	4.26	74.2	4.25	69.74	4.25	64.68	4.25	60.22	4.26	86.71	4.26	82.04	4.25	76.19	4.25	65.07	4.25	58.9	4.26
		3.57		3.34		3.34		3.34		3.34		3.34		3.34		3.34		3.34		3.34
		3.27		2.45		2.45		2.45		2.46		2.46		2.45		2.45		2.45		2.46
Muscovite 2 M1	8.06	10.04	8.32	10.07	8.88	10.05	9.21	10.11	8.34	10.02	2.53	10.05	3.13	10.03	3.2	10.01	2.36	10.01	1.85	9.93
		4.49		4.48		4.99		5.02		5.00		5.02		4.45		4.44		4.44		4.96
		3.35		3.5		4.48		4.47		3.31		3.52		3.48		3.48		3.51		3.49
Illite	3.12	4.46	—	—	—	—	—	—	—	—	0.94	20.04	—	—	—	—	—	—	—	—
		3.34										4.50								
		2.56										3.35								
Anorthoclase	1.93	4.08	2.81	4.05	3.09	4.07	4.53	4.08	4.16	4.08	0.92	4.02	1.28	4.02	1.79	4.06	3.83	4.08	4.38	4.09
		3.80		3.52		3.50		3.23		3.78		3.75		3.76		3.21		3.24		3.74
		3.25		3.24		3.24		3.47		3.24		2.53		3.09		2.99		3.0		3.23
Microcline	1.26	4.26	2.34	4.21	2.83	4.23	5.21	4.19	6.83	4.21	1.32	3.88	2	3.96	2.06	3.97	3.04	3.99	3.62	4.00
		3.57		3.51		3.51		3.51		3.49		3.50		3.5		3.51		3.44		3.20
		3.27		3.30		3.31		3.30		2.88		3.23		3.21		3.18		3.18		3.09
Cristobalite	—	—	0.16	4.1	0.36	4.04	0.64	4.06	0.85	4.06	—	—	0.72	4.06	1.21	4.05	1.42	4.05	2.18	4.04
				3.19		2.89		3.15		3.13				3.12		2.95		3.14		2.8
				2.85		3.12		2.84		2.90				2.92		2.52		2.48		2.52
Titanium oxide	0.44	3.24	0.5	3.29	0.75	3.24	0.44	3.24	0.7	3.18	0.31	3.25	0.31	3.23	0.19	3.24	0.54	3.22	0.7	3.23
		2.49		2.46		2.48		2.48		2.50		2.49		2.48		2.48		2.51		2.49
		2.19		2.17		2.29		2.18		2.18		2.29		2.28		2.28		2.19		2.19
Diopside	0.67	2.94	1.68	3.2	1.7	3.24	3.23	3.29	3.03	2.98	0.76	3.04	0.95	3.02	2.89	3.21	5.38	3.23	5.67	2.95
		3.04		2.98		2.99		3.22		2.55		2.54		2.93		2.97		2.99		2.98
		2.50		2.92		2.94		2.97		2.92		2.94		2.88		2.81		2.90		2.53
Wollastonite 2 M	—	—	0.85	3.86	1.36	3.84	1.43	3.82	3.1	4.04	—	—	1.29	3.87	1.68	3.33	2.93	3.5	4.13	3.82
				3.46		3.5		3.5		3.31				3.49		2.95		3.07		3.32
				3.0		2.96		2.96		2.97				2.97		2.78		2.97		2.97
Hematite	0.15	3.68	0.49	3.67	0.93	3.67	0.94	3.68	2.04	3.68	0.36	3.68	0.89	3.67	1.26	3.67	1.83	3.68	1.94	3.34
		2.70		2.69		2.69		2.69		2.70		2.70		2.69		2.69		2.69		2.68
		2.52		2.51		2.51		2.51		2.51		2.51		2.51		2.51		2.51		2.51
Gehlenite	0.18	2.76	0.2	3.05	0.56	3.04	0.75	3.04	1.22	2.82	0.17	2.88	0.51	3.05	0.9	3.23	0.8	3.19	1.7	2.86
		3.0		2.81		2.83		2.83		2.47		3.06		2.83		2.81		2.97		3.08
		2.98		3.0		3.83		3.67		3.02		2.76		2.42		2.72		2.57		3.71
Akermanite	0.24	2.79	0.63	3.7	1.28	3.07	1.75	3.06	2.06	2.85	0.43	2.87	0.59	2.85	0.84	3.69	1.79	3.06	1.1	2.84
		2.99		3.07		3.7		3.7		3.07		3.09		3.07		3.06		2.85		3.06
		2.37		2.85		2.85		2.85		3.71		3.73		3.71		2.85		3.7		3.7
Labradorite		—								—	—	—	—		1.5	4.09	3.39	4.08	5.45	4.08
																3.23		3.77		3.77
																2.5		3.21		3.21

experiments for samples fired at 900 °C and 1000 °C show a different trend when BA from 10% to 40% is included in the clay and at two firing temperatures. The BET-based method was performed using nitrogen as the adsorbate at a 77.35 K. The relationship between pore diameter, and the surface area was determined by the DFT method is shown in Fig. 14.

Fig. 14 shows that in the reference samples fired at 900 °C and samples with the addition of BA10, BA20 and fired at 1000 °C, micropores predominate in the remaining mesopores. Surface area and adsorption were obtained from the adsorption isotherm and calculated using a BET-based method. In addition, the total pore volume and average pore diameter were estimated using the DFT method, and all these data can be seen in Table 6.

The table data shows that the surface area of clay samples and the total pore volume decrease when BA is added to the base material for both firing temperatures. In addition, the average pore diameter of the samples without BA and with BA10, BA20 and fired at 900 °C had the same value (3.385 nm). However, with an increase in the amount of BA (30% and 40%) and a firing of 900 °C, the average pore diameter of the samples increased sharply and amounted to 26.12 and 33.242 nm, respectively.

Nevertheless, the average pore diameter of samples fired at 1000 °C has a different dependence. The pore size of samples without the addition of BA is 36 nm. Adding BA to the clay demonstrates a decrease in the pore diameter value at the same size. A positive correlation was found between the specific surface area and pore volume for samples fired at 900 °C. A similar trend is observed for samples fired at 1000 °C.

The data of nitrogen porosimetry can be compared with the studied microstructure of the samples. Samples fired at 900 °C demonstrate two groups of porosity, 3 nm and 4.5 nm. The pores of the first group correlated to the porosity of BA0, BA10 and BA20 samples, and the second group to the porosity with BA30 and BA40 samples. In all samples fired at 900 °C, the group of pores had a bimodal distribution, where pores of smaller diameter referred to slotted pores of clay material, and pores of larger diameter referred to slotted and cylindrical pores, which are formed as a result of thermo-chemical transformations of BA and clay minerals. The formation of cylindrical pores and an increase in the pore diameter in samples BA30 and BA40 fired at 900 °C is explained by the rise in the percentage of BA. This is explained characterized by compaction of the structure of ceramic materials as a result of contact sintering of the spherical vitreous substance of particles of amorphous clay aggregates and other components of the clay mixture, as well as by the merging of small pores into larger ones and by thickening of the pore walls and partitions [48].

In the reference samples and samples with BA10 and BA20 and fired at 1000 °C, slit pores are formed. An increase in porosity is observed in samples BA30 and BA40. This temperature range is characterized by three pore sizes: 1.5 nm, 1.8 nm, and 2 nm. A pore size of 1.5 nm is typical for reference samples and BA10 and BA20 samples. The pore size of 1.8 nm refers to the BA30 samples, the predominance of pores with a diameter of 2 nm is characteristic of samples with the BA40. The shape of slit and cylindrical pores can explain this: the cylindrical pores are isolated and are typical of the material, which is used as an additive; the slit porosity of the samples is interconnected with clay. The BA contains minerals that enter into thermo-chemical transformations resulting in the release of gaseous components (CO_2, H_2) in crystalline water and, as a result, lead to the formation of pores.

4. Conclusions

The bottom ash, formed in incinerating MSW in the CPP, belongs to non-hazardous waste and can be used as an additive in clay bricks production. There are clays with a high CaO content (2.71%) in Lithuania, making it impossible to use additives with a high CaO content. In the presented experimental study, clay raw materials with a low CaO content (0.2%). It has been established that BA particles stabilise shrinkage during drying and reduce shrinkage during firing. The shrinkage is within the acceptable range. The burnout of the small residual amount of organic substances in the clay, the decomposition of calcium carbonate, and the release of gaseous substances and crystalline water during firing lead to a change in the microstructure of clay samples. The result of these transformations is the formation of open porosity and a change in the shape of the pores, leading to a change in the samples' physical

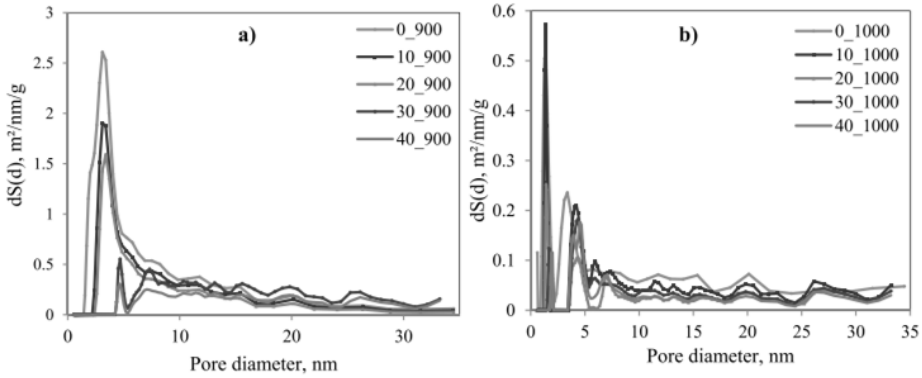

Fig. 14. Pore size distribution from nitrogen adsorption test: a — fired samples at 900 °C; b — fired samples at 1000 °C.

Table 6
N_2 adsorption measurements for clay samples at different firing temperature and amount of BA (DFT method).

Parameters	Temperature firing 900 °C					Temperature firing 1000 °C				
	Amount BA, %									
	0	10	20	30	40	0	10	20	30	40
Specific surface area, m^2/g	11.444	7.923	6.311	6.478	4.513	1.992	1.592	1.122	1.123	0.930
Total pore volume, cc/g	0.051	0.038	0.030	0.027	0.019	0.017	0.006	0.004	0.004	0.003
Pore diameter, nm	3.385	3.385	3.385	26.12	33.24	36.00	33.24	33.24	33.24	33.24

and mechanical properties, frost resistance, and mineralogical composition.

The infrared spectra of clay, BA and clay brick samples fired at 900 and 1000 °C showed the presence of hydroxyl groups (OH) in clay, a small amount of adsorbed water in clay and BA, the C-O bond, which corroborated the presence of $CaCO_3$ in BA and Si-O, Si-O-Mg, Si-O-Al and Al-OH-Al bond for clay, BA and clay brick samples. These results are consistent with the XRD analysis.

Clay bricks containing 10–20% BA and fired at 900 °C had density of 1.93 and 1.92 g/cm^3, shrinkage of approximately 5.9% and 5.5%, the compressive strength of 22.6 and 17 MPa, water absorption of 14% and 14.2%, open porosity is 27.3% and 28.4%, and frost resistance 23 cycles. Frost resistance was determined by repeated freezing and thawing. The clay bricks fired at 1000 °C and containing 10–30% BA had a density approximately of 1.92–1.99 g/cm^3; shrinkage of 6.6–5.8%, compressive strength of 14.5–22.6 MPa, water absorption of 11.7–13.1%, the total open porosity of 25–26%, and frost resistance 25 cycles.

The samples fired at 900 °C and containing 10–20% BA predominated slit pores with a size of 3.3 nm. The clay body samples containing 10–20% BA and fired at 1000 °C had slit pores with a pore diameter of 1.5 nm, but clay brick samples containing 30% BA and fired at the same temperature predominated slit cylindrical pores with a pore diameter of 1.8 nm.

According to LST EN 772–22:2019, clay bricks containing up to 10–20% of BA and fired at 900 and 1000 °C can be utilized in moderately aggressive environments (F1 class). However, specimens containing 30% BA and fired at 1000 °C can be used in passively aggressive environments. Samples can be used for internal use; if used externally bricks are liable to be damaged by frost action if not protected by impermeable cladding or render (F0 class).

According to the results of the thermal conductivity analysis, it was found that the thermal conductivity values directly depend on the porosity of the samples. The values of the measured thermal conductivity for the samples were in the range from 0.49 W to 1.1 W/m·K. In accordance with ASTM D 78896, it can be argued that the addition of bottom ash during clay brick production does not impair the technical properties of the fired samples.

The results of this study point to the possibility of the development of fired clay bricks using up to 30% replacement of clay with bottom ash. However, such a brick depends on its characteristics, particularly the class of frost resistance. In addition, bottom ash used as an additive will reduce the amount of accumulated waste.

Declaration of Competing Interest

The authors declare that they have no known competing financial interests or personal relationships that could have appeared to influence the work reported in this paper.

Acknowledgements

We acknowledge Marius Praspaliauskas, Senior research associate, Laboratory of Heat-Equipment Research and Testing, Lithuanian Energetic Institute (LEI) to help in preparing materials for the experiment.

We would like to say our great gratitude to the staff of the Centre for Hydrogen Energy Technologies, LEI to help with research.

We acknowledge the staff of the Kaunas cogeneration power plant for helping in providing material for research and informational support.

References

[1] M.H. Abdullah, A.S. A. Rashid, U.H. M. Anuar, A. Marto, R. Abuelgasim. Bottom ash utilization: A review on engineering applications and environmental aspects. IOP Conf. Ser.: Mater. Sci. Eng. 527 (2019) 012006, (https://doi:10.1088/1757–899X/527/1/012006).

[2] D. Blasenbauer, F. Huber, J. Lederer, M.J. Quina, D. Blanc-Biscarat, A. Bogush, E. Bontempi, J. Blondeau, J.M. Chimenos, H. Dahlbo, Legal situation and current practice of waste incineration bottom ash utilization in Europe (https://doi), Waste Manag 102 (2020) 868–883, https://doi.org/10.1016/j.wasman.2019.11.031.

[3] Vilnius cogeneration power plant (https://vkj.lt/en/about-us/eu-funding/147).

[4] Kaunas cogeneration power plant (https://kkj.lt/en/about-us/power-plant/93).

[5] Klaipeda cogeneration power plant (https://gren.com/lt/).

[6] B.H. Cho, B.H. Nam, J. An, H. Youn, Municipal solid waste incineration (MSWI) ashes as construction materials-A review (https://doi), Materials 13 (14) (2020) 3143, https://doi.org/10.3390/ma13143143.

[7] R. Taurino, E. Karamanova, L. Barbieri, S. Atanasova-Vladimirova, F. Andreola, A. Karamanov, New fired bricks based on municipal solid waste incinerator bottom ash (https://doi), Waste Manag. Res. (2017) 1–9, https://doi.org/10.1177/0734242×17721343.

[8] A.M. Saleh, M.N. Rahmat, Potential use of municipal solid waste ash (MSWA) as sustainable construction bricks (https://doi), Mater. Sci. Eng. 620 (2019), 012073, https://doi.org/10.1088/1757-899X/620/1/012073.

[9] F.A.M. Lino, K.A.R. Ismail, Recycling and thermal treatment of MSW in a developing country, IOSR J. Eng. 7 (7) (2017) 30–38.

[10] A. Maldonado-Alameda, J. Giro-Paloma, A. Alfocea-Roig, J. Formosa, J. Maria Chimenos, Municipal solid waste incineration bottom ash as sole precursor in the alkali-activated binder formulation (https://doi), Appl. Sci. 10 (2020) 4129, https://doi.org/10.3390/app10124129.
[11] D. Fernández-González, I. Ruiz-Bustinza, J. Mochón, C. González-Gasca, L.F. Verdeja, Iron ore sintering: process, Miner. Process. Extr. Metall. Rev. 38 (2017) 215–227, https://doi.org/10.1080/08827508.2017.1288115.
[12] Y. Xiao, M. Yunusa, D. Jelagin, H. Tan, B. Strnadel, Special Issue on Silicate Solid Waste Recycling, in: Materials, 14, Basel, 2021, p. 3776, https://doi.org/10.3390/ma14143776.
[13] X. Dou, F. Ren, M. Quan Nguyen, A. Ahamed, K. Yin, W. Ping Chan, V. Wei-Chung Chang, Review of MSWI bottom ash utilization from perspectives of collective characterization, treatment and existing application, Renew. Sustain. Energy Rev. 79 (2017) 24–38, https://doi.org/10.1016/j.rser.2017.05.044.
[14] B. Hooi Cho, B. Hyun Nam, J. An, H. Youn, Municipal solid waste incineration (MSWI) ashes as construction materials-A review (https://doi), Materials 13 (2020) 3143, https://doi.org/10.3390/ma13143143.
[15] M. Van Praagh, M. Johansson, J. Fagerqvist, R. Grönholm, N. Hansson, H. Svensson, Recycling of MSWI-bottom ash in paved constructions in Sweden–A risk assessment, Waste Manag 79 (2018) 428–434, https://doi.org/10.1016/j.wasman.2018.07.025.
[16] L.A. Sormunen, P. Kolisoja, Construction of an interim storage field using recovered municipal solid waste incineration bottom ash: Field performance study, Waste Manag 64 (2017) 107–116. (https://urn.fi/URN:ISBN:978-952-15-4019-6).
[17] (https://www.vesco.com.ua/media/brochure-ru.pdf).
[18] L.F. Dutra, M.E. Freitas, A.-C. Grillet, N. Mendes, M. Woloszyn, Microstructural characterization of porous clay-based ceramic composites (https://doi), Materials 12 (2019) 946, https://doi.org/10.3390/ma12060946.
[19] U. Kuila, M. Prasad, Specific surface area and pore-size distribution in clays and shales. European Association of Geoscientists & Engineers, Geophys. Prospect. 61 (2013) 341–362, https://doi.org/10.1111/1365-2478.12028.
[20] A.I. Gusev. Nanomaterials, nanostructures, nanotechnologies. Moskow: Fizmatlit (2005) 416.
[21] M. Thommes, Physical adsorption characterization of nanoporous materials, Chem. Ing. Tech. 82 (2010) 1059–1073, https://doi.org/10.1002/cite.201000064.
[22] N.N. Greenwood, A. Earnshaw (1997) Chemistry of the Elements, second edition. School of chemistry, University of Leeds, U.K. 357 p.
[23] (https://portalkeramiki.ru/index.php/eshop/materials/chemisrtry/59/s-4530-detail).
[24] 2014/955/EU: Commission Decision of 18 December 2014 amending Decision 2000/532/EC on the list of waste pursuant to Directive 2008/98/EC of the European Parliament and of the Council Text with EEA relevance.
[25] J.C.T. Rezende1, V.H.S. Ramos, H.A. Oliveira, R.M.P.B. Oliveira, E. Jesus, Removal of Cr(VI) from aqueous solutions using clay from calumbi geological formation, N. Sra. Socorro, SE State, Brazil, Mater. Sci. Forum 912 (2018) 1–6, https://doi.org/10.4028/www.scientific.net/MSF.912.1.
[26] M.S. Conconi, M. Morosi, J. Maggi, P.E. Zalba, F. Cravero, N.M. Rendtorff, Thermal behavior (TG-DTA-TMA), sintering and properties of a kaolinitic clay from Buenos Aires Province, Argentina, Cerâmica 65 (2019) 227–235, https://doi.org/10.1590/0366-69132019653742621.
[27] H.B. Hadjltaiefa, S.B. Ameurb, P.D. Costac, M.B. Zinaa, M.E. Galvez, Photocatalytic decolorization of cationic and anionic dyes over ZnO nanoparticle immobilized on natural Tunisian clay, Appl. Clay Sci. (2017), https://doi.org/10.1016/j.clay.2017.11.008.
[28] I. Aliu, Comparative analysis of the compressive strengths of clay and sandcrete blocks for low cost housing, J. Eng. Archit. 4 (2) (2021) 19.
[29] (https://www.gobrick.com/docs/default-source/read-research-documents/technicalnotes/9a-specifications-for-and-classification-of-brick.pdf/).
[30] M. Sutcu, E. Erdogmus, O. Gencel, A. Gholampour, E. Atan, T. Ozbakkaloglu, Recycling of bottom ash and fly ash wastes in eco-friendly clay brick production, J. Clean. Prod. 233 (2019) 753–764, https://doi.org/10.1016/j.jclepro.2019.06.017.
[31] O. Kizinievič, V. Voišnienė, V. Kizinievič, I. Pundienė, Impact of municipal solid waste incineration bottom ash on the properties and frost resistance of clay bricks, J. Mater. Cycles Waste Manag. 24 (2022) 237–249, https://doi.org/10.1007/s10163-021-01314-4.
[32] S. Louati, S. Baklouti, B. Samet, Geopolymers base don phosphoric acidand illito-kaolinitic clay, Adv. Mater. Sci. Eng. 7 (2016) 1–7, https://doi.org/10.1155/2016/2359759.
[33] J. Götze, Y. Pan, A. Müller, Mineralogy and mineral chemistry of quartz: a review, Mineral. Mag. 85 (5) (2021) 639–664, https://doi.org/10.1180/mgm.2021.72.
[34] N. Kumari, C. Mohan Basics of Clay Minerals and Their Characteristic Properties. (2021) 1–29, (https://doi:10.5772/intechopen.97672).
[35] Illite mineral data Available from (http://webmineral.com/data/Illite.shtml)#.XyAKkJ4zZPY, (Acces.: 2020-08-29).
[36] R. Schoonheydt, C.T. Johnston, F. Bergaya, Surface and interface chemistry of clay minerals 9 (2018) 1–410.
[37] J.-C. Boulliard, E. Gaillou, Twinning in anorthoclase megacrysts from phonolitic eruptions, Erebus volcano, Antarctica (https://doi), Eur. J. Mineral., Copernic. 31 (1) (2019) 99–110, https://doi.org/10.1127/ejm/2019/0031-2804.
[38] S.K. Haldar, J. Tišljar, Introduction to mineralogy and petrology, Chapter 2. Basic Mineral. (2014) 39–79, https://doi.org/10.1016/B978-0-12-408133-8.00002-X.
[39] Ma del Carmen Gutiérrez-Castorena, Interpretation of micromorphological features of soils and regoliths (secondedition), Chapter 6 – Pedogenic Siliceous Features (2018) 127–155, https://doi.org/10.1016/B978-0-444-63522-8.00006-1.
[40] Wollastonite mineral data available from (https://www.ima-na.org/page/what_is_wollastonite).
[41] Y. Lu, Y. Wang, Y. Zhao, Z. Wei, Y. Li, W. Hao, Y. Zhang, The characteristics of mineralogy, morphology and sintering during co-combustion of Zhundong coal and oil shale, RSC Adv. 7 (2017) 51036–51045, https://doi.org/10.1039/C7RA10340A.
[42] J. Kotowski, K. Nejbert, D. Olszewska-Nejbert, Rutile mineral chemistry and Zr-in-rutile thermometry in provenance study of Albian (Uppermost Lower Cretaceous) terrigenous quartz sands and sandstones in southern extra-carpathian Poland, Miner 11 (2021) 553, https://doi.org/10.3390/min11060553.
[43] M. Muhammad, A. Fatmaliana, Z. Jalil. Study of hematite mineral (Fe2O3) extracted from natural iron ore prepared by co-precipitation method, IOP Conference Series: Earth and Environmental Science (2019) 348 012135.
[44] Labrodarite mineral data available from (https://www.mindat.org/min-2308.html).
[45] Diopside mineral data available from (https://www.mindat.org/min-1294.html).
[46] T. Safonova, Y. Zykova, Malacolite- an efficient admixture in brick production, Bull. Irkutsk State Tech. Univ. 3 (39) (2009) 174–180.
[47] A. Alothman, Z.A Review: Fundamental aspects of silicate mesoporous materials, Materials 5 (12) (2012) 2874–2902, https://doi.org/10.3390/ma5122874.
[48] N. Grubeša, M. Vračević, J. Ranogajec, V. Vučetić, Influence of pore-size distribution on the resistance of clay brick to freeze-thaw cycles, Materials 13 (10) (2020) 2364, https://doi.org/10.3390/ma13102364.

Construction and Building Materials 326 (2022) 126902

Contents lists available at ScienceDirect

Construction and Building Materials

journal homepage: www.elsevier.com/locate/conbuildmat

Cement substitution by sludge-biomass gasification residue: Synergy with silica fume

Regina Kalpokaitė-Dičkuvienė *, Inna Pitak, Arūnas Baltušnikas, Stasė Irena Lukošiūtė, Gintaras Denafas, Jūratė Čėsnienė

Laboratory of Materials Research and Testing, Lithuanian Energy Institute (LEI), Breslaujos 3, LT-44403 Kaunas, Lithuania

ARTICLE INFO

Keywords:
Silica fume
Gasification residue
Cement
Pore size
Hydration
Microstructure

ABSTRACT

The increasing volumes of sewage sludge and other wastes of biological origin force the use of downdraft gasifiers for waste utilization; however, thermal processes produce residues that need to be treated in an environmentally acceptable way. The object of the study is to evaluate the possible application of residue, derived from industrial sewage sludge-biomass gasification plants, with silica fume as a partial binder substitute in cement-based materials. At total cement replacement levels of 10 and 12%, the dosages of gasification residue and silica fume varied in the range of 2–6% and 6–10% by cement mass, respectively. The impact of synergy between silica fume and gasification residue on the hydration and microstructure development of cement paste was analysed using SEM-EDS, XRD, TGA and N_2 sorption methods. The synergy of wastes was found to change the morphology and assemblage of hydration products and to accelerate the consumption of portlandite. N_2 physisorption revealed that the synergy of both substitutes had a significant impact on the distribution of pores in the mesoporosity range up to 30 nm, representing small microcapillary pores. The synergistic impact of the substitutes on selected properties of cement mortars was determined after 7, 28 and 56 days. Compared with the reference, all blended mortars showed 5–40% higher mechanical strength and 25–50% lower water ingress during the entire hydration period. The compressive strength increased with the reduction in the residue-to-silica fume (R/SF) ratio, while the flexural strength and sorptivity were less dependent on the ratio. The results revealed that the total cement substitution level may be increased up to 12%, within 4–6% covered by gasification residue, without losing the mechanical strength and consequently, to reduce the resources of Portland cement and silica fume.

1. Introduction

In the last few decades, global concern over the growing amount of sewage sludge (SS) generation has risen [1]. As a consequence, SS recycling or utilization issues have recently been a focus of much research [2]. According to [3], the rise of limitations of SS disposal in landfills forced researchers to focus on developing appropriate methods for the thermal processing of sludge. Thermal treatment of SS performed by mono-incineration or co-incineration with other fuels, such as coal or municipal solid wastes, has been intensively investigated due to its several advantages, such as a significant reduction in volume, minimization of odours and production of heat [2]. Therefore, most European countries still consider it to be a reasonable method for SS utilization research [2].

On the other hand, alternative thermal processes such as pyrolysis, gasification or wet oxidation have become attractive due to the generation or extraction of valuable liquid or gaseous products from SS that can be further reused [3–8]. The gasification process comprises the conversion of a solid/liquid organic compound in gaseous (syngas) and solid (char, tar) phases [6]. Most commercial gasifiers are designed for biomass gasification; however, the growing amount of SS or other wastes of biological origin forces the use of downdraft gasifiers for waste utilization, especially in countries that do not have available fossil fuel resources [8].

From an environmental sustainability point of view, the gasification process is preferable to pyrolysis or incineration [9]. Moreover, for biomass treatment with other wastes, the application of the thermal plasma gasification process favours the minimization of toxic compound release [8]. J. Dong et al. [9] calculated that gasification more than pyrolysis contributes to the substantial reduction of acid gas formation.

* Corresponding author.
E-mail address: Regina.Kalpokaite-Dickuviene@lei.lt (R. Kalpokaitė-Dičkuvienė).

https://doi.org/10.1016/j.conbuildmat.2022.126902
Received 16 November 2021; Received in revised form 15 February 2022; Accepted 16 February 2022
Available online 24 February 2022

Meanwhile, co-pyrolysis of SS with biochar has a lower impact on global warming potential and freshwater ecotoxicity [10]. For example, researchers [10] calculated that incineration of SS with gaseous product generation reduces carbon emissions nearly three times compared with incineration without energy recovery. S. Singh et al. [11] pointed out that the overall production of sewage sludge biochar generates up to 24% lower CO_2 emissions than that required for the production of activated charcoal. Despite the lower greenhouse gas emissions, the outputs of the aforementioned thermal processes are ash or charros residues, the amount of which represents nearly 12–18% [9]. Consequently, these residues (or thermal process wastes) also require an environmentally acceptable treatment, allowing them to become more sustainable.

A prevalent path for industrial waste or byproduct recycling is their use in the construction industry. Similarly, replacing cement or aggregates with byproducts is the most popular strategy for concrete production sustainability to decrease the environmental impact and the resources of binder and aggregates [12]. Some industrial wastes, such as coal combustion fly ash, blast furnace slag, silica fume, rice husk ash or zeolites, possess pozzolanic activity, which is related to the ability of the material to react in the presence of water with hydration products of cement and thus can strengthen cementitious material [13,14]. Consequently, these byproducts have found their potential application as supplementary cementitious materials [12,15–20], allowing a reduction in cement demand whose production is also responsible for greenhouse gas emissions.

On the other hand, SS ash or char residue does not typically possess strong pozzolanic properties, and therefore, their application in building materials mostly carries filler characteristics [20–23]. The fineness and mineralogical composition of ash or char vary based on the operational conditions of the thermal process systems and supplementary processing treatments. As a result, the properties of cementitious materials mixed with residual waste (ash or char) can range from moderate to valuably low, depending on the amount of residues added. Typically, after thermal treatment processes, such as pyrolysis or incineration, particles of residual ash are highly porous. Their incorporation worsens the properties of cement-based materials, although ball milling of residual ash helps overcome that reduction [24–31].

According to the existing literature, the application of SS ash or biochar for cement or aggregate replacement decreases the durability of mortars even after prolonged hydration time; however, a relatively small content of residue (2–5%) can result in a mechanical strength similar to that of the control material [12,24,32]. Consequently, to increase the performance of blended cement-based materials, pozzolanic materials are used in combination with residual ash. For example, better performance was achieved from blending residual ash or biochar with metakaolin, quartz powder, silica fume, rice husk ash, fly ash or blast furnace slag [17,19,25,27,28,33–35].

Despite the variety of pozzolans, the impact of silica fume on the hydration of plain or blended cement-based materials has attracted more attention, as its reactivity strongly depends on its fineness, application level and hydration duration [36–40]. Thermodynamic calculations [36] have shown that the blending of cement with more than 15 % silica fume reduces both the pH of the pore solution and the total volume of hydrates, resulting in changes in the portlandite morphology and composition of CSH, especially after longer hydration times. According to data presented in [39], the finer particles of silica fume (35–80 μm) accelerate cement hydration and contribute to the mechanical strength increment. The substitution level may also influence the effectiveness of coarser or finer particles [36,38]. Silica fume possesses a strong pore size refinement effect, but the large amount tends to increase the autogenous and drying shrinkage of cement-based materials, so that the replacement level for mortars should not exceed 12% [41].

To our knowledge, few studies [25,27,40] have addressed the application of SS ash or biochar in combination with silica fume for cement substitution. However, in those studies, the employed residue was collected after pyrolysis or incineration at a temperature range of 500–850 °C in the laboratory, while the level of silica fume was strictly confined to either 10% or 25%. Despite incorporating silica fume, the improvement in functional properties was moderate or comparable with the control. On the other hand, the performance of blended composites was studied within 28 days of application. According to Skibsted and Snellings [13], the significant impact of silica fume on phase composition is more evident after long-term hydration. Nevertheless, a contradiction remains regarding the impact of SS ash and biochar on cement hydration.

A literature review showed that although the impact of SS ash or biochar on the properties of cement-based materials has been widely studied, the utilization of residue produced during co-gasification of SS with biomass has been studied to a lesser extent, whereas its synergistic effect with silica fume remains undiscussed. Therefore, the aim of this study is to investigate the potential application of solid residue remaining after gasification of SS with biomass, in binary compositions with silica fume to implement a valuable utilization of solid wastes. For this purpose, the contribution of each substitute to the hydration process within two month was determined by applying thermogravimetric analysis (TGA) and X-ray diffraction (XRD) for phase quantification; scanning electron microscopy (SEM) and nitrogen (N_2) physisorption methods for microstructure characterization. Experimental investigation of key properties of cement-based material blended with various dosages of gasification residue (2–6 % by mass of cement) and silica fume (6–10 % by mass of cement) involved mechanical strength and water sorptivity, and were accompanied by the estimation of the economic performance of binary substitutes.

2. Materials and methods

2.1. Materials

In this study, industrial materials such as commercial Portland cement type CEM II/A-LL 42.5 N with specific gravity 2.95 (Lithuania), silica fume of particle size 0.1–0.45 μm and specific gravity 2.00 ("RW-Füller", RW silicium GmbH) and sand of particle size 0–2 mm and specific gravity 2.52 (Sakret, Lithuania) were used for the cement blends formulations. The chemical composition of cement and silica fume, declared by suppliers, is summarized in Table 1.

Gasification residual waste (hereafter *Residue)* was collected by thermal treatment of pelleted woody biomass with sewage sludge in a downdraft gasifier coupled with a secondary thermal plasma reactor. The detailed technical parameters of the gasification process, which are not the focus of this research, are described and published elsewhere [8]. It should be noted that no additional chemical or thermal pretreatment was applied for the residue; however, to use it in cement compositions, the milling operation was performed in a laboratory ball-milling machine. The milling was continued until nearly no material remained on a sieve of mesh size No. 45, which was selected for the fineness inspection. The median particle size of the residue, determined by laser granulometry, was 7.95 μm. The particle size distributions of the materials are given in Fig. 1.

2.2. Experimental methods

2.2.1. Mechanical strength and water sorption

For mechanical strength determination, mortar cubes (20 × 20 × 20 mm) and prisms (20 × 20 × 100 mm) were prepared at a binder-to-sand ratio of 2.5 and a water-to-binder (w/b) ratio of 0.4. Binder is considered the sum of cement, silica fume (SF) and gasification residue (R). Various combinations of silica fume with gasification residue were used for cement substitution at replacement levels of 10 % and 12 % by weight of cement. The compositions of the studied mortars are presented in Table 2. The dry content of the superplasticizer Gaia (pH = 5, ρ = 1.15 g /ml; Ulmen, Spain) was constant at 0.8 g for all mortar compositions.

Table 1
Chemical composition of raw materials.

Material	CaO	SiO_2	Al_2O_3	Fe_2O_3	MgO	SO_3	P_2O_5	K_2O	Na_2O	SiC
Cement	63.42	20.61	5.45	3.36	3.84	0.8	–	0.50	0.41	–
Silica Fume	0.25	96.0	0.20	0.05	0.25	–	–	0.50	0.08	0.60

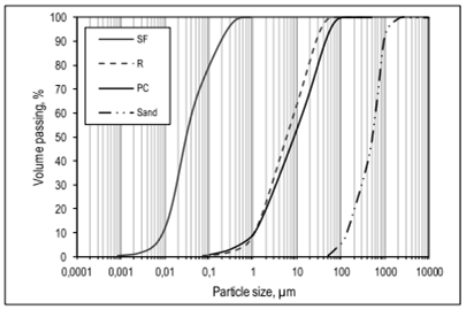

Fig. 1. Particle size distribution of silica fume (SF), gasification residue (R), Portland cement (PC) and sand.

For the preparation of each batch of samples, all components of the binder (cement, silica fume and gasification residue) were dry mixed until homogeneous before adding the required amount of water. The fresh mortar paste was cast into moulds and left for 24 h. Then, demoulded samples were cured at (21 ± 2) °C and a relative humidity of 95 % for a certain period. Eight cubic and three prismatic samples of each formulation were used for compressive and flexural strength determination, respectively. Tests were carried out on a universal test machine at a constant speed rate of 0.5 mm/min in accordance with the EN 196 standard [42]. After flexural strength testing, the broken prismatic samples were used in the capillary imbibition test under the procedure described in EN 1015–18 [43]. Monitoring of the mass change increment during the defined periods was performed to calculate the cumulative water content. From the plot of the absorption graph, a sorptivity coefficient was derived. The standard deviation in the average of three samples was less than 0.006 (mm^3/mm^2) Water absorption by total immersion was calculated with test method ASTM C642 [44] from the differences of mass values determined for samples oven-dried in air, after immersion in air, after immersion and boiling in air and water.

2.2.2. Hydration study

To investigate the impact of additives on the hydration process, four modular cement pastes without sand were prepared. Pure cement paste was denoted as pc; in two other pastes, denoted pSF and pR, cement was substituted at the 5 wt% level by silica fume (SF) or gasification residue (R), respectively. The final paste, denoted as pSFR contained up to 10 wt % cement replaced by two equal parts of silica fume and residue.

The morphology and elemental composition analysis (SEM-EDS) of both gasification residue and blended cement paste samples was performed on a ZEISS EVO MA10 microscope equipped with an energy dispersive spectrometer (EDS) at an accelerating voltage of 15 kV in secondary electron mode. At selected intervals, severed pieces of cementitious samples were soaked in isopropanol for several days and then vacuum-dried. Dry specimens were coated with gold to produce a conductive layer.

Thermogravimetric measurements (TGA) were performed on a LINSEIS STA PT1600 thermal analyzer by selecting N_2 atmosphere and a heating rate of 20 °C/min. The obtained TG data were used to calculate the amount of portlandite (*CH*) and chemically bound water (w_b) by the following equations:

$$CH = \frac{m_{410} - m_{490}}{m_{490}} \times \frac{74}{18} \times 100\% \quad (1)$$

$$w_b = \frac{m_{40} - m_{490}}{m_{490}} \times 100\% \quad (2)$$

where m_{40}, m_{410} and m_{490} represent the sample weights at 40 °C, 410 °C and 490 °C, respectively; the values represent the molecular masses of portlandite and water. *CH* and w_b were normalized to 100 g of anhydrous material for comparison purposes.

Crystalline phase analysis of hydrated cement pastes was carried out on a BRUKER D8 ADVANCE diffractometer with CuKα radiation at 40 kV and 30 mA. Data were collected in a 2Θ (3 °÷70 °) interval range at a scanning step of 0.02 °.

For TGA and XRD analysis methods, paste specimens were ground to powder and immersed in isopropanol for 20 min by subsequent drying in an oven at 40 °C for 15 min and then left in a vacuum until testing.

A nitrogen physisorption (N_2 physisorption) test was carried out on an Autosorb iQ analyzer from Quantachrome. For the test, each sample was crushed, while pieces of 1–1.5 mm in size were selected for the measurement. Three grams of each crushed specimen was immersed in isopropanol for three days with periodic solvent renewing each hour for the first day and once per day for the next two days. After exchange, the samples were vacuum-dried prior testing. The outgassing was performed for 2 h at 60 °C.

The quenched solid density functional theory (QSDFT) and Barett-Joyner-Halenda (BJH) models were used to obtain the pore size distribution based on N_2 gas sorption isotherms. According to the International Union of Pure and Applied Chemistry (IUPAC) [45,46], there are six types of isotherms and four types of hysteresis loops classified by their shape. The shape of the hysteresis loop correlates with the texture of mesoporous material, such as the pore size distribution, shape and connectivity [45]. Based on IUPAC, pores with internal widths between 2 and 50 nm are classified as mesopores, while pores larger than 50 nm

Table 2
Mix design for the cement - silica fume – gasification residue mortars.

Sample code	Cement,[% wt]	Silica Fume (SF),[% wt]	Gasification residue (R),[% wt]	Water/Binder ratio,[-]	Sand/Binder ratio[-]	Gasification residue/Silica Fume ratio, (R/SF)[-]	Silica Fume/Cement ratio (SF/C),[-]
Ref.	100	–	–	0.4	2.5	–	–
SF10	90	10	–	0.4	2.5	0	0.11
SF8R2	90	8	2	0.4	2.5	0.25	0.09
SF6R4	90	6	4	0.4	2.5	0.7	0.07
SF10R2	88	10	2	0.4	2.5	0.2	0.11
SF8R4	88	8	4	0.4	2.5	0.5	0.09
SF6R6	88	6	6	0.4	2.5	1	0.07

are macropores. The QSDFT and BJH methods are both applicable for mesoporous materials, yet BJH underestimates pores with diameters less than 15 nm [46]. Meanwhile, the QSDFT method considers pore wall heterogeneity and is capable of reliably characterizing mesopores in the range from 2 to 35 nm [46]. Combining both methods, wider spectra of pores can be analysed.

3. Results and discussion

3.1. Characterization of gasification residue

After the ball-milling procedure, the gasification residue powder was examined by SEM. From the image presented in Fig. 2 the morphology of milled gasification residue is seen. The surface of the particles is nearly smooth and without visible pores or holes, while the shape of the particles is nonregular, varying from plate-like to rectangular-like shape. The elemental composition obtained by SEM-EDS analysis is presented in Table 3. According to the data, the dominant element is carbon, while other non-hazardous elements, such as Ca, Fe, Si, P, Mg and Al, do not exceed the level of 3 wt%. Although Zn is on the list of environmentally harmful elements, based on waste acceptance criteria [47], its relatively small amount (less than 1 wt%) can be interpreted as inert.

The performed XRD analysis presented in Fig. 2 shows that the residue contains both crystalline calcium-bearing phases such as phosphates and carbonates, and amorphous non-crystalline phases. The presence of a non-crystalline phase is favourable since it may contain a soluble fraction able to participate in reactions with cement [48,49].

3.2. Impact of gasification residue and silica fume on the hydration of cement pastes

3.2.1. Thermogravimetric analysis

To investigate the impact of both substitutes on the hydration of cement, thermal analysis was performed, and representative thermogravimetric (TG) and differential thermogravimetric (DTG) curves are presented in Fig. 3. The plain and blended cement pastes after being hydrated for 28 days are compared in Fig. 3 a, whereas the impact of hydration time for cement paste with silica fume and gasification residue both (pSFR) is shown in Fig. 3 b.

As shown in Fig. 3 all curves contain three main temperature regions. According to [50–52], the dehydration of calcium silicate hydrate (CSH), ettringite (AF_t), calcium monosulfo-, hemicarboaluminate or calcium monocarboaluminate (all phases are denoted as AF_m) takes place up to 200 °C. Dehydroxylation of portlandite (CH) occurs at 400–500 °C, while decarbonation of calcium carbonates (CC) takes place at 700–800 °C. From DTG patterns, the AF_t and AF_m phases are hard to distinguish, as their decomposition temperatures are very narrow and overlay each other.

The comparison of the investigated systems shows that with respect to the reference paste, a large peak at approximately 110 °C, attributed to the decomposition of CSH, is the most intense for the pSFR paste (Fig. 3a), and a distinct peak at approximately 160 °C corresponds to the formation of AF_m compounds [26,49]. The third peak at approximately 450 °C, characterizing dehydration of CH, is much smaller for pastes with silica fume (pSF and pSFR samples). This is reasonable since silica fume is a highly reactive pozzolan that reacts with CH in the presence of water and forms CSH compounds [13]. In the temperature region from 710 °C to 780 °C the decomposition of calcium carbonate, mostly coming from the raw cement, together with various polymorphs or less crystalline forms of carbonates takes place [53]. In blended pastes, the small peaks above 720 °C may suggest the decomposition of compounds from waste or crystallization of silica fume (Fig. 3). In general, samples with cement substituted by residue are distinguished by the highest mass losses, while for the pc and pSF pastes, the TG curves are nearly the same shape. The hydration time increment has the most significant impact on mass losses resulting in a more intensive rise in the CSH (and AF_m) peak than CH and CC (Fg. 3 b).

For comparison purposes, based on TG data, the normalized amounts of bound water w_b and portlandite *CH* are presented in Fig. 4. It is considered that w_b indicates the volume of reaction products (including CSH, AF_t, AF_m and CH) formed during cement hydration, while normalized *CH* can be interpreted as an indication of changes in the assemblage of reaction products (CH consumption in the formation of additional CSH) [54]. The data in Fig. 4a show that the normalized w_b content continuously increases for all compositions over hydration time; however, the substitute containing pastes w_b are significantly higher than that for the reference paste. Moreover, during the first seven days, the bound water is the highest for the sample with both substitutes (pSFR), while after 14 days, a higher normalized w_b content gives paste with silica fume (pF). According to [13], the enhanced hydration at an early age is caused by the filler effect, while chemical reactions involving the dissolution-precipitation mechanism start later. The rise in w_b for the pSF paste is related to pozzolanic reactions when silica fume chemically reacts with calcium hydroxide and produces additional CSH phases. Due to CH consumption, the normalized *CH* value is 15 to 40 % lower than the reference paste (pc). These data correlate well with those reported in [39,55] where w_b and *CH* values for both pure and blended with silica fume pastes were estimated and measured.

With respect to the reference paste, a sample with cement substituted by the residue (pR) is characterized by more bound water and a lower *CH* content. M. Mejdi et al. [49] observed a similar tendency for samples with cement replaced by sewage sludge ash and explained that by the formation of different types of hydration products, in particular precipitation of ettringite and monocarbonate. Moreover, it seems that

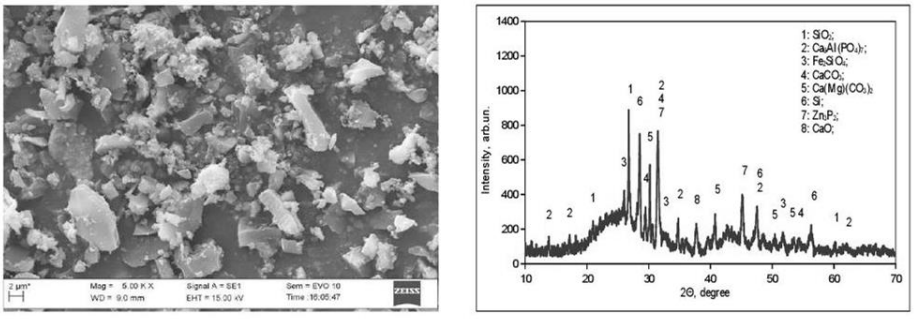

Fig. 2. SEM image (left) and X-ray diffraction pattern (right) of gasification residue after ball milling.

Table 3
Elemental composition of gasification residue based on SEM/EDS measurements.

Elements	C	O	Ca	Fe	Si	P	Zn	Mg	Al	S	Total
wt.%	72.22	20.75	2.83	1.64	0.95	0.64	0.46	0.27	0.23	0.12	100
at.%	80.19	17.30	0.94	0.39	0.45	0.27	0.16	0.15	0.12	0.05	100

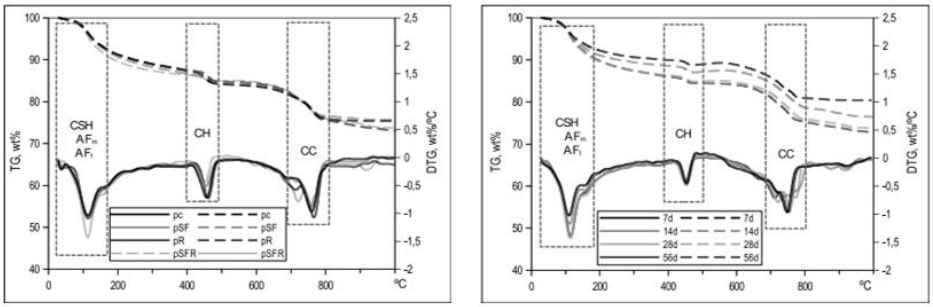

Fig. 3. TG and DTG curves for plain and blended cement pastes hydrated for 28 days (a) and for pSFR cement paste hydrated at various hydration periods (b).

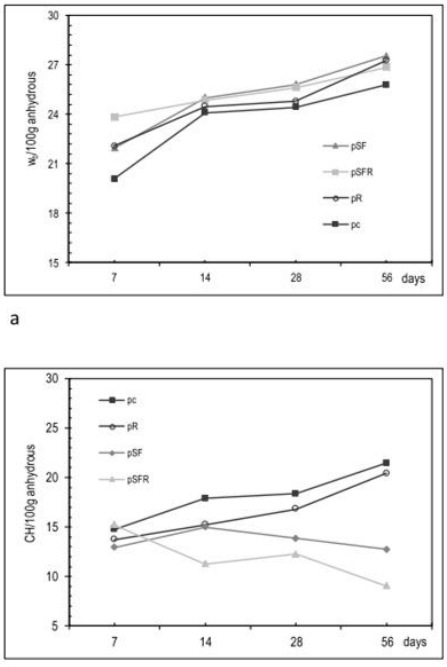

Fig. 4. Evolution of normalized to 100 g anhydrous amount of : a - bound water (w_b) b - portlandite (*CH*).

residue more likely promoted the hydration process through the "filler effect", according to which, the substitute provides additional space for the precipitation and growth of hydration products since the effective water-to-cement ratio changes [13].

It seems, on the other hand, that cement replacement by both substitutes (pSFR) enhanced the reactivity of cement paste and resulted in even faster CH consumption than in the pSF sample, even though the normalized w_b is nearly the same or lower (Fig. 4). These data are inconsistent with observations obtained by Gupta et al. [27], where a *CH* content increment was reported for samples with cement replaced by a mixture of commercial biochar (5 %) and silica fume (10 %). Based on observations presented in [39], the delay in CH consumption indicates a weak dispersion of silica fume in the matrix. On the other hand, it was pointed out in [13] that the reactivity of silica fume is mainly limited by water and pore space availability, whereas the latter is essential at later hydration ages when a higher degree of cement hydration reduces the activity of CH. According to our results (Fig. 4), after 28 days, the reduction of normalized *CH* for the pSFR paste proceeds even faster than that for the pSF sample, indicating that the filler effect of residue promoted the reactivity of silica fume.

3.2.2. Morphology analysis

SEM images of the fraction surfaces of reference and blended cement pastes after being hydrated for 56 days are shown in Fig. 5 with the elemental compositions of analysed crystals (Au was detected due to the coverage of samples with gold before analysis).

After two months of hydration (Fig. 5), as expected, in a paste with silica fume, portlandite crystals are small without well-defined edges due to its partial consumption by pozzolan. On the other hand, very massive CH crystals are still present in both the reference paste and the gasification residue paste (Fig. 5 a,c). On the contrary, needle-like hydrates of various thicknesses (AF_t) were mostly found in blends with residue, while they were less visible in the reference paste. The excessive formation of ettringite in cement compositions with sulfate-rich sewage sludge ash was also observed by C. Gu et al. [26]. It was assumed that AF_t formation was caused by a high content of sulfates (23 %) in ash. On the other hand, M. Mejdi et al. [49] pointed out that after 56 days in systems with sewage sludge ash, the precipitation of AF_t crystals takes

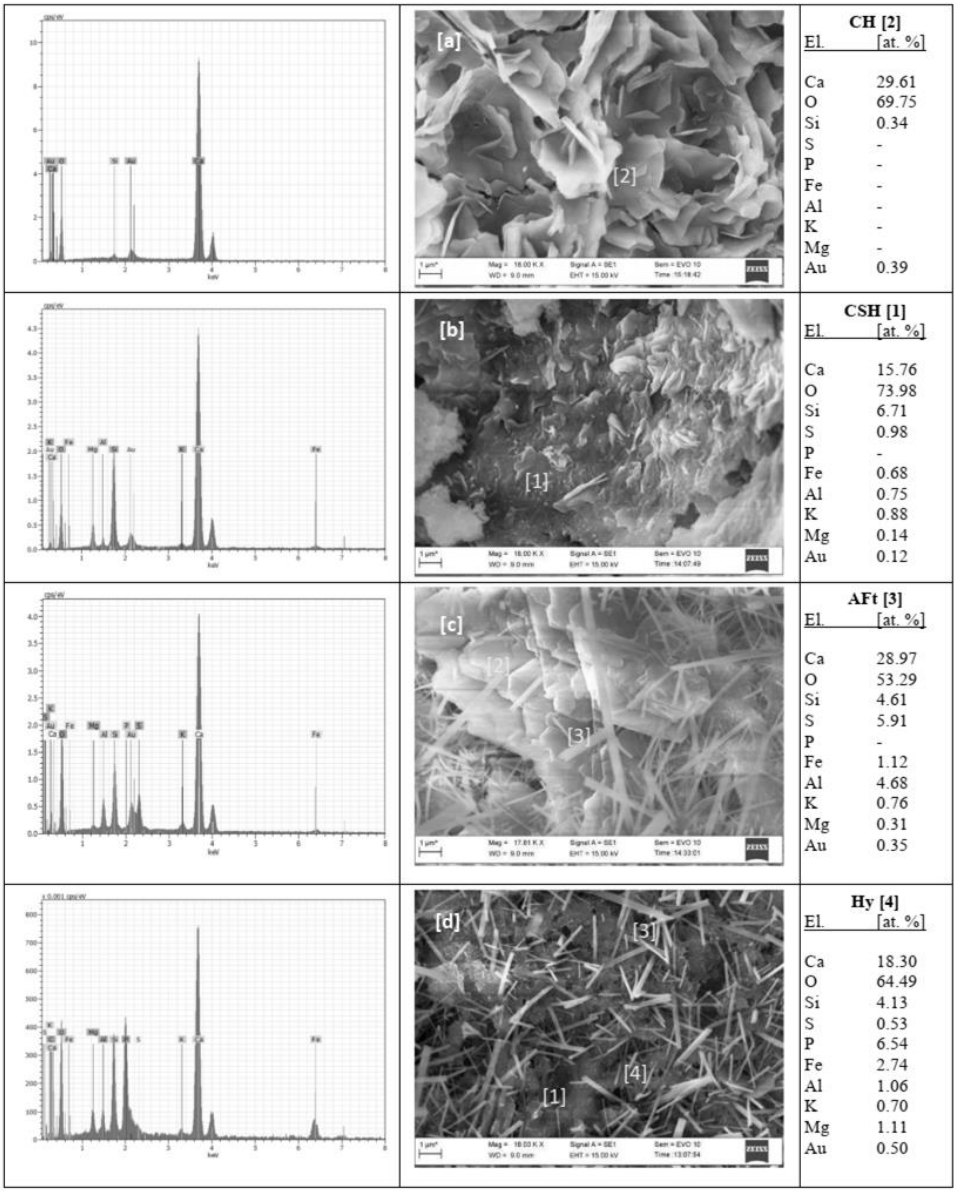

Fig. 5. Morphology of blended cement pastes hydrated for 56 days: a – pc; b – pSF; c - pR; d – pSFR.

place due to dissolution of the amorphous phase of ash, and thus, it may have a link with the enhancement of chemically bound water content. In our case, gasification residue did not contain a high amount of sulfates; however, with respect to the reference paste, a much higher normalized w_b (Fig. 4) obtained for pSFR composition suggests that the precipitation of ettringite crystals after such a long period is probable. On the other hand, a deeper examination of crystals revealed that some of needle-like hydrates contain a higher phosphorus content and thus, inferring the possible formation of calcium phosphate hydrates (Hy). According to [34,48], the formation of other calcium-bearing phosphate compounds

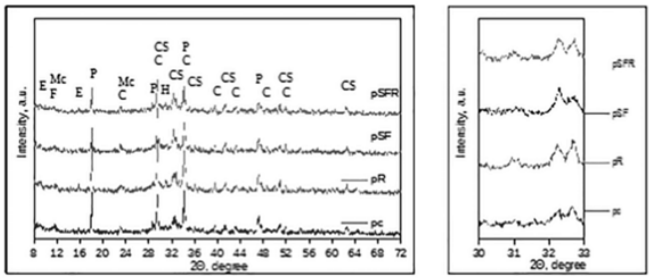

Fig. 6. XRD patterns for hydrated pastes: E – ettringite, F – ferrite, Mc – monocarboaluminate, P – portlandite, C – calcite, CS – alite/belite, H – hydroxyapatite.

arising from the incorporation of sewage sludge ash may even result in an increase in the compressive strength of blended compositions. The amorphous phase intermixed with needle-like hydrates was also detected in pSFR samples; however, even though the elemental compositions of that phase were similar to those of CSH gel (1), its visual shape and overall porosity differed from those observed in the pSF system (Fig. 5d).

3.2.3. X-ray diffraction analysis

Fig. 6 presents X-ray diffraction patterns of plain and blended cement pastes hydrated for 56 days. The main distinction among patterns is the intensity of CH (2Θ = 18°), which is much lower in pastes with silica fume and therefore, it is in good agreement with the thermal analysis results (Fig. 3). The small ettringite peak (2Θ = 9°) is less visible in the pSF paste, while most of the other peaks are identical. Although the peak intensity varies slightly among samples, there is one small broad peak at 31°2Θ, that is only characteristic to systems with gasification residue (the enlarged X-ray pattern Fig. 6).

The gasification residue used in this study contains an amorphous phase (2Θ = 20-30°) (Fig. 2), which, according to [48,49], due to the presence of phosphates, may become a reactive fraction inducing the formation of poorly crystalline hydroxyapatite ($Ca_5(PO_4)_3OH$) possessing reinforcing properties. H. Zhang et al. [56] showed that hydroxyapatite crystals possess various forms from fibrous to zigzag or needle-like shapes, while I. Neira et al. [57] demonstrated that both fibrous and plate-like particles of hydroxyapatite result in the enhanced mechanical strength of calcium phosphate cement.

Although SEM-EDS analysis showed the formation of needle-like crystals with a higher content of phosphorus, it is very difficult to justify or distinguish the formation of hydroxyapatite since its main peak is situated at 32°2Θ and thus, overlaps with the peaks of other cement products. According to findings presented in [58], hydroxyapatite might also be in a carbonated form, in which peaks are broader and shift to lower 2Θ angles up to one degree. Thus, due to the availability of calcite from cement, a small peak at 31°2Θ (Fig. 5), characteristic only for systems with gasification residue, could be assigned to the possibly carbonated form of hydroxyapatite, whose formation could take place only from the amorphous phase of gasification residue, as assumed in [49].

3.2.4. Nitrogen gas physisorption analysis

Nitrogen physisorption experiments are useful for the characterization of cement-based material microstructures, as by applying different models, the distribution of pores in the microporosity (less than 2 nm) and mesoporosity (2–50 nm) ranges [45] can be obtained. Due to the variety in definitions of pores available in literature, A.R. Santos et al. [59] summarized and classified the pore range below 10 nm as CSH gel pores, pores from 10 to 50 nm as medium capillaries or microcapillary, and pores up to 10 μm as large capillary pores. Gel pores are related to the hydration rate and pozzolanic reactions, while medium and large capillary pores affect the permeability and strength of the structure [59].

The impact of cement substitutes on the pore volume development during the hydration is shown in Fig. 7. The comparison shows that the volume of pores in the pSFR paste decreases rapidly up to 28 days and mainly in the pore range of more than 12 nm (Fig. 7a). This tendency compares well with the observations presented in [61,61]. A longer hydration time predominantly affects the pore region up to 20 nm, which, according to [62], is very sensitive to the formation and packing density of hydration products. Fig. 7b shows that the percentage of relative pore volume for blended compositions with silica fume is higher than that for the reference paste. Thus, it can be assumed that a

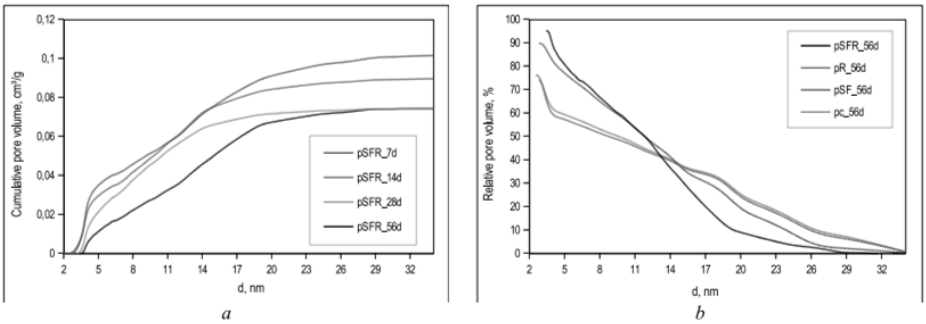

Fig. 7. Impact of hydration time and additives on distribution of pore volume: a - cumulative and b – relative to total.

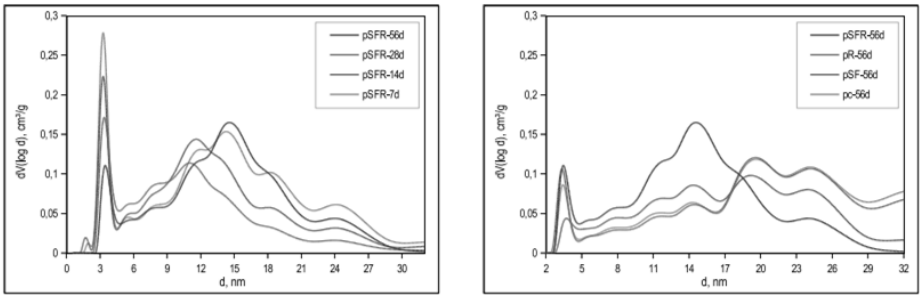

Fig. 8. Pore size distribution by QSDFT method. Impact of hydration time (a) and additives (b).

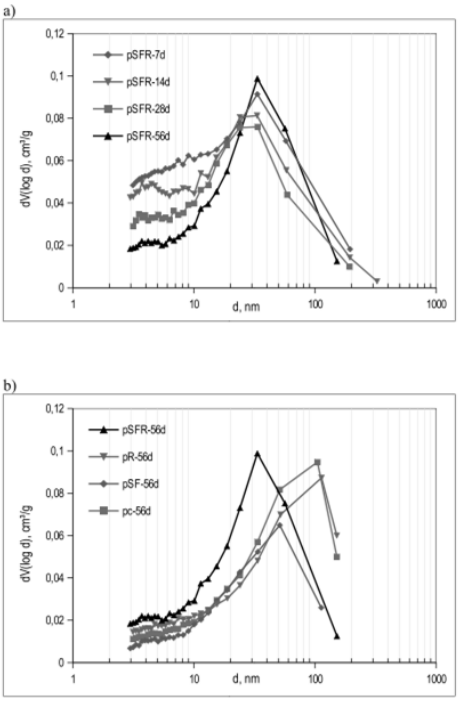

Fig. 9. Pore size distribution by BJH method. Impact of hydration time (a) and additives (b).

reduction of the pore volume indicates pore structure refinement that might occur due to the potential of pozzolan, or reactive phase assemblage, to fill the pore space by hydration products [13,60]. The highest consumption of portlandite in the pSFR system (Fig. 4b) with the excessive formation of needle-like hydrates at 56 days (Fig. 5) supports these assumptions.

To obtain the pore size distribution, two methods, QSDFT and BJH, were applied on the adsorption branch of the isotherms. The distribution of pores in the range up to 35 nm, characteristic to CSH gel and microcapillary pores, was obtained by the QSDFT method (Fig. 8), while the BJH method was useful for the distribution of larger capillary pores (Fig. 9).

In the range up to 10 nm, corresponding to the CSH gel region, the BJH method gives no distinctive peaks (Fig. 9a), whereas two narrow characteristic peaks, situated at approximately 2 nm and 3.5 nm, are distinguished with the QSDFT method (Fig. 8a). It was observed that the largest peak (3.5 nm) reduces with increasing hydration time, while the smaller peaks (2 nm) disappear after 14 days, thus indicating the filling of pore space by hydration products predominantly by CSH gel [60]. This reduction tendency, also seen in the BJH method, compares well with the distribution of critical pore entry, measured by the mercury intrusion method, proposed by E. Berodier and K. Skrivener [60] for the characterization of connected porosity. The pore width value (3.5 nm) obtained for the blended composition (Fig. 8a) is very close to the range of critical pore radii (2 – 8 nm) measured for the various cement compositions mentioned in [13,63].

In the mesoporosity range (10–50 nm), there is one distinct maximum peak obtained from the BJH method (Fig. 9a), while the QSDFT method (Fig. 8a) shows several non-well defined peaks, the magnitude of which varies significantly over time. After the shortest hydration time, four peaks are situated at nearly 12 nm, 14 nm, 18 nm and 25 nm (Fig. 8a). The volume of pores with the largest opening (18 and 25 nm) decreases with increasing hydration; meanwhile, two other peaks shift to a smaller size bordering the CSH gel region (2–10 nm). At 56 days, pore opening of 15 nm prevails in the pSFR system; suggesting significant changes in the connections of pores [60,64]. Moreover, in contrast to the pSFR composition, other formulations, hydrated for the same period, show a higher volume of pores at widths of 20–24 nm and 30–150 nm in the QSDFT and BJH methods, respectively (Fig. 8b, Fig. 9b).

The comparison of data obtained by both methods reveals that after 56 days of hydration, the pSF system contains the lowest volume of pores in the range from 2 nm to 100 nm (Fig. 8b, 9b). A significantly higher pore volume with increasing pore width shows the reference paste (pc) and sample with cement substituted by residue (pR). Among all samples, the pSFR paste generates the highest pore volume, but the peak maximum shifts to a smaller pore size and occurs at 15 nm and 34 nm, for the QSDFT and BJH methods, respectively (Fig. 9b). This implies that the pSFR paste contains more but refined and possibly water-filled capillary pores that are still available for the deposition of hydration products. The highest consumption of CH (Fig. 4) together with the formation of crystalline and amorphous hydration products (Fig. 5) infers that the incorporation of both substitutes promotes cement

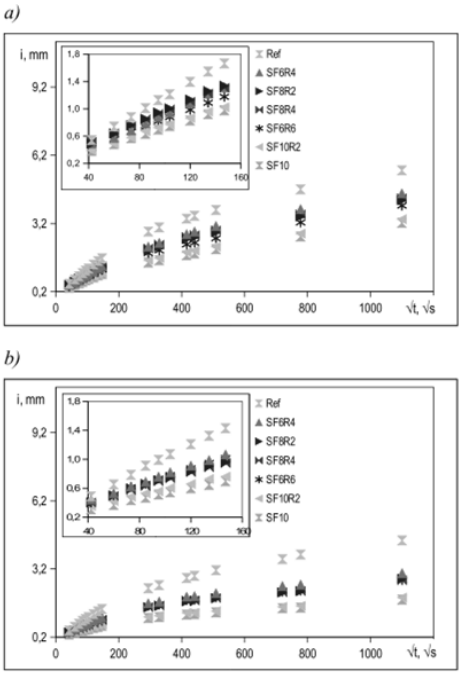

Fig. 10. Capillary absorption as a function of square root of time for mortar samples hydrated for 28 (a) and 56 (b) days.

hydration since, due to the dilution of the system by residue, the reactivity of silica fume increases as it may act both as filler and as pozzolan [13]. The formation of additional hydration products assists in the refinement of pores leading to the formation of a more compact structure [60,63,64].

3.3. Impact of gasification residue and silica fume on the properties of mortars

3.3.1. Resistance to water absorption

The water absorption rate by capillary suction reflects the water intake into medium capillary pores (10–50 nm) [55] and thus, capillary imbibition curves for cement mortars (Table 2) cured for 28 and 56 days are presented in Fig. 10.

For cement-based materials, water imbibition curves are generally divided into two linear parts defined by time. In the period of up to 6 h, strong capillary forces rule the water uptake, whereas; beyond one day, the diffusion phenomena take place [65]. From the enlarged view of the curves presented in Fig. 10, the imbibition by capillary forces takes a longer time, and therefore, the transition period starts approximately after 30 h (or 147 $s^{0.5}$). Although this transition period, visible as a decline from the linearity, indicates the conversion of the main driving forces [65], it can even last up to 7 days for the given cement formulations (Fig. 10). Moreover, the comparison of curves obtained after two hydration periods reveals that the rate of water intake slows (over 25 %) with increasing hydration age and mostly for compositions mixed with residue and silica fume. The highest water uptake is attributed to the reference sample, while the lowest ingress belongs to the SF10 mortar sample, whereas curves of other samples are distributed in between (Fig. 10). Although the deviation among samples with gasification residue is nearly slight, mortar SF10R2 is distinguished by the lowest moisture intake, which is almost identical to the SF10 sample. S. Gupta [27] reported a nearly similar tendency of reduced water imbibition for mortars containing 5 % biochar and 10 % SF, which was comparable to the control sample with cement replaced by 15 % of silica fume.

A correlation between sorption capacity and residue percentage is fairly well reflected in the sorptivity coefficient results presented in Fig. 11. The sorptivity coefficient decreases with increasing hydration age and a reduction in the R/SF ratio (higher silica fume content and lower residue content). Although the lowest sorptivity was observed for sample SF10 (R/SF = 0), compared with the reference sample, the sorptivity coefficients of all other samples with residue were 24–47 % and 33–57 % lower after 28 and 56 hydration days, respectively. Even though the sorptivity values are of the same magnitude, the impact of the cement substitution level is visible. According to Table 2, in mortar compositions, at the constant amount of silica fume, the replacement level of cement increases from 10 % to 12 % because of the residue content increment. Thus, by comparing data at either R/SF = 0.7 and 1.0 or 0.25 and 0.5, it is clear that a higher percentage of gasification residue (and higher total cement replacement level) leads to the reduction of sorptivity by almost 8 % (Fig. 11a). Nonetheless, an exception is in the SF10 and SF10R2 samples (R/SF = 0 and 0.2), where the sorptivity

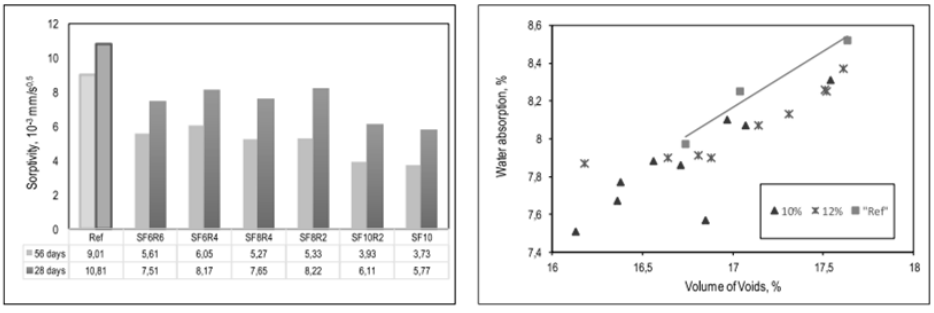

Fig. 11. Average values of sorptivity (a) and water absorption (b) for mortar samples.

increased up to 6 % due to the incorporation of residue (Fig. 11a).

An opposite situation shows water absorption by total immersion results even though the variation among data is marginal (Fig. 11b). As shown in Fig. 10, the water absorption of all blended samples is nevertheless lower than that of the reference paste. In contrast to sorptivity results, water absorption is lower for samples with a 10 % cement replacement level instead of 12 %. Moreover, the comparison of absolute values revealed that the lowest water absorption (7.77 % and 7.51 %, at 28 and 56 days, respectively) showed the SF6R4 sample while the SF10 composition reached similar values (7.57 %) only after the longest hydration period. This suggests that the substitution of cement by a mixture of silica fume with residue mostly affects the size and distribution of capillary pores, whose level of fineness, interconnection or tortuosity are mainly responsible for the sorptivity [65]. Nitrogen physisorption results support this assumption since pSFR cement paste showed a high pore volume $V_T = 78.06\ (mm^3/g)$, far lower than the reference paste ($V_T = 82.15\ mm^3/g$) and much higher than for paste with silica fume ($V_T = 60.15\ mm^3/g$). Despite its high porosity, it demonstrated the lowest pore opening among all tested samples (Fig. 9). This is consistent with the reduction of the primary water ingress rate for compositions blended with a residue (Fig. 10b), which also indicates a redistribution of moisture from the capillary towards more refined pores [61].

3.3.2. Compressive and flexural strength

The results presented in Fig. 12, show that blended compositions possessed a significantly higher mechanical strength than the reference sample over hydration time. The compressive strength tends to increase with decreasing R/SF ratios. For flexural strength, this tendency is less defined as the best performance was obtained at R/SF ratios of 0.2 and 1.0, corresponding to the highest and lowest SF/C contents. Fig. 12 also reveals that the rate of compressive strength development changes with time and varies among samples. For example, for the reference composition, the compressive strength increases up to 12 % and to more than 20 % after one and two months, respectively. Blended mortars give a significant strength increment of 30 %-47 % during the first month, while over this period, the strength development slows up to 9–19 % (Fig. 12).

Fig. 13 shows the mechanical strength increment or reduction relative to the reference paste. For compositions with R/SF greater than 0.2 the increment in compressive strength is nearly 7–14 %, 26–44 % and 22–32 % at 7, 28 and 56 days, respectively (Fig. 13). The exception is the sample without a residue (R/SF = 0) whose strength rate increases nearly uniformly both with time (Fig. 12) and relative to the reference paste (Fig. 13). This is consistent with results obtained in [71]. Nonetheless, compared with compositions containing the residue, the SF10 mortar shows a moderate strength (Fig. 12, Fig. 13).

The data presented in Fig. 12 and Fig. 13, reveal that among all samples, compositions at R/SF ratios of 0.2, 0.25 and 0.5 showed the highest compressive strength values. Nevertheless, the strongest was the SF10R2 sample (R/SF = 0.2), which also gave a high resistance to flexure comparable to those at R/SF greater than 0.7, especially after longer hydration (Fig. 13). Although the incorporation of a higher content of residue (R/SF $\geq$ 0.7) gives a reduction in compressive strength of as little as 5 % (Fig. 12), these compositions distinguish lower water absorption with a moderate sorptivity (Fig. 11). This result infers that in combination with gasification residue, the level of silica fume could be reduced from 10 to 6 % without a significant loss in functional properties.

3.4. Discussion

J. Skibsted and R. Snallings [13] noted that early cement hydration largely depends on the interparticle distance rather than on the dissolution rate of silica fume particles. Although the connectivity of the solid-to-solid phase increases with the addition of silica fume [Meng-38], higher contents of silica fume (more than 20 %) tend to agglomerate, which obstructs the pozzolanic activity of silica fume. Due to the reduced reactivity of pozzolan, the dilution effect becomes a dominant and influences the porosity of the structure [38]. On the other hand, due to cement substitution by silica fume, the morphology of CH changes from massive crystals to platelet shapes [66].

In the composition involving cement replaced by only silica fume (pSF), a delay of pozzolanic reaction up to 14 days (Fig. 4) together with the formation of much smaller CH crystals, without well-defined edges, was observed in this study (Fig. 5). This is in line with the results presented in [38,66], where CH consumption by silica fume (10 %) starts over seven days. In cement formulation with both substitutes (pSFR), the significant increment in the volume of hydration products with changes in their assemblage occurred much earlier - after seven days (Fig. 4). Evidence of significant changes in the morphology of hydration products was observed in SEM-EDS spectra (Fig. 5). Consequently, it could be inferred that the synergy of silica fume and residue may have increased the number of reactions, such as cement hydration, pozzolanic reactivity of silica fume or partial dissolution of amorphous phases of residue. All these reactions impacted the assemblage and microstructure of hydration products.

Fig. 14 shows the evolution of bound water consumed for CSH and ettringite formation (weight loss up to decomposition of CH (Fig. 3) versus the degree of hydration. It is apparent that the hydration degree

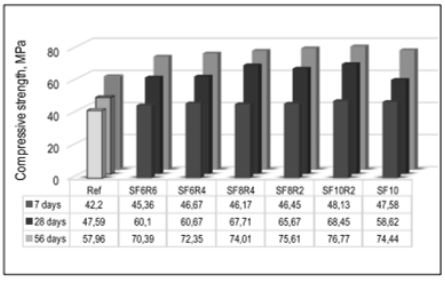

a

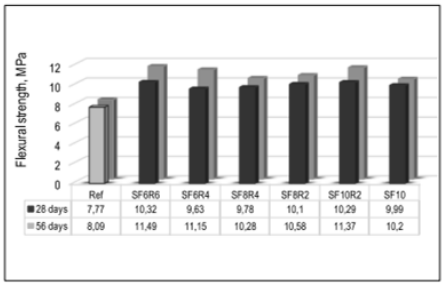

b

Fig. 12. Compressive (a) and flexural (b) strength results (average) for mortar samples. Standard error range for compressive (0.2–1.2) and flexural (0.2–0.5) strength.

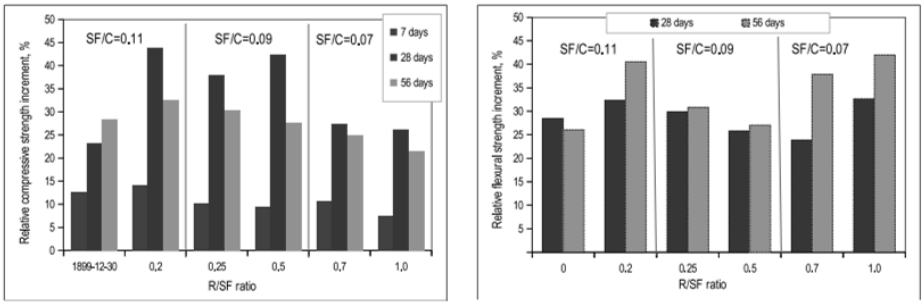

Fig. 13. Comparison of compressive (left) and flexural (right) strength increments relative to the reference mortar; SF/C – silica fume-to-cement ratio, R/SF – gasification residue-to-silica fume ratio.

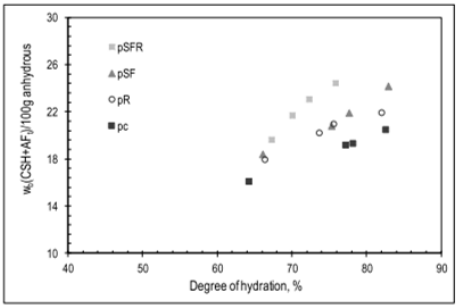

Fig. 14. Normalized bound water of CSH and AF_t versus hydration degree.

for the pSFR system is higher during the first seven days with a delay at later ages; but the amount of CSH seems to be higher than that in other pastes. This suggests that pozzolanic reactions prevail over cement hydration, which seems to be not restricted. On the other hand, the increasing degree of hydration with the bound water increment implies that there is still free space for the deposition and growth of hydration products. This assumption aligns with the nitrogen physisorption results, according to which, the increased amount of small capillary pores and their shifting to the CSH pore region (Fig. 8) was found only in the pSFR system. This suggests that the formation of needle-like hydrates intermixed with the amorphous phase assists in the refinement or "rearrangement" of the pore structure, even though, the volume of pores tends to increase. The refinement of the pore structure, on the other hand, could explain the macroscale properties of the compositions. Despite the improvement in compressive strength (Fig. 12) and resistance to capillary water uptake (Fig. 10), the enhancement of flexural strength at R/SF greater than 0.5 implies that the effect of both substitutes lies in the strengthening of the internal transition zone between matrix and aggregate grain [71–73].

Overall the findings of this study extend those presented in [25–27,40], by confirming that char residue in conjunction with reactive silica fume contributes to the changes in phase assemblage and total volume of hydration products. However, the application of the BJH and QSDFT methods provided more information on the distribution of pores and revealed that the synergy of silica fume with a residue significantly affects the range of small capillary pores (less than 30 nm) and leads to the refinement of the pore structure, one of the factors behind the improvement of the functional properties [13].

3.5. Carbon footprint

For the recycling of wastes in cement-based materials, the environmental impact should be considered, and therefore, the estimation of CO_2 emissions is typically selected as the main parameter for the evaluation of waste potential. Based on the data and methodology proposed

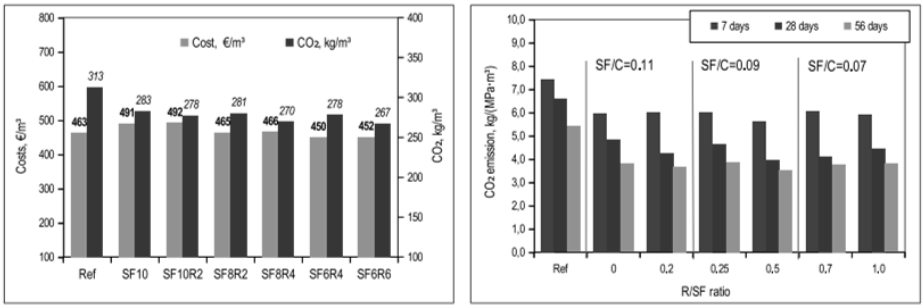

Fig. 15. Comparison of cost and CO_2 emission for the production of cement mortars blended with silica fume (SF) and gasification residue (R.)

by [18,67,68], cost analysis and environmental impact for compositions of this study were performed, while the estimated values are presented in Fig. 15. It should be noted that the silica fume used in this investigation was quite expensive, resulting in a 6% increase in the cost of the blended samples compared to the reference sample. Meanwhile, the reduction in cost was lowered by only 3 %, mostly caused by the increment of residue content.

Fig. 15 reveals that the incorporating both wastes significantly affected CO_2 emissions by reducing them by 10–15 %. Moreover, CO_2 emissions are slightly lower for samples with 12 % than 10 % cement replacement level (Fig. 15). Although not all parameters were included in the calculations, the obtained data are comparable to those presented by others [26,69,70]. On the other hand, it is reasonable to evaluate the effectiveness of the selected amount of mineral admixtures by combining the environmental impact with engineering properties such as mechanical strength, as was proposed in [67]. Fig. 15 illustrates how much each composition produces CO_2 per cubic compressive strength. It can be seen that compositions blended with a residue produce nearly the same (and in some cases slightly lower) emission as composition with cement substituted only by silica fume (R/SF = 0). Moreover, examination of Fig. 15 shows that due to very low data variation among samples with 10 % and 12 % cement replacement levels, an R/SF ratio of 0.5–1.0 could be considered a beneficial amount of substitutes from environmental and engineering points. Despite the improvement in strength, the very low level of water imbibition, obtained for compositions with R/SF ratios higher than 0.5 suggests the possibility of recycling gasification residues in combination with silica fume for the production of cement-based rain-screens or boards applicable in areas where water flows prevail.

4. Conclusions

The present study investigated the potential utilization of two types of waste, sewage sludge-biomass gasification residue and silica fume, as a means for cement replacement and analysed their synergistic impact on the hydration and properties of construction materials. According to the obtained data, the following conclusions can be drawn:

- As evidenced by the TGA results, cement replacement by both substitutes increases the volume of hydration products and promotes CH consumption that starts earlier than in compositions containing only silica fume.
- According to XRD and SEM analysis, the incorporation of both substitutes promotes the formation of higher amount of amorphous CSH phase intermixed with needle-like hydrates, mostly ettringite and small amount of calcium phosphate-bearing hydrates.
- Nitrogen physisorption results revealed that the synergy of silica fume and residue most significantly contributes to the micro- and mesopore range (up to 30 nm), representing the CSH structure and small capillary pores.
- The capillary water uptake of mortars is more dependent on the total cement substitution level and hydration time than on the residue-to-silica fume (R/SF) ratio. Although the incorporation of both substitutes reduces sorptivity from 24 to 56 %, the sample with cement replaced by only silica fume showed the lowest values.
- The compressive strength of mortars decreases with an increasing R/SF ratio, while the flexural strength is less dependent on the substitute ratio. Compared with the reference sample, all blended mortars showed a much higher compressive (7–44 %) and flexural (24–40 %) strength. Nevertheless, the best performance was observed for the sample with the lowest amount of gasification residue.
- Estimated costs and CO_2 emission results indicate that the total cement substitution level may be increased up to 12 %, within 4–6 % covered by gasification residue, without losing the mechanical strength. At the same time, the reduced amount of silica fume (up to 6 %) would save on resources as well.

CRediT authorship contribution statement

Regina Kalpokaitė-Dičkuvienė: Conceptualization, Methodology, Investigation, Validation, Writing – original draft, Writing – review & editing. **Inna Pitak:** Writing – original draft, Visualization, Formal analysis. **Arūnas Baltuśnikas:** Investigation, Methodology, Formal analysis, Validation. **Stasė Irena Lukošiūtė:** Conceptualization, Resources, Supervision, Funding acquisition. **Gintaras Denafas:** Formal analysis. **Jūratė Čėsnienė:** Formal analysis.

Declaration of Competing Interest

The authors declare that they have no known competing financial interests or personal relationships that could have appeared to influence the work reported in this paper.

Acknowledgement

The authors would like to thank the Department of Combustion Science for the supply of materials.

References

[1] European Commission. Eurostat. https://ec.europa.eu/eurostat/web/main/data/database.
[2] A. Kelessidis, A.S. Stasinakis, Comparative study of the methods used for treatment and final disposal of sewage sludge in European countries, Waste Management 32 (6) (2012) 1186–1195.
[3] M. Smol, J. Kulczycka, A. Henclik, G. Katarzyna, Z. Wzorek, The possible use of sewage sludge ash (SSA) in the construction industry as a way towards a circular economy, J. Clean. Prod. 95 (15) (2015) 45–54, https://doi.org/10.1016/j.jclepro.2015.02.051.
[4] I. Fonts, G. Gea, M. Azuara, J. Ábrego, J. Arauzo, Sewage sludge pyrolysis for liquid production: A review, Renewable and Sustainable Energy Reviews. 16 (5) (2012) 2781–2805, https://doi.org/10.1016/j.rser.2012.02.070.
[5] R. Migliaccio, P. Brachi, F. Montagnaro, S. Papa, A. Tavano, P. Montesarchio, G. Ruoppolo, M. Urciuolo, Sewage Sludge Gasification in a Fluidized Bed: Experimental Investigation and Modeling, Ind. Eng. Chem. Res. 60 (13) (2021) 5034–5047, https://doi.org/10.1021/acs.iecr.1c00084 10.1021/acs.iecr.1c00084.s001.
[6] A. Molino, S. Chianese, D. Musmarra, Biomass gasification technology: The state of the art overview, J. Energ. Chem. 25 (2016) 10–25. https://10.1016/j.jechem.2015.11.005.
[7] M. Praspaliauskas, N. Pedišius, N. Striu ̄gas, Elemental Migration and Transformation from Sewage Sludge to Residual Products during the Pyrolysis Process, Energy Fuels. 32 (4) (2018) 5199–5208. https://pubs.acs.org/doi/10.1021/acs.energyfuels.8b00196.
[8] N. Striugas, V. Valinčius, N. Pedišius, R. Poškas, K. Zakarauskas, Investigation of sewage sludge treatment using air plasma assisted gasification, Waste Manag. 64 (2017) 149–160, https://doi.org/10.1016/j.wasman.2017.03.024.
[9] J. Dong, Y. Tang, A. Nzihou, Y. Chi, E. Weiss-Hortala, M. Ni, Life cycle assessment of pyrolysis, gasification and incineration waste-to-energy technologies: Theoretical analysis and case study of commercial plants, J. Sci. Total Environ. 626 (1) (2018) 744–753, https://doi.org/10.1016/j.scitotenv.2018.01.151.
[10] D. Barry, C. Barbiero, C. Briens, F. Berruti, Pyrolysis as an economical and ecological treatment option for municipal sewage sludge, Biomass and Bioenergy. 122 (2019) 472–480, https://doi.org/10.1016/j.biombioe.2019.01.041.
[11] S. Singh, V. Kumar, D.S. Dhanjal, S. Datta, D. Bhatia, J. Dhiman, J. Samuel, R. Prasad, J. Singh, A sustainable paradigm of sewage sludge biochar: Volarization, opportunities, challenges and future prospects, J. Clean. Prod. 269 (1) (2020), 122259, https://doi.org/10.1016/j.jclepro.2020.122259.
[12] J. De Brito, R. Kurda, The past and future of sustainable concrete: A critical review and new strategies on cement-based materials, J. Clean. Prod. 281 (25) (2021), 123558, https://doi.org/10.1016/j.jclepro.2020.123558.
[13] J. Skibsted, R. Snellings, Reactivity of supplementary cementitious materials (SCMs) in cement blends, Cem. Concr. Res. 124 (2019) 105799, https://doi.org/10.1016/j.cemconres.2019.105799.
[14] A. Sadrmomtazi, Z. Noorollahi, B. Tahmouresi, A. Saradar, Effects of hauling time on self-consolidating mortars containing metakaolin and natural zeolite, Constr. Build. Mater. 221 (10) (2019) 283–291, https://doi.org/10.1016/j.conbuildmat.2019.06.037.
[15] F. Boukhelf, R. Cherif, A. Trabelsi, R. Belardi, M.B. Bouiadjra, On the hygrothermal behaviour of concrete containing glass powder and silica fume, J. Clean. Prod. 318 (10) (2021), 128647, https://doi.org/10.1016/j.jclepro.2021.128647.
[16] M. Saridemir, M.H. Severcan, M. Ciflikli, S. Celikten, F. Ozcan, C.D. Atis, The influence of elevated temperature on strength and microstructure of high strength concrete containing ground pumice and metakaolin, Constr. Build. Mater. 124 (15) (2016) 244–257, https://doi.org/10.1016/j.conbuildmat.2016.07.109.

[17] S. Chakraborty, B.W. Jo, J.H. Jo, Z. Baloch, Effectiveness of sewage sludge ash combined with waste pozzolanic minerals in developing sustainable construction material: An alternative approach for waste management, J. Clean. Prod. 153 (1) (2017) 253–263, https://doi.org/10.1016/j.jclepro.2017.03.059.
[18] X. Sun, Y. Zhao, Y. Tian, W. Pingi, Z. Guo, J. Qiu, J. Xing, G. Xiaowei, Modification of high-volume fly ash cement with metakaolin for its utilization in cement paste backfill: The effects of metakaolin content and particle size, Powder Tech. 393 (2021) 539–549, https://doi.org/10.1016/j.powtec.2021.07.067.
[19] R. Kalpokaite-Dičkuviene, I. Lukošiūtė, K. Brinkienė, N. Striūgas, A. Baltušnikas, R. Lukauskaitė, J. Česnienė, Utilization of sewage sludge-biomass gasification residue in cement based materials: effect of pozzolan type, Environ. Tech. 39 (22) (2018) 2937–2950, https://doi.org/10.1080/09593330.2017.1370020.
[20] A.A. Raheem, R. Abdulwahab, M.A. Kareem, Incorporation of metakaolin and nanosilica in blended cement mortar and concrete-A review, J. Clean. Prod. 290 (25) (2021), 125852, https://doi.org/10.1016/j.jclepro.2021.125852.
[21] A. Sirico, P. Bernardi, B. Belletti, A. Malcevschi, E. Dalcanele, I. Domenichelli, P. Fornoni, E. Moretti, Mechanical characterization of cement-based materials containing biochar from gasification, Constr. Build. Mater. 246 (20) (2020), 118496, https://doi.org/10.1016/j.conbuildmat.2020.118490.
[22] A. Danish, M.A. Mosaberpanah, M.U. Salim, N. Ahmad, F. Ahmad, A. Ahmad, Reusing biochar as a filler or cement replacement material in cementitious composites: A review, Constr. Build. Mater. 300 (20) (2021), 124295, https://doi.org/10.1016/j.conbuildmat.2021.124295.
[23] C.J. Lynn, R.K. Dhir, G.S. Ghataora, R.P. West, Sewage sludge ash characteristics and potential for use in concrete, Constr. Build. Mater. 98 (15) (2015) 767–779, https://doi.org/10.1016/j.conbuildmat.2015.08.122.
[24] L. Swierczek, B. Michał Cieślik, P. Konieczka, Challenges and opportunities related to the use of sewage sludge ash in cement-based building materials – A review, J. Clean. Prod. 287 (10) (2021), 125054, https://doi.org/10.1016/j.jclepro.2020.125054.
[25] A. Dixit, S. Gupta, S.D. Pang, H.W. Kua, Waste Valorisation using biochar for cement replacement and internal curing in ultra-high performance concrete, J. Clean. Prod. 238 (2019) 117876, https://doi.org/10.1016/j.jclepro.2019.117876.
[26] C. Gu, Y. Ji, Y. Zhang, Y. Yang, J. Liu, T. Ni, Recycling use of sulfate-rich sewage sludge ash (SR-SSA) in cement-based materials: Assessment on the basic properties, volume deformation and microstructure of SR-SSA blended cement pastes, J. Clean. Prod. 282 (2021) 124511, https://doi.org/10.1016/j.jclepro.2020.124511.
[27] S. Gupta, P. Krishnan, A. Kashani, H.W. Kua, Application of biochar from coconut and wood waste to reduce shrinkage and improve physical properties of silica fume-cement mortar, Constr. Build. Mater. 262 (30) (2020), 120688, https://doi.org/10.1016/j.conbuildmat.2020.120688.
[28] Z. Chen, C.S. Poon, Comparative studies on the effects of sewage sludge ash and fly ash on cement hydration and properties of cement mortars, Constr. Build. Mater. 154 (15) (2017) 791–803, https://doi.org/10.1016/j.conbuildmat.2017.08.003.
[29] S. Gupta, H.W. Kua, Carbonaceous micro-filler for cement: Effect of particle size and dosage of biochar on fresh and hardened properties of cement mortar, Sci. Total Env. 662 (20) (2019) 952–962, https://doi.org/10.1016/j.scitotenv.2019.01.269.
[30] A. Kappel, L.M. Ottosen, G.M. Kirkelund, Colour, compressive strength and workability of mortars with an iron rich sewage sludge ash, Constr. Build. Mater. 157 (30) (2017) 1199–1205, https://doi.org/10.1016/j.conbuildmat.2017.09.157.
[31] G. Rutkowska, P. Wichowski, J. Fronczyk, M. Franus, M. Chalecki, Use of fly ashes from municipal sewage sludge combustion in production of ash concretes, Constr. Build. Mater. 188 (2018) 874–883, https://doi.org/10.1016/j.conbuildmat.2018.08.167.
[32] Z. Chang, G. Long, J.L. Zhou, C. Ma, Valorization of sewage sludge on the fabrication of construction and building metarials: A review, Res. Conv. Recycling 154 (2020), 104606, https://doi.org/10.1016/j.resconrec.2019.104606.
[33] G. Chand, S.K. Happy, S. Ram, Assessment of the properties of sustainable concrete produced from quaternary blend of portland cement, glass powder, metakaolin and silica fume, Clean. Eng. Tech. 4 (2021) 100179, https://doi.org/10.1016/j.clet.2021.100179.
[34] M. Cyr, R. Idir, G. Escadeillas, Use of metakaolin to stabilize sewage sludge ash and municipal solid waste incineration fly ash in cement-based materials, J. Hazard. Mater. 243 (2012) 193–203.
[35] R. Kalpokaite-Dičkuviene, A. Baltušnikas, R. Levinskas, J. Česnienė, Incinerator residual ash - Metakaolin blended cements: Effect on cement hydration and properties, Constr. Build. Mater. 206 (10) (2019) 297–306, https://doi.org/10.1016/j.conbuildmat.2019.02.060.
[36] B. Lothenbach, M. Zajac, Application of thermodynamic modelling to hydrated cements, Com. Concr. Res. 123 (2019) 105779, https://doi.org/10.1016/j.cemconres.2019.105779.
[37] A. Sadrmomtazi, B. Tahmouresi, R.K. Khoshkbijari, Effect of fly ash and silica fume on transition zone, pore structure and permeability of concrete, Mag. Concr. Res. 70 (10) (2018) 519–532, https://doi.org/10.1680/jmacr.16.00537.
[38] W. Meng, A. Kumar, K.H. Khayat, Effect of silica fume and slump-retaining polycarboxylate-based dispersant on the development of properties of portland cement paste, Cem. Concr. Comp. 99 (2019) 181–190, https://doi.org/10.1016/j.cemconcomp.2019.03.021.
[39] C. Ni, Q. Wu, Z. Yu, X. Shen, Hydration of Portland cement paste mixed with densified silica fume: from the point of view of fineness, Constr. Build. Mater. 272 (22) (2021), 121906, https://doi.org/10.1016/j.conbuildmat.2020.121906.
[40] D. Vouk, M. Serdar, A.A. Vučinic, Use of incinerated sewage sludge ash in cement mortars: Case study in Croatia, Tehnički vjesnik 24 (1) (2017) 43–51. https://doi.org/10.17559/TV-20150901095705.
[41] L. Wang, M. Jin, Y. Wu, Y. Zhou, S. Tang, Hydration, shrinkage, pore structure and fractal dimension of silica fume modified low Portland cement-based materials, Constr. Build. Mater. 272 (22) (2021), 121952, https://doi.org/10.1016/j.conbuildmat.2020.121952.
[42] European Standard EN 196, Methods of testing cement – Part 1: Determination of strength.
[43] European Standard EN 1015, Methods of test for mortar for masonry – Part 18: Determination of water absorption coefficient due to capillary action of hardened mortar.
[44] International Standard ASTM C 642-06: Standard Test Methods for Density, Absorption, and Voids in Hardened Concrete.
[45] K.S.W. Sing, D.H. Everett, R.A.W. Haul, I. Mouscou, R.A. Pierotti, J. Rouquerol, T. Siemieniewska, Reporting physisorption data for gas/liquid systems with special reference to the determination of surface area and porosity, Pure Appl, Chem. 57 (1985) 603–619.
[46] M. Thommes, Physical adsorption characterization of nanoporous materials, Chemie Ingenieur Technik 82 (2010) (2010) 1059–1073, https://doi.org/10.1002/cite.201000064.
[47] 2003/33/EC: Council Decision of 19 December 2002 establishing criteria and procedures for the acceptance of waste at landfills pursuant to Article 16 of and Annex II to Directive 1999/31/EC. 2003. Official J European Comm. 46:27-49.
[48] T.D. Dyer, J.E. Halliday, R.K. Dhir, Hydration chemistry of sewage sludge ash used as a cement component, J. Mater. Civil. Eng. 23 (5) (2011) 648–655, https://doi.org/10.1016/(ASCE)MT.1943-5533.0000221.
[49] M. Mejdi, M. Saillio, T. Chaussadent, L. Divet, A. Tagnit-Hamou, Hydration mechanisms of sewage sludge ashes used as cement replacement, Cem. Concr. Res. 135 (2020) 106115, https://doi.org/10.1016/j.cemconres.2020.106115.
[50] E.T. Stepkowska, J.M. Blanes, F. Franco, C. Real, J.L. Pérez-Rodríguez, Phase transformation on heating of an aged cement paste, Thermochimica Acta 420 (1-2) (2004) 79–87, https://doi.org/10.1016/j.tca.2003.11.057.
[51] K. Vance, M. Aguayo, T. Oey, G. Sant, N. Neithalath, Hydration and strength development in ternary portland cement blends containing limestone and fly ash or metakaolin, Cem. Concr. Com. 39 (2013) 93–103, https://doi.org/10.1016/j.cemconcomp.2013.03.028.
[52] R. Gabrovšek, T. Vuk, V. Kaučič, Evaluation of the hydration of Portland cement containing various carbonates by means of thermal analysis, Acta Chim. Slov. 53 (2006) 159–165.
[53] A. Hidalgo, C. Domingo, C. Garcia, S. Petit, C. Andrade, C. Alonso, Microstructural changes induced in Portland cement-based materials due to natural and supercritical carbonation, J. Mater. Sci. 43 (2008) 3101–3111. https://10.1007/s10853-008-2521-5.
[54] D. Damidot, B. Lothenbach, D. Herfort, F.P. Glasser, Thermodynamics and cement science, Cem. Concr. Res. 41 (7) (2011) 679–695, https://doi.org/10.1016/j.cemconres.2011.03.018.
[55] F. Lavergne, A. Ben Fraj, I. Bayane, J.F. Barthelemy, Estimating the mechanical properties of hydrating blended cementitious materials: An investigation based on micromechanics, Cem. Concr. Res. 104 (2018) 37–60, https://doi.org/10.1016/j.cemconres.2017.10.018.
[56] H. Zhang, W. Darvel, B.,, Morphology and structural characteristics of hydroxyapatite whiskers: Effect of the initial Ca concentration, Ca/P ratio and pH, Acta Biomater. 7 (7) (2011) 2960–2968, https://doi.org/10.1016/j.actbio.2011.03.020.
[57] I.S. Neira, Y.V. Kolen'ko, K.P. Kommareddy, I. Manjubala, M. Yoshimura, F. Guitián, Reinforcing of a Calcium Phosphate Cement with Hydroxyapatite Crystals of Various Morphologies, ACS Appl. Mater. Interfaces. 2 (11) (2010) 3276–3284, https://doi.org/10.1021/am100710b.
[58] S. Li, W. Yu, W. Zhang, G. Zhang, L. Yu, E. Lu, Evaluation of highly carbonated hydroxyapatite bioceramic implant coatings with hierarchical micro-/nanorod topography optimized for osseointegration, Inter. J. Nanomedicine 13 (2018) 3643–3659, https://doi.org/10.2147/IJN.S159989.
[59] A.R. Santos, M.R. Veiga, A.S. Silva, J. de Brito, J.I. Alvarez, Evolution of the microstructure of lime based mortar and influence on the mechanical behaviour: The role of aggregates, Constr. Build. Mater. 187 (30) (2018) 907–922, https://doi.org/10.1016/j.conbuildmat.2018.07.223.
[60] E. Berodier, K. Scrivener, Evolution of pore structure in blended systems, Cem. Concr. Res. 73 (2015) 25–35, https://doi.org/10.1016/j.cemconres.2015.02.025.
[61] W. Huang, H. Kazemi-Kamyab, W. Sun, K. Scrivener, Effect of cement substitution by limestone on the hydration and microstructure development of ultra-high performance concrete (UHPC), Cem. Concr. Res. 77 (2017) 86–101, https://doi.org/10.1016/j.cemconcomp.2016.12.009.
[62] Q. Zeng, K. Li, T. Fen-Chong, P. Dangla, Pore structure characterization of cement pastes blended with high volume fly-ash, Cem. Concr. Res. 42 (1) (2012) 194–204, https://doi.org/10.1016/j.cemconres.2011.09.012.
[63] W. Huang, H. Kazemi-Kamyab, W. Sun, K. Scrivener, Effect of replacement of silica fume with calcined clay on the hydration and microstructural development of eco-UHPFRC, Mater. Design. 121 (5) (2017) 36–46, https://doi.org/10.1016/j.matdes.2017.02.052.
[64] Z. Zhang, G.W. Scherer, Evaluation of drying methods by nitrogen adsorption, Cem. Concr. Res. 120 (2019) 13–26, https://doi.org/10.1016/j.cemconres.2019.02.016.
[65] N.M. Alderete, Y.A. Villagran Zaccardi, N. De Belio, Physical evidence of swelling as the cause of anomalous capillary water uptake by cementitious materials, Cem.

Concr. Res. 120 (2019) 256–266, https://doi.org/10.1016/j.cemconres.2019.04.001.
[66] J.E. Rossen, B. Lothenbach, K.L. Scrivener, Composition of C-S-H in pastes with increasing levels of silica fume addition, Cem. Concr. Res. 75 (2015) 14–22, https://doi.org/10.1016/j.cemconres.2015.04.016.
[67] G. Long, Y. Gao, Y. Xie, Designing more sustainable and greener self-compacting concrete, Constr. Build. Mater. 84 (1) (2015) 301–306, https://doi.org/10.1016/j.conbuildmat.2015.02.072.
[68] Z. Pavlik, M. Pavlikova, M. Zalecka, G. Lagod, Z. Suchorad, L. Guz, Life cycle assesment of the use of sewage sludge as Portland cement replacement, IOP Conf. Series: Mater. Sci. Eng. 710 (2019), 012038, https://doi.org/10.1088/1757-899X/710/1/012038.
[69] M. Záleská, Z. Pavlík, M. Pavlíková, L. Scheinherrová, J. Pokorný, A. Trník, P. Svora, J. Foit, O. Jankovský, Z. Suchorab, R. Černý, Biomass ash-based mineral admixture prepared from municipal sewage sludge and its application in cement composites, Clean Techn. Environ. Policy 20 (1) (2018) 159–171, https://doi.org/10.1007/s10098-017-1465-3.
[70] D. Nakic, Environmental evaluation of concrete with sewage sludge ash based on LCA, Sustain. Prod. Consump. 16 (2018) 193–201, https://doi.org/10.1016/j.spc.2018.08.003.
[71] M. Gruszczyński, M. Lenart, Durability of mortars modified with the addition of amorphous aluminum silicate and silica fume, Theoret. Appl. Fract. Mech. 107 (2020) 102526, https://doi.org/10.1016/j.tafmec.2020.102526.
[72] H. Eker, A. Bascetin, Influence of silica fume on mechanical property of cemented paste backfill, Constr. Build. Mater. 317 (2022) 126089, https://doi.org/10.1016/j.conbuildmat.2021.126089.
[73] M.F. Junaid, Z.u. Rehman, M. Kuruc, I. Medveď, D. Bačinskas, J. Čurpek, M. Čekon, N. Ijaz, W.S. Ansari, Lightweight concrete from a perspective of sustainable reuse of waste byproducts, Constr. Build. Mater. 319 (2022) 126061, https://doi.org/10.1016/j.conbuildmat.2021.126061.

ACKNOWLEDGMENTS

I'd like sincerely thank to Prof Dr Gintaras Denafas for supervising my doctoral research, consultations, valuable advice and great support and faith in me as a scientist.

I want to kindly thank Dr Stasė Irena Lukošiutė, Head of the Laboratory of Materials Research and Testing, Lithuanian Energy Institute, for her invaluable advice on my study, for sharing knowledge in materials testing and for perfect scientific discussion and emotional support.

I am incredibly grateful dr Arūnas Baltušnikas for helping with my study, measuring materials properties using various analyses, sharing knowledge in pore size distribution studies, XRD analysis by Rietveld refinement and for great valuable scientific discussion, emotional and friendly support.

Special thanks to Sigitas Rimkevičius, director of the Lithuanian Energy Institute, for the opportunity to study and work, for invaluable moral support.

I thank scientists Regina Kalpokaitė-Dičkuvienė, Jūraite Čėsnienė, Rita Kriūkienė and Vidas Makarevičius for their invaluable advice, assistance in conducting experiments, in scientific discussions; Algis Marštys and Virgis Kazlauskas for organising my work in the laboratory, exciting and valuable discussions.

Many thanks to all the employees of the Lithuanian Energy Institute and Kaunas University of Technology for the technical and scientific support of my research.

Special thanks to the Kaunas and Alytus regional waste management centre employees for their help in experimenting and for information support.

I want to express my deep gratitude to all those who have contributed to my development and formation as a scientist; thank you very much for your intellectual and emotional support.

I also want to express special gratitude to my family for their support, faith, understanding and patience.

APPENDIXES

Appendix 1. Parameters, methodology and results of calculation economic efficiency of using the SRF during clinker firing

№	Parameters	Limit value	Symbol
1	Daily kiln production quantity	3056 ton/day	KP[61]
2	Total operating day	360 day/year	OD[61]
3	Emission factor of coal	85 %	CA_{CO2}[61]
4	The energy required to produce one kg of clinker	840 kcal/kg	Ec[28]
5	The calorific value of coal	7400 kcal/kg	HCV_{coal}[62]
6	Price 1 ton of coal	137 USD	P_{coal}[63]
7	The cost price of one-ton SRF	25 USD	P_{SRF}[64]
8	The calorific value of SRF	5000 kcal/kg	CV_{SRF}
9	Emission cost of one ton CO_2	58 USD	P_{CO2}[65]
10	Replacement ratio of SRF	10, 15, 20, 25%	RR
11	Coal consumption by initial situation	16.1 t/h	C^0_{coal}

Methodology of calculation

The energy consumption of coal to produce clinker tons per day, kcal/kg (*E*):

$$En = KP \times 1000 \times Ec, \quad (1)$$

The coal energy consumption savings by using the replacement ratio of SRF, kcal/kg (*Esav*):

$$Esav = En \times RR \quad (2)$$

The SRF amount to be replaced per hour to achieve the required energy, ton/h (A_{SRF}):

$$A_{SRF} = \left(Esav / HCV_{SRF}\right) / 1000 / 24 \quad (3)$$

The coal amount per hour required to achieve the energy, ton/h (C_{coal}):

$$C_{coal} = \left(REn / CV_{coal}\right) / 1000 / 24 \quad (4)$$

where *RE* is the required energy to produce one kg of clinker taking into account the replacement ratio of SRF (kcal/kg):

$$REn = KP \times Ec_{calc} \times RR \times 1000 \quad (5)$$

where Ec_{calc} is the calculation energy required to produce 1 kg of clinker (kcal/kg):

$$Ec_{calc} = \left(Ec \times AC\right) / 100 \quad (6)$$

where *AC* is the coal consumption (t/h) and was calculated by Eq. 7:

$$AC = C^0_{coal} - C_{coal} \quad (7)$$

where C_{coal} – coal consumption calculated by different replacement ratios of SRF (t/h).

The amount of SRF required for replacing one ton of coal (Q_{SRF}) was:

$$Q_{SRF} = A_{SRF} / AC \quad (8)$$

Using SRF as a replacement fuel, the annual coal savings, t/year (AS_{coal}), were calculated using Eq. 9:

$$AS_{coal} = AC \times OD \times 24 \tag{9}$$

The annual income in coal savings, USD/year (AI), was calculated by Eq. 10:

$$AI = AS_{coal} \times P_{coal} \tag{10}$$

The annual consumption of SRF, t/year (AC_{SRF}), was calculated using Eq. 11:

$$AC_{SRF} = A_{SRF} \times OD \times 24 \tag{11}$$

By Eq. 12, the annual costs of SRF, USD/year (C_{SRF}), were calculated:

$$C_{SRF} = AC_{SRF} \times P_{SRF} \tag{12}$$

The actual financial savings, USD/year (FS), were calculated using Eq. 13:

$$FS = AI - C_{SRF} \tag{13}$$

The annual CO_2 emission savings for the cement plant using coal, USD/year (CS_{CO2}), was calculated by Eq. 14:

$$CS_{CO2} = AC \times CA_{CO2} \times TOD \times 24 \tag{14}$$

Reducing CO_2 emissions from coal, USD/year (ES_{CO_2}), was calculated using Eq. 15:

$$ES_{CO_2} = CS_{CO_2} \times P_{CO_2} \tag{15}$$

Loss of efficiency taking into account the use of SRF, % (LEf), was calculated by Eq. 16:

$$LEf = 0.20 \times RR \times 100 \tag{16}$$

The net cost savings was calculated according to Eq. 17:

$$NCS = \frac{(AI + ES_{CO2} - C_{SRF}) \times (100 - LEf)}{100} \tag{17}$$

UDK UDK 662.6/.9+628.4](043.3)
SL 344. 2023-10-20, 15,5 leidyb. apsk. l. Tiražas 14 egz. Užsakymas 195. Išleido Kauno technologijos universitetas, K. Donelaičio g. 73, 44249 Kaunas Spausdino leidyklos „Technologija“ spaustuvė, Studentų g. 54, 51424 Kaunas